2009

CHAPERONE EXPRESSION AND EFFECTS OF ITS INHIBITION ON BREAST CANCER SENSITIZATION

Malissa Diehl
Virginia Commonwealth University

CHAPERONE EXPRESSION AND EFFECTS OF ITS INHIBITION ON BREAST CANCER SENSITIZATION

A dissertation submitted in partial fulfillment of the requirements for the degree of Doctor of Philosophy at Virginia Commonwealth University

By Malissa Chang Diehl
B.S. Biochemistry and Molecular Biology
The Pennsylvania State University, 2002

Director: Shawn E. Holt, Associate Professor
Department of Pathology, Department Human and Molecular Genetics,
Department of Pharmacology & Toxicology, and Massey Cancer Center

Virginia Commonwealth University
Richmond, Virginia
July 2009

Acknowledgements

These past few years have been the most rewarding, exciting, and frequently frustrating times of my life. This work would not have been possible without the support of so many great people since I would not be where I am today without them. First and foremost, a huge thanks goes to Dr. Shawn Holt for teaching me to think critically and offering his patience, his continued guidance and advice, and his humor. You have given me thoughtful direction through this project, but have also allowed me to develop my own ideas and interests as a scientist. Thank you for everything you've done in the past and the present, and for preparing me for the future. To Dr. Lynne Elmore, thank you for answering all my insistent questions. To the rest of my committee members, Dr. Joy Ware, Dr. Jolene Windle, and Dr. Michael Idowu, I appreciate all the constructive suggestions and discussions on how to progress my research. To Dr. Tim York, a big thanks for taking the time to meticulously explain advanced statistics, which was a significant portion of the study. To all my past and current lab mates, Patrick, Michael, Kennon, and Sarah, our academic and personal conversations were invaluable, and especially to Amy, thank you for providing daily encouragement, assurance, and amusement. Special mention also goes to VCU's Department of Anatomy and Neurobiology Microscopy Facility, supported in part with funding from NIH-NINDS Center core grant (5P30NS047463-02) and Clinical Pathology of VCU's School of Medicine for allowing me to use their digital microscope at will.

To my parents, thank you for pushing me, and not just in academics. For that, I owe you everything. To my husband Brian, you have always been so supportive and believed in me, even when I didn't. Thank you for being so encouraging through this difficult process. Thanks also go to my father- and mother-in-law, for your unwavering fostering of my goals. Last, but not least, to all my wonderful friends, I couldn't have done it without your laughter and companionship. Thanks for keeping me grounded and helping me keep things in perspective.

Table of Contents

Page

Acknowledgements ii

List of Tables vii

List of Figures viii

List of Abbreviations xi

Abstract xiii

Chapter 1: Introduction and Review of Current Literature 1

1.1 Hallmarks of Cancer 1

1.2 Role of p53 in Breast Cancer 4

1.3 Telomere Biology and Function 8

1.4 Maintenance of Telomeres by Telomerase 14

1.5 Cellular Fates 18

1.6 Molecular Chaperones, Heat Shock Proteins, and Hsp90 20

1.7 Hsp90 Inhibition 31

1.8 Current Breast Cancer Therapeutics 37

1.9 Aims and Rationale for Study 47

Chapter 2: Materials and Methods 50

Chapter 3: Differential expression of Hsp90 and its co-chaperone, p23, in human breast tissue 61

3.1 Introduction and Rationale 61

3.2 Results 63

3.2.1 Hsp90 and p23 protein levels are elevated in breast cancer cells 63

3.2.2 Established cancer cell lines on TMA consistently express higher Hsp90 and p23 levels 65

3.2.3 Hsp90 expression in clinical tissues is predominantly cytoplasmic.....70

3.2.4 p23 nuclear expression differs between disease types 71

3.2.5 Hsp90 and p23 expression differs between disease types but not between locations.....74

3.2.6 Breast cancer related clinical parameters are significantly associated with chaperone upregulation 77

3.2.7 Total Hsp90 in tumor cells is associated with an increase in both complexed and uncomplexed Hsp90.....79

Chapter 4: Effect of Hsp90 Inhibition on Breast Cancer Sensitization 90

4.1 Introduction and Rationale 90

4.2 Results 94

4.2.1 RAD affects cellular proliferation and telomerase activity in breast cancer cells.....94

4.2.2 RAD and Adr in combination more than additively alters growth properties 102

4.2.3 RAD and Adr in combination affects cell fate and the expression of cell cycle associated proteins and HSPs 105

4.2.4 Radicicol pretreatment elicits a stronger senescence response but no apoptotic response 112

4.2.5 No change in p53 or p21 expression in MDA-MB231 cells.....117

4.2.6 CIS and TAX are associated with differential expression of cell fate proteins and HSPs 120

4.2.7 CIS and TAX affect Hsp90 client protein expression.....125

4.2.8 CIS and TAX induce apoptotic cell death.....127

4.2.9 TAM treatment affects cellular proliferation and p53/p21 expression 134

Chapter 5: Discussion 140

5.1 Preface 140

5.2 Differential expression of Hsp90 and p23 in breast cancer.....140

5.3 Client-bound and free forms of Hsp90 co-exist in cancer cells 147

5.4 Radicicol, alone and in combination, affects cellular proliferation 149

5.5 Telomerase activity decreases in response to RAD 152

5.6 p53, p21, and cell cycle regulation.....154

5.7 Radicicol affects co-chaperones of the Hsp90 cycle.....158

5.8 Expression of c-Abl is altered in response to CIS but not TAX 160

5.9 Induction of senescence or apoptosis 161

5.10 Perspective 164

References.....166

Appendix: Telomere-associated TRF2 Expression during Breast Cancer Progression.....196

A.1 Introduction 196

A.2 Results 198

A.2.1 Invasive breast carcinomas express less nuclear TRF2.....198

A.2.2 Consistently high nuclear TRF2 in breast and non-breast cell lines 200

A.2.3 Highly variable FISH signal indicative of nonhomogeneous telomere

length 202

A.2.4 No difference in TRF2 score, but considerable difference in FISH score ..206

A.2.5 Age influences TRF2 expression.....208

A.2.6 Association of TRF2 and telomere length.....208

A.3 Discussion 211

Vita.....215

List of Tables

Table **Page**

1: Summary of chaperone intensity of established cells lines on TMAs. 68

2: Cell line cytoplasmic and nuclear immunostaining 69

3: Hsp90 cytoplasmic and nuclear immunostaining. 73

4: p23 cytoplasmic and nuclear immunostaining. 76

5: Summary of disease type-specific differences. 78

6: Correlations between TNM stage and average chaperone scores in invasive cores. 80

7: Correlations between ER/PR status and chaperone expression in invasive cores. 81

8: Relationship between TNM stage and hormone receptor status in invasive cores. 82

9: Summary of complexed vs. uncomplexed Hsp90 in normal and cancer cells. 88

10: TRF2 nuclear immunostaining. 201

11: Average TRF2 immunostaining and FISH scores. 207

12: Correlations between chronologic age or TNM stage and average TRF2 score. 209

13: Correlations between TRF2 score or clinical parameters and FISH. 210

List of Figures

Figure **Page**

1: The six hallmarks of cancer....2

2: p53 mediates the DNA damage response....5

3: Telomere binding- and associated-proteins localize on the telomeric structure 11

4: Telomerase reactivation in cancer cells could be therapeutically targeted 15

5: Heat shock proteins have multifunctional responsibilities on client protein maturation....22

6: Schematic of the domains of the Hsp90 monomer....24

7: Structure and features of the Hsp90 homodimer....26

8: Hsp90 ATP-driven chaperoning cycle 27

9: Hsp90 client proteins are involved in the hallmarks of cancer 30

10: Hsp90 inhibitors 34

11: Current anticancer drugs for breast cancer....40

12: Design of Tissue Microarrays 53

13: Hsp90 and p23 protein levels increase with population doubling in normal cells and are high in established breast cancer cell lines....64

14: High Hsp90 and p23 expression in established immortal and cancer cell lines 66

15: Cell lines of TMA consistently express high levels of both Hsp90 and p23 67

16: Hsp90 cytoplasmic expression is elevated in invasive breast carcinomas as compared to normal and DCIS tissues....72

17: Level of p23 is higher in normal breast tissue than in invasive breast carcinomas 75

18: Hsp90 in cancer cells exists in both a complexed and uncomplexed state 84

19: Schematic of modified immunoprecipitation technique 85

20: Method of immunoprecipitation affects detection of Hsp90 complexes 87

21: Cell growth decreases with increasing RAD concentrations. 96

22: Assembly of telomerase 97

23: Radicicol-responsive telomerase activity.....98

24: RAD-dependent cell growth at low RAD doses 100

25: Telomerase activity declines at lower RAD concentrations 101

26: Average cell counts decrease in the presence of RAD pretreatment 103

27: Greater decline in population doubling with RAD and Adr combination treatment ..104

28: Induction of p53 and p21 upon single agent and combination treatments.....106

29: Greater induction of p53 upon Adr alone treatment.....108

30: Greater induction of p21 levels upon Adr alone treatment 109

31: Expression of cochaperones and a cell cycle-regulatory protein in Adr treated cancer cells.....110

32: Expression of cochaperones and a cell cycle-regulatory protein in RAD and Adr treated cancer cells 111

33: No change in overall telomere length upon drug treatment.....113

34: Drug treated cells exhibit positive senescence-associated β-gal staining 115

35: Increase in senescent cells upon treatment with RAD and Adr 116

36: Apoptotic cells are undetectable upon RAD + Adr treatment 118

37: No change in p53 or p21 levels in singe agent or combination treated MDA-MB231 cells.....119

38: No change in chaperone expression in MDA-MB231 cells upon Adr or RAD + Adr treatment.....121

39: Differential expression of cell fate related proteins and the Hsp90-related co-chaperone after CIS or TAX treatment.....123

40: Altered expression of Hsp90 client proteins post CIS or TAX treatment.....126

41: Small percentage of morphological cell death in response to treatment with Cisplatin.....128

42: Cell death upon CIS treatment 129

43: Indiscernable change in apoptotic cells between CIS alone and with RAD pretreatment.....131

44: Massive morphological cell death occurs in response to treatment with Taxol.....132

45: Greater cell death upon TAX treatment 133

46: Apoptotic cell emergence not affected by RAD pretreatment with TAX.....135

47: Cell growth declines in response to tamoxifen treatment 137

48: Decreased expression of cell fate related proteins with TAM treatment 138

49: TRF2 expression in normal, DCIS, and invasive breast carcinomas from tissue arrays 199

50: Established cell lines consistently express high levels of nuclear TRF2 203

51: Variability in telomeric signal in invasive cores.....204

52: Tumor and surrounding normal tissue express varying telomeric intensity 205

List of Abbreviations

17-AAG	17-allyamino, 17-demethoxy geldanamycin
17-DMAG	17-(2-dimethylaminoethyl) amino-17-demethoxygeldanamycin
Adr	Adriamycin
ATM	Ataxia telangiectasia mutated protein
ATR	ATM and Rad3-related protein
Cdk4	Cyclin-dependent kinase 4
CIS	Cisplatin
DCIS	Ductal carcinoma *in situ*
DNA-PK	DNA-activated protein kinase
EGF	Epidermal growth factor
ER	Estrogen receptor
GA	Geldanamycin
HER2/neu	Human epidermal growth factor receptor 2
HME	Human mammary epithelial cell
Hsp90	Heat shock protein 90
Hsp70	Heat shock protein 70
ICC	Immunocytochemistry
IHC	Immunohistochemistry
PD	Population doubling
pRb	Retinoblastoma protein

PR	Progesterone receptor
RAD	Radicicol
SA β-Gal	Senescence associated beta galactosidase
SERM	Selective estrogen receptor modulator
TAM	Tamoxifen
TAX	Taxol
TGFβ	Transforming growth factor β
TMA	Tissue microarray
TNM	Tumor-Node-Metastasis

Abstract

CHAPERONE EXPRESSION AND EFFECTS OF ITS INHIBITION ON BREAST CANCER SENSITIZATION

A dissertation submitted in partial fulfillment of the requirements for the degree of Doctor of Philosophy at Virginia Commonwealth University

By Malissa Chang Diehl
B.S. Biochemistry and Molecular Biology
The Pennsylvania State University, 2002

Director: Shawn E. Holt, Associate Professor
Department of Pathology, Department Human and Molecular Genetics,
Department of Pharmacology & Toxicology, and Massey Cancer Center

Virginia Commonwealth University
Richmond, Virginia
July 2009

Breast cancer is one of the most prevalent and deadly forms of cancer in women and is not restricted by race or ethnicity. Although a wealth of knowledge has been amassed on the biology of breast cancer, including its risk factors, diagnosis, prognosis, prevention, and treatment, it remains a serious health concern and active area of research. Initial response to standard chemotherapeutic and radiotherapeutic regimens is generally strong for many patients, yet breast tumors often recur, leading to more aggressive and resistant tumors. Because recurrence is such a clinical issue, more effective therapeutic approaches are needed to eliminate partial clinical responses and undesirable side effects.

Molecular chaperones like the heat shock protein 90 (Hsp90) family are regarded as ubiquitous, highly conserved proteins that mainly respond upon induction of stress or disruption in cellular homeostasis. Chaperones are critically involved in controlling the conformation,

stability, function, and degradation of many oncogenic client proteins by assisting in trafficking, remodeling of improperly folded client proteins, and suppression of protein aggregation. Hsp90-mediated folding events are an ATP-dependent process that involves the association with various co-chaperones and stimulators, including Hsp70, Hsp40, HOP, p23, and Aha1 for client stabilization and modification. Notably, Hsp90 seems to be particularly associated with cell signaling clientele, such as nuclear hormone receptors, protein kinases, and many other oncogenic proteins that directly influence the hallmarks of cancer.

In order to define the role of chaperones in breast cancer progression, we assessed chaperone expression levels in normal and tumor lines. Based on our initial finding of increased expression of Hsp90 and p23 in immortal and cancer cell lines, it is possible that this phenomenon may be reflected in normal breast tissue as well as breast carcinoma specimens. Indeed, we observed high Hsp90 expression in invasive carcinomas, such that high nuclear expression correlates with a greater TNM stage, while high cytoplasmic Hsp90 correlates with ER negativity, suggesting that elevated Hsp90 may be an indicator or marker of advanced disease. p23 expression also increases appreciably in established breast cancer cell lines with invasive breast tissue specimens displaying an opposite trend. Although p23 does not appear to have any relationship with TNM stage, significant relationships with ER and PR emerged, with higher nuclear p23 correlating to ER positivity and higher total p23 being positively associated with PR presence. Due to the differential expression of Hsp90 in normal, DCIS, and invasive breast carcinomas, we determined the impact on Hsp90 function, finding that total Hsp90 in tumor cells is associated with an increase in both complexed and uncomplexed Hsp90, which is in contrast to a previously reported study.

The intrinsic nature of heat shock proteins makes them especially relevant to a cell's defense against cancer initiation. The preferential accumulation of Hsp90 in cancer cells also forms the basis for the unique sensitivity of tumor cells to Hsp90 inhibition. The Hsp90 specific inhibitor, radicicol, is more potent in terms of blocking ATPase activity than other Hsp90-related compounds like geldanamycin, which is much more toxic. All Hsp90 inhibitors prevent the association of the co-chaperone p23 with Hsp90, resulting in destabilization of the client protein. For these reasons, it may be possible that Hsp90 inhibition would sensitize breast cancer cells to be more responsive to standard chemotherapeutics. We determined that radicicol negatively alters cellular proliferation, and in combination with Adriamycin, elicits a more robust decline in growth and the expression of Hsp90 client proteins. This finding was associated with an increase in senescent cells without a detectable affect on apoptosis. Radicicol in combination with cisplatin or Taxol contributed to an increase in cell death (apoptosis) and differentially altered the expression of client proteins. Finally, ER negative breast cancer cells do not display altered p53 expression upon radicicol and Adriamycin treatment. Blockade of ER activity in ER positive cells with tamoxifen induced significant reductions in proliferation and decreased p53 expression without a corresponding decrease in p21 levels. In conclusion, these results point to the utility of Hsp90 inhibition as a valid form of targeted therapy for breast cancer, and the value of radicicol as a potential adjuvant treatment option in combination with standard chemotherapeutics.

Chapter 1

Introduction and Review of Current Literature

1.1 Hallmarks of Cancer

Breast cancer is one of the most prevalent forms of cancer and cause of mortality in women and is not restricted by race or ethnicity.[1] Although a wealth of knowledge has been amassed on the biology of breast cancer, including its risk factors, diagnosis, prognosis, prevention, and treatment, it remains a serious health concern and active area of research. It is an especially multifaceted disease with both genetic and environmental factors contributing to its layers of complexity. Despite the unpredictable nature of cancer, it still adheres to fundamental principles and patterns of transformation, although the pathways and mechanisms may vary between cancer types. On a basic level, a collection of genomic alterations need to accrue, persist, and bypass defenses in order for normal cells to convert into tumor cells. In doing so, homeostasis within the cell and in the surrounding environment is disrupted, leading to a malignant phenotype.

As general features, the hallmarks of any cancer include self-sufficient growth signals, insensitivity to anti-growth signals, limitless replication potential, evasion of apoptosis, continual angiogenesis, and invasion and metastasis (Figure 1) (Hanahan and Weinberg, 2000). Although the mechanisms by which a tumor cell acquires these capabilities may vary, these six alterations nevertheless reflect the intricacy of cancer development. In addressing the first capability, normal cells require growth signals in order to proliferate, while tumor cells have a reduced dependence on such exogenous factors since they produce and respond to their own signals. Such autocrine stimulation obviates the need for growth factors from neighboring cells (Fedi *et*

[1] http://www.cancer.gov/cancertopics/types/breast

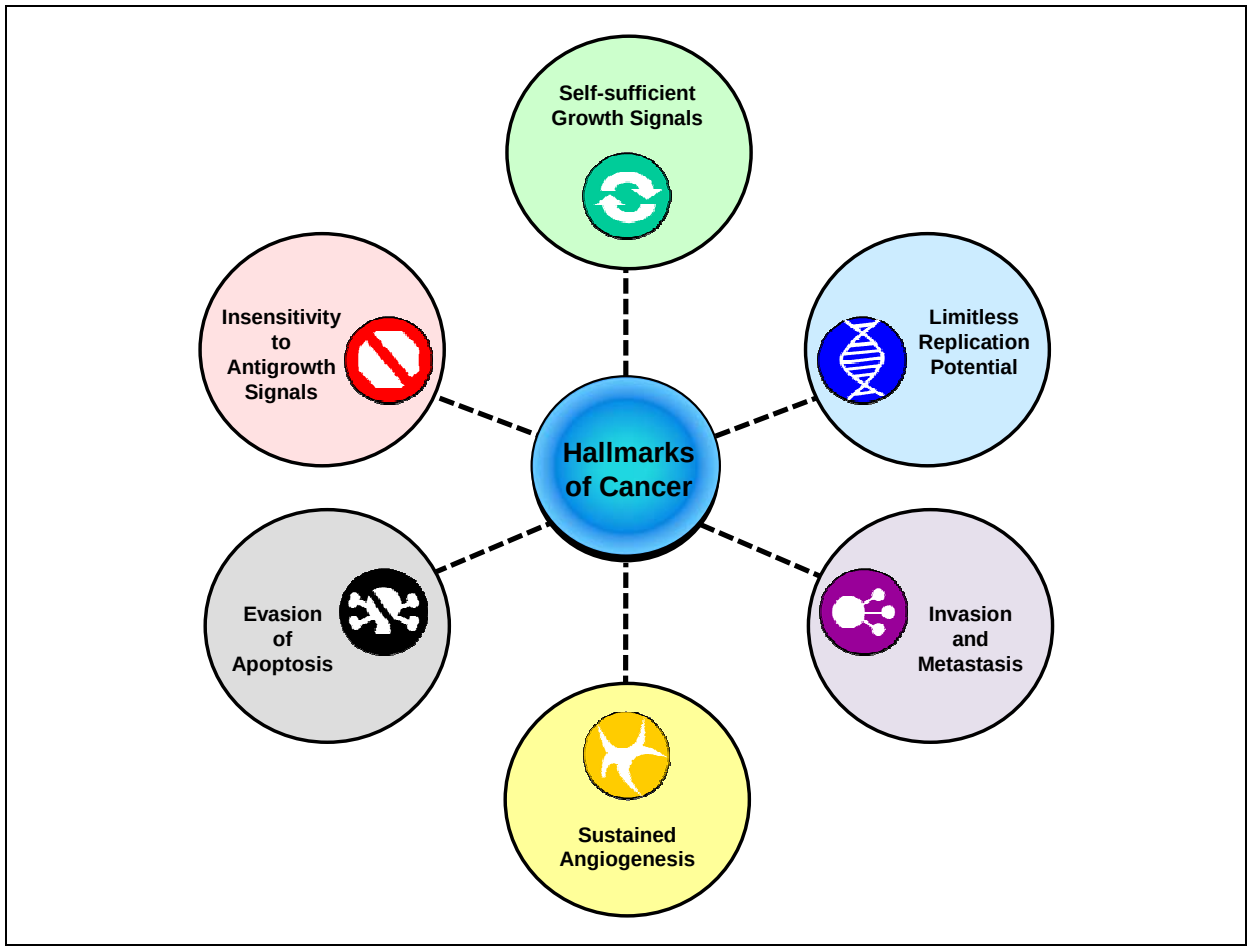

Figure 1: The six hallmarks of cancer. Although the mechanisms by which these characteristics are obtained vary, cancer cells fundamentally are armed with the ability to fulfill these alterations. As a reflection of the complexity and intricacy of cancer development, these hallmarks include self-sufficient growth signals, insensitivity to anti-growth signals, limitless replication potential, evasion of apoptosis, continual angiogenesis, and invasion and metastasis. Adapted from Hanahan and Weinberg, 2000.

al., 2000). However, it is important to realize that contributions from surrounding stroma and other nearby normal cells may also facilitate tumor progression (Weigelt and Bissell, 2008). Additionally, growth factor receptors may be overexpressed in cancer cells, allowing for hypersensitivity to such signals, or may become ligand-independent. For example, the HER2/neu receptor is overexpressed in mammary cancers and associates with aggressiveness while a truncated EGF receptor lacking its cytoplasmic domain remains constitutively active (Kurebayashi, 2001; Wiley, 2003; Khazaie *et al*., 1993). The presence of pro-growth signals is balanced by the action of anti-growth signals. Normal cells respond to growth inhibitory factors by entering quiescence or a postmitotic state, thereby surrendering their proliferative potential (Hanahan and Weinberg, 2000). Mediated mostly by p53, and pRb and its effector TGFβ, anti-growth signaling pathways are disrupted in cancer cells (Weinberg, 1995). This occurs via downregulation or mutation of the TGFβ receptor or detrimental modification of downstream signaling factors, cell cycle inhibitors, or cyclin-CDK complexes (Fynan and Reiss, 1993; Chin *et al*., 1998; Zuo *et al*., 1996). In order to ensure continued cell growth, tumor cells have also acquired the potential to propagate indefinitely. In this state of immortalization, normal growth boundaries are breached in part by maintaining telomere length (Wright and Shay, 2005).

In addition to altered growth properties, cancer cells also have deregulated cell death processes. Evolutionarily conserved, programmed cell death is mainly mediated by death receptors (extrinsic pathway) or the mitochondria (intrinsic pathway), either of which can be dysfunctional in tumor cells (Fulda, 2008). As an example, loss of TRAIL (TNF-related apoptosis inducing ligand) death receptors from the cell surface attenuates TRAIL-induced apoptosis and is associated with TRAIL-resistance in breast cancer cells (Zhang *et al*., 2009; Zhang and Zhang, 2008). Once a tumor has been established with these malignant properties, it

must further ensure survival and increase in size by gaining angiogenic abilities (Hanahan and Folkman, 1996). In breast carcinomas, increased microvascularization was found to be associated with metastasis and poorer prognosis (Weidner *et al*., 1992). Finally, in later stages, cells from the primary tumor acquire the capability to invade adjacent tissues and migrate to other distant sites. This cascade of events is initiated by the escape of tumor cells from the primary mass followed by intravasation, survival in the blood stream, extravasation, and colonization and growth at secondary sites (Mazzocca and Carloni, 2009). For breast cancer, metastases primarily form in the bone, an environment that contains stromal cells with osteolytic properties that facilitate tumor establishment (Suva *et al*., 2009). The effects of invasion and metastasis are ultimately the main factors contributing to cancer mortality, accounting for over 90% of deaths in breast cancer (Bendre *et* al., 2003; Couzin J, 2003; Sporn, 1997).

1.2 Role of p53 in Breast Cancer

One key feature that the hallmarks of cancer share in common is the involvement of the tumor suppressor protein, p53. The p53 signaling pathway is essential in preventing malignant transformation since malfunction of this regulator is the most common alteration in human cancers (Gasco *et al*., 2002). Furthermore, patients with Li-Fraumeni syndrome, in which a germline mutation of p53 exists, are greatly predisposed to tumor development, especially of the breast, brain, and soft tissue sarcomas (Akashi and Koeffler, 1998). Upon cellular stress, activation of this pathway occurs via ATM, ATR, or DNA-PK, all of which act as sensors in the cascade (Figure 2) (McGowan and Russell, 2004). These sensors can then phosphorylate p53 at specific serine residues, releasing it from its normal interaction with MDM2 and stabilizing it. The subsequent increase in p53 levels results in upregulation of $p21^{Waf1/Cip1}$, a cyclin-dependent

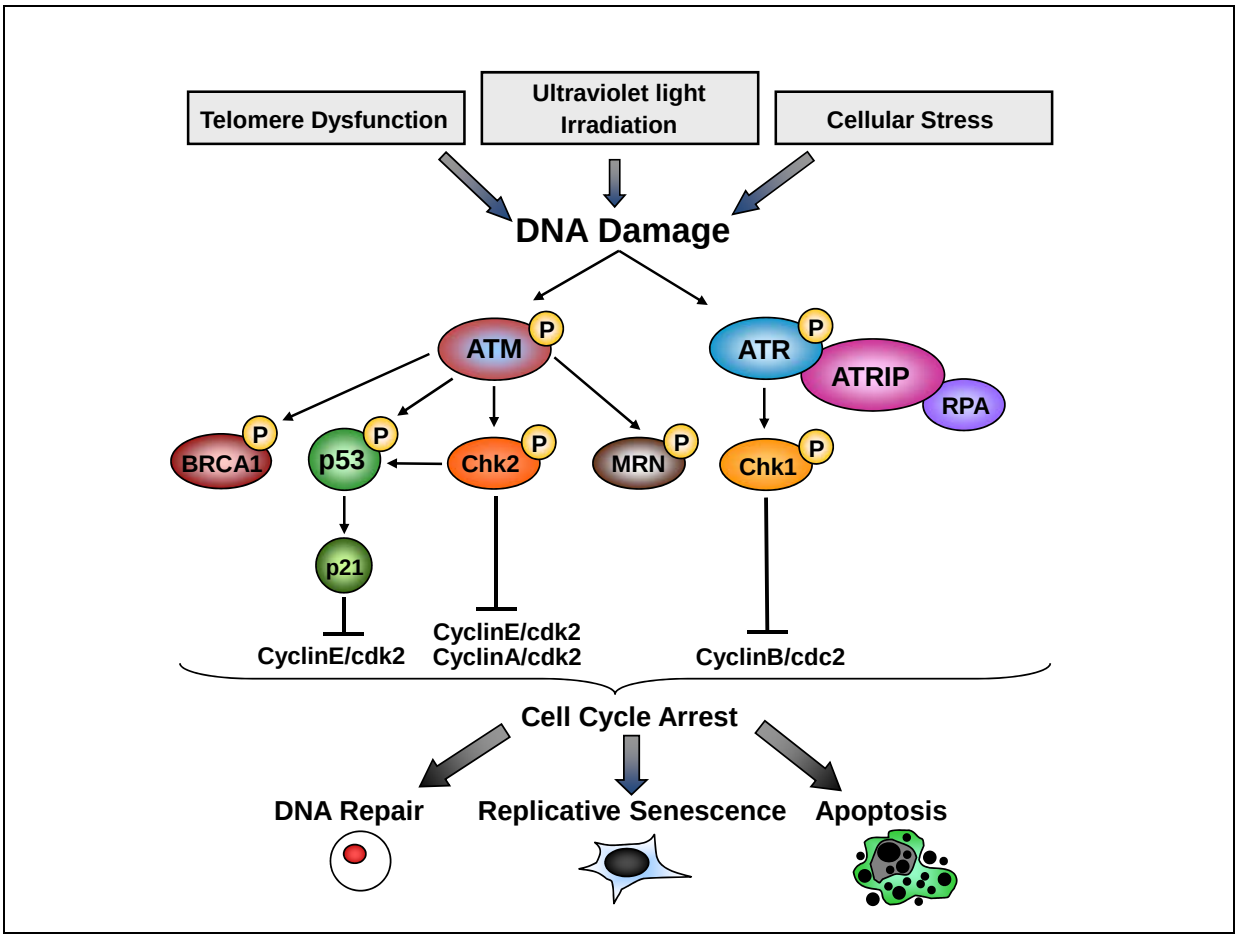

Figure 2: p53 mediates the DNA damage response. A variety of insults can lead to activate checkpoint mechanism and trigger a DNA damage response. Signaling occurs mainly via ATM and ATR, which in turn stimulates a cascade of events, including activation of p53. The culmination of these activities contributes to cell cycle arrest followed by resolution of the damage via DNA repair, or other cellular fates, including senescence and apoptosis. Replicative senescence may have evolved as part of an anti-tumor protective mechanism, whereby bypassing this checkpoint may lead to neoplastic transformation. Apoptosis may have evolved as a mechanism of ensuring survival of only undamaged cells and thus maintaining genomic integrity. Adapted from Diehl *et al*., 2009.

kinase inhibitor that acts to suppress the kinase activity of cyclinE/cdk2 (Bartek and Lukas, 2001). Activation of p53 ultimately triggers its sequence-specific DNA binding to target genes, allowing for their transcription.

The role of p53 has been extensively studied in breast carcinogenesis and it is now known that inactivation of p53 occurs through a variety of mechanisms (Gasco *et al*., 2002). The p53 gene is the most commonly mutated gene, occurring in approximately 50% of all human cancers. Most mutations, about 85%, are missense mutations that generate mutant p53 that lacks the ability to bind target gene DNA in a sequence-specific manner, either through mutation of the codons within this region or alteration of p53 conformation (Wong *et al*., 1999). The mutations in DNA binding domains of p53, but not in non-conserved domains, were found to be associated with more aggressive mammary cancers (Alsner *et al*., 2000). Specifically for breast cancer, coding mutations create somatic changes, but the generation of these mutant p53 proteins occurs only about 20% of the time (Pharoah *et al*., 1999). This percentage increases in patients with concurrent germline mutations in the breast cancer susceptibility genes, BRCA1 and BRCA2 (Greenblatt *et al*., 2001). In addition to mutations of p53 itself, modification of p53 interactors may occur. For instance, reduced protein expression of the upstream kinase, ATM, or of Chk2, which also activates p53, is apparent in sporadic breast cancer (Angele *et al*., 2000; Sullivan *et al*., 2002). The role of $p21^{Waf1/Cip1}$ in modulating breast cancer is less clear, but the general consensus indicates that this CDK inhibitor is associated with poorer prognosis and drug resistance (Abukhdeir and Park, 2008). Finally, p53 inactivation may be due to cytoplasmic sequestration in which wild-type p53 is excluded from the nucleus, thus prohibiting its transcriptional activity (Moll *et al*., 1992).

In all, descriptive and mechanistic studies of p53 have produced abundant data on the

biology and function of wild-type and mutant p53, including the compilation of a growing list of its target genes and protein interactors (Vousden and Lu, 2002).[2] Since its first description in 1979, it is clearly evident that this tumor suppressor protein is involved in the pathways contributing to the classic cancer hallmarks (Lane and Crawford, 1979; Lacroix *et al*., 2006). Upon DNA damage, p53 induces cell cycle arrest to allow for DNA repair or apoptosis when damage is beyond repair, but this process malfunctions when p53 is mutated, thus leading to loss of growth regulation. In this manner, normally latent genes controlling cell proliferation and survival are transcriptionally activated, thus increasing tumorigenic potential. Negative cell cycle regulation by wild-type p53 primarily occurs via $p21^{Waf1/Cip1}$ (CDK inhibitor family member), which, in concert with p16 (member of INK4 family specific to Cdk4 and Cdk6) inhibits cyclin-cdk complexes (Sherr, 1996). These actions thereby prevent phosphorylation (inactivation) of pRb and subsequent G1/S phase cell cycle arrest (Cadwell and Zambetti¸ 2001). Similar to mice that are p21 null, mice deficient in p53 fail to induce $p21^{Waf1/Cip1}$ upon UV exposure and cannot properly arrest (Deng *et al*., 1995). Upon ionizing radiation (IR) exposure, wild-type 53 also frequently induces Gadd45α (growth arrest and DNA damage-inducible), which normally associates with Cdc2/cyclin B1 and exerts control over the G2/M transition (Zhan, 2005). This role is reflected in p53-/- mouse embryonic fibroblasts that show undetectable Gadd45α induction in response to IR (Kastan *et al*., 1992). Along these lines, siRNA-mediated silencing of Gadd45 alleviated the G2/M blockade upon zinc toxicity in normal bronchial epithelial cells and was associated with reduced phosphorylation of p53 (Shih *et al*., 2008).

The process of immortalization also requires the deregulation of growth promoting and inhibiting genes. In general, p53 levels are drastically elevated in transformed cells as compared to normal cells due to increased stability of the protein (Finlay, 1992). In other cases, the lack of

[2] http://www.hprd.org/interactions?hprd_id=01859&isoform_id=01859_1&isoform_name=

functional p53, represented as mutant p53, was found in lymphoid transformed cells and in tumors (Wolf *et al*., 1984; Masuda *et al*., 1987). One study compared mortal and parentally-derived immortal chick embryo fibroblasts (CEF) in terms of p53 and Rb status (Ulrich *et al*., 1992). In this instance, they found that all immortal cell lines demonstrated loss of wild-type p53 RNA expression, without any concurrent change in Rb levels. In another instance, spontaneously immortalized CEFs were found to have abundant p53 mRNA levels, but no corresponding functional activity, as measured by $p21^{Waf1/Cip1}$ levels, was detectable (Christman *et al*., 2006). These data suggest that p53 must be inactivated in order for immortalization to ensue. Since indefinite proliferation requires the maintenance of telomere length, the interaction of telomerase with p53 has also become an area of interest. Telomerase reactivation occurs in approximately 98% of immortal cell lines and in over 90% of invasive breast carcinomas (Kim *et al*., 1994; Herbert *et al*., 2001). In light of this phenomenon, elevated telomerase activity has been found to be loosely associated with p53 expression (Mueller *et al*., 2002).

In addition to cell cycle control, wild-type p53 also modulates the apoptotic response. For example, p53 inactivation leads to a loss of repression of Bcl-2 (anti-apoptotic protein), which subsequently abrogates apoptosis (Cadwell and Zambetti, 2001). Maspin, an inhibitor of angiogenesis that is transcriptionally activated by p53, serially decreases as DCIS progresses to invasive carcinomas and then onto lymph node metastases (Maass *et al*., 2001). All this evidence highlights the essential function of the p53 pathway in maintaining the balance between survival and death.

1.3 Telomere Biology and Function

From initial work with yeast and *Tetrahymena* to the more recent trend of studying

mammalian telomeres, a wealth of information has been amassed on telomere biology and function. The protection provided by chromosome ends is essential for maintaining chromosomal and genomic stability. Telomeres are specialized structures found at the ends of linear chromosomes that are distinct from the remainder of the genomic chromatin in many ways, both structurally and functionally. These nucleoprotein complexes contain non-coding DNA distinguished by the highly conserved 5'-(TTAGGG)-3' sequence in humans. The presence of multiple guanine residues allows the telomere to inherently form G-quadruplex structures under physiological conditions (Rhodes, 2006). The telomeric region consists of an area of double-stranded DNA followed by a stretch of single-stranded DNA to produce a G'-overhang at the 3' end. Telomeres exist in variable lengths among different organisms or cells of different origins. Telomeric DNA is maintained at a defined equilibrium, although repeats vary in number between different chromosomes, and so telomeric length is quite heterogeneous. In mammalian cells, telomere-binding proteins establish this equilibrium (Hemann *et al*., 2000). For instance, the average length ranges from 3 to 20 kb in humans, while inbred strains of mice have been shown to have telomeres as long as 150 kb (Matulić *et al*., 2007).

As dynamic structures, the primary function of telomeres is to provide a capping mechanism, and to this end, telomeres fulfill three such roles (Baykal *et al*., 2004). First, intact telomeres protect natural DNA ends from being recognized as double-stranded breaks and consequently activating a DNA damage response (Deng and Chang, 2007). In other words, telomeres assure that the ends of normal linear chromosomes are not subjected to unwarranted mechanisms of repair. Second, telomeres provide protection from inappropriate exonuclease degradation, and third, telomere structure prevents formation of end-to-end fusions (Deng and Chang, 2007; Bhattacharyya and Lustig, 2006). Normal cells without a capping mechanism are

also vulnerable to recombination due to their highly repetitive sequence (Baykal *et al*., 2004). Other downstream chromosomal instabilities including translocations, non-disjunction, and aneuploidy may occur at later rounds of cell division, which likely contribute to tumorigenesis (Karlseder, 2003). Thus, maintaining telomere integrity and avoiding dysfunction are critical for genomic stability.

A host of telomere binding proteins assure that telomeres do not trigger a DNA damage response, since an unfolded telomere could be sensed as a double strand DNA break (Figure 3). Some of these capping proteins include telomeric repeat binding protein factor 1 and 2 (TRF1 and 2), TIN2 (TRF1-interacting nuclear factor 2), POT1 (protection of telomeres), RAP1 (repressor/activator protein), MRE11 complex, Ku, PTOP/PIP1, and tankyrase 1/2 (Shay and Bacchetti, 1997). These proteins cooperatively establish the telomere loop, or T-loop, in which the single-stranded 3'overhang folds back and invades duplex DNA (de Lange, 2005; Kanoh and Ishikawa, 2003). The region of double strand invasion is referred to as the displacement loop, or D-loop (de Lange, 2005; Neidle and Parkinson, 2003). The existence of apparently evolutionarily conserved T-loops supports the presence of higher-order structure in telomeres (Rhodes, 2006; Neidle and Parkinson, 2003).

Of these telomere binding proteins, six integral proteins, TRF1, TRF2, TIN2, RAP1, TPP1, and POT1, constitute the Shelterin complex. Unlike other telomere-associated proteins, this complex is abundant only at chromosome ends and remains associated at the telomere throughout the cell cycle (de Lange, 2005). Two of the shelterin components, TRF1 and TRF2, contain DNA-binding domains that recognize the double-stranded portion of telomeric DNA, and thus are necessary for the proper formation and stabilization of the T/D-loop (Rhodes, 2006). TRF2 is also found at the junction of duplex DNA invasion, around the D-loop (Wai, 2004).

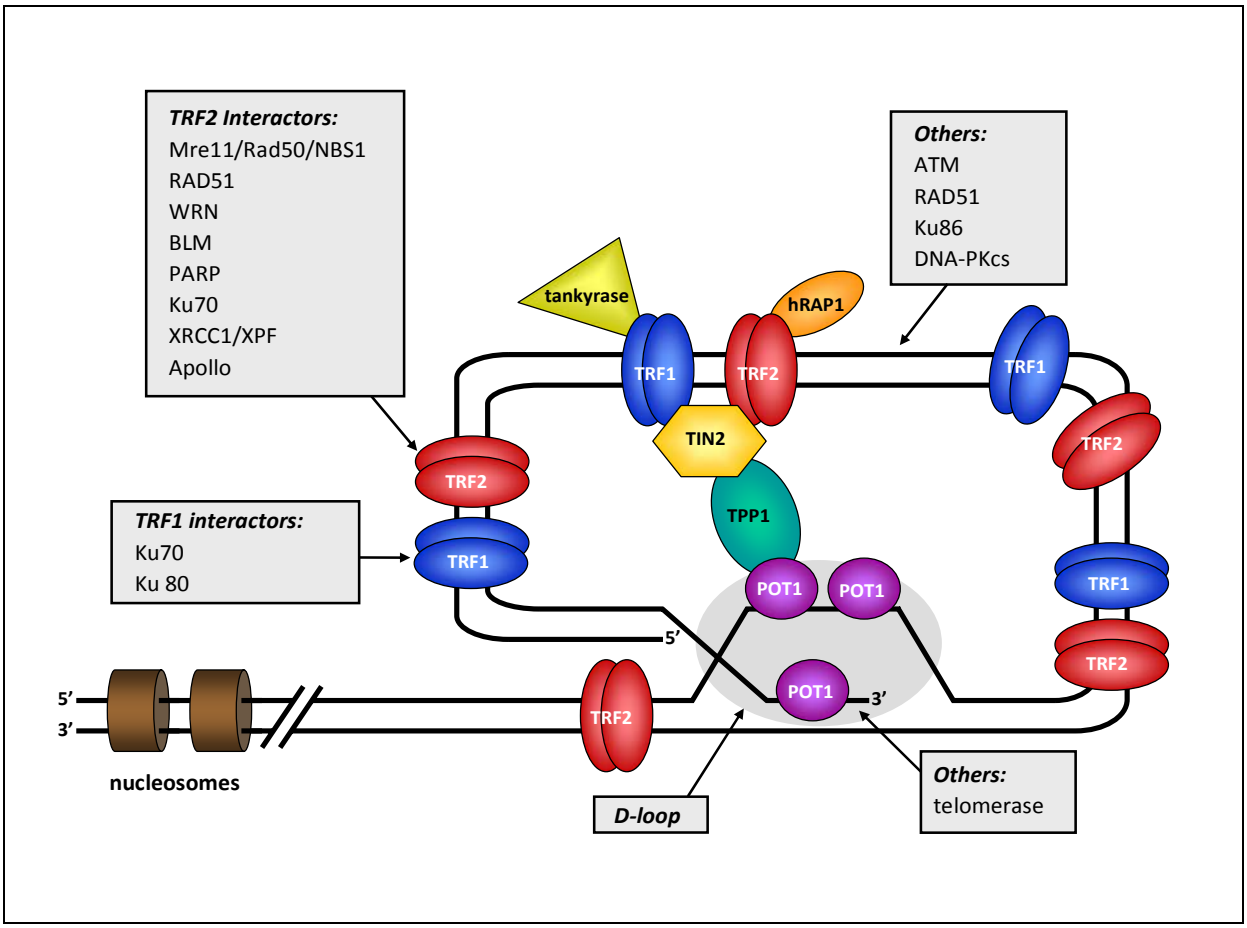

Figure 3: Telomere binding- and associated-proteins localize on the telomeric structure. Formation of the T-loop and D-loop require the assistance of several telomere-binding proteins. Of these, the shelterin complex, consisting of TRF1, TRF2, TIN2, TPP1, RAP1, and POT1, collectively contains five DNA-binding domains (two each in TRF1 and TRF2 and one in POT1), thus making it uniquely suited to recognize telomeric DNA. The role of other telomere associated proteins in homologous recombination or non-homologous end joining implicates DNA damage sensing and repair to be intimately connected to telomere biology. The absence or deficiency in telomere-based or DNA damage and repair proteins may lead to telomere dysfunction and ultimately, genomic instability. Taken from Diehl *et al*., 2009.

These proteins bind as preformed homodimers and are able to form higher order oligomers (de Lange, 2005). Homodimerization of TRF1 and TRF2 is essential to their proper functioning since loss of this ability results in a failure to localize to the telomere (Rhodes, 2006).

Although TRF1 and TRF2 localize to the same region of the telomere, they serve different functions. TRF1 mainly acts as a negative regulator of telomere length, partially through inhibition of telomerase. Overexpression of TRF1 results in gradual telomere shortening, while dominant-negative TRF1 causes elongation in the presence of telomerase (Matulić *et al*., 2007). In contrast, TRF2 has emerged as the major protective factor at chromosome ends, acting as a positive regulator of telomere length (Karlseder, 2003). In support of this role, overexpression of TRF2 results in increased telomere shortening, without an associated increase in replicative senescence rate (Karlseder *et al*., 2002), indicating that TRF2 acts to stabilize and protect shortened telomeres and prevents the induction of senescence. Functional inactivation of TRF2 via a dominant-negative mutant results in a loss of T-loop formation, leading to the production of non-homologous end joining (NHEJ)-mediated end-to-end fusions. These fusions presumably arise from the cell's inability to distinguish natural ends and broken DNA (Karlseder, 2003; Karlseder *et al*., 1999). Additionally, recent data indicate that TRF2 may assume other (non-telomeric) cellular roles. For instance, TRF2 has been implicated in sensing and responding to irradiation-induced non-telomeric interstitial DNA damage (Bradshaw *et al*., 1999). In this context, the interaction of TRF2 with numerous mediators of DNA repair implicates this protein in serving multiple functional roles.

Other factors involved in telomere capping include TIN2 and tankyrase (a poly (ADP-ribose) polymerase), which act as negative and positive regulators of telomere length, respectively (Neidle and Parkinson, 2003). TIN2 is believed to provide a scaffolding unit for

other proteins to dock and modulate TRF1 function (Matulić *et al*., 2007). Tankyrase is required for resolution and complete separation of sister telomeres during mitosis. Tankyrase is recruited by TRF1 to the telomere where it interacts with the acidic N-terminal domain of TRF1 (Kanoh J and Ishikawa, 2003; Hsiao and Smith, 2008). Human RAP1 indirectly binds to the telomere via TRF2 and has been reported to have both negative and positive roles (Matulić *et al*., 2007; Neidle and Parkinson 2003). POT1 specifically binds single-stranded telomeric sequences of both the 3' overhang portion of the telomere and internally displaced regions in order to regulate telomere elongation (de Lange, 2005; Loazya and de Lange, 2003). Loss of POT1 results in loss of telomeric sequences and the appearance of fusions that may solicit a damage response. TPP1 negatively regulates length by interacting with POT1 and TIN2 using different domains (Matulić *et al*., 2007), and in doing so, it apparently holds all the components of the shelterin complex together (de Lange, 2005).

In addition to members of the shelterin complex, the lariat T-loop structure is also associated with proteins involved in DNA repair, DNA processing, and proteins that specifically bind single-stranded DNA. The many DNA repair factors that localize to chromosome ends include ATM, DNA-PKcs, RAD51, Ku70, Ku86, and the RAD50-MRE11-NBS1 complex (Figure 3) (Matulić *et al*., 2007). Furthermore, additional DNA processing enzymes interact at the telomere, including WRN, BLM, ERCC1-XPF1, and Apollo (Matulić *et al*., 2007). Interestingly, the normal localization of these DNA damage and repair proteins does not trigger a DNA damage response or cell cycle arrest (Karlseder, 2003). The fact that these DNA damage response proteins and telomere-binding proteins reside at chromosome ends and their involvement in both telomere maintenance and the damage response suggests interdependency for ensuring genomic integrity (Slijepcevic, 2006; Slijepcevic and Al-Wahiby, 2005). Loss of

any telomere binding or telomere-localized proteins could lead to compromised structure, function, and protective failure. Given that many of these proteins participate in repair mechanisms, the convergence of the coexistence of the DNA damage response and telomere homeostasis has been a subject of great interest. A global picture is emerging that intrinsically implicates repair mechanisms as contributors of telomere maintenance.

Taken together, information about both linear and three-dimensional structure and associated proteins has provided valuable insight into telomere biology and function. The plethora of mediators that aid in preserving this function and the complexity of the telomeric structure indicate that telomere dysfunction is intolerable and must be prevented. Therefore, ensuring the presence of a protected state at chromosome ends is necessary for upholding chromosomal and genomic integrity.

1.4 Maintenance of Telomeres by Telomerase

During normal replication, the discontinuous property of lagging-strand synthesis produces a stretch of unreplicated DNA between the final RNA priming event and the terminus of the chromosome due to DNA polymerase inaccessibility. This phenomenon, termed the "end replication problem", effectively shortens telomeres in somatic cells by 20-200 bases with each round of cell division until a critically short length is reached (Neidle and Parkinson, 2003). The progressive accumulation of short telomeres directs cells with functional tumor suppressors into senescence, characterized as an irreversible G1 growth arrested state (Figure 4) (Feldser *et al*., 2003; Shay *et al*., 1991). In rare cases, immortal and tumor cells are able to spontaneously reactivate the processive ribonucleoprotein enzyme, telomerase, in an attempt to counteract the end replication problem and extend or maintain these shortened ends. This activation leads to the

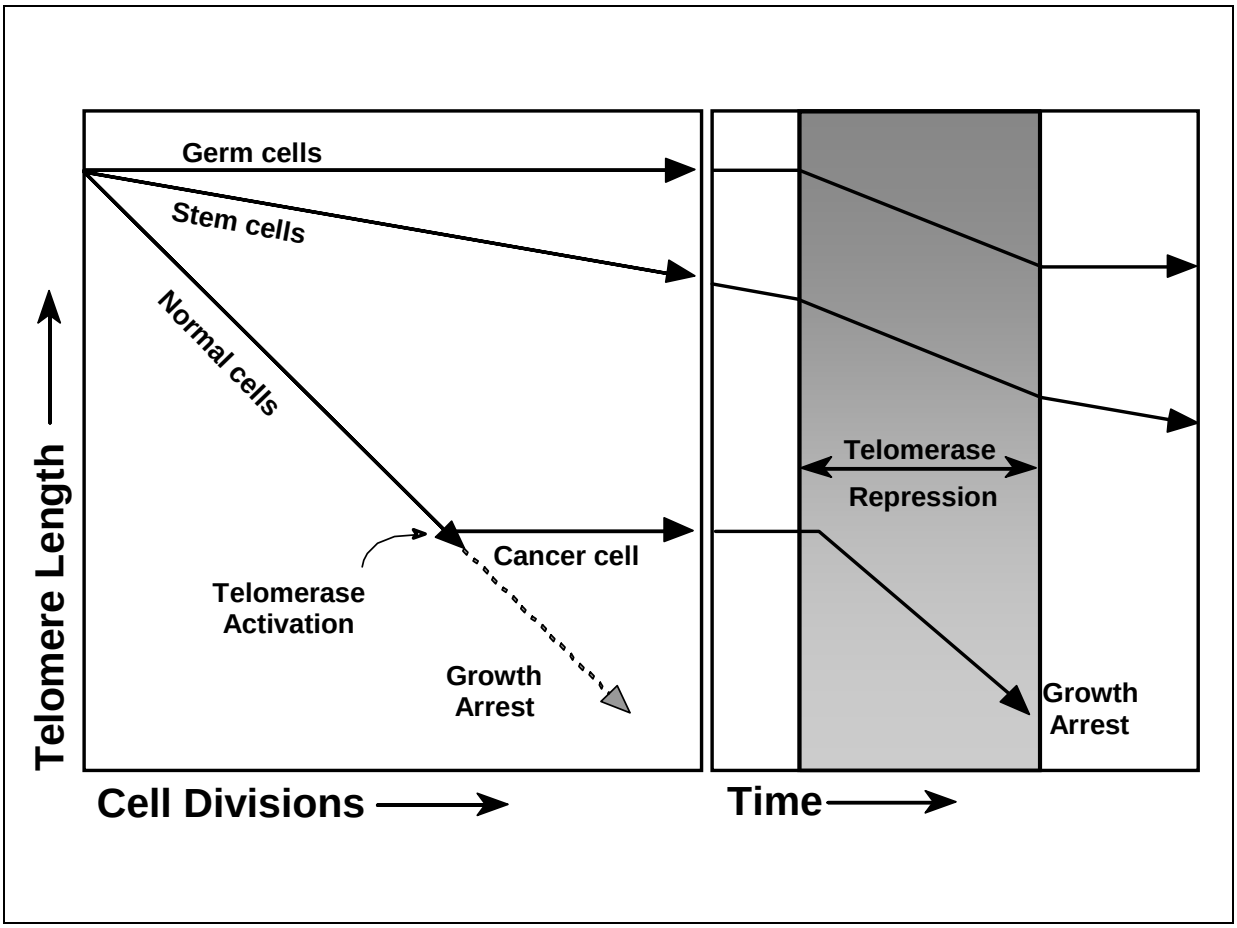

Figure 4: Telomerase reactivation in cancer cells could be therapeutically targeted. Telomerase activity is upregulated in more than 85% of all malignant human cancers, making it a logical therapeutic target and practicable molecular marker for human tumorigenic conversion. Proliferative cells, such as germ and stem cells, normally express telomerase and so maintain telomeres at longer lengths even with many population doublings. The progressive accumulation of short telomeres directs normal cells with functional tumor suppressors into senescence, characterized as an irreversible G1 growth arrested state. In rare cases, a subset of these cells is able to spontaneously reactivate telomerase, in an attempt to counteract the end replication problem. This occurrence leads to immortalization and risk of accumulation of mutations that predispose the cell to tumorigenesis. Continued proliferation and shortening of telomeres in these escaped cells eventually leads to crisis or mortality stage II. Taken from Holt *et al*., 1996.

formation of immortal cells that may accumulate further mutations to predispose the cell to tumorigenesis. Continued proliferation and shortening of telomeres in these escaped cells eventually leads to crisis or mortality stage II (Herbert *et al*., 2001). In contrast, proliferative cells, such as germ and stem cells, normally express telomerase and therefore maintain telomeres at longer lengths even after many population doublings.

First identified in *Tetrahymena* by Greider and Blackburn (Greider and Blackburn, 1985), telomerase consists of an internal RNA template (hTR in humans) that recognizes the single stranded overhang produced as a result of DNA replication and a catalytic reverse transcriptase (hTERT in humans) that uses the template to add on telomeric DNA (Holt *et* al., 1999; Lin and Yan, 2005). As mentioned above, normal somatic human cells lack telomerase activity beyond the developmental period, while tumor, stem, and germ cells have reactivated telomerase activity (Neidle and Parkinson, 2003; Shay and Bacchetti, 1997; Holt and Shay, 1999). Proper telomerase assembly requires the association of various proteins including the heat shock protein 90 multichaperone complex, consisting of Hsp90, p23, Hsp70, p60, and Hsp40/ydj (Holt *et al*., 1999). However, only Hsp90 and p23 have been shown to stably associate with active enzyme (Forsythe *et al*., 2001).

Telomerase activity has been detected in more than 85% of all malignant human cancers, making it a logical therapeutic target and practicable molecular marker for human tumorigenic conversion. For breast cancer, the percentage of tumors with telomerase is closer to 95%, including 75% of *in situ* carcinomas, 88% of ductal and lobular carcinomas, and 5% of adjacent tissue (Carey *et al*., 1998; Shay and Bacchetti, 1997). Furthermore, more severe breast cancers as determined by histologic alterations, tumor size, lymph node status, and staging are associated with increased telomerase activity (Yashima *et al*., 1998; Hoos *et al*., 1998). The telomerase

mRNA transcript (hTERT) is also upregulated in more aggressive breast carcinomas (Bieche *et al*., 2000). However, despite high levels of telomerase activity in cancer cells, telomeres are nevertheless maintained at a relatively short length. In fact, telomere length abnormalities occur early in the initiation of epithelial carcinogenesis (Meeker *et al*., 2004b), for example, in ductal carcinoma *in situ* (DCIS) of the breast (Meeker *et al*., 2004a). The mechanism for shortened, stable telomeres in tumors is likely related to access of telomerase to the telomere, which may be regulated by telomeric structure as determined by the presence of telomere binding proteins (Lei *et al*., 2005).

The association of telomerase with severity in breast cancer has implicated this protein as a potential prognostic marker. In support of this notion, a significant association has been determined between positive telomerase activity and lymphovascular invasion, an important step in breast cancer metastasis and indicator of prognosis (Mokbel *et al*., 2000). Clinical studies have also demonstrated that high telomerase activity correlates with reduced disease-free survival in patients (Clark *et al*., 1997). For these reasons, telomerase inhibition may be an appropriate adjuvant anticancer approach to treating breast cancer. Treatment would be specific since only telomerase-positive (i.e. cancer) cells would be susceptible, thereby limiting toxicity to normal cells. A variety of inhibitors exist, including those that target hTR and hTERT, compounds that stabilize the G-quadruplex, and immunotherapeutics (White *et al*., 2001).

The lack of telomerase reactivation in a small fraction of cancers points to the existence of secondary mechanism of proliferation and survival. Approximately 10% of human tumors, immortalized human cell lines, and telomerase-null mouse cell lines employ the alternative lengthening of telomeres (ALT) pathway (Bryan *et al*., 1997; Niida *et al*., 2000; Reddel and Bryan, 2003). ALT cells display telomere dynamics in which telomeres with various critically

short lengths are targeted and elongated to various lengths, which is suggestive of an inter-telomeric recombination method in mammalian cells (Henson *et al*., 2002). Recombinatorial proteins characteristically found in cells with undetectable telomerase activity, but exhibiting ALT activity, include RAD51, RAD52, MRN, RPA, WRN, and BLM (Henson *et al*., 2002), all of which localize to the telomere. Additionally, poly(ADP-ribose) polymerase (PARP), which binds single and double-stranded breaks and interacts with p53 to modulate base excision repair, may also be involved in ALT since loss of PARP induces an ALT-like telomere phenotype (Tong *et al*., 2001). Moreover, PARP binds with high affinity to TRF2, making the telomere connection to DNA repair even more sound (Neidle and Parkinson, 2003).

1.5 Cellular Fates

When cell cycle checkpoint mechanisms are intact, cells respond to damage by undergoing senescence or apoptosis. In the absence of such checkpoints, cells continue to proliferate leading to increased genomic instability (Callén and Surrallés, 2004). Functional checkpoints ensure cellular integrity by allowing time for the damage to be repaired. In the case of DNA damage, successful DNA repair drives the cells to either undergo checkpoint recovery or adaptation (Bartek and Lukas, 2007). In recovery, progression into M phase is associated with inactivation of Chk1 via the ubiquitin/proteasome-mediated degradation of Claspin and Wee1, a mitosis inhibiting kinase (Bartek and Lukas, 2007), which is closely followed by accumulation of Cdc25A, subsequent activation of Cdc25C, and entry into mitosis. Recovery may be mediated by the removal or dephosphorylation of γH2AX, a phosphorylated histone tightly associated with DNA damage-induced foci (Keogh *et al*., 2006). Adaptation, on the other hand, involves entering mitosis even in the presence of unaddressed checkpoints and unrepaired DNA damage (Harrison

and Haber, 2006). This mechanism is not completely understood and may entail elimination of damaged cells via mitotic catastrophe (Castedo *et al*., 2004). Regardless of the final cellular outcome, it is evident that cell cycle checkpoints ensure that appropriate signals are elicited and transduced in response to DNA damage.

Progressive telomere shortening destabilizes the T-loop structure and predisposes the chromosome to deleterious uncapping events and dysfunction (Griffith *et al*., 1999). Although other forms of senescence exist, loss of protection from telomeres can lead to replicative senescence in which cell growth is irreversibly arrested after a certain amount of population doublings, i.e. once the cell has reached the Hayflick limit (Hayflick and Moorhead, 1961; Hayflick 2000; Shay and Roninson, 2004; von Zglinicki *et al*, 2005). This supports the thought that cellular senescence may have evolved as part of an anti-tumor protective mechanism, and that bypassing this checkpoint leads to neoplastic transformation (Wright and Shay, 1992). In addition to telomere-dependent growth arrest, stress-induced senescence is triggered by DNA damaging agents, such as irradiation, chemicals, and oxidative stress, all generating double-strand breaks, some of which occur at the telomere (Herskind and Rodemann, 2000; Robles and Adami, 1998; von Zglinicki *et al*., 1995). In this way, DNA damage responders can sense aberrations in telomeres and halt proliferation to avoid the accumulation of detrimental mutations (Artandi and Attardi, 2005).

As an alternative to senescence, short unprotected telomeres and DNA or cellular damage may also trigger apoptosis (Matulić *et al*., 2007; Verdun and Karlseder, 2007). p53-dependent apoptosis is mediated by cell cycle checkpoints and the transcriptional activation of DNA repair factors and pro-apoptotic proteins, such as Apaf1 and Bcl-2 (Su, 2006). On the other hand, p53-independent mechanisms of apoptosis also exist. The transcription of the p53 family member,

p73, is stimulated by the transcription factor, E2F1, which is implicated in inducing cell death in the absence of p53 (Irwin *et al*., 2000). In support of the role of p73 in apoptosis, high levels of this protein are found in cells with inactivated pRb (or unrepressed E2F1) as well as cells undergoing malignant transformation (Kaelin, 1999). Furthermore, reactivation of telomerase or inactivation of p53 and pRb (or aberrant expression of p16) allows continued proliferation by bypassing senescence (Karlseder, 2003; Narita *et al*., 2003). In this scenario, cells continue to divide beyond their normal replicative capacity, producing telomeres that lack a protective structure. At this point, the cell enters a crisis stage marked by severe chromosomal instability and cell death (Artandi and Attardi, 2005; Verdun and Karlseder, 2007). Cells that achieve immortalization, most likely via reactivation of telomerase, also display properties of transformation, regardless of whether telomerase is activated (Seger *et al*., 2002). The decision to follow the apoptotic route has most likely evolved as a way to preserve genomic integrity via selective killing of damaged cells (Su, 2006). In summary, cellular responses to DNA damage, including telomeric damage, are triggered by various signals, but ultimately contribute to cell cycle arrest, repair, and replicative senescence or apoptosis.

1.6 Molecular Chaperones, Heat Shock Proteins, and Hsp90

Protein assembly is not a simple, spontaneous process, but rather entails a multistep series that requires assistance from a class of proteins termed molecular chaperones. These proteins have evolved in response to the highly flexible and unstable nature of higher order structures that are held together via non-covalent interactions (Chang, 2009). In aiding in accurate folding, chaperones effectively prohibit improper associations with other proteins as they assist in the maturation of their substrates or clients. Chaperones generally are not

components of the final structure of their clients, but rather associate with substrates in a transient manner. Otherwise referred to as heat shock proteins (HSPs), these proteins were discovered based on their ability to induce a heat shock response upon chemical or physical stress to the cell or a disruption in cellular homeostasis (Lindquist and Craig, 1988; Ritossa, 1962). These stresses include proteotoxic stressors, such as high heat, heavy metals presence, or hypoxia. Although these stimuli trigger dramatic upregulation of HSPs in times of stress, normal conditions also require their assistance in protein folding (or refolding), translocation across membranes, preventing aggregation or self-association, maintaining complexes in an activation competent state, and directing misfolded or otherwise non-functional proteins towards degradation (Figure 5) (Mosser and Morimoto, 2004; Whitesell and Lindquist, 2005). Thus, the presence and action of HSPs is akin to an adaptive response that is needed more during unfavorable conditions to ensure cell survival.

Heat shock protein 90 (Hsp90) is uniquely distinguished from other chaperones since it behaves in the most passive manner. While chaperones like Hsp70 are involved in nascent protein folding, Hsp90 appears to specifically hold client proteins in an intermediate activation-primed state, not just in unfolded states (Mosser and Morimoto, 2004). The Hsp90 family consists of multiple members found in different locations within the cell. The two main cytoplasmic isoforms share 85% sequence identity and include Hsp90α, which is inducible upon cellular stress or shock, and Hsp90β, which is constitutively expressed (Hickey *et al*., 1989). Additionally, GRP94 is mainly found in the endoplasmic reticulum while TRAP1 (TNF receptor-associated protein) is located in the mitochondria (Argon and Simen, 1999; Felts *et al*., 2000). Homologous members in mice include Hsp86 and Hsp84 in mice, Hsp83 in *Drosophila*, Hsc82 and Hsp82 in yeast, and HtpG in bacteria (Young *et al*., 2001). Collectively, they are

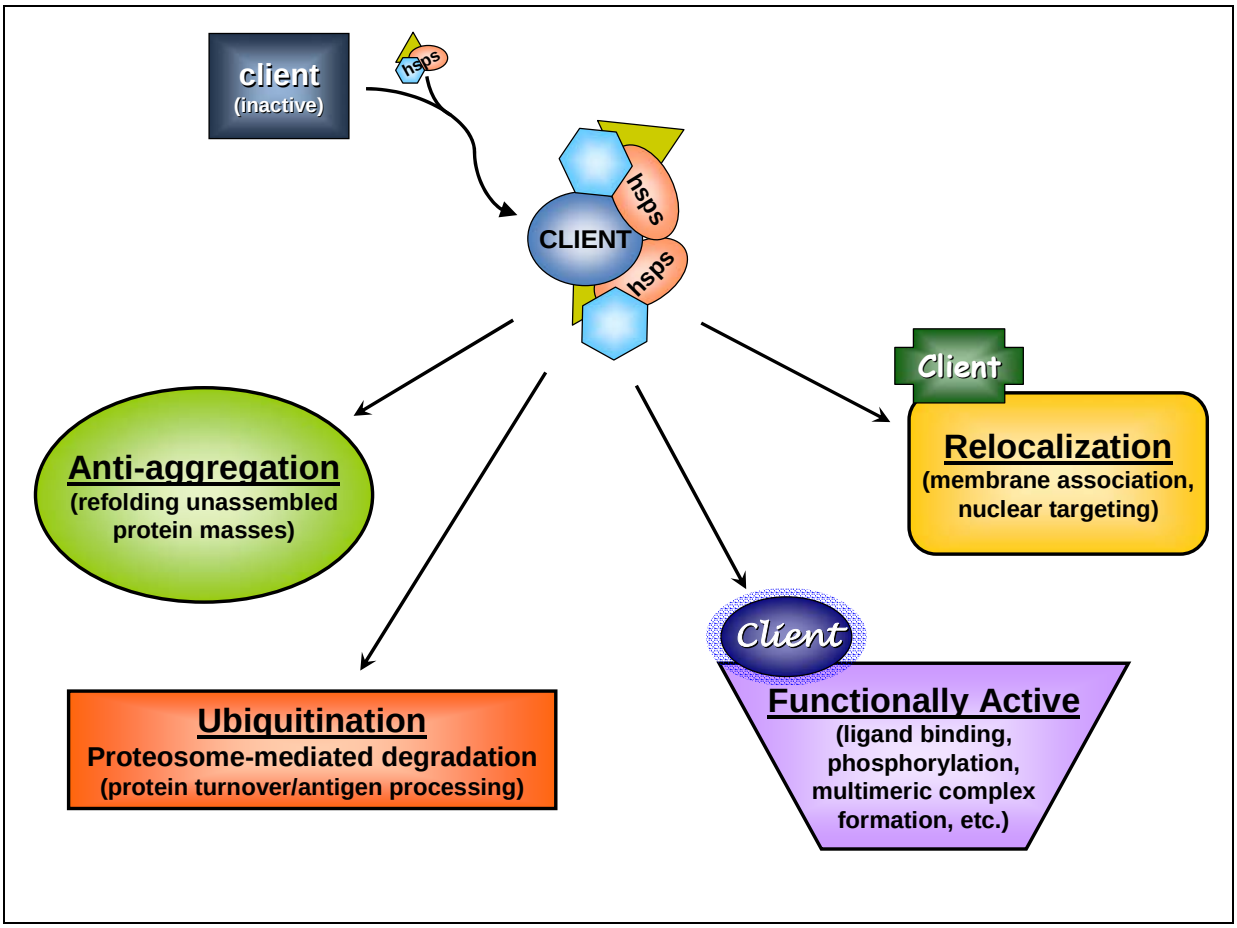

Figure 5: Heat shock proteins have multifunctional responsibilities on client protein maturation. Molecular chaperones such as heat shock proteins aid in accurate folding and maturation of their substrates, effectively prohibiting improper associations with other proteins. HSPs are dramatically upregulated by a variety of chemical and physical stressors, but are also needed under normal conditions. In addition to their assistance in protein folding (or refolding), HSPs also participate in translocation of clientele across membranes, preventing protein aggregation or self-association, maintaining complexes in an activation competent state, and directing misfolded or otherwise non-functional proteins towards degradation.

regarded as ubiquitous, highly conserved proteins that are critically involved in controlling the conformation, stability, function, and degradation of many oncogenic client proteins, thus determining their cellular fate (Beliakoff and Whitesell, 2004; Csermely *et al*., 1998). The essentiality of this protein for cell viability is evident since genetic knockdown of Hsp90 proves to be lethal in eukaryotic cells (Chiosis, 2006). Furthermore, Hsp90 is abundantly found in the cell, comprising 1-2% of total protein content even under non-stressed conditions. In tumor cells, this percentage increases to approximately 4-6% (Chiosis and Neckers, 2006).

Recent advances in determining the structure of Hsp90 has led to important advances in elucidating its function. As shown in Figure 6, the Hsp90 protein consists of three main conserved domains, as this structural arrangement is shared across species (Young *et al*., 2001). Hsp90 exists as an obligate homodimer, whose protomers consists of an N-terminal domain, a middle domain, and a C-terminal dimerization domain (Nemoto *et al*., 1995). The 24-28 kDa N-terminus contains the primary binding site of client proteins and a separate, distinct ATP-binding site. These binding pockets include highly conserved residues, indicating that the specificity between the client and Hsp90 interaction is structure-dependent (Pearl and Prodromou, 2006). Crystallography has also indicated that the N-terminus contains a nucleotide-binding cleft where specific Hsp90 inhibitors bind (Stebbins *et al*., 1997). A shorter linker region tethers the N-terminal domain to the 38-44 kDa middle domain. This linker is highly susceptible to proteolysis and contains charged residues such as Asp, Glu, and Lys (Prodromou and Pearl, 2003). It is possible that the linker regulates Hsp90 function by increasing substrate affinity at the N-terminus and mediating cross-talk between protein and ATP binding (Scheibel *et al*., 1999). However, this linker is not essential for ATPase activity, since its removal still allows for ATP hydrolysis (Meyer *et al*., 2003). Deletion of this linker region has also been shown to cause

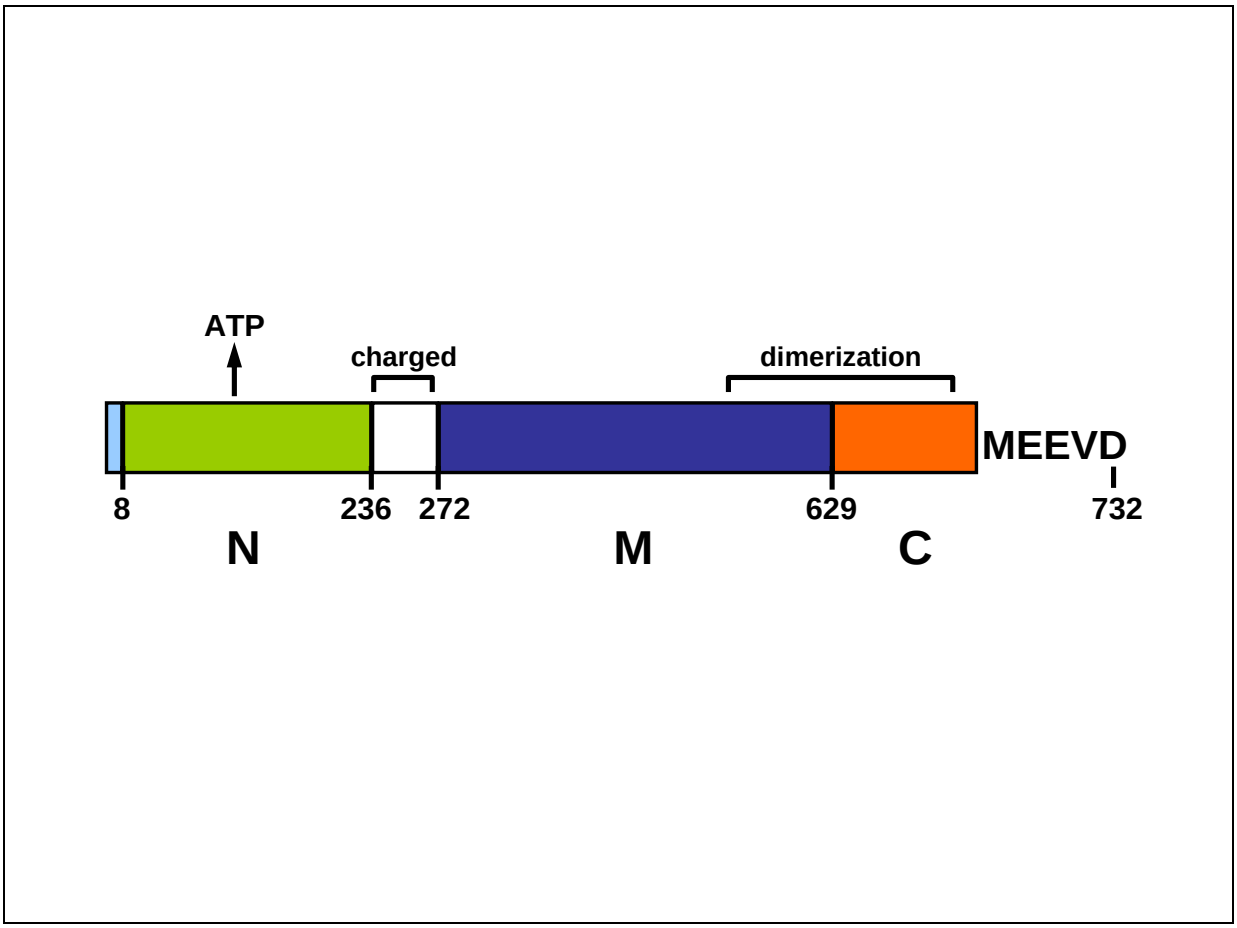

Figure 6: Schematic of the domains of the Hsp90 monomer. Hsp90 is a highly conserved protein that consists of three main domains, of which, the structural arrangement is shared across species. A short linker region tethers the 24-28 kDa ATP-binding N-terminal domain ("N", green) to the flexible 38-44 kDa middle domain ("M", dark blue). This linker is highly susceptible to proteolysis and contains charged residues such as Asp, Glu, and Lys. The final 12 kDa C-terminal domain ("C", orange) contains the obligate dimerization site and contains an MEEVD motif that recruits select co-chaperones that recognize this sequence. Numbers indicate amino acid position. Adapted from Young *et al*., 2001.

defects in the heat shock response and a decrease in Aha1-stimulated ATPase activity and loss of p23 binding, suggesting that this region imparts a regulatory function (Hainzl *et al*., 2009). The flexible 35 kDa middle domain contains a series of α-β-α sandwiches and α-helical coils (Prodromou and Pearl, 2003). Client protein and ATP binding induces a conformational change in structure such that the N-terminal and middle domains act in concert to form a lid that clamps down over the open pocket (Figure 7). This action induces twisting of the middle domains around each other, subsequent transient N-terminal dimerization in Hsp90 protomers, and ATP hydrolysis (Dollins *et al*., 2007). The middle domain also contains a hidden recognition site for nuclear localization signals in the interior of the protein that is activated upon heat shock (Daniel *et al*., 2008). The final 12 kDa C-terminal domain is the obligate dimerization site and contains an MEEVD motif that recruits select co-chaperones that recognize this sequence (Young *et al*., 1998). This domain has also been implicated in binding client proteins and may also contain a secondary ATP binding site, although this is still controversial (Csemerly *et al*., 1998; Young *et al*., 1997; Scheibel *et al*., 1998; Soti *et al*., 2002).

Functionally, the Hsp90 multiprotein machinery assists in cellular trafficking, the remodeling of improperly folded client proteins, and the suppression of protein aggregation (Whitesell and Lindquist, 2005; Sarto *et al*. 2000). This machinery is a cytosolic multiprotein complex that is supplemented with a variety of cochaperones, whose interactions are dependent upon the binding state of ATP. Accordingly, the association of Hsp90 and client proteins behaves in a cyclic manner such that the ADP-bound state is amenable to binding of clientele while the ATP-bound state leads to clientele stabilization and modification (Figure 8). In the initial step, an immature client protein associates with Hsp70, Hsp40, and heat shock organizing protein (HOP) (Hernandez *et al*., 2002). This complex then transfers the client to the open form

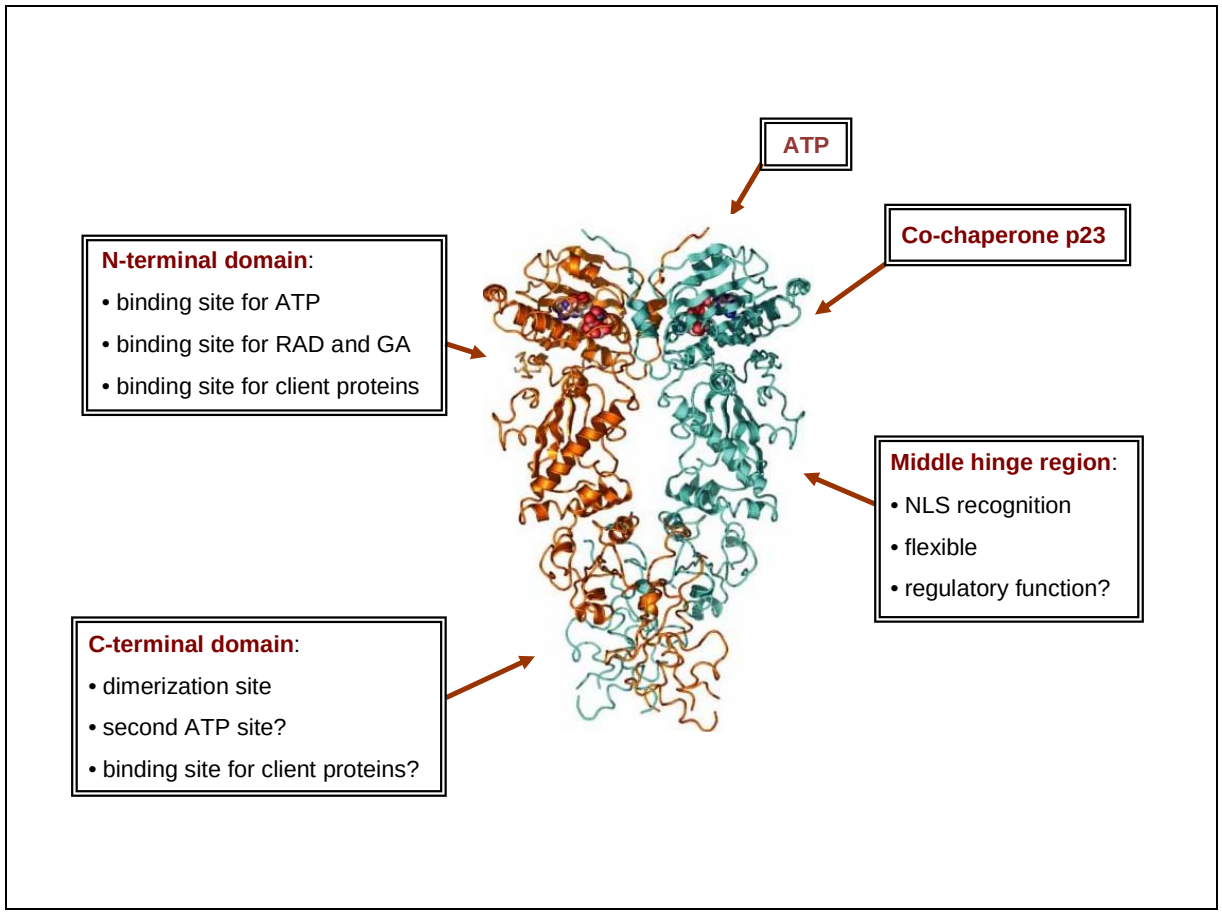

Figure 7: Structure and features of the Hsp90 homodimer. As an obligate homodimer, Hsp90 protomers consists of an N-terminal domain, a middle domain, and a C-terminal dimerization domain. The N-terminus contains the primary binding site of client proteins, and the co-chaperone, p23, and a separate, distinct ATP-binding site. It is also region where Hsp90 inhibitors are targeted. These binding pockets include highly conserved residues, indicating that the specificity between the client and Hsp90 interaction is structure-dependent. The flexible middle domain contains a series of α-β-α sandwiches and α-helical coils that induces a conformational change in Hsp90 structure upon client binding. A region for the recognition of nuclear localization signals (NLS) is located within the interior of the middle domain and is activated upon heat shock. The C-terminus has also been implicated in binding client proteins and may also contain a secondary ATP binding site. Adapted from Pearl and Prodromou, 2006.

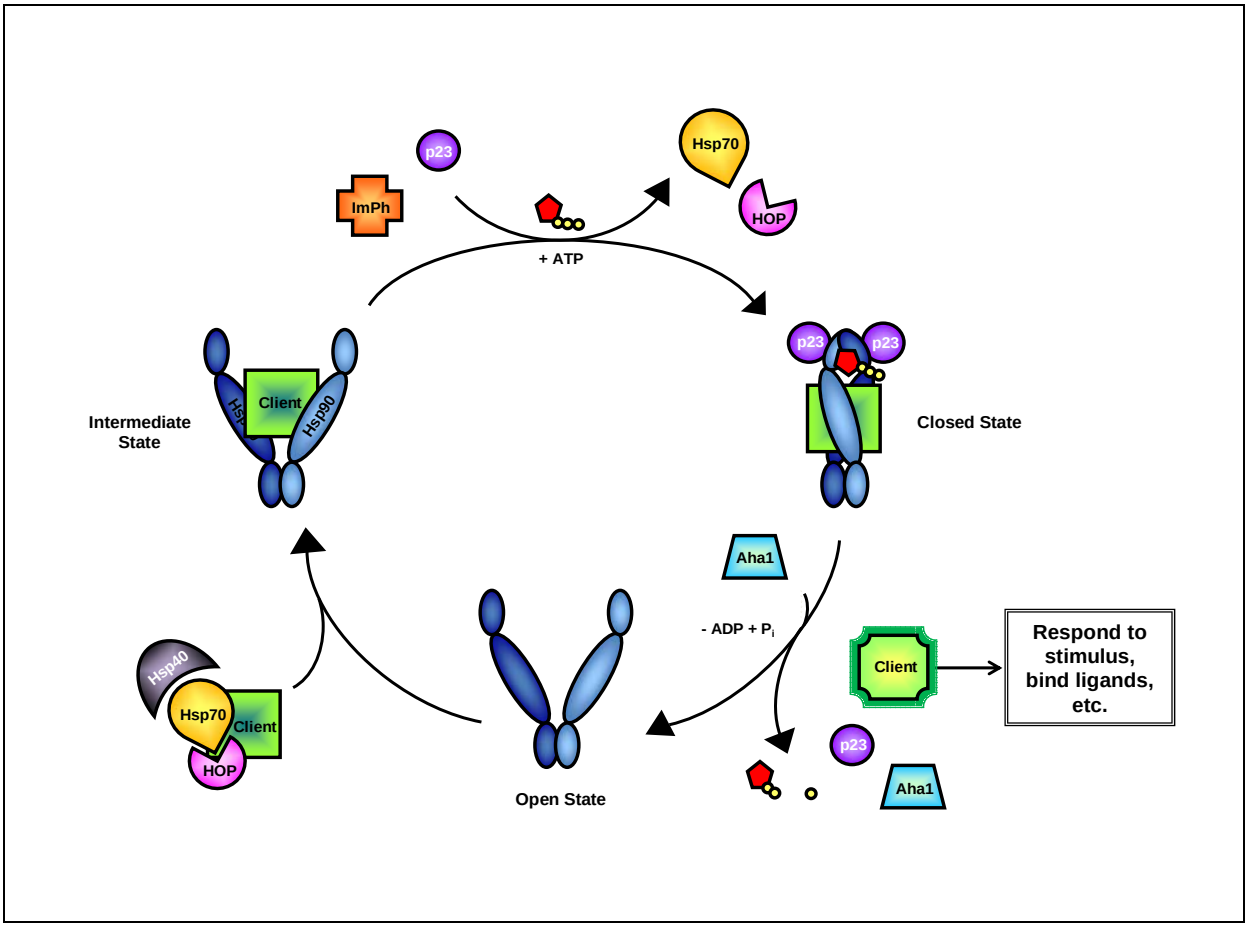

Figure 8: Hsp90 ATP-driven chaperoning cycle. The Hsp90 cycle is supplemented with a multitude of cochaperones, whose interactions are dependent upon the binding state of ATP. Accordingly, the association of Hsp90 and client proteins behaves in a cyclic manner such that the ADP-bound state is amenable to binding of clientele while the ATP-bound state leads to clientele stabilization and modification. An immature client protein initially is presented by Hsp70, Hsp40, and heat shock organizing protein (HOP). This complex then transfers the client to the open form of Hsp90, creating an intermediate chaperone assembly. Following the dissociation of Hsp70/40 and displacement by the introduction of co-chaperones (p23) and immunophilins, the client-bound complex accepts ATP. This triggers N-terminal dimerization of Hsp90 such that the middle domains intersect, resulting in the formation of the closed or clamped state. Upon ATP hydrolysis in the presence of Aha1, a mature client protein is released. Adapted from Bracher and Hartl, 2006.

of Hsp90, creating an intermediate chaperone assembly. Following the dissociation of Hsp70/40 and displacement by the introduction of co-chaperones (p23) and immunophilins, the complex is then able to accept ATP. Binding of ATP triggers N-terminal dimerization of Hsp90 such that the middle domains intersect, resulting in the formation of the closed or clamped state. Upon ATP hydrolysis in the presence of Aha1, a mature client protein is released (Bracher and Hartl, 2006). It is notable from kinetic studies that Hsp90 has a very slow ATPase activity that is dramatically accelerated in the presence of Aha1 (Hessling *et al*., 2008). The ADP generated in this reaction is unfavorable for the closed conformation, which promotes Hsp90 to resume the open conformation. In this manner, client proteins achieve stability, allowing them to bind to ligands or undergo post-translational modifications to activate signaling pathways (Sharp and Workman, 2006).

Regulation of Hsp90 activity occurs through a variety of mechanisms. In one mode, heat shock factor 1 (HSF1) is sequestered by an Hsp90 monomer under basal conditions. Upon stress, client proteins compete with HSF1 for Hsp90 binding and thus displace HSF1, which subsequently timerizes to initiate the heat shock response (Zou *et al*., 1998). Another mechanism of regulation occurs allosterically via the binding of nucleotides (i.e. ATP or ADP) at sites distinct from active sites. These effectors cause a change in conformation in Hsp90, which subsequently affects its activity level (Prodromou *et al*., 1997). On a second level, regulation of Hsp90 ATPase and client binding activities occurs through binding of essential co-chaperones, many of which are chaperones themselves (Riggs *et al*., 2004). Co-chaperones are not considered client proteins, but may impart specificity to Hsp90 by recognizing certain clientele and presenting it to Hsp90 (Caplan, 2003). In addition to client protein selection, co-chaperones aid in other Hsp90 functional aspects, including client protein activation and degradation, Hsp90-

client stabilization, and ATP hydrolysis. Hsp90 enlists the aid of the largest number of co-chaperones, and these can be classified into two broad groups. One type contains a tetratricopeptide (TRP) motif that recognizes the EEVD domain in Hsp90 and includes Hop and immunophilins, while the second type does not contain this domain and includes Cdc37, Aha1, and p23, which is able to act independently of Hsp90 (Buchner, 1999; Freeman and Yamamoto, 2002). The p23 co-chaperone has been studied for its role in breast cancer, although the majority of studies involving p23 focus on the relationship of this protein with steroid hormone receptors. Specifically, overexpression of p23 positively regulates the activity of the estrogen receptor, resulting in enhanced invasiveness of breast cancer cells without an effect on proliferation (Knoblauch and Garabedian, 1999). Furthermore, p23 expression increases accordingly as tumor grade increases (Oxelmark *et al*., 2006). Finally, the third level of regulation involves the reversible covalent modification of Hsp90. Hsp90 has been shown to undergo S-nitrosylation at endothelial nitric oxide synthase (eNOS) specific cysteine residues, resulting in inhibition of ATPase and eNOS activities (Martínez-Ruiz *et al*., 2005).

Currently, Hsp90 has been found to interact with over 200 client proteins and the list is continually expanding.[3] Many client proteins, such as kinases, transcription factors, hormone receptors, and telomerase, undergo post-translational maturation via the Hsp90 chaperone cycle to determine their cellular fate (Csermely, *et al*., 1998; Dai and Whitesell, 2005; Holt and Shay, 1999; Sharp and Workman, 2006). It is notable that Hsp90 seems to selectively associate with cell signaling clientele, such as nuclear hormone receptors and protein kinases (Pratt and Toft, 2003; Brown *et al*., 2007). Furthermore, many Hsp90 client proteins directly influence the six hallmarks of cancer (Figure 9). For example, oncoproteins and proteins involved in cell signaling, such as Akt, HER2, Bcr-Abl, and EGFR, require Hsp90-mediated stability and

[3] http://www.picard.ch/downloads/downloads.htm

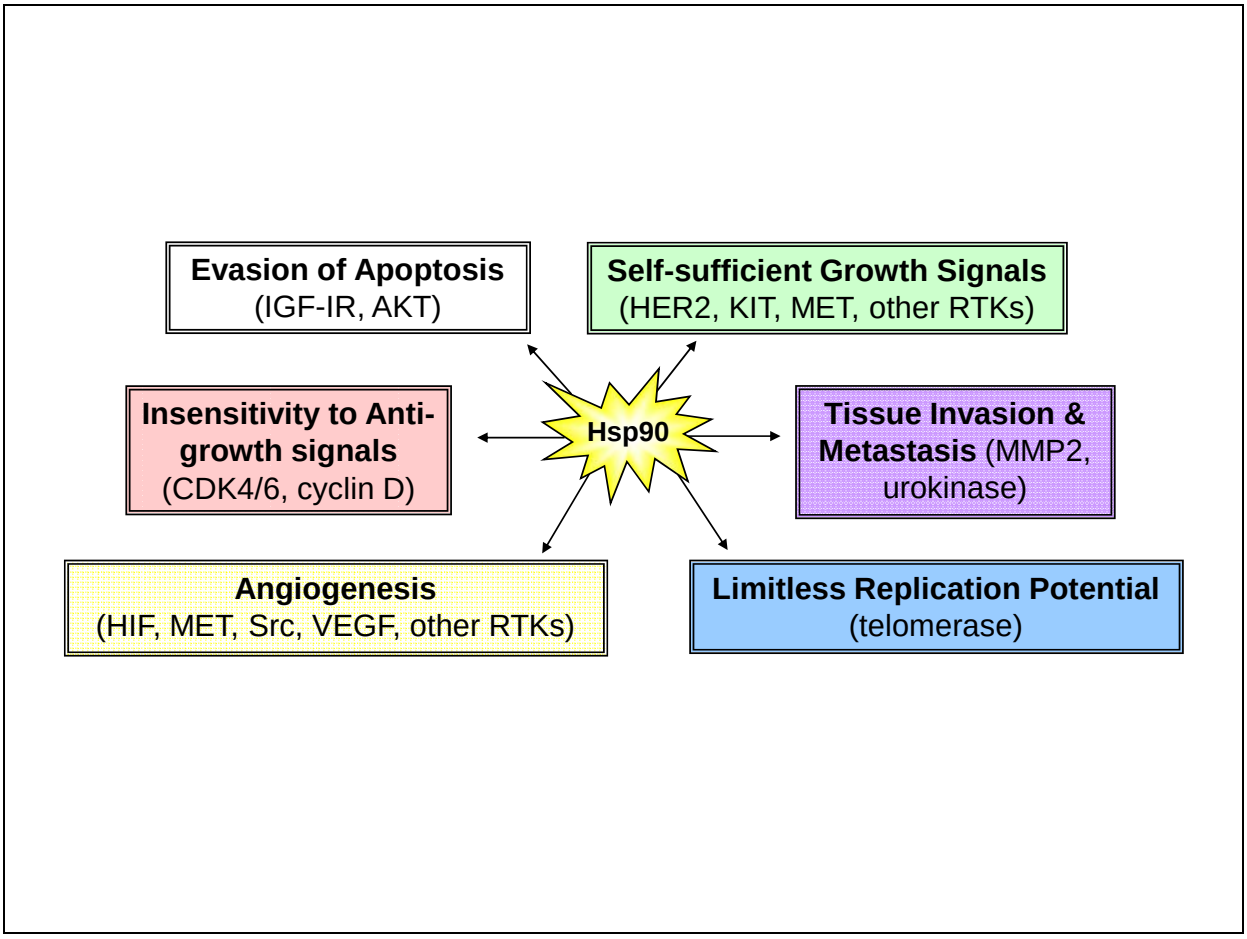

Figure 9: Hsp90 client proteins are involved in the hallmarks of cancer. Currently, Hsp90 has been found to interact with over 200 clientele proteins and the list is continually expanding. Many oncogenic client proteins, such as kinases, transcription factors, hormone receptors, and telomerase, undergo post-translational maturation via the Hsp90 chaperone cycle. Hsp90 seems to particularly associate with cell signaling clientele, such as nuclear hormone receptors and protein kinases. Many of these Hsp90 client proteins directly influence the establishment of the six hallmarks of cancer. The interaction of Hsp90 with these clientele clearly implicates this chaperone in transformation and tumorigenesis. Adapted from Neckers, 2006.

functional activation (Zhang and Burrows, 2004). Thus, the role of Hsp90 in signal transduction inherently implicates this chaperone in transformation and tumorigenesis.

1.7 Hsp90 inhibition

Cancer is clearly not a simple disease, but rather employs the involvement of multiple pathways and a variety of abnormalities. Even when the targeting of a malignant cell is specific and induces less cytotoxicity, non-responsive cells eventually emerge due to their highly plastic and adaptive nature. Hormone-dependent cells become hormone-independent, chemotherapeutic resistance develops, and survival persists even in unfavorable environments (Neckers, 2006). In the face of such obstacles in successful cancer treatment, it may be more effective to assume a multi-nodal approach by simultaneously targeting a common factor. Namely, by blocking the Hsp90 machinery, it is possible to inhibit many of those pathways and mechanisms of survival.

The intrinsic nature of heat shock proteins makes them especially relevant to cellular defense against cancer initiation. Previous studies have reported an overexpression of Hsp90 in human breast cancer; however, only tumor specimens and breast cancer cell lines were examined (Pick *et al*., 2007). The stress-inducible isoform Hsp90α has also been reported to be preferentially increased in cancer tissues compared to non-cancerous tissues (Yano *et al*., 1996, 1999). In addition to significantly elevated total levels in cancer cells, Hsp90 has been found predominantly in a form that is bound to its client proteins, while most normal cells have uncomplexed Hsp90 (Kamal *et al*., 2003; Ferrarini *et al*., 1992). Despite the higher Hsp90 levels in cancer cells, Hsp90 inhibitors negatively affect tumor growth even though only a small fraction of available binding sites are occupied (Banerji *et al*., 2005; Eiseman *et al*., 2005; Vilenchik *et al*., 2004). These observations suggest that Hsp90 in stressful conditions (as in

tumor cells) exists in a highly activated state as a multiprotein complex capable of supporting the transformed phenotype (Chiosis and Neckers, 2006). As a corollary, normal cells must maintain Hsp90 in an inactive state that undergoes more dynamic interactions with client partners. Thus, the balance between activated and latent Hsp90 must be tipped in favor of multichaperone assembly in order for transformation to occur or progress.

The preferential accumulation of Hsp90 in cancer cells also forms the basis for the unique sensitivity of tumor cells to Hsp90 inhibition. In particular, Hsp90 in cancer cells has a higher affinity for anti-Hsp90 compounds compared to that in normal cells, thus providing tumor selectivity via, as yet, an unknown mechanism (Kamal *et al*., 2003). In light of this finding, it is possible that malignant cells are more dependent on Hsp90-mediated stability and activation of oncogenic pathways than normal cells, and so are more sensitive to Hsp90 inhibitors (He *et al*., 2006; Vilenchik *et al*., 2004; Whitesell *et al*., 1992). In addition to its tumor selectivity, Hsp90 inhibitors also act in a specific manner. Since Hsp90 inhibition is tailored against one specific protein, it has been considered a targeted therapy for cancer. Because of the dependence of Hsp90 function on ATP hydrolysis, many Hsp90 inhibitors interfere with this intrinsic activity by binding at the N-terminal ATP site. In this way, Hsp90-dependent client proteins bound at the N-terminus can be tagged for ubiquitination and subsequently directed toward proteasomal degradation (Eleuteri *et* al., 2002; Pearl *et al*., 2008). Thus, Hsp90 inhibition has earned great interest as a promising approach for cancer therapy since many oncogenic client proteins can be simultaneously targeted and disrupted (Goetz *et al*., 2003; Sharp and Workman, 2006).

From the first Hsp90 inhibitor to be discovered and developed, a multitude of derivatives and additional classes of inhibitors have been identified. These inhibitors do not necessarily interfere with binding of client proteins; rather, they prevent their maturation. Two of the most

potent naturally occurring Hsp90 inhibitors identified thus far are geldanamycin and radicicol. Initially discovered in 1970 as an antimicrobial agent, geldanamycin (GA, Figure 10A) is a benzoquinone ansamycin antibiotic that has exhibited antigrowth properties (DeBoer *et al*., 1970). Originally believed to operate via direct inhibition of v-Src, a tyrosine kinase involved in proliferation in tumor cells, GA was later shown to actually bind a 90 kDa protein that directed its activity (Whitesell *et al*., 1994). Although GA binds with higher affinity to Hsp90 than ATP, it displayed high *in vivo* hepatotoxicity in preclinical studies due to the unstable nature of the 17-methoxy group (Supko *et al*., 1995). For this reason, GA analogues were created, of which 17-allylamino, 17-demethoxy geldanamycin (17-AAG, Figure 10B), developed at Kosan Biosciences, showed the most promise. This agent is less hepatotoxic, more stable, and has more inhibitory activity than its parent compound, even in animal models (Schulte and Neckers, 1998b; Pacey *et al*., 2006). For instance, it has demonstrated anticancer activity at nontoxic doses in prostate cancer xenografts as measured by the dose-dependent degradation of androgen receptor, HER2, and Akt expression (Solit *et al*., 2002). As such, it was the first Hsp90 inhibitor to enter clinical trials and has now progressed to phase II trials for melanoma, breast, prostate, and thyroid cancers (Sausville, 2003). The success of this inhibitor is evidenced by the formulation of an injectable version of the drug labeled tanespimycin (KOS-953, Kosan Biosciences), which shows antitumor activity in HER2 (+) metastatic breast cancer, and retaspimycin (IPI-504, Infinity Pharmaceuticals), which is currently undergoing trials for breast cancer (Taldone *et al*., 2008; Modi *et al*., 2007; Sydor *et al*., 2006).

Despite the advantages of 17-AAG, drug solubility remained problematic. To circumvent this issue, the second generation 17-(2-dimethylaminoethyl) amino-17-demethoxygeldanamycin (17-DMAG, Figure 10C) was synthesized and showed greater physiologic solubility (Tian *et al*.,

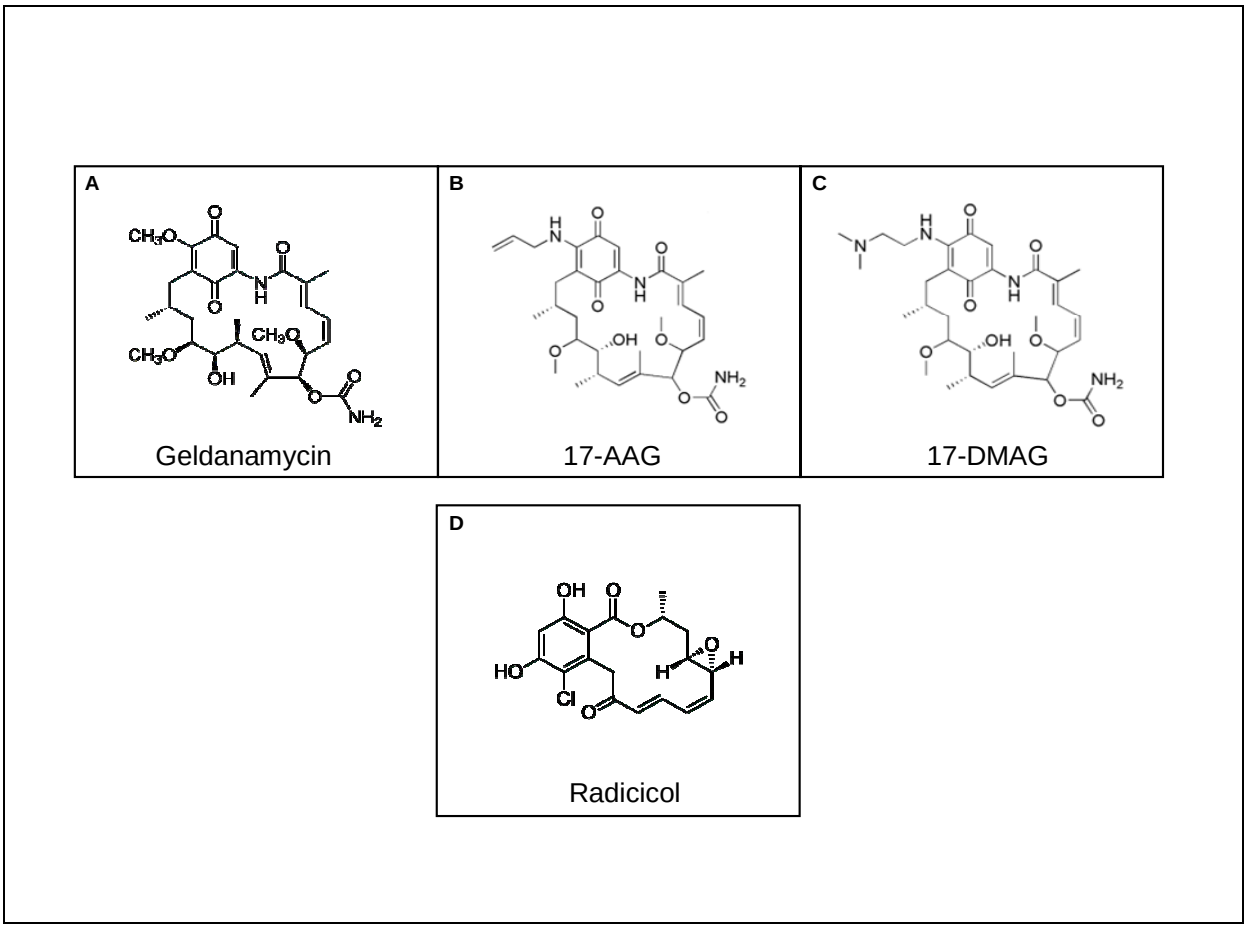

Figure 10: Hsp90 inhibitors. Geldanamycin (A) is a benzoquinone ansamycin antibiotic and radicicol is a non-ansamycin macrocyclic agent, and both have exhibited antigrowth properties. Derivatives of geldanamycin, 17-AAG (B) and 17-DMAG (C), have shown less cytotoxic effects and are currently in clinical trials for a variety of cancers. The radicicol parent compound (D) lacks *in vivo* activity due to its chemical structure, so derivatives have been synthesized that show greater antitumor promise. These Hsp90-specific inhibitors competitively bind at the N-terminal ATP-binding site, effectively blocking Hsp90 chaperoning function.

2004). It has also demonstrated activity in mice with MDA-MB-231 xenografts as evidenced by a greater retention of 17-DMAG in tumor tissue than normal, as well as a reduction in Hsp90 levels (Eiseman *et al*., 2005). Also known as alvespimycin (KOS-1022, Kosan Biosciences), it has entered phase I clinical testing and also shows activity against hormone refractory HER2 (+) metastatic breast cancer (Miller *et al*., 2007). Thus, HER2 is an especially sensitive target of Hsp90 inhibition, undergoing degradation in response to exposure to both 17-AAG and 17-DMAG (Neckers, 2000). A variety of other synthetic GA derivatives with a mixture of side chains and conjugated moieties is reviewed in Hadden *et al*., 2006, but is beyond the scope of this introduction.

Similar to GA, radicicol (RAD, Figure 10D) is also an antifungal antibiotic that was originally identified in *Monosporium bonorden* based on its ability to inhibit growth of mold and bacteria (Delmotte and Delmotte-Plaque, 1953). This non-ansamycin macrocyclic agent was also believed to exert inhibitory effects on v-Src and was later realized to be an Hsp90 inhibitor (Kwon *et al*., 1992b). It is able to revert the transformed phenotype, such that transformed fibroblast cells treated with RAD undergo morphologic changes to resemble normal cells (Kwon *et al*., 1992). Like GA, RAD binds in the N-terminal ATP binding site of Hsp90 and exerts its anticancer effect through inhibition of the Hsp90 machinery. In fact, RAD has a higher affinity for Hsp90 and competes with GA for binding in the N-terminal domain (Schulte *et al*., 1998a). Furthermore, RAD is more potent in terms of blocking ATPase activity and prevents the association of the co-chaperone p23 with Hsp90 (Roe *et al*., 1999). In breast cancer cells, RAD has been shown to affect the level of Hsp90 client proteins (Schulte *et al*., 1998a). Other advantages of RAD include activity in GA-resistant cells and a lack of hepatotoxicity (Chiosis *et al*., 2003; Yamamoto *et al*., 2003). However, RAD lacks *in vivo* activity since its electrophilic

structure undergoes modifications that render it biologically inactive when injected into the bloodstream (Geng *et al*., 2004). Thus, the native RAD molecule is still in preclinical development, but RAD derivatives (KF25706 and KF58333) are showing greater promise since they exhibit antiproliferative abilities while maintaining *in vivo* activity in tumor xenograft models (Soga *et al*., 1999; Soga *et al*., 2001).

In addition to benozquinone ansamycins and radicicol, more recently identified Hsp90 inhibitors include pyrazoles, purines, and novobiocin. All exhibit inhibitory effects on Hsp90 chaperoning function, although their potency and mechanisms vary. Pyrazoles, exemplified by CCT018159, are able to induce Hsp70 expression while reducing levels of client proteins c-raf, Cdk4, and ErbB2 in melanoma cells (Cheung *et al*., 2005; Sharp *et al*., 2003). Treatment with small molecule purines, specifically PU3 and PU24F-Cl, also affects ErbB2, AKT, and c-raf levels in breast cancer cells and in *in vivo* xenograft tumors (Chiosis *et al*. 2002: Vilenchik *et al*., 2004). Coumarin antibiotics such as novobiocin are believed to bind in a secondary ATP binding site located within the C-terminus of Hsp90 (Marcu *et al*., 2000a). Although it also negatively affects ErbB2, c-raf, v-Src, and mutant p53, its action is not as potent as other inhibitors (Marcu *et al*., 2000b; Yun *et al*., 2004). The putative C-terminal ATP site is also the reported binding site for cisplatin, whose presence prevents Hsp90 from interacting with hormone receptors (Itoh *et al*., 1999; Rosenhagen *et al*., 2003). However, no significant effects on client protein levels were detected nor any cellular response, suggesting that cisplatin alone cannot induce anticancer reactions (Sharp and Workman, 2006).

Although the exact mechanism by which inhibition of Hsp90 disrupts the stability of its client proteins is unclear, it most likely involves the ubiquitin-proteasome system. In this pathway, destabilized client proteins are covalently tagged for degradation by the three-step

transfer of multiple ubiquitin molecules from ubiquitin-related enzymes (Marques *et al*., 2006). Ubiquitin is initially bound and activated by ubiquitin-activating enzyme (E1). An ubiquitin-conjugatin enzyme (E2) then transfers this ubiquitin from E1 to the damaged protein, which is sequestered by a ubiquitin-ligase enzyme (E3). The polyubiquitinated protein is then degraded by the 26S proteasome, which entails recognition by the 19S regulatory subunit of the proteasome and subsequent entry into the interior 20S core subunit (Schwartz and Ciechanover, 2009). In the presence of ATP, unfolding of proteins occurs, which leads to proteolysis that produces short polypeptide fragments.

In summary, a vast amount of information has been amassed on Hsp90 biology and function, yet much remains to be elucidated in terms of mechanism. Although Hsp90 has previously been shown to be moderately uninformative on a diagnostic level, it is clear that Hsp90 plays a role in tumor progression and response to therapy. Continuing progress in identifying clientele and understanding Hsp90 inhibition will surely contribute to advancing the global Hsp90 story.

1.8 Current Breast Cancer Therapeutics

While breast cancer patients now have a wide range of therapeutics available to them, occurrence of the disease is still common and treatment challenges still remain. Although many patients initially respond to standard chemotherapeutic regimens, breast tumors may redevelop leading to localized, regional, or distant recurrence that may be more aggressive and resistant to further treatment. Clearly, more effective approaches are needed since conventional therapy is typically associated with partial clinical responses and undesirable side effects, including the destruction of normal non-cancerous surrounding cells. For this reason, there is a great need for

the identification of new therapeutic options that specifically target tumor cells. With the current trend for early breast cancer detection, there is also a growing demand for discovering markers to assist in the risk stratification of patients.

Breast cancer treatments can generally be categorized into groups of surgical intervention, radiotherapy, chemotherapy, hormone therapy, or targeted therapy.[4] Depending on the type and stage of the cancer, different treatment options are more suitable than others. Removal of the lump (lumpectomy) or of the entire breast (mastectomy) are established and appropriate options in less advanced forms of breast cancer (Benson *et al*., 2009). With these procedures, assessment of the resected tissue may be used in a diagnostic as well as therapeutic capacity. Radiation therapy is most successful when combined with surgical options; however, long-term side effects due to off-target effects remain major concerns (Fisher *et al*., 2002). For this reason, two new techniques have been developed to reduce normal tissue toxicity and non-uniform irradiation dosage. Accelerated partial breast irradiation (APBI) refers to a collection of methods that targets the primary region of the affected breast for a shorter duration of time, thus eliminating the need for whole-breast treatment (Van Limbergen and Weltens, 2006). APBI is recommended for patients with smaller tumors and with low risk of developing multifocal recurrence (Van Limbergen and Weltens, 2006). The second technique, intensity modulated radiation therapy (IMRT), addresses dose homogeneity by attempting to improve delivery (Yu *et al*., 2008). Although long-term clinical outcome data is scarce, these methods nevertheless have enhanced the radiotherapy option.

Chemotherapy refers to the range of anti-cancer compounds that are used to treat inoperable breast cancer and either pre- or post-operatively as part of a breast conserving surgery regimen. Since this type of treatment destroys both tumor and normal cells, it is not especially

[4] http://www.mayoclinic.com/health/breast-cancer/DS00328/DSECTION=treatments-and-drugs

selective in killing and is thus associated with significant side effects. By the 1980's, anthracycline antibiotics were developed and continue to be used as first-line treatments or in combinations with other chemotherapeutics (Fisher *et al*., 1989). Specifically, doxorubicin (Adriamycin®) has been a mainstay in the treatment of various solid tumors, including breast, ovary, liver, lung, and soft tissue sarcomas, and has been used as both a single agent and in combination therapies (Figure 11A) (Murphy *et al*., 1995; DeVita *et al*., 1993). A variety of mechanisms of action have been proposed that are based on the ability of this antineoplastic drug to intercalate into DNA and induce apoptosis (Gewirtz, 1999). In this manner, doxorubicin can block macromolecular DNA biosynthesis by inhibiting DNA polymerase (Zunino *et al*., 1975; Gewirtz, 1999). Another mechanism involves free radical formation, in which the electron accepting quinone structure in the presence of electron donors allows for the generation of free radicals, which then cause DNA damage (Feinstein *et al*., 1993). The addition of Adriamycin has also been shown to create drug-DNA adducts in a dose-dependent manner (Cullinane *et al*., 2000). These covalently tethered adducts serve as interstrand cross-links that impart exceptional stabilization in the DNA (Fornari *et al*., 1994). This stability may reflect the drug's preferential binding to GC sites, which contributes to obstruction of duplex strand separation or unwinding and subsequent interference with helicase activity (Bachur *et al*., 1993). Finally, Adriamycin has been shown to exert its activity via the induction of DNA strand breaks due to inhibition of topoisomerase II (Tewey *et al*., 1984). Accepted as the primary target of Adriamycin, this enzyme exhibits reduced or altered activity in Adriamycin-resistant cells that have correspondingly fewer DNA breaks (Son *et al*., 1998).

Despite its frequent application and efficacy in breast cancer treatment, Adriamycin resistance is a major clinical concern. Response rates average between 40-60%, but development

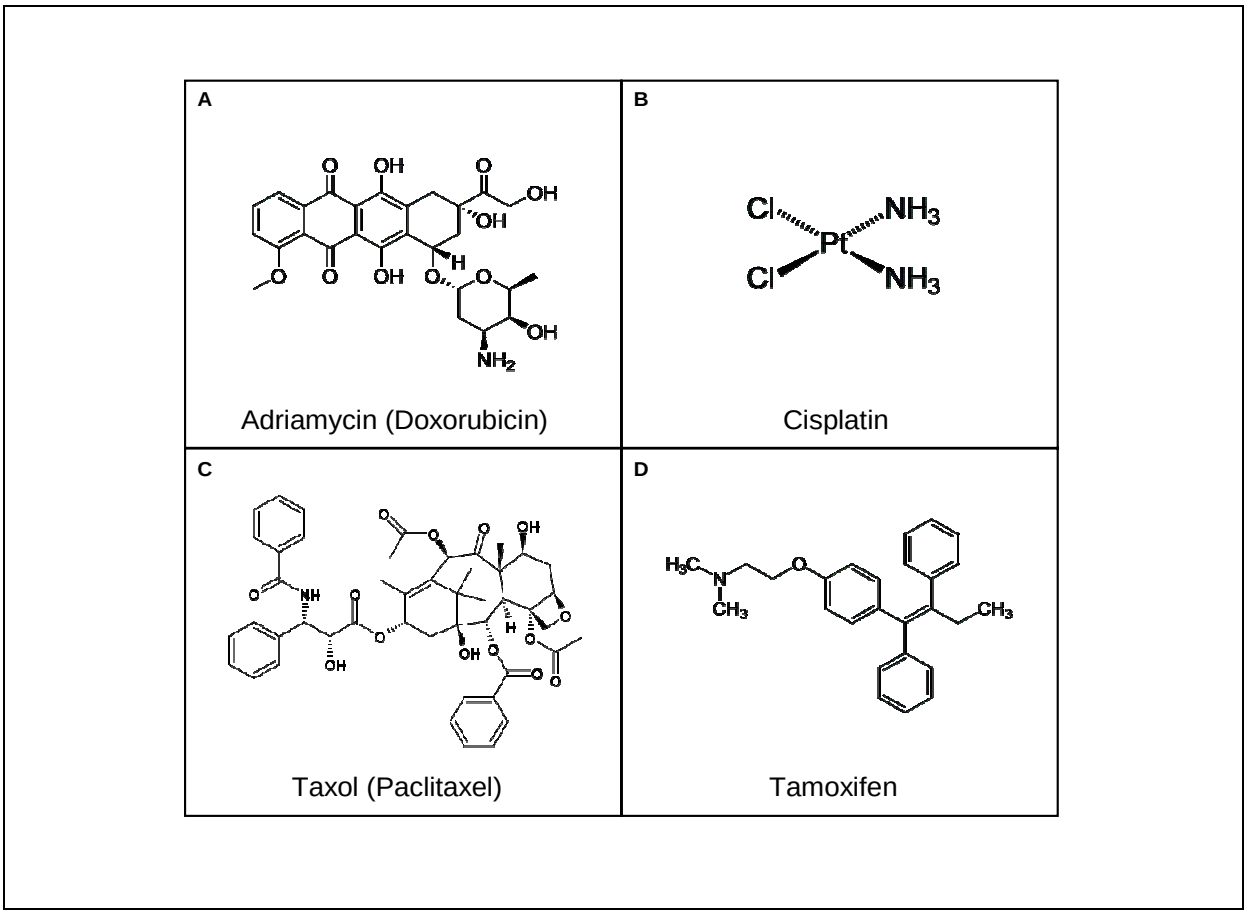

Figure 11: Current anticancer drugs for breast cancer. The chemotherapeutics, Adriamycin (A) and Taxol (C), have been a mainstay in treatment of various cancers. Adriamycin acts as a DNA damaging agent by forming DNA cross-links and inhibiting topoisomerase II, while Taxol acts as a microtubule stabilizing agent. Cisplatin (B) is a novel platinum-based chemotherapeutic that creates DNA adducts which effectively block transcription. Tamoxifen (D) is a selective estrogen receptor modulator (SERM) that antagonizes ER activity. However, its mode of action is limited to those breast cancers that have retained expression of the ER. Resistance is a serious concern for all current therapies, but further advancement in the field of drug development shows promise in overcoming these challenges.

of resistance leads to complete treatment failure (Ta *et al*., 2008). One proposed mechanism of breast cancer resistance towards anthracyclines occurs via the overexpression of plasma membrane transporter proteins, such as breast cancer resistance protein (BCRP), which is expressed at low levels in parental MCF7 cells but higher in MCF7/AdrVp cells that have multidrug resistance (Faneyte *et al*., 2002; Doyle *et al*., 1998). Furthermore, alterations in apoptosis-mediating proteins, such as those in the Bcl-2 pro- and anti-apoptotic family, or in drug targets, such as topoisomerase II, may lead to a resistant phenotype (Pommier *et al*., 2004; Prost, 1995).

Although antitumor drugs like Adriamycin have garnered much attention and use as standard chemotherapeutics, novel platinum-based compounds are rapidly gaining research interest as cancer combatants. Initially described in *E.coli* as a cell division inhibitor in response to an electric current applied to the growth medium, cisplatin (cis-diamminedichloroplatinum (II) or cis-DDP) has exhibited anticancer activity in solid tumors such as those of testicular, ovarian, and advanced breast cancers (Rosenberg *et al*., 1965; Jordan and Carmo-Fonseca, 2000; Muggia, 2009; Martín, 2001). The reactivity of cisplatin is based on its platinum and chlorine containing chemical structure, which is conducive for the formation of DNA adducts (Figure 11B). In an aqueous environment, the chlorine ions are displaced, allowing for amino acid side chains or purine bases within DNA to pair with platinum (Jordan and Carmo-Fonseca, 2000). Subsequently, DNA adducts form, of which intrastrand 1,2-d(GpG) and -d(ApG) cross-links are the most common. This platinum-modified structure creates bends in the DNA which results in the recruitment of high mobility group (HMG) proteins (Gelasco and Lippard, 1998). The presence of HMG proteins shields the adducts from being recognized by nucleotide excision repair (NER) proteins, and consequently, are poorly repaired (Huang *et al*., 1994).

In this manner, the mechanism of action of cisplatin lies in its ability to inhibit transcription and trigger apoptosis. In particular, cisplatin-induced cross-links do not interfere with priming events but block further elongation by RNA polymerase II, resulting in a stalled complex (Corda *et al*., 1991). Since rRNA synthesis is elevated in rapidly proliferating cells like cancer cells, cisplatin may preferentially affect only these cells only (Moss and Stefanovsky, 1995). Furthermore, cisplatin may induce cell death by triggering G2 cell cycle arrest in a p53-dependent manner since p53 deficient cells are less responsive to cisplatin treatment (Allday *et al*., 1995; Anthoney *et al*., 1996). Alternatively, apoptosis may be mediated by a p53-independent pathway, namely that of p73, since cisplatin activates c-Abl, which induces the p73 cascade (Gong *et al*., 1999). Intrinsic cisplatin resistance exists, but advancement of the understanding of the platinum-DNA interaction will aid in overcoming these challenges.

In addition to DNA damaging agents, microtubule stabilizing agents have been successful as chemotherapeutic compounds, especially in the treatment of breast cancer. Namely, by the 1990's, taxanes, including paclitaxel (Taxol®) and docetaxel (Taxotere®), were developed as viable options and are now widely recognized as being extremely active against advanced breast cancer as well as a promising initial line of treatment for early breast cancer (Figure 11C) (Ring and Ellis, 2005). Besides their role in cell division and chromosome separation in mitosis, microtubules are also essential for other cellular activities, including maintenance of cell shape, intracellular transport, and cell signaling (Jordan and Wilson, 2004). As components of the cytoskeleton, microtubules are highly dynamic structures that are characterized by dynamic instability and treadmilling, which refer to processes of tubulin polymerization that is regulated by microtubule-associated proteins (Mitchison and Kirschner, 1984; Honore *et al*., 2005). Electron crystallography has shown that Taxol binds to β-tubulin on the inside of the cylindrical

core, thus preventing polymer disassembly (Downing and Nogales, 1999). In this case, the mechanism of action lies within the ability to stabilize microtubules and effectively block the metaphase to anaphase transition, resulting in apoptosis or mitotic catastrophe (Jordan and Wilson, 2004; Castedo *et al*., 2004).

Similar to anthracyclines, natural and acquired resistance to taxanes is multifaceted and not uncommon (McGrogan *et al*., 2007). Mutations in β-tubulin or changes in β-tubulin isotype composition, alterations in microtubule-associated proteins, or cell cycle anomalies can all contribute to the development of resistant cells (Berrieman *et al*., 2004; Burkhart *et al*., 2001; Goncalves *et al*., 2001; Villeneuve *et al*., 2006). Despite this hurdle, many clinical studies have reported that Taxol in combination with other antimitotics or anthracyclines is more effective and associated with a better outcome (Henderson *et al*., 2003; Jordan and Wilson, 2004). It is clear that rational design of chemotherapeutic combinations will enhance antitumor activity and possibly overcome multidrug resistance.

Since breast cancer initiation and progression are dependent on the production of endocrine factors and sex hormones, hormone or endocrine therapy has also been developed as another therapeutic option. Not only does it regulate reproductive processes in hormone-dependent cancers such as those of the breast or prostate, estrogen participates in the advancement of disease. Three natural forms of estrogen exist, including 17β-estradiol (E_2), which is most predominant and has the highest affinity for its receptors, and estrone (E_1) and estriol (E_3), both of which are estradiol metabolites (Chen *et al*., 2008). Part of the nuclear receptor superfamily, two isoforms of the estrogen receptor (ER) exist, ERα , which is the more prevalent form in breast cancer and promotes proliferation, and ERβ, found mainly in normal breast tissue (Pearce and Jordan, 2004; Herynk and Fuqua, 2004). In the classical pathway of ER

signaling, E2 binds to ligand-binding domains on estrogen receptors in the nucleus while mitogen-actived protein kinase (MAPK)-related growth factors bind in a secondary coactivation domain, in turn triggering receptor dimerization (Shiau *et al*., 1998; Kato *et al*., 1995). This estrogen-ER complex then binds to estrogen response elements within the promoter region of target genes involved in cell growth, stimulating their transcription (Björnström and Sjöberg, 2005).

It has long been known that reducing endogenous estrogen levels can ameliorate the progression of breast cancer. Limiting estrogen production can reduce the frequency of breast cancer emergence as well as induce remission in patients with advanced cancer (Dorssers *et al*., 2001). Furthermore, about 60% of breast cancers are positive for ER and are therefore responsive to estrogen-mediated growth signals (Putti *et al*., 2005). These findings have resulted in the development of a new promising category of chemotherapeutics. Specifically, selective estrogen receptor modulators (SERMs) have gained immense interest for its antitumor and cancer prevention capabilities. The unique quality of SERMs lies in its ability to act as both antagonists and agonists in select tissues. Indeed, SERMs display antagonistic properties in the breast and brain, while they behave agonistically in the bone, liver, and cardiovascular system (Lewis and Jordan, 2005).

One of the most well known and studied SERM is the nonsteroidal ER antagonist, tamoxifen (Figure 11D). The mechanism of action of this drug lies in its ability to interrupt the ER signaling cascade. Tamoxifen serves as a competitive inhibitor of estrogen binding by occupying the normal ligand-binding site on ER and altering its conformation (Shiau *et al*., 1998). Once tamoxifen binds the ER, dimerization of receptors still occurs; however, subsequent transcriptional activation of target genes is obstructed (Lønning and Lien, 1995). Consequently,

inhibition of tumor cell proliferation may occur, as shown by an accumulation of MCF7 cells in G1 phase due to their inability to transition through the cell cycle (Osborne *et al*., 1983). Induction of cell death also occurs since ER(+) MCF7 cells treated with tamoxifen display apoptotic morphology and DNA cleavage at a lower dose and more rapidly than ER(-) MDA-MB231 breast cancer cells (Perry *et al*., 1995). Furthermore, although it lacks activity in a portion of ER-positive cancers, tamoxifen acts as an effective antiestrogen by targeting ERα for degradation in ER-positive breast cancer cells (Wu *et al*., 2009).

Mechanisms of acquired and intrinsic resistance to tamoxifen are not completely elucidated; however, three possibilities have been proposed that address the metabolism of the drug, including alterations in ER, interaction with the tumor environment, and involvement of alternative signaling pathways. In the body, tamoxifen is metabolized into the primary compounds, 4-hydroxy-tamoxifen and N-desmethyl-tamoxifen, followed by secondary metabolism of both into the active metabolite, 4-hydroxy-N-desmethyl-tamoxifen (endoxifen) (Algeciras-Schimnich, *et al*., 2008). If alternative metabolic pathways emerge, tamoxifen may be converted instead into ER agonists and thus stimulate tumor growth (Crewe *et al*., 2002). In the second mechanism, although mutations in ERα are rare, splice variants are more common (Karnik *et al*., 1994; Dowsett *et al*., 1997). Surprisingly, acquired resistance is usually not concurrent with loss of ER expression or ineffective DNA binding to estrogen-response elements (Johnston *et al*., 1995; 1997). Signaling between the tumor mass and neighboring cells may promote tumor progression. For example, high levels of stromal cell-secreted proteolytic factors, such as urokinase-type plasminogen activator (uPA) and its inhibitor PAI-1 are associated with a poorer response to tamoxifen (Meijer-van Gelder ME *et al*., 2004). Finally, phosphorylation of ER by MAPK or Akt, which are activated by the HER-2 receptor, may stimulate tumor

proliferation. Indeed, an inverse correlation exists between Her-2/neu and ER expression, in which patients with high Her-2/neu are less responsive to tamoxifen treatment (Lewis and Jordan, 2005).

As an alternative or possible solution to tamoxifen resistance, another hormonal therapy employing aromatase inhibitors was developed to treat women with ER(+) breast cancer. Aromatase inhibitors (AIs) function by inhibiting the aromatase enzyme responsible for the conversion of androgens into estrogens, thereby reducing physiologic levels of circulating hormone (Pietras, 2006). Unlike tamoxifen, AIs lack agonist activity and so are more effective in this respect as an adjuvant therapy. Current third-generation AIs are extremely potent and selective and show less toxicity as compared to the first-generation drug, and thus are the standard first-line therapy for hormone-dependent metastatic breast cancer (Samphao *et al*., 2009).

In addition to the standard chemo- and hormonal-therapeutics previously described, improved understanding of the molecular events in carcinogenesis has spurned the discovery of targeted therapies for breast cancer. Due to the specific nature of their action, these novel drugs are limited to the subset of tumors that display dependence on the target in question. A key pathogenic feature of breast cancer is the contribution of the epidermal growth factor receptor (EGFR) in disease progression (Normanno *et al*., 2006). The advent of gefitinib (Irresa®) was initially promising, but phase II clinical trials proved that it was ineffective for metastatic breast cancer, even when combined with chemotherapy (Agrawal *et al*., 2005; Ferrer-Soler *et al*., 2007). Currently, trastuzumab (Herceptin®), which targets the HER2/ErbB2 receptor, a member of the epidermal growth factor receptor (EGFR) family, is designated as one of the most well used targeted inhibitors (Di Cosimo and Baselga, 2008). Activation of this tyrosine kinase

receptor leads to stimulation of signaling pathways involved in cellular proliferation, including the Akt, MAPK, and Jak/Stat pathways (Schlessinger, 2004). Overexpression of Her-2/neu occurs in about 30% of breast cancers and is associated with poor survival outcome (Slamon *et al*., 1989; Muller *et al*., 2004). Moreover, elevated Her-2/neu leads to a greater metastatic potential and resistance to p53-mediated apoptosis (Dittmar *et al*., 2002; Huang *et al*., 2002). Lepatinib (Tykerb®) is another targeted therapy that is dually directed towards EGFR and HER2. Treatment with either trastuzumab or lepatinib in combination with chemotherapy in patients with HER2 amplification improves disease-free survival (Slamon *et al*., 2001; Geyer, *et al*., 2006). Although described briefly here, the list of viable targets in scientific and clinical development is continually expanding and will ultimately lead to the advancement of patient-tailored therapies.

1.9 Aims and Rationale for Study

Due to the development of acquired drug resistance with single agents as well as with current combination treatments, there is a need to identify therapeutic regimens able to overcome this limitation. Despite numerous studies in a variety of solid tumors (Becker *et al*., 2004; Kato *et al*., 1995; Kurahashi *et al*., 2005; Ogata *et al*., 2000; Romanucci *et al*., 2006), the roles of Hsp90 and p23 during mammary carcinogenesis and progression and particularly how inhibiting these proteins may influence breast tumor biology remains unclear. Our laboratory has previously shown that in an experimental model for prostate cancer, Hsp90 and p23 are upregulated during malignant progression (Akalin *et al*., 2001). This study was then extended to clinical prostate specimens, in which normal tissue and benign prostatic hyperplasia (BPH)

demonstrate relatively low levels of both Hsp90 and p23 while carcinomas consistently express high levels (Elmore *et al*., 2008).

Based on these studies, we assessed expression levels and cellular localization of Hsp90 and p23 in normal and malignant breast tissues. Although examining Hsp90 expression in cancer cells is not a novel undertaking, current literature lacks comprehensive studies that assess Hsp90 in normal tissue or in stages of breast cancer development, as well as its association to clinical variables. The present study assesses chaperone expression during the advancement of malignancy. We conjectured that chaperone expression would increase according to malignancy in breast tissue, as was observed for prostate specimens. This initial assessment was used to determine whether chaperone expression and localization patterns correlate with stage or advancement of disease.

Based on the positive findings in the first study, it proved necessary to characterize the effects of Hsp90 inhibition in breast cancer cells. This entailed the characterization of this inhibition by pharmacologic methods using the Hsp90 specific drug, radicicol, which specifically targets the essential ATP binding site at the N-terminus of Hsp90 and binds with higher affinity to this pocket than client proteins, effectively blocking its ATPase activity. The rationale behind pharmacologic inhibition is based on the idea that lack of functional Hsp90 may cause telomere erosion and/or dysfunction, leading to apoptosis in breast tumor cells. In addition to the Hsp90 inhibitor alone, various combinations of radicicol with other chemotherapeutics provided insight into the possibility of sensitization of breast cancer cells. Because nonspecific cytotoxicity is associated with these standard regimens, we speculated that inhibiting Hsp90 before initiating conventional therapy would help reduce the amount of exposure, drug dose, or duration of treatment, potentially leading to a better response with fewer side effects. In other words, we

hypothesized that Hsp90 inhibition would be an effective means to sensitize tumor cells to be more responsive to standard treatments. Chemotherapeutic and hormonal drugs used in combination treatments included Adriamycin, Cisplatin, Taxol, and Tamoxifen, all of which are currently used to treat both early and advanced breast cancer. The goal of the following experiments was to define and characterize the consequences of Hsp90 inhibition specifically on cellular proliferation, telomerase stability and function, telomere length, expression of client proteins, and ultimately on senescence or apoptosis in breast cancer cells.

Chapter 2

Materials and Methods

Drug Reagents

Radicicol and cisplatin were purchased from Sigma and solubilized in DMSO (St. Louis, MO). Adriamycin, taxol, and tamoxifen were suspended in DMSO and were kindly provided by Dr. David Gewirtz, Pharmacology and Toxicology, VCU. All drugs were stored at -20^{o}C until ready for use, at which time stock reagents were diluted in culture media.

Cell Culture and Protein Extraction

BJ fibroblasts were cultured in DMEM medium supplemented with 10% cosmic calf serum (HyClone Laboratories, Logan, UT), 0.36% 10x medium 199 (Invitrogen, Carlsbad, CA), and 0.03 mg/ml gentamicin (Invitrogen). Human mammary epithelial MCF10A cells were cultured in DMEM/F12 (Invitrogen) supplemented with 10 μg/ml insulin (Sigma), 0.5 μg/ml hydrocortisone (Sigma), 20 ng/ml EGF (BD Bioscience, San Jose, CA,), 5% horse serum (Invitrogen), 100 ng/ml cholera toxin (Calbiochem, Gibbstown, NJ), and 1% pen/strep (Invitrogen). Breast cancer cell lines, MCF7 (obtained from American Type Culture Collection), MDA-MB 231, and ZR75-1 were grown in RPMI 1640 medium supplemented with 0.03 mg/ml gentamicin (Quality Biologicals, Gaithersburg, MD) and 10% fetal bovine serum (Fisher Scientific, Pittsburgh, PA). All cells were maintained as monolayers and cultured at 37^{o}C in 5% CO_2 and 100% humidity, as previously described (Elmore *et al*., 2002). Upon near confluence or conclusion of drug treatments, cells were washed with 1x phosphate-buffered saline (PBS) and briefly treated with trypsin-EDTA (Invitrogen). Cells were harvested for lysing in a standard

radioimmune precipitation assay buffer (RIPA: 1% Nonidet-P40, 1% sodium deoxycholate, 150mM Tris, 50mM NaCl, 1mM EDTA) and a protease inhibitor cocktail (EMD Chemicals, Gibbstown, NJ). Lysates were cleared by centrifugation at 11,000 rpm for 20 min. Extracted total protein content in the supernatant was quantified using a Lowry-based colorimetric assay (Bio-Rad, Hercules, CA) according to manufacturer's protocol. Li-Fraumeni human mammary epithelial (HME) cell protein lysates were prepared as above and generously provided by Dr. Lauren Gollahon of Texas Tech University (Lubbock, TX).

Western Blot Analysis and Quantitation

A 15 μg (for Hsp90, p23, and β-actin proteins) or 50 μg (for all other proteins) aliquot of total cell protein was separated in a 10% SDS-polyacrylamide gel and transferred onto a nitrocellulose membrane. Standard blotting protocol included blocking of non-specific reactions by incubation in 5% dry milk (Bio-Rad), followed by washing three times for 10 min each in 1x PBS/0.1% Tween 20 and incubation with primary antibody. Antibodies used include anti-Hsp90 monoclonal (recognizes both α and β isoforms), anti-p23 monoclonal, and anti-Hsp70 monoclonal (1:5000, all kindly provided by Dr. David Toft, Mayo Clinic); anti-p53 pantropic (1:1500, Calbiochem); anti-Cip1/WAF1 (1:1500, BD Transduction Laboratories); anti-Cdk4 (1:1500, Santa Cruz Biotechnology, Santa Cruz, CA); anti-Hsp27 (1:1500, Stressgen, Ann Arbor, MI); and anti-c-abl (1:1000, Santa Cruz Biotechnology). Anti-β-actin monoclonal (1:5000, Sigma) antibody was included as a loading control. The membrane was then washed again three times and incubated with horseradish peroxidase-conjugated goat anti-mouse IgG secondary antibody (1:3000, Bio-Rad). Transferred proteins were detected by chemiluminescence reaction (Pierce Super Signal West Pico, Rockford, IL) according to

manufacturer's protocol. Quantitation was performed via densitometry using the ChemiImager 4400 software program (Alpha Innotech, San Leandro, CA).

Design of Tissue Microarrays (TMAs)

Breast tissue arrays were obtained from the National Cancer Institute's Cooperative Breast Cancer Tissue Resource (CBCTR) (http://cbctr.nci.nih.gov). The second generation case sets were created from 679 breast tissue specimens divided into six non-overlapping sets (Figure 12). Each tissue specimen was arrayed in quadruplicate to address possible tissue heterogeneity, such that four cores were taken from each breast tissue specimen, with one core per specimen appearing in each of the four replicate paraffin tissue microarray (TMA) blocks. A collection of these blocks is referred to as a case set. A complete array set, representing the minimum number of cores recommended for an experiment, includes sections from three case sets. We have obtained sections from three individual case sets (#3, #5, and #7). Assembled TMA blocks were cross-sectioned, formalin-fixed, and paraffin-embedded onto slides (one section per slide). Each slide contains between 133-135 cores, including 79-80 invasive breast cancer, 23 normal, and 10-11 ductal carcinoma *in situ* (DCIS) breast specimens. Also included are 21 control cores, with normal spleen arrayed in triplicate, breast cancer cell lines selected based on expression of several mammary cancer-associated proteins, and non-breast specific cell lines. A total of six slides each were stained for Hsp90, p23, and TRF2 (two slides each from three case sets). One slide from case set #3 served as a PBS negative control, in which no primary antibody was applied, yet was processed in exactly the same manner as the experimental slides. Relevant clinical data provided for each case included age at diagnosis, estrogen receptor (ER) and progesterone receptor (PR) status, and tumor-node-metastasis (TNM) stage.

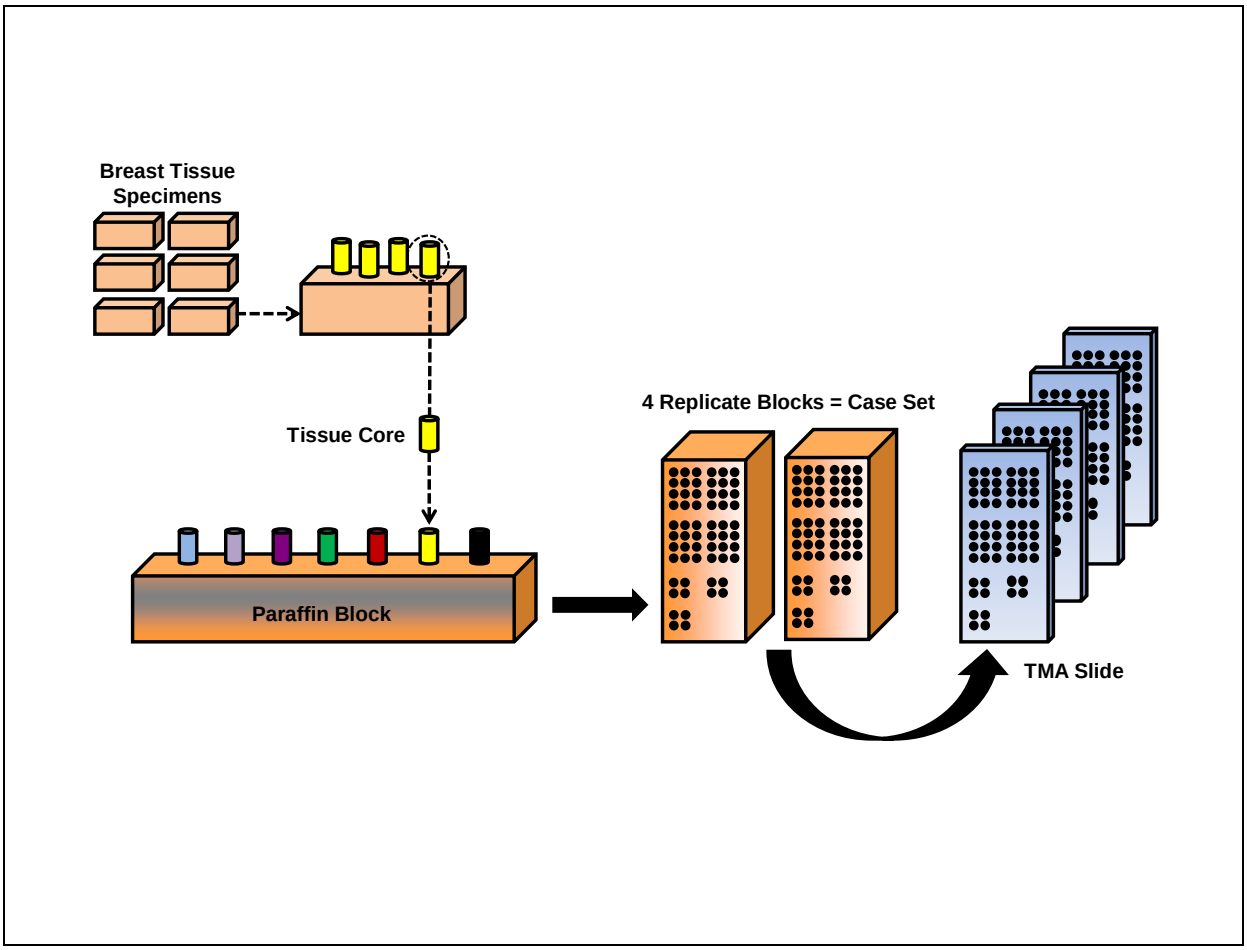

Figure 12: Design of Tissue Microarrays. Second generation breast tissue arrays were obtained from the National Cancer Institute's Cooperative Breast Cancer Tissue Resource. Each tissue specimen was arrayed in quadruplicate to address possible tissue heterogeneity, with one core per specimen appearing in each of the four replicate paraffin tissue microarray (TMA) blocks. A collection of these blocks is referred to as a case set. A complete array set, representing the minimum number of cores recommended for an experiment, includes sections from three case sets. Sections were sliced from each paraffin block and embedded onto slides.

Immunohistochemistry (IHC) / Immunocytochemistry (ICC)

A standard immunohistochemical staining procedure (Akalin *et al* 2001) was used to detect Hsp90 and p23 in breast tissue arrays. A VectaStain ABC immunoperoxidase IgG detection kit (Vector Labs, Burlingame, CA) was used according to the manufacturer's recommendations, using diaminobenzidine (Vector Labs) as the substrate. Slides were deparaffinized in CitriSolv (Fisher Scientific), rehydrated in graded ethanol series, and steamed for antigen retrieval in a modified citrate buffer (pH 6.1) (Dako Cytomation, Carpinteria, CA). Endogenous peroxidase activity was quenched, followed by blocking in horse serum, overnight incubation with primary Hsp90 or p23 antibody (provided by Dr. David Toft, Mayo Clinic) or primary TRF2 antibody (Upstate, Charlottesville, VA), 1 hr incubation with biotinylated secondary antibody, 30 min incubation with avidin-biotin complex, and 10 min incubation with DAB substrate. Slides were then lightly counterstained with Gill's Hematoxylin (Poly Scientific, Bay Shore, NY) prior to dehydration in increasing ethanol gradients, clearing, and permanent mounting with Permount (Fisher Scientific).

Immunoprecipitation

Sub-confluent untreated cells were harvested and lysed as described above. A 100 μg or 300 μg aliquot of lysate was precleared with protein G agarose (Roche, Indianapolis, IN) or protein L agarose (Santa Cruz Biotechnology) beads, respectively. Following primary antibody incubation with complexed Hsp90 (Stressgen, SPA-845) or uncomplexed Hsp90 (Stressgen, SPA-830) for 2 hr, prewashed protein G (for uncomplexed Hsp90) or L (for complexed Hsp90) beads were added to the sample and agitated overnight. Bead-protein mixtures were spun down and supernatant collected as the unbound fraction. Bead-bound fraction was washed three times with

TRAP lysis buffer (0.1% Nonidet-P40, 1 M Tris-Cl pH 7.5, 0.5 M KCl, 1 M $MgCl_2$, 1 M dithiothreitol, 20% glycerol). All samples were heat denatured at 95^{o}C for 10 min and bead-bound fraction was briefly spun down prior to being electrophoresed on a 10% SDS-polyacrylamide gel.

Drug Treatments

To determine the optimal RAD concentration to use for chronic drug studies, approximately 1 x 10^5 MCF7 cells were plated in 6-well dishes. The next day, cells were treated with a range of RAD concentrations including 0.01 μM, 0.03 μM, 0.1 μM, 0.3 μM, 1 μM, 3 μM, and 10 μM for 4 hr, 24 hr, or 48 hr. For chronic drug treatments, approximately 5 x 10^5 MCF7 cells were plated in 100 cm^2 dishes or 5 x 10^4 cells were plated in 6-well dishes. The next day, cells were either not treated (Adr only cells) or treated with 0.03 μM RAD for 48 hr (for RAD+Adr cells), followed by acute treatment for all cells with Adr for 2 hr. The range of Adr used included 0.0075 μM, 0.025 μM, 0.075 μM, 0.25 μM, and 0.75 μM. For combination treatments with CIS and TAX, cells were either not treated (for CIS or TAX only cells) or treated with 0.03 μM RAD (for RAD+CIS or RAD+TAX cells) for 48 hr beginning the day after original plating. All cells were then washed with 1x PBS, and treated with either 0.1 μM CIS or 100 nM TAX, respectively, for 24 hr. For combination treatments with TAM, all cells were treated with 1 μM TAM for 24 hr beginning the day after original plating. The next day, cells were either not treated (TAM+Adr only cells) or treated with RAD (TAM+RAD+Adr cells) for 48 hr. This was followed by acute treatment with Adr for 2 hr. The concentrations of Adr used included 0.075 μM and 0.75 μM. Upon completion of treatments for each drug series, cells were washed with 1x PBS (Invitrogen) and fresh media was added.

Cell Growth Assays

MCF7 cells were plated and treated with various drug combinations as described above. At the conclusion of each treatment period, cells were washed once in 1x PBS and harvested using trypsin-EDTA (Invitrogen). Cell growth was measured by counting in triplicate using a hemocytometer (Hausser Scientific, Horsham, PA). Population doubling was calculated using the formula $[\log_{10}(\text{cell count post treatment/original cell count})]/0.3$.

Telomere Repeat Amplification Protocol (TRAP) Assay

After drug treatment, telomerase activity was measured using the TRAPeze® telomerase detection kit (Chemicon/Millipore, Billerica, MA) according to the manufacturer's recommendations, as previously described (Forsythe *et al*., 2001). Each 100,000 cell sample was lysed in 1x CHAPS lysis buffer (Chemicon/Millipore) with protease inhibitor cocktail (EMD Chemicals). TS primer was labeled with [γ-^{32}P]ATP (Perkin Elmer, Boston, MA) for 30 min, followed by telomerase-mediated extension incubation with cell extract equivalent to 1000 cells for 25 min. Extended products were then amplified by PCR via a two-step process (94°C for 30 s, 60°C for 30 s) for 27 cycles. Amplified products were separated on a 10% polyacrylamide gel, which was subsequently fixed and exposed to a PhosphorImager screen (Molecular Dynamics, Sunnyvale, CA) overnight. Relative telomerase activity was quantified using ImageQuant 5.2 software (Molecular Dynamics) by determining the ratio of the sample telomerase ladder activity to the standard internal 36 bp ladder.

Terminal Restriction Fragment (TRF) Assay

Telomere length was determined via the terminal restriction fragment (TRF) assay. Genomic

DNA was isolated from cells using Blood and Cell Culture Midi Kit and columns (Qiagen, Santa Clarita, CA) according to manufacturer's instructions. Following quantitation using the NanoDrop 100 Spectrophotomer (Thermo Scientific, Waltham, MA), 8-10 μg of DNA was digested with a mixture of *Alu*I, *Hae*III, *Hinf*I, *Msp*I, and *Rsa*I restriction enzymes (New England BioLabs, Ipswich, MA) for 4 hr and resolved on a 0.7% agarose gel that included a 1 kb (Invitrogen) and *Hind*III DNA digest ladder (New England Biolabs). These ladders, as well as a G-rich telomere specific $(TTAGGG)_4$ probe (IDT, San Diego, CA), were labeled with [γ-^{32}P]ATP for 30 min at 37^{o}C. Unincorporated radioactive ATP was removed using the QIAquick nucleotide removal kit (Qiagen). The gel was then denatured in 1.5 M NaCl, 0.5 M NaOH for 30 min, dried until thin (Gel Dryer 583, BioRad), and neutralized in 1.5 M NaCl, 0.5 M Tris for 15 min. Following this series, the dried gel was hybridized with labeled probe overnight, washed at least three times in 0.1X SSC, 0.1% SDS, and exposed on a PhosphorImager cassette (Molecular Dynamics) overnight.

Senescence associated β-Galactosidase Staining and Quantitation

MCF7 cells were plated in 6-well dishes and treated with RAD alone or RAD and Adr. At 4 d post-treatment, cells were washed twice in 1x PBS, followed by fixation in 2% formaldehyde, 0.2% glutaraldehyde for 5 min at room temperature. After washing twice in PBS, cells were incubated for 4 h in the dark at 37^{o}C with 1 mg/ml β-galactosidase substrate (X-gal, Gold BioTechnology, St. Louis, MO) prepared fresh in 40 mM citric acid/NaP buffer, pH 6.0, 5 mM potassium ferrocyanide, 5 mM potassium ferricyanide, 150 mM NaCl, and 2 mM MgCl, as previously described (Elmore *et al*., 2002). After two washes in PBS, the percentage of positively stained cells was quantified by counting three random fields.

Terminal deoxynucleotidyl transferase dUTP nick end labeling (TUNEL) Assay

Upon completion of drug treatments, both floating and adherent fractions of MCF7 cells were collected and approximately 2 x 10^4 MCF7 cells were cytospun (Shandon Cytospin 4, Thermo Scientific). Cells were fixed in 4% formaldehyde for 10 min, washed twice in 1x PBS, postfixed in -20^{o}C cold glacial acetic acid:ethanol (1:2) for 5 min, and washed twice again. Subsequent steps were performed in a covered humidifying chamber in the dark. These steps included blocking in 1 mg/ml bovine serum albumin (New England Biolabs) for 30 min and incubation with terminal transferase (Roche) in the presence of fluorescein 12-dUTP (Roche) for 60 min at 37^{o}C in the dark. Cells were washed with 1x PBS and mounted in Vectashield with DAPI (Vector Labs).

Fluorescence *in situ* hybridization (FISH). To assess telomere length, a pantelomeric, FITC-labeled peptide nucleic acid (PNA) probe was used to detect telomeres on TMAs. The probe hybridization followed standard procedures that have been shown to be successful in breast cancer cell lines and adapted to test the TMAs (Bradshaw *et al*., 2005; Jones *et al*., 2005). Each slide was pretreated with heat incubation overnight at 60^{o}C, followed by deparaffinization and rehydration in a graded ethanol series. Slides were microwaved in citric acid (pH 6.0) and digested in pepsin solution (4 mg/ml in 0.9% NaCl, pH 1.9). After immersion in 3:1 fix of methanol:acetic acid for 1 hr and fixation in 4% formaldehyde in PBS (pH 7.2), tissue cores and FITC-labeled telomeric probe $(C_3TA_2)_3$ and PNA probe were codenatured for 3 min at 80^{o}C. Hybridization overnight at 37^{o}C was followed by washing in denaturation solution (70% fo rmaldehyde/2x SSC for 15 min at 31^{o}C) to remove excess probe. After washing in 2x SSC and

2x SSC with 0.1% NP-40, slides were air dried and counterstained with DAPI (Cytocell, Windsor, CT).

Scoring of Slides

For IHC, mounted slides were semi-quantitatively scored by two independent pathologists in terms of reactivity (positive if >10% of the cells are immunostained), intensity based on an ordinal scale (negative/very weak = 0, weak = 1, moderate = 2, strong = 3), and cellular localization (nuclear or cytoplasmic). Inter-rater agreement was measured using a weighted kappa test. For FISH, one slide was scored by Dr. Colleen Jackson-Cook, Director of Cytogenetics Diagnostic Laboratory at VCU, and the rest by Kristi Turner, Cytogenetics Research Specialist at VCU. Relative telomeric DNA lengths are assessed by visual inspection of telomere-specific hybridization probe fluorescent intensities between pre-malignant and malignant breast tissue and their normal counterparts. A semi-quantitative assessment of telomere signals was performed. Lesions categorized as “normal” are scored “2” and have telomeric signals comparable to those of normal stromal fibroblasts, endothelial cells, and normal mammary epithelial cells. Lesions categorized as “short” are scored “1” and have signal intensities dimmer than the normal stroma, but are still readily detectable and within the normal range of normal cells. Lesions categorized as “very short” are scored “0” and have such low telomeric signal that they are barely detectable and dimmer than any normal cell. Lesions categorized as “long” are scored “3” and have signal stronger than that found in normal cells.

Statistical Analysis

For western blot analysis, changes in population doublings, and telomerase activity, a student's t-test was performed to assess statistical significance of mean sample differences. For IHC, rigorous statistical analysis was performed using R version 2.9.1 to definitively assess Hsp90, p23, and TRF2 expression differences across all disease types using analysis of variance methods with significance set at $p<0.05$. Analyses that involved prediction of intensity scores were handled using a mixed effects modeling approach (Faraway, 2006) to handle the presence of both fixed and random effects. Pearson's correlations were calculated to assess the relationship between protein expression and TNM stage, ER/PR, or age, with significance set at $p<0.05$. Intensity scores were treated as ordered categorical values while localization was a nominal outcome. The design of the TMA further identifies multiple cores from the same case and replicate sections. Student's t-test was used to determine significance for changes in cellular localization.

Image Acquisition

All images of Hsp90, p23, and TRF2 immunostained tissue microarrays were magnified by Nikon Eclipse E600 and captured by Nikon Digital Camera DXM1200F, using the Nikon ACT-1 image editing program. FISH images were obtained using a Zeiss AxioScope2, equipped with DAPI, FITC and dual color filters. All phase contrast, β-Galactosidase, and TUNEL images were obtained by a Zeiss Axiovert 40 microscope, maintained by the microscopy facility of VCU's Anatomy and Neurobiology. All TRAP and TRF images were scanned on a Typhoon 9410 Variable Mode Imager (GE, Piscataway, NJ), maintained by the Massey Cancer Center of VCU.

Chapter 3

Differential expression of Hsp90 and its co-chaperone, p23, in human breast tissue

3.1 Introduction and Rationale

Molecular chaperones, like the heat shock protein 90 (Hsp90) family, are regarded as ubiquitous, highly conserved proteins that mainly respond upon induction of stress or disruption of cellular homeostasis. Chaperones are involved in controlling the conformation, stability, function, and degradation of many oncogenic client proteins, thus determining their cellular fate (Beliakoff and Whitesell, 2004; Csermely *et al*., 1998). Functionally, the Hsp90 multiprotein machinery assists in trafficking, the remodeling of improperly folded client proteins, and the suppression of protein aggregation (Whitesell and Lindquist, 2005; Sarto *et al*. 2000). Kinases, transcription factors, hormone receptors, and certain polymerases, like telomerase, all undergo post-translational maturation via the Hsp90 chaperone cycle (Dai and Whitesell, 2005; Holt and Shay, 1999).

The intrinsic nature of heat shock proteins makes them especially relevant to a cell's defense against cancer initiation. Previous studies have reported an overexpression of Hsp90 in human breast cancer; however, only tumor specimens and breast cancer cell lines, but not normal and pre-malignant specimens, were examined (Pick *et al*., 2007). The stress-inducible isoform Hsp90α has also been reported to be preferentially increased in cancer tissues compared to non-cancerous tissues, but this study did not assess total Hsp90 levels in normal tissues (Yano *et al*., 1996, 1999). Because upregulation of Hsp90 was reported in these previous findings, Hsp90 inhibition has attracted great interest as a promising approach for cancer therapy since many client proteins can be simultaneously targeted and disrupted (Goetz *et al*., 2003; Sharp and

Workman, 2006), which would likely result in tagging of client proteins with polyubiquitin molecules and subsequent proteasomal degradation (Pearl *et al*., 2008). As such, the Hsp90 inhibitor, 17-allyamino, 17-demethoxy geldanamycin (17-AAG), is in phase II clinical trials and is a promising anticancer drug, since it is less hepatotoxic and more stable than its parent compound, geldanamycin (Pacey *et al*., 2006).

The co-chaperone p23 has also been studied for its role in breast cancer, although the majority of studies involving p23 focus on the relationship of this protein with steroid hormone receptors. Specifically, overexpression of p23 positively regulates the activity of the estrogen receptor, which regulates growth-promoting gene transcription, resulting in enhanced invasiveness of breast cancer cells without any effect on proliferation (Björnström and Sjöberg, 2005; Knoblauch and Garabedian, 1999; Oxelmark *et al*., 2006). The expression of p23 in breast cancer cell lines also increases according to tumor grade (Oxelmark *et al*., 2006), with higher expression in high-grade tumors. Furthermore, p23 has been shown to be significantly increased in mammary tumors and metastatic lung carcinomas and very weak in normal tissue (Krebs *et al*., 2002; Mollerup *et al*., 2003). These findings implicate p23 in cancer cell growth, and may suggest a novel role for this co-chaperone in tumor cell invasion or metastasis and breast cancer progression.

Despite these studies and others in a variety of solid tumors (Becker *et al*., 2004; Kato *et al*., 1995; Kurahashi *et al*., 2005; Ogata *et al*., 2000; Romanucci *et al*., 2006), the role of Hsp90 and p23 during mammary carcinogenesis and progression remain unclear, particularly how inhibiting these proteins may influence breast tumor biology. Our laboratory has previously shown that in an experimental model for prostate cancer, Hsp90 and p23 are upregulated during malignant progression (Akalin *et al*., 2001). This study was then extended to clinical prostate

specimens, where we demonstrated that normal tissue and benign prostatic hyperplasia (BPH) express relatively low levels of both Hsp90 and p23 while carcinomas consistently express high levels (Elmore *et al*., 2008).

We now assess expression levels and localization of Hsp90 and p23 in normal and malignant breast tissues, which will then be used to determine whether chaperone expression correlates with stage or advancement of malignancy, with particular attention on subcellular localization and tumor grade. The results obtained in this study will provide the rationale behind whether inhibition of chaperones is an appropriate means to sensitize tumor cells to be more responsive to traditional cancer therapeutics.

3.2 Results

3.2.1 Hsp90 and p23 protein levels are elevated in breast cancer cells.

Since little is known about the roles of Hsp90 and its co-chaperone, p23, in mammary carcinogenesis and progression, we initially assessed their expression in human cell lines. Total cellular levels of Hsp90 and p23 were examined in normal human mammary epithelial cells (HMEs) at various population doublings, as well as in established human breast cancer cell lines. Pre-immortal HMEs at lower population doublings displayed significantly lower levels of both Hsp90 and p23 as compared to their isogenic immortal HME (PD>100) cell line and breast cancer cell lines (Figure 13A). Western analysis of Hsp90 shows relatively equal levels of this chaperone, however, upon quantitation, it is evident that Hsp90 is moderately elevated 1.2-fold in immortal HMEs, 1.4-fold in MCF7, 1.6-fold in MDA-MB231, and 1.3-fold in ZR75-1 (Figure 13B). Compared to HMEs at PD 11.8, p23 is almost two-fold greater in immortal HMEs, 3.2-fold greater in MCF7, 2.4-fold greater in MDA-MB231, and 2.1-fold greater in ZR75-1. It is

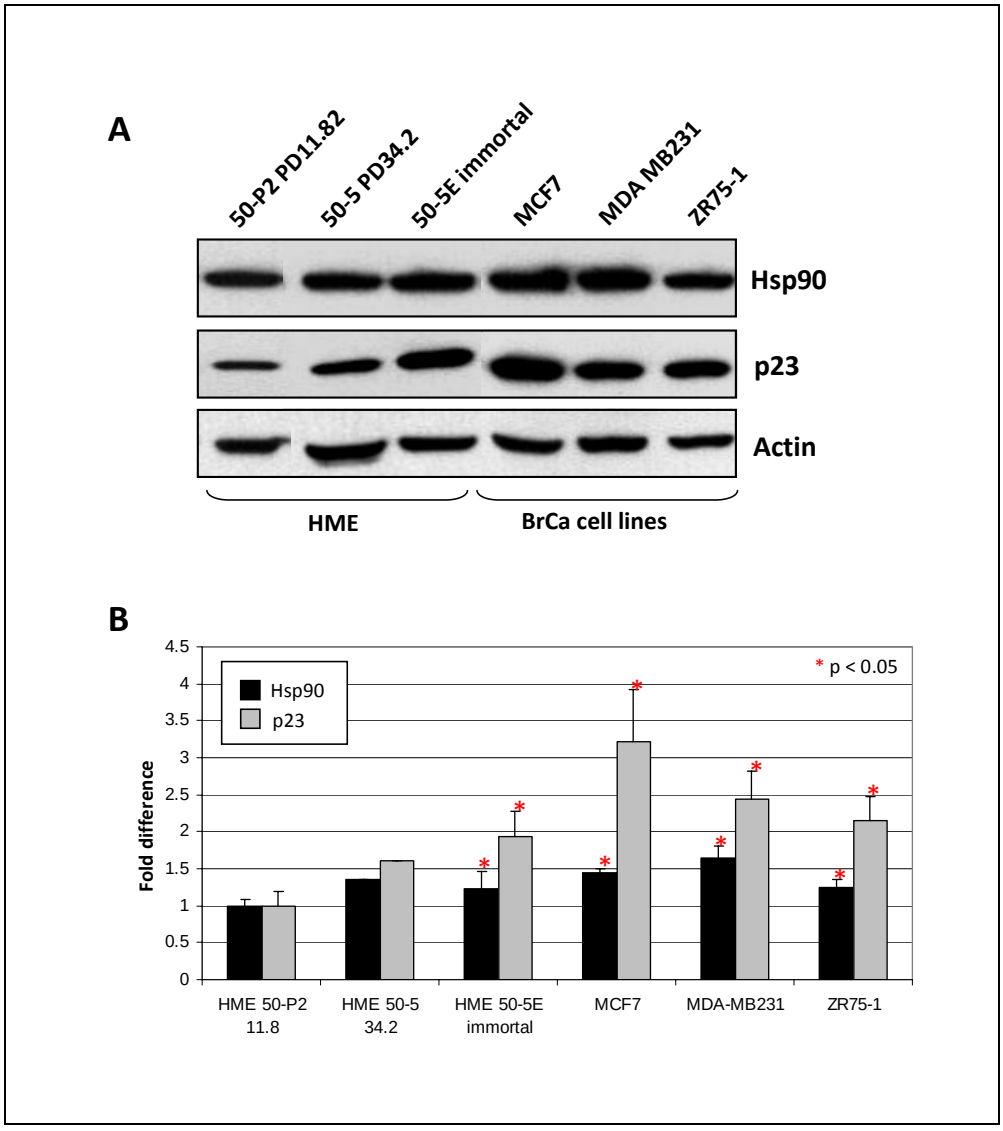

Figure 13. Hsp90 and p23 protein levels increase with population doubling in normal cells and are high in established breast cancer cell lines. (A) 15 µg of total cellular lysate from pre-immortal Li-Fraumeni human mammary epithelial cells (HMEs) at low passage numbers, isogenic immortal HMEs, and breast cancer cell lines (MCF7, MDA-MB231, ZR75-1) was subjected to western analysis. Immunoblots were probed with antibodies against Hsp90, p23, and β-actin, which served as a loading control. (B) Quantitation of western blot by densitometry. All experiments were performed in triplicate, unless other wise noted. Significance was set at $p < 0.05$. HME 50-5 PD 34.2 was only analyzed once and so was not able to be assessed for significance.

notable that within the HME cells, p23 protein expression increases as cells progress toward immortality with high passage cells displaying higher levels.

In order to confirm the increased expression of Hsp90 and p23 in these cancer cell lines, immunostaining was performed on live cells, including immortalized human mammary epithelial MCF10A cells, breast cancer MCF7 and MDA-MB231 cells, and prostate cancer PC-3 cells. All immortal and cancer cells lines tested display extremely high levels of Hsp90 and p23 that appear in both nuclear and cytoplasmic locations (Figure 14).

3.2.2 Established cancer cell lines on TMA consistently express higher Hsp90 and p23 levels.

As an extension of the *in vitro* finding of increased Hsp90 and p23 in cancer cells, we wanted to determine whether cell lines included in the tissue arrays also reflect an upregulation of these chaperones. Each array contained cores of the established cell lines MCF10A, MCF7, T47D, PC-3, and the human colon adenocarcinoma cell line HT-29. For Hsp90 and p23 expression, a total of 106 and 104 cell line cores, respectively, were examined. Representative images of Hsp90 and p23 immunostaining for these cell lines (data not shown for HT-29) reveal that these proteins are localized to both the nucleus and cytoplasm, although to varying degrees (Figure 15). For Hsp90, expression of this chaperone is always greater in the cytoplasm than in the nucleus, such that cytoplasmic scores indicate consistently strong staining (Table 1). When assessing average Hsp90 scores, it is again clear that this chaperone is abundantly expressed in the cytoplasm, with the majority of cell line cores (75.8%) staining very strongly (Table 2). Nuclear Hsp90 expression is only moderately reduced with the majority of cores staining either +1 or +2 in intensity (71.3%) (Table 2).

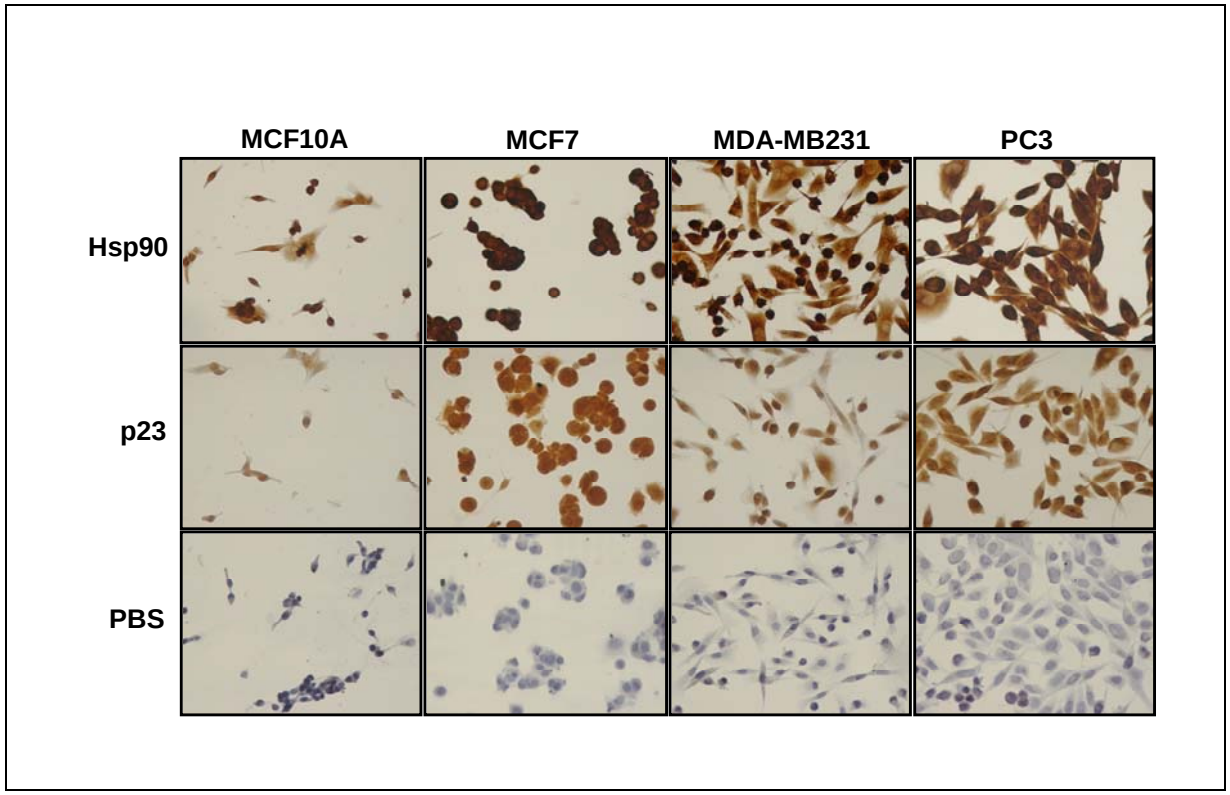

Figure 14: High Hsp90 and p23 expression in established immortal and cancer cell lines. Immunocytochemical staining of immortalized breast epithelial MCF10A cells, breast cancer MCF7 and MDA-MB231 cells, and prostate cancer PC3 cells show abundant Hsp90 and p23 expression. Bottom panel represents PBS-incubated negative control cells, in which no primary antibody was added.

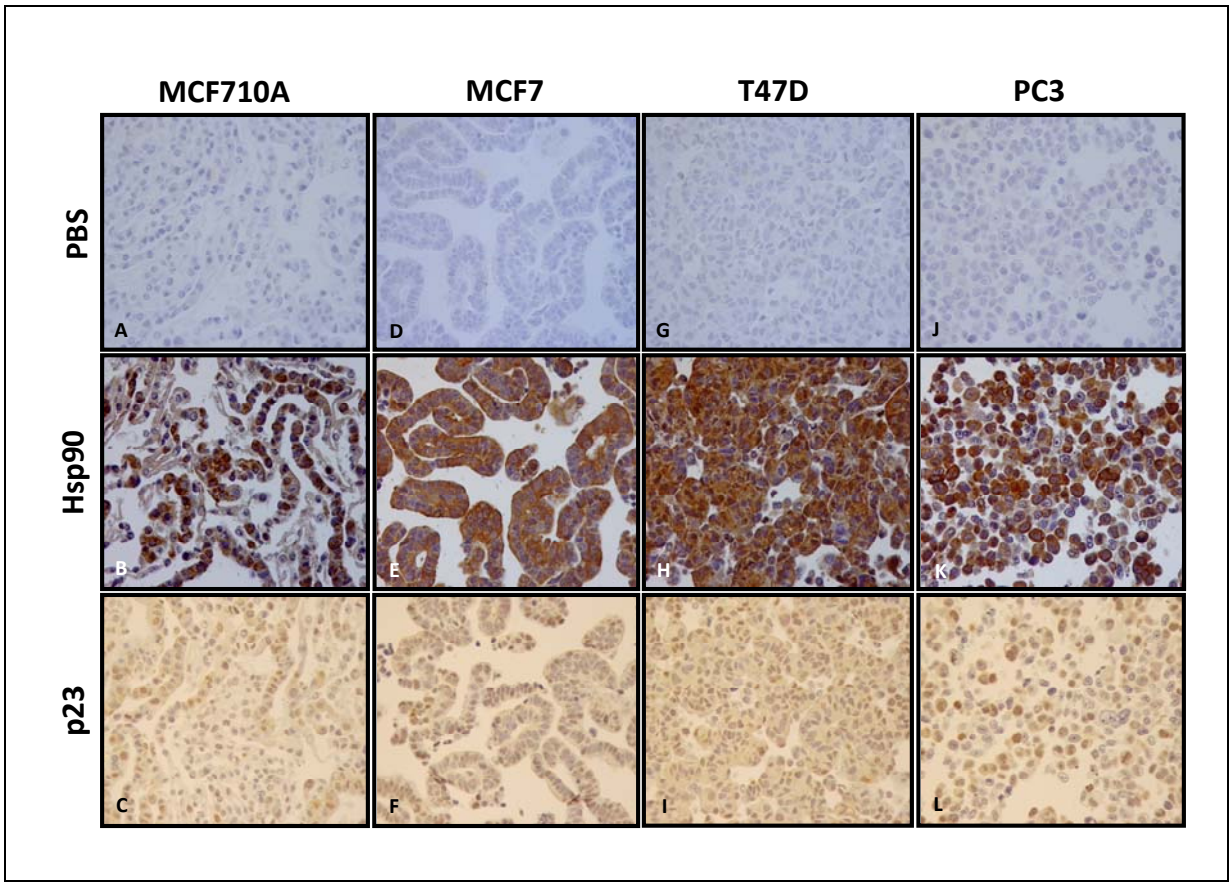

Figure 15. Cell lines of TMA consistently express high levels of both Hsp90 and p23. Established cell lines included in the TMAs were also subjected to immunohistochemical processing. Representative images of the immortalized breast epithelial cell line MCF10A (B); breast cancer cell lines MCF7 (E) and T47D (H); and the prostate cancer cell line PC3 (K), are shown stained with an antibody against Hsp90. MCF10A (C), MCF7 (F), T47D (I), and PC3 (L) cores were also stained with an antibody for p23. PBS-treated MCF10A (A), MCF7 (D), T47D (G), and PC3 (J) served as a negative control (no primary antibody). Total numbers of cores stained for Hsp90 and p23 was n = 106 and n = 104, respectively. All images shown are at 40x. moderately intense in the cytoplasm (41.7% ± 0.04%) and a greater proportion of moderately intense nuclear p23-staining cell lines (45% ± 0.03%) as compared to Hsp90. Taken together, our data reveal that Hsp90 and p23 protein expression in detectable in both cellular locations, although to different extents, in established immortal and cancer cell lines.

Table 1: Summary of chaperone intensity of established cell lines on TMAs.

	Mean Hsp90 Score		Mean p23 Score	
Cell Line	**Nuclear**	**Cytoplasmic**	**Nuclear**	**Cytoplasmic**
MCF10A	1.04	2.67	1.95	1.82
MCF7	0.63	2.79	1.54	1.25
T47D	1.75	2.96	1.78	1.35
PC3	1.42	3.00	1.54	1.63
HT-29	1.46	3.00	0.82	1.09

Table 2: Cell Line cytoplasmic and nuclear immunostaining

Intensity	Hsp90		p23	
	Nuclear % (stdev)	**Cytoplasmic % (stdev)**	**Nuclear % (stdev)**	**Cytoplasmic % (stdev)**
0	24.1 (0.02)	1.4 (0.004)	19.8 (0.01)	8.4 (0.01)
1	**40.6 (0.03)**	1.4 (0.004)	29.2 (0.03)	**47.3 (0.04)**
2	30.7 (0.02)	21.4 (0.01)	**45.0 (0.03)**	41.7 (0.04)
3	4.6 (0.02)	**75.8 (0.02)**	6.0 (0.01)	2.6 (0.007)

As a group, it appears that the levels of p23 in nuclear and cytoplasmic locations are comparable to each other (Table 1). Interestingly, immortalized breast epithelial and breast cancer cell lines have less intense cytoplasmic p23 than nuclear, while the opposite situation is found in prostate and colon cancer cells (higher cytoplasmic and lower nuclear). A comparison of average p23 scores reveals that the expression of cytoplasmic p23 in cell lines is simply not as strong as that of Hsp90, with only 2.6% staining very strongly (compare to 75.8% for Hsp90, Table 2). Rather, the majority of cell lines express relatively lower cytoplasmic p23 levels (47.3%). Furthermore, there is a greater proportion of cell lines staining moderately intense in the cytoplasm (41.7%) and a greater proportion of moderately intense nuclear p23-staining cell lines (45%) as compared to Hsp90. Taken together, our data reveal that Hsp90 and p23 protein expression is detectable in both cellular locations, although to different extents, in established immortal and cancer cell lines.

3.2.3 Hsp90 expression in clinical tissues is predominantly cytoplasmic.

Based on the finding in tumor cell lines, we wanted to determine whether Hsp90 expression is also relatively higher in malignant breast tissue specimens. Tissue arrays containing the three disease states, normal, ductal carcinomas in situ (DCIS), and invasive breast carcinomas, were immunohistochemically stained for Hsp90. Briefly, clinical samples including each of these three tissue types were obtained and arrayed (tissue cores punched out) in quadruplicate to address tissue heterogeneity. Each of these four cores was then paraffin-embedded onto separate slides such that a group of six slides constitutes a case set. We have obtained three case sets and have used two slides from each case set to assess Hsp90 and p23 levels, while the remaining two slides were treated as negative controls. Each slide thus contains

hundreds of representative cores that can be processed and analyzed simultaneously. For Hsp90 and p23 expression, a total of 107 and 111 normal cores; 55 and 56 DCIS cores; and 457 and 426 invasive breast carcinomas, respectively, were examined.

As shown in Figure 16A and 16B, normal breast tissues predominantly show lower Hsp90 staining intensity, with the majority of cores staining very weakly for Hsp90 in the nucleus (68.3%) (Table 3). Similarly, approximately 69.1% of DCIS (Figure 16C, D) and 72.9% of invasive breast carcinomas (Figure 16E, G) also stained weakly in the nucleus for Hsp90 (Table 3). Representative images of invasive carcinomas show that Hsp90 expression is variable, ranging from very weak nuclear staining (or mainly cytoplasmic) to very strong (Figure 16F, G). Based on this data, we therefore conclude that nuclear Hsp90 staining does not appear to vary between the disease types.

Unlike nuclear Hsp90 expression, cytoplasmic staining is moderately strong in all clinical specimens in these tissue arrays. Namely, the majority of normal cores (38.7%), DCIS (59%), and invasive carcinomas (51.2%) all express moderate levels of Hsp90 in the cytoplasm (Table 3). Interestingly, over half of the DCIS and invasive carcinomas show moderately intense Hsp90 staining while this intensity is observed in just over a third of normal cores. As a corollary, a small fraction of normal tissue (2.4%) express very strong Hsp90 staining, while DCIS and invasive tissues have ~8.4-fold (20.2%) and ~6.3-fold (15.1%) more, respectively (Table 3). Thus, cytoplasmic Hsp90 expression is generally greater in malignant tissue.

3.2.4 p23 nuclear expression differs between disease types.

Since p23 protein levels were shown to be significantly elevated in tumor cell lines, we wanted to assess p23 expression and localization in breast tissue counterparts. Normal, DCIS,

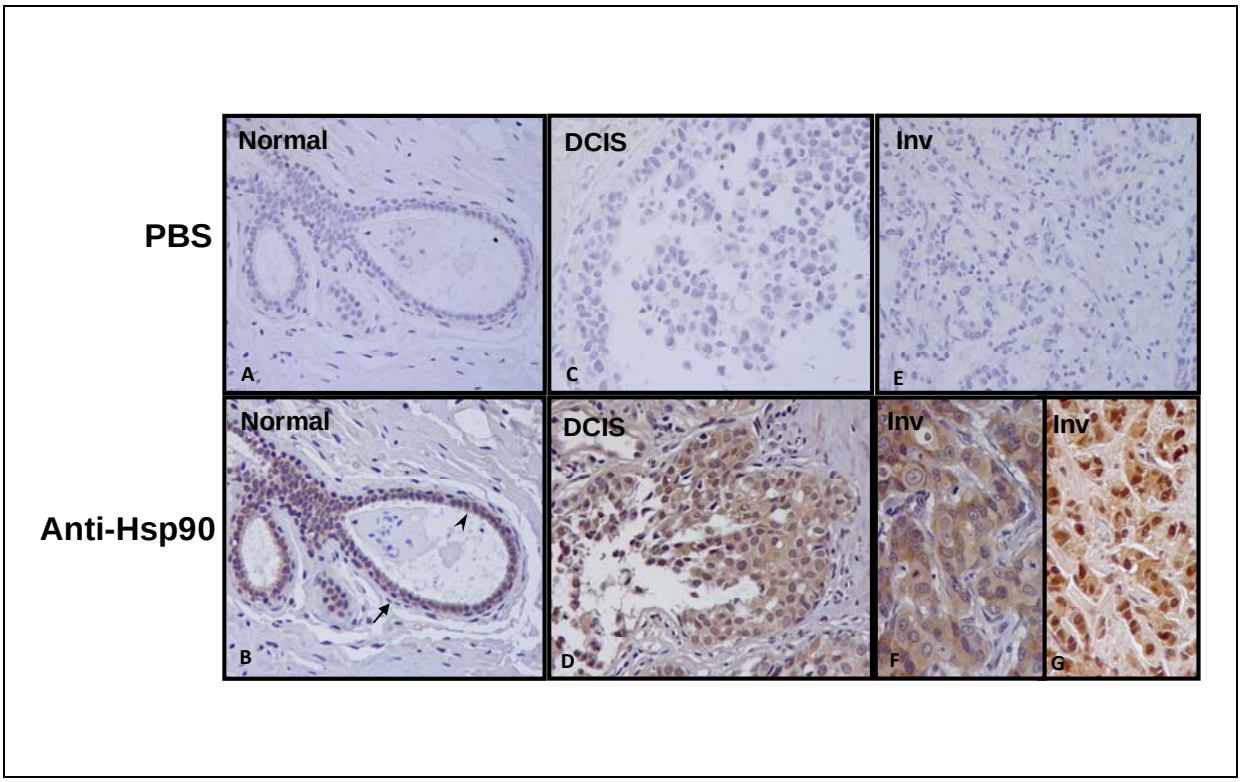

Figure 16. Hsp90 cytoplasmic expression is elevated in invasive breast carcinomas as compared to normal and DCIS tissues. Immunohistochemical analysis of negative control (no primary antibody) PBS-treated normal (A), DCIS (C), and invasive (E) breast tissues and Hsp90-stained normal (B), DCIS (D), and invasive (F, G) breast carcinomas. Six slides were processed for Hsp90 that included an overnight incubation with primary antibody, 10 min. DAB incubation, and light hematoxylin counterstain. Total numbers of cores stained was n = 107 for normal, n = 55 for DCIS, and n = 457 for invasive carcinomas. Myoepithelial and epithelial cells are denoted by the arrow and arrowhead, respectively. All representative images shown are at 40x. Overall weighted kappa = 0.8358.

Table 3: Hsp90 cytoplasmic and nuclear immunostaining

	Cytoplasmic Score % (stdev)			Nuclear Score % (stdev)		
Intensity	**Normal**	**DCIS**	**Invasive**	**Normal**	**DCIS**	**Invasive**
0	24.3 (0.05)	3.9 (0.01)	12.4 (0.03)	**68.3 (0.07)**	**69.1 (0.04)**	**72.9 (0.03)**
1	34.6 (0.02)	16.9 (0.02)	21.3 (0.02)	29.7 (0.04)	30.0 (0.03)	22.5 (0.02)
2	**38.7 (0.04)**	**59.0 (0.03)**	**51.2 (0.03)**	2.0 (0.006)	0.9 (0.003)	4.1 (0.007)
3	2.4 (0.008)	20.2 (0.03)	15.1 (0.01)	0	0	0.5 (0.001)

and invasive breast carcinoma sections were processed for p23 immunoreactivity in the same manner as Hsp90. Based on tissue array data, nuclear p23 immunostaining noticeably differs among the disease types. Similar to the finding for Hsp90, it is evident that p23 expression is variable among invasive carcinomas. Additionally, p23 expression also shows differences between clinical tissues and established cell lines. Specifically, the majority of normal breast tissue (47.2%, Figure 17A, B) displays moderately strong nuclear staining while most DCIS (38.8%, Figure 17C, D) cores stain relatively weakly and invasive carcinomas (53.5%, Figure 17E, G) stain very weakly (Table 4). This is in contrast to the cancer cell line finding, in which a greater proportion of established cell line cores stained moderately intense and very strong in the cytoplasm and a larger percentage score moderately intense in the nucleus (Table 2). This data suggests that a trend exists wherein p23 nuclear expression decreases with advanced malignancy, which is opposite of our *in vitro* cell strain/line results.

An initial assessment of p23 immunostaining in cytoplasmic fractions reveals no apparent difference in the intensity of the majority of disease types. Specifically, normal (53.5%), DCIS (46.1%), and invasive (41.8%) cores all stain relatively weakly (Table 4). However, it is noteworthy that a greater proportion of normal cores but a smaller proportion of invasive cores stain at this intensity. As an extension of this finding, fewer invasive cores stain moderately intense (24.4%) compared to normal tissue, while more invasive cancers stain very weakly (33.2%) compared to normal tissue (9.0%) (Table 4). Hence, these data also suggest reduced p23 levels in more advanced cancers.

3.2.5 Hsp90 and p23 expression differs between disease types but not between locations.

In order to assess disease group-specific differences, normal, DCIS, and invasive

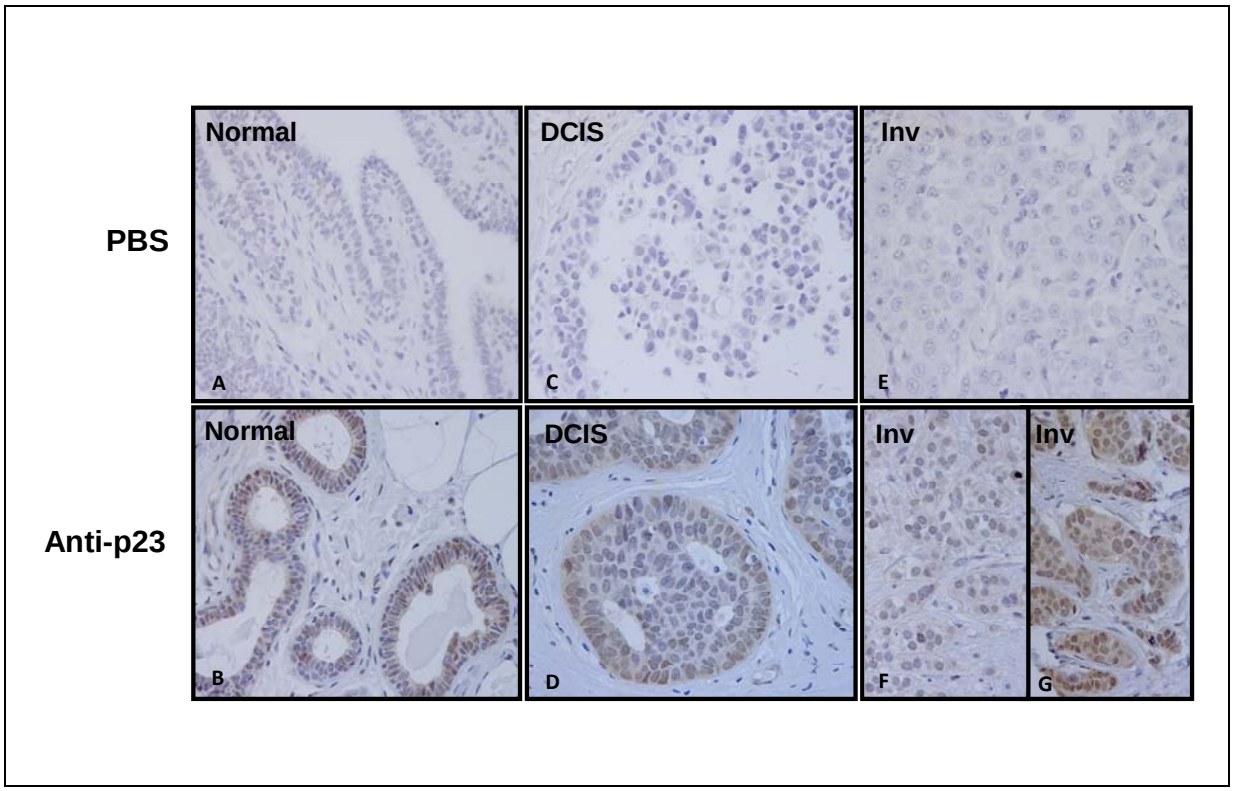

Figure 17. Level of p23 is higher in normal breast tissue than in invasive breast carcinomas. Immunohistochemical analysis of negative control (no primary antibody) PBS-treated normal (A), DCIS (C), and invasive (E) breast tissues and p23 primary antibody-stained normal (B), DCIS (D), and weakly staining invasive (F) and strongly staining invasive (G) breast carcinomas. Six slides were processed for p23 in the same manner as Hsp90. Total numbers of cores stained was n = 111 for normal, n = 56 for DCIS, and n = 426 for invasive carcinomas. All images shown are at 40x. Overall weighted kappa = 0.4957.

Table 4: p23 cytoplasmic and nuclear immunostaining

	Cytoplasmic Score % (stdev)			Nuclear Score % (stdev)		
Intensity	**Normal**	**DCIS**	**Invasive**	**Normal**	**DCIS**	**Invasive**
0	9.0 (0.02)	19.8 (0.03)	33.2 (0.05)	12.9 (0.02)	26.2 (0.03)	**53.5 (0.05)**
1	**53.5 (0.04)**	**46.1 (0.03)**	**41.8 (0.03)**	27.3 (0.02)	**38.8 (0.04)**	26.2 (0.01)
2	37.1 (0.05)	34.1 (0.04)	24.4 (0.03)	**47.2 (0.03)**	28.8 (0.04)	18.4 (0.02)
3	0.4 (0.002)	0	0.6 (0.002)	12.6 (0.02)	6.2 (0.01)	1.9 (0.004)

carcinomas were analyzed as separate groups. On a scale of 0 to 3, observed average scores for Hsp90 nuclear expression is fairly consistent between the disease types with normal tissues scoring 0.35, DCIS scoring 0.32, and invasive carcinomas scoring 0.32 (Table 5). These results do not suggest any significant differences in nuclear Hsp90 staining as cells progress from a normal to invasive state ($p = 0.7468$). In contrast, cytoplasmic Hsp90 expression does significantly differ between the disease types with normal breast tissue generally scoring lower (1.19) than both DCIS (1.95) and invasive carcinomas (1.69) ($p<0.0001$, Table 5). Although Hsp90 expression increases with advanced malignancy, there is no apparent change in cellular localization patterns ($p>0.05$) with cytoplasmic Hsp90 nearly always greater than nuclear levels.

In the case of p23, both nuclear and cytoplasmic fractions exhibit the same trend in which higher p23 levels are associated with benign states and lower p23 levels with invasiveness. Again, disease specific differences exist in which normal, DCIS, and invasive carcinomas on average have significantly varied scores ($p<0.0001$, Table 5). Similar to the finding for Hsp90, no localization changes were noted for p23 ($p>0.05$).

3.2.6 Breast cancer related clinical parameters are significantly associated with chaperone upregulation.

Due to the variability in Hsp90 and p23 immunoreactivity within the invasive carcinoma group, we sought to determine whether this variability correlated with TNM stage and/or steroid hormone receptor status. Clinical data was provided by the CBCTR on the status of ER and PR, which are both Hsp90 client proteins. Breast cancers can be broadly grouped according to disease progression by assigning TNM scores, which takes into account the tumor-node-metastasis stage of a particular cancer, wherein a higher score is associated with greater severity. Invasive breast

Table 5: Summary of disease type-specific differences

		Observed means (s.e.)			
Chaperone	**Location**	**Normal**	**DCIS**	**Invasive**	**p-value***
Hsp90	Nuclear	0.3480 (0.5171)	0.3235 (0.4907)	0.3191 (0.5702)	0.7468
Hsp90	Cytoplasmic	1.1921 (0.8310)	1.9515 (0.7327)	1.6932 (0.8731)	**<0.0001**
p23	Nuclear	1.6099 (0.8465)	1.1892 (0.8583)	0.7214 (0.8395)	**<0.0001**
p23	Cytoplasmic	1.2870 (0.6354)	1.1441 (0.7242)	0.8607 (0.7746)	**<0.0001**

*p<0.05 are significant

carcinomas included in our case sets represented various levels of TNM stages. In our study, we found that a positive correlation exists between nuclear Hsp90 and TNM stage, in which higher Hsp90 expression is directly associated with a higher TNM score ($p = 0.0023$, Table 6). The co-chaperone p23 does not appear to have any relationship with TNM stage (Table 6). Likewise, ER and PR negativity typically signify poorer prognosis since most available therapeutics depend on the presence of these receptors. Cytoplasmic Hsp90 expression has an inverse correlation with ER status, such that higher expression is associated with ER negativity ($p = 0.0112$, Table 7). Significant relationships between p23 and ER/PR also emerged, with higher nuclear p23 correlating to ER positivity ($p = 0.0003$) and higher total p23 being positively associated with PR presence (nuc: $p = 0.0044$; cyto: $p = 0.353$, Table 7).

Finally, in addition to significant relationships with chaperone expression, TNM stage also displays an inverse, or negative correlation with both ER and PR presence ($p<0.0001$ for both, Table 8), which is to say that a higher TNM stage, corresponding to a higher grade breast cancer, is significantly associated with ER and PR negativity. Collectively, these data suggest the involvement of the chaperones, Hsp90 and p23, in participating in breast cancer progression. Their influence on clinical parameters of prognosis are specifically observed in that nuclear Hsp90 is associated with more advanced breast cancer, while elevated p23 correlated with ER/PR positive tumors.

3.2.7 Total Hsp90 in tumor cells is associated with an increase in both complexed and uncomplexed Hsp90.

Due to the differential expression of Hsp90 in normal, DCIS, and invasive breast carcinomas, we wanted to determine whether these changes in protein levels impacted the activity

Table 6: Correlations between TNM stage and average chaperone scores in invasive cores

Chaperone	Location	Correlation	p-value*
Hsp90	Nuclear	+	**0.0023**
Hsp90	Cytoplasmic	None	0.6018
p23	Nuclear	None	0.4690
p23	Cytoplasmic	None	0.2323

*p<0.05 are significant

Table 7: Correlations between ER/PR status and chaperone expression in invasive cores

Receptor	Chaperone	Location	Correlation	p-value*
ER	Hsp90	Nuclear	None	0.1441
		Cytoplasmic	-	**0.0112**
PR	Hsp90	Nuclear	None	0.6706
		Cytoplasmic	None	0.0933
ER	p23	Nuclear	+	**0.0003**
		Cytoplasmic	None	0.0506
PR	p23	Nuclear	+	**0.0044**
		Cytoplasmic	+	**0.0353**

*$p<0.05$ are significant

Table 8: Relationship between TNM stage and hormone receptor status in invasive cores

Receptor	Correlation	p-value*
ER	-	**<0.0001**
PR	-	**<0.0001**

*p<0.05 are significant

state of Hsp90. As a rationale for Hsp90 as a viable therapeutic target for breast cancer, previous data reports that the Hsp90 found in tumor cells is nearly all in a complex with its client proteins, while Hsp90 in most normal cell types remains predominantly in an unbound state (Kamal *et al*., 2003). Our results suggest differential expression of Hsp90 in normal, DCIS, and invasive breast carcinomas based on the cancer staging, rather than alterations in Hsp90/client protein binding status. In an effort to recapitulate the study by Kamal *et al.*, we compared normal fibroblasts, MCF10A cells, and MCF7 breast cancer cells for the presence of bound (active) and free (inactive) forms of Hsp90 (Figure 18). Our results show that while there is an increase in the client-complexed form of Hsp90 in immortal and tumor cell lines pulled down by protein G beads compared to fibroblast cell strains, there is considerably detectable complexed Hsp90 in normal cells. It is significant, in contrast to previous results, that there is also an abundance of the uncomplexed form of Hsp90 in immortal and tumor cells. Furthermore, there is a significant portion of Hsp90 protein that is not at all bound to protein G beads, suggesting that the immunoprecipitation may have been inefficient.

In the course of troubleshooting these experiments, we discovered that the complexed Hsp90 form used in the Kamal *et al*., 2003 paper was actually an IgM antibody and that protein G beads were ineffective in recognition of this immunoglobulin type. For this reason, a modified immunoprecipitation technique was implemented in which we compared the ability of protein G and L beads to pull down uncomplexed Hsp90 (IgG antibody) and complexed Hsp90 (IgM) (Figure 19). For both the protein G and L beads, a variety of lysate concentrations were tested to determine the optimal concentrations – 100μg of lysate for G beads because lesser amounts failed to precipitate sufficient detectable Hsp90, which is consistent with previous report (Kamal et al., 2003), and a maximal recommended concentration of 300μg for L beads. In this procedure,

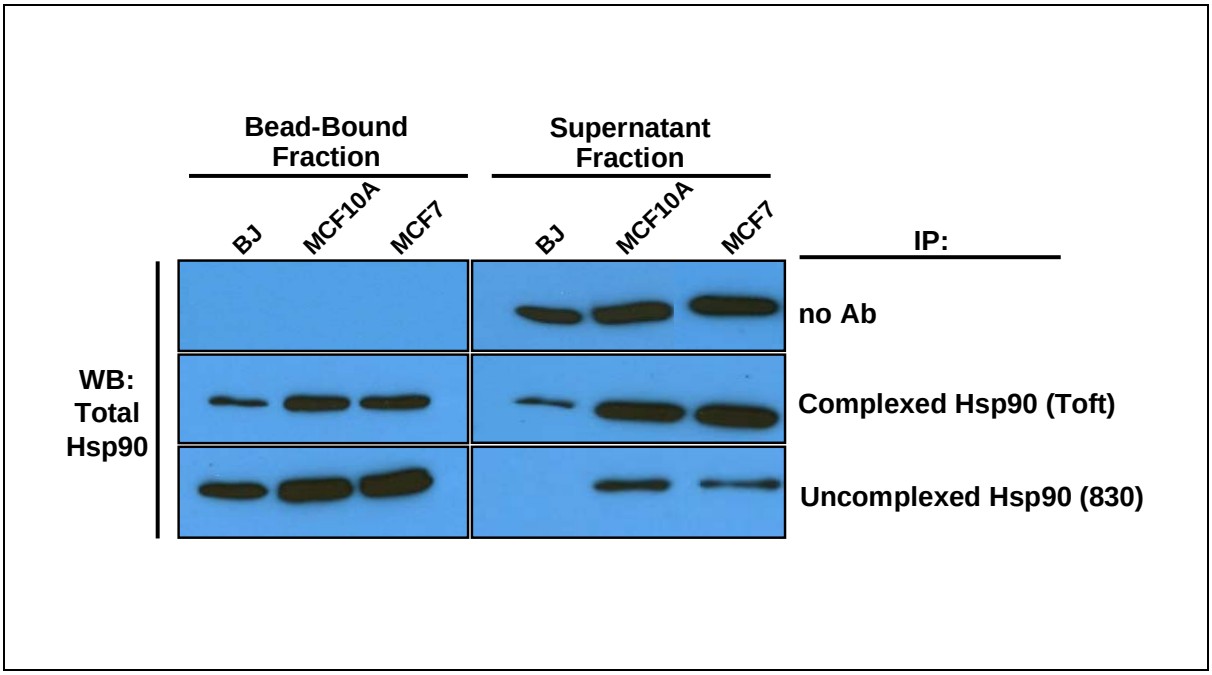

Figure 18. Hsp90 in cancer cells exists in both a complexed and uncomplexed state. Normal BJ fibroblasts, MCF10A immortal mammary epithelial cells, and MCF7 breast cancer cells were subjected to immunoprecipitation using antibodies against the client-bound and client-free forms of Hsp90. Immunoprecipitation utilizing protein G beads was performed on 100 μg of total protein lysate. Left panels show fraction bound to beads (immunoprecipitated), while the right panels show the supernatant fraction (non-immunoprecipitated). Following IP, immunoblot was probed for total Hsp90 (Toft, recognizes both complexed and uncomplexed and both isoforms of Hsp90).

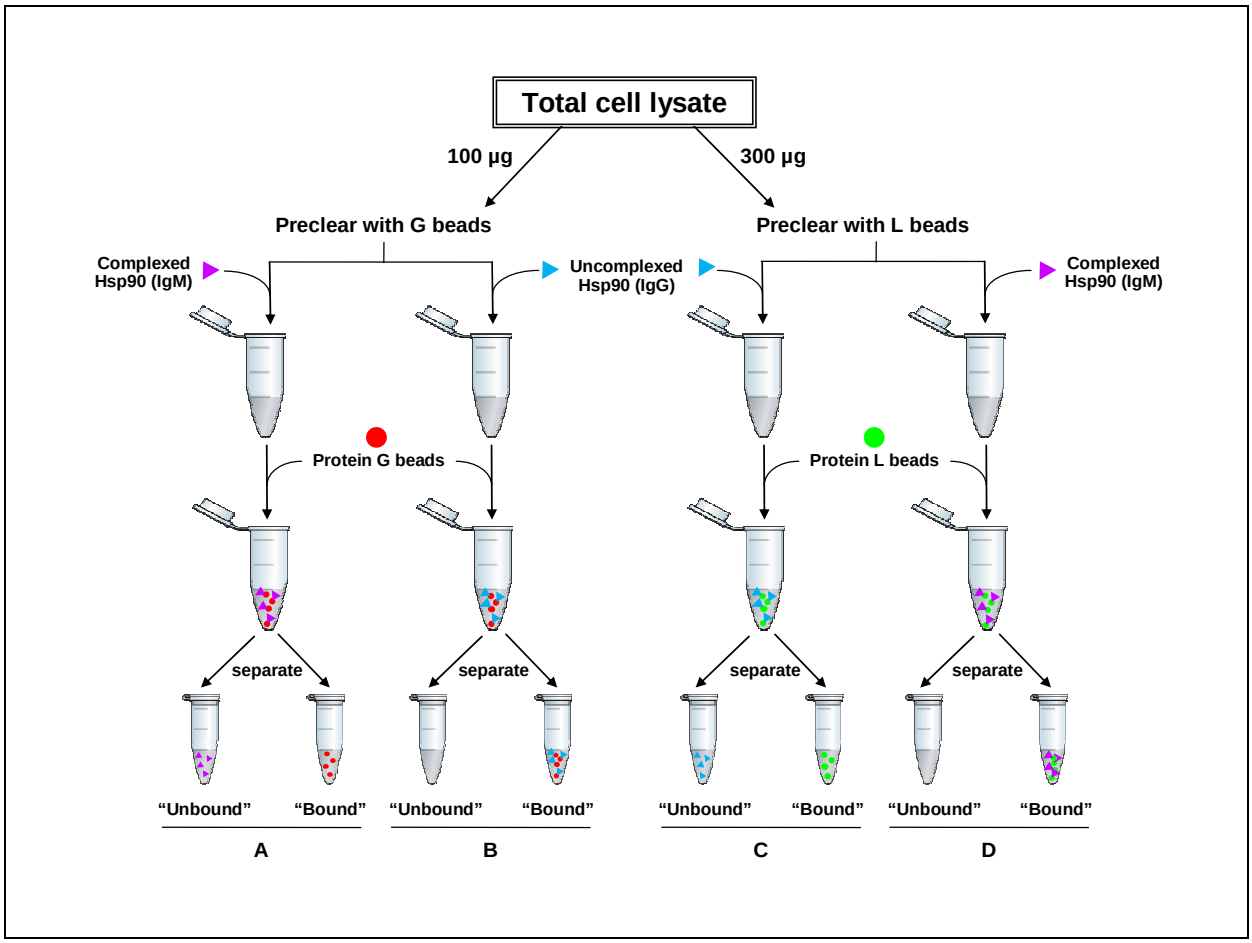

Figure 19: Schematic of modified immunoprecipitation technique. Total cell lysate was subjected to immunoprecipitation using two different agarose beads that recognize different immunoglobulins. Either 100 µg (for protein G) or 300 µg (for protein L) of lysate was precleared, followed by incubation with primary antibody, either complexed Hsp90 (IgM) or uncomplexed Hsp90 (IgG). Prewashed G or L beads were then added to each precleared G or L mixture, respectively, and incubated overnight with agitation. Each sample was spun down and supernatant collected as the "unbound" fraction, while bead-bound protein was labeled the "bound" fraction. In theory, protein G beads do not recognize IgM antibodies, and so complexed Hsp90 in the IgM form would be found in the "unbound" fraction (A). These G beads preferentially bind IgG antibody, so the uncomplexed Hsp90 form would be found in the "bound" fraction (B). Similarly, protein L beads have a distinct affinity for IgM antibodies, and so the "bound" fraction would only contain complexed Hsp90 (C, D).

optimal amounts of protein lysate from normal fibroblasts and breast cancer cells were precleared with either G or L beads, followed by incubation with primary antibody (complexed or uncomplexed Hsp90). Protein G or L beads were then added to the lysate-antibody mixture, incubated together, and bead-bound fractions separated from unbound fractions. Protein G beads do not recognize IgM antibodies, and so complexed Hsp90 would be found in the supernatant or "unbound" fraction (Figure 19A). Since G beads preferentially bind IgG antibody, the uncomplexed Hsp90 form would be found in the "bound" fraction (Figure 19B). Similarly, protein L beads have a distinct affinity for IgM antibodies, and the unbound fraction would contain uncomplexed Hsp90 (Figure 19C) while the bound fraction would only contain complexed Hsp90 (Figure 19D).

Given the number of technical issues with immunoprecipitation-type assays in general, experiments employing this modified method were repeated a minimum of 10 times with differing protein concentrations, antibody types, incubation periods, and lysis conditions, with representative results shown (Figure 20) and compiled (Table 9). Indeed, protein G beads do not pull down IgM antibodies, as evidenced by the lack of complexed Hsp90 in the bound fraction. We again show that there is clearly detectable uncomplexed Hsp90 in cancer cells. However, upon immunoprecipitation with L beads, we do not detect either complexed or uncomplexed Hsp90 in the bead-bound fractions. The results presented here are in significant contrast with that reported by Kamal *et al*, as shown by the abundance of the uncomplexed form of Hsp90 in immortal and tumor cells. While they report detectable complexed Hsp90 with G bead incubation, we consistently could not repeat this finding. We are confident that our immunoprecipitation technique accurately represents biologically relevant findings, indicating

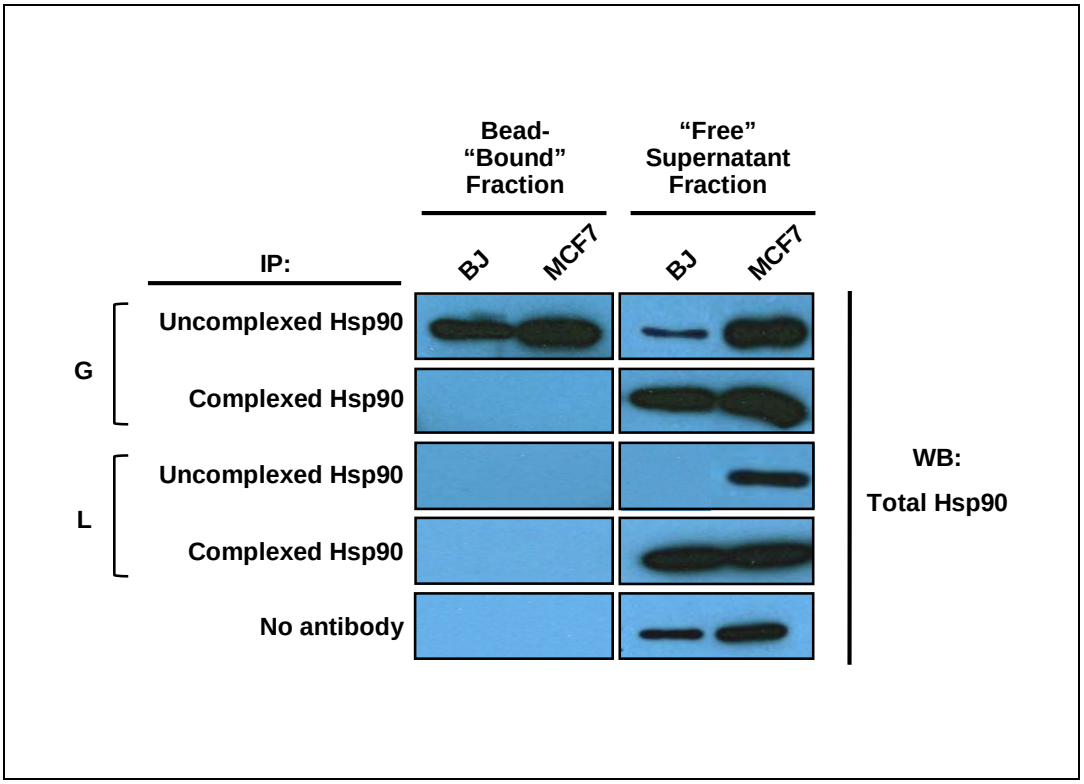

Figure 20: Method of immunoprecipitation affects detection of Hsp90 complexes. Normal BJ fibroblasts and MCF7 breast cancer cells were compared for differential presence of client-bound or free form of Hsp90. A 100 µg or 300 µg aliquot of total cell lysate was immunoprecipitated for uncomplexed Hsp90 (SPA-830, IgG) and complexed Hsp90 (SPA-845, IgM) using protein G or protein L beads, respectively. Left panels show fraction bound to beads (immunoprecipitated), while the right panels show the supernatant fraction (non-immunoprecipitated). Following IP, immunoblot was probed for total Hsp90 (Toft).

Table 9: Summary of complexed vs. uncomplexed Hsp90 in normal and cancer cells

Beads		Present Study				Kamal *et al*., 2003			
		Uncomplexed Hsp90 (830 IgG)		Complexed Hsp90 (845 IgM)		Uncomplexed Hsp90 (830 IgG)		Complexed Hsp90 (845 IgM)	
		BJ	MCF7	BJ	MCF7	Normal	Cancer	Normal	Cancer
G	Bound	+	++	–	–	+	–	+	+
	Free	+	++	++	++	–	+	–	–
L	Bound	–	–	–	–	ND	ND	ND	ND
	Free	–	+	++	++	ND	ND	ND	ND

*representative of at least 10 separate experiments; ND = not done

that the Kamal *et al*.'s result is an artifact of inappropriate method. Taken together, our data may suggest that the differences between normal and immortal or cancer cells in terms of functional Hsp90 levels may be related to either its overall expression level or its subcellular location, rather than the client-binding status of Hsp90.

Chapter 4

Effect of Hsp90 Inhibition on Breast Cancer Sensitization

4.1 Introduction and Rationale

While breast cancer patients now have a wide range of therapeutics available to them, occurrence of the disease is still common and treatment challenges still remain. Chemotherapy and hormonal therapy have been valuable therapeutic options that are widely used to treat inoperable breast cancer and either pre- or postoperatively as part of a breast conserving surgery regimen. Since this type of treatment destroys both tumor and normal cells, it is not especially selective in killing and is thus associated with significant side effects.

Doxorubicin (Adriamycin®) has been a mainstay in the treatment of various solid tumors, including breast, ovary, liver, lung, and soft tissue sarcomas, and has been used as both a single agent and in combination therapies (Murphy *et al*., 1995; DeVita *et al*., 1993; Gewirtz, 1999). Additionally, novel platinum-based compounds are rapidly gaining research interest as cancer combatants. Cisplatin has exhibited anticancer activity in solid tumors such as those of testicular, ovarian, and advanced breast cancers (Rosenberg *et al*., 1965; Jordan and Carmo-Fonseca, 2000; Muggia, 2009; Martín, 2001). In addition to DNA damaging agents, microtubule stabilizing agents such as paclitaxel (Taxol®) have been successful as chemotherapeutic compounds, especially in the treatment of both early and advanced breast cancer. Since breast cancer initiation and progression are dependent on the production of estrogen, hormone therapy targeted against the estrogen receptor has also been developed as another therapeutic option. About 60% of breast cancers are positive for ER and so are responsive to estrogen-mediated growth signals (Putti *et al*., 2005). As a selective ER modulator, tamoxifen has been shown to inhibit tumor cell

proliferation by blocking the G1 to S phase transition in (ER+) MCF7 cells, which also display apoptotic morphology and DNA cleavage at a lower dose more rapidly than ER(-) MDA-231 breast cancer cells when treated with tamoxifen (Osborne *et al*., 1983; Perry *et al*., 1995). Furthermore, although it lacks activity in a portion of ER-positive cancers, tamoxifen acts as an effective antiestrogen by targeting ERα for degradation in ER-positive breast cancer cells (Wu *et al*., 2009).

As is evident from basic research and clinical studies, intrinsic and acquired resistance via a variety of mechanisms to these chemotherapeutic and anti-hormonal drugs is a major concern. Hence, more effective approaches are necessary since conventional therapy is typically associated with partial clinical responses and undesirable side effects, including the destruction of normal non-cancerous surrounding cells. Rational design of chemotherapeutic combinations may thus enhance antitumor activity and possibly overcome multidrug resistance, providing new therapeutic options that specifically target tumor cells.

Molecular chaperones aid in accurate protein assembly by prohibiting improper associations with other proteins as they assist in the maturation of their substrates or clients. These proteins are dramatically upregulated in times of stress, but are also present under normal basal conditions, thus highlighting their essential nature in cell viability. Heat shock protein 90 (Hsp90) is unique from other chaperones since it is critically involved in controlling the conformation, stability, function, and degradation of many oncogenic client proteins, thus determining their cellular fate (Beliakoff and Whitesell, 2004; Csermely *et al*., 1998). This chaperone is abundantly found in the cell, comprising 1-2% of total protein content even under non-stressed conditions, while in tumor cells, this percentage increases to approximately 4-6% (Chiosis and Neckers, 2006). Functionally, the Hsp90 multiprotein machinery, assists in cellular

trafficking, the remodeling of improperly folded client proteins, and the suppression of protein aggregation (Whitesell and Lindquist, 2005; Sarto *et al*. 2000). In this manner, client proteins achieve stability, allowing them to bind to ligands or undergo post-translational modifications to activate signaling pathways (Sharp and Workman, 2006). Currently, Hsp90 has been found to interact with over 200 clientele proteins, many of which are associated with cell signaling, including kinases, transcription factors, and hormone receptors. Thus, the role of Hsp90 in affecting the maturation of client proteins involved in signal transduction inherently implicates this chaperone in transformation and tumorigenesis. Hsp90 acts in conjunction with co-chaperones and other cofactors that stimulate or enhance its activity. The p23 co-chaperone has been studied for its role in breast cancer, although the majority of studies involving p23 focus on the relationship of this protein with steroid hormone receptors. Specifically, overexpression of p23 is associated with increased tumor grade and positively regulates the activity of the estrogen receptor, resulting in enhanced invasiveness of breast cancer cells without any effect on proliferation (Knoblauch and Garabedian, 1999; Oxelmark *et al*., 2006).

The intrinsic nature of heat shock proteins makes them especially relevant to a cell's defense against cancer initiation. Previous studies have reported an overexpression of Hsp90 in human breast cancer; however, only tumor specimens and breast cancer cell lines were examined (Pick *et al*., 2007). The preferential accumulation of Hsp90 in cancer cells also forms the basis for the unique sensitivity of tumor cells to Hsp90 inhibition. In particular, Hsp90 in cancer cells have a higher affinity for anti-Hsp90 compounds compared to that in normal cells, thus providing tumor selectivity via, as yet, an unknown manner (Kamal *et al*., 2003). In light of this finding, it is possible that malignant cells are more dependent on Hsp90-mediated stability and activation of oncogenic pathways than normal cells, and so are more sensitive to Hsp90

inhibitors (He *et al*., 2006; Vilenchik *et al*., 2004; Whitesell *et al*., 1992). The tumor selectivity of Hsp90 inhibitors allows it to act in a specific manner, and is thus considered a targeted therapy for cancer. Because of the dependence of Hsp90 function on ATP hydrolysis, Hsp90 inhibitors like radicicol interfere with this intrinsic activity by binding at the N-terminal ATP site. In this way, Hsp90-dependent client proteins can be tagged for ubiquitination and subsequently directed toward proteasomal degradation (Eleuteri *et* al., 2002; Pearl *et al*., 2008). Thus, Hsp90 inhibition has earned great interest as a promising approach for cancer therapy since many client proteins can be simultaneously targeted and disrupted (Goetz *et al*., 2003; Sharp and Workman, 2006).

Radicicol is also an antifungal antibiotic that is able to revert the transformed phenotype, such that transformed fibroblast cells treated with RAD undergo morphologic changes to resemble normal cells (Kwon *et al*., 1992). In fact, RAD has a higher affinity for Hsp90 and competes with GA for binding in the N-terminal domain (Schulte *et al*., 1998a). Furthermore, RAD is more potent in terms of blocking ATPase activity and prevents the association of the co-chaperone p23 with Hsp90 (Roe *et al*., 1999). In breast cancer cells, RAD has been shown to affect the level of Hsp90 client proteins (Schulte *et al*., 1998a). Other advantages of RAD include activity in GA-resistant cells and a lack of hepatotoxicity (Chiosis *et al*., 2003; Yamamoto *et al*., 2003).

Based on the findings in our first study, it is necessary to characterize the effects of Hsp90 inhibition in breast cancer cells. This entails the characterization of this inhibition by pharmacologic methods using radicicol. Studies utilizing radicicol as a means to examine the role of Hsp90 in cancer progression are far fewer in comparison to those employing geldanamycin. Pharmacologic inhibition is partly based on the idea that lack of functional Hsp90 may cause telomere erosion and/or dysfunction, leading to apoptosis in breast tumor cells.

Previous work in our lab has shown that M12 metastatic prostate cancer cells show a decline in cell growth upon Hsp90 inhibition that coincides with a transient reduction in telomerase activity and telomere erosion (Compton *et al*., 2001). However, it remains to be determined whether breast cancer cells also behave in a similar manner.

In addition to the Hsp90 inhibitor alone, various combinations of radicicol with other chemotherapeutics will provide insight on the possibility of sensitization of breast cancer cells. Because nonspecific cytotoxicity is associated with these standard regimens, inhibiting Hsp90 before initiating conventional therapy may help reduce the amount of exposure, drug dose, or duration of treatment, potentially leading to a better response with fewer side effects. Chemotherapeutic and hormonal drugs utilized in the combination treatments include adriamycin, cisplatin, taxol, and tamoxifen, all of which are currently used to treat breast cancer. The goal of the following experiments is to define and characterize the consequences of Hsp90 inhibition specifically on cellular proliferation, telomerase stability and function, telomere length, expression of client proteins, and ultimately on senescence or apoptosis.

4.2 Results

4.2.1RAD affects cellular proliferation and telomerase activity in breast cancer cells.

Since Hsp90 inhibition in breast cancer progression is not well defined, we wanted to begin our assessment of the effect of radicicol (RAD) on the ability of tumor cells to continuously proliferate. The human breast adenocarcinoma MCF7 cell line was used for the majority of studies because it is an established, well-characterized cell line that is routinely used as an *in vitro* breast cancer model. MCF7 cells were initially treated with RAD at 0.1 μM, 0.3 μM, 1 μM, 3 μM, and 10 μM for either 24 hr or 48 hr. Upon completion of treatment at each time

point, cells were harvested and cell growth was assessed. It is evident that MCF7 cells display a dose-dependent growth effect upon RAD treatment, such that cellular proliferation begins to display a reduction even at the lowest concentration tested (Figure 21). At each time point, 24 hrs or 48 hrs, there is a steady decline in population doubling as the RAD concentration increases, with the highest concentrations of RAD eliciting the greatest effect on growth. Specifically, at 0.3 μM, 1 μM, 3 μM, and 10 μM, MCF7 cells are undergoing cell death, reflected as significant negative population doublings. Interestingly, MCF7 cells begin to display aberrant growth effects at 0.1 μM RAD, whereas M12 prostate cancer cells require a higher dose (0.3 μM) to elicit an Hsp90 inhibition-mediated growth reduction (Compton *et al*., 2001).

The assembly of the active form of the ribonucleoprotein enzyme telomerase has been shown to require the assistance of various chaperones. Hsp90 and p23 specifically aid in this process by mediating the joining of the hTERT catalytic subunit and its internal RNA template, hTR. As telomerase is folded into the active state, Hsp70, Hsp40, and HOP dissociate from the initial complex while Hsp90 and p23 remain stably associated with the final product (Figure 22). Because this association is necessary for efficient and functional telomerase assembly, we wanted to determine whether inhibition of Hsp90 adversely affected its activity. MCF7 cells were treated with various RAD concentrations as just described above and harvested at 4 hr, 24 hr, and 48 hrs post-treatment.

As shown in Figure 23, telomerase activity, as measured by the TRAP assay, shows a steady decline over time with RAD treatment as compared to non-treated cells. At each RAD concentration, the intensity of the laddering effect progressively decreases with increasing post treatment time. This decrease in telomerase activity is not dose-dependent (i.e. activity does not decrease or increase according to RAD dose), but rather, it appears that the effect on

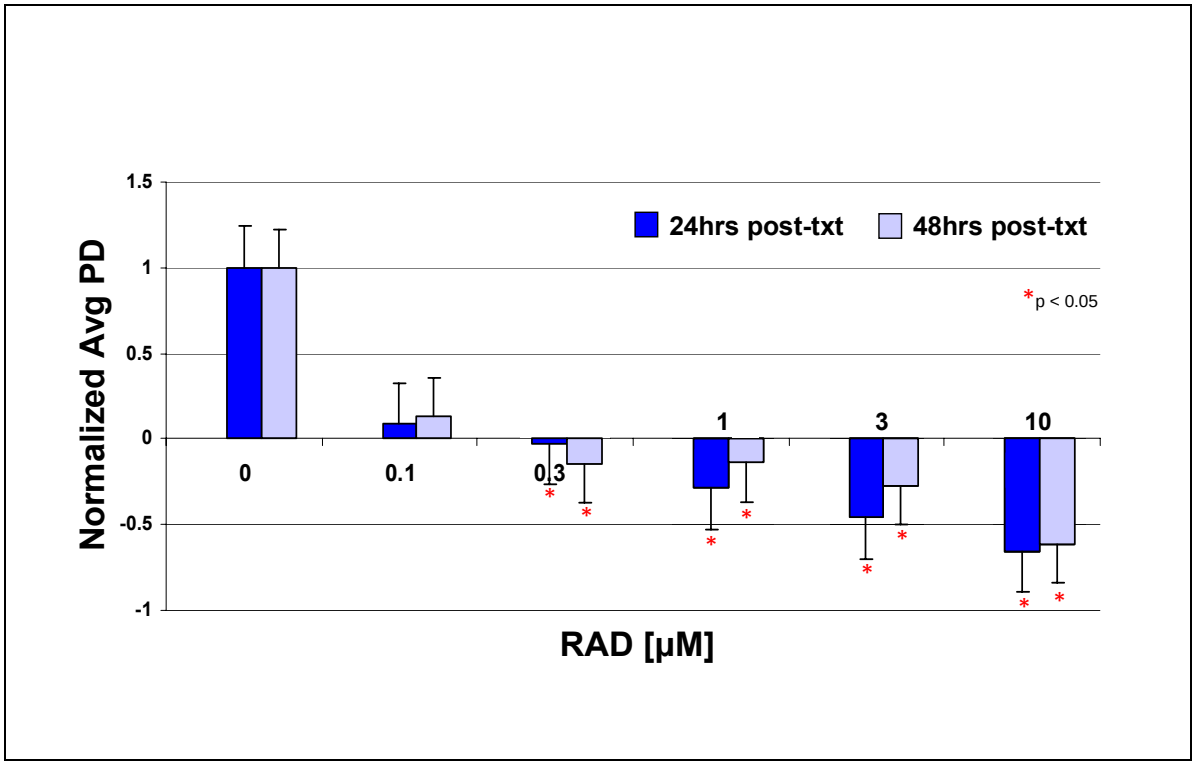

Figure 21: Cell growth decreases with increasing RAD concentrations. Breast cancer MCF7 cells were treated for 48 hrs with RAD at varying concentrations, including high doses of 3 μM and 10 μM. For each RAD concentration, cells were treated and harvested at 24 hr or 48 hr post-treatment. Cells at each time point were counted in triplicate and population doubling (PD) calculated as described in the Methods section. Untreated MCF7 cells served as the negative control and this PD was set to a value of 1, to which all other PDs were normalized. Results represent at least 3 individual experiments. Asterisks (*) denote significant reduction ($p < 0.05$) in PD as compared to untreated cells.

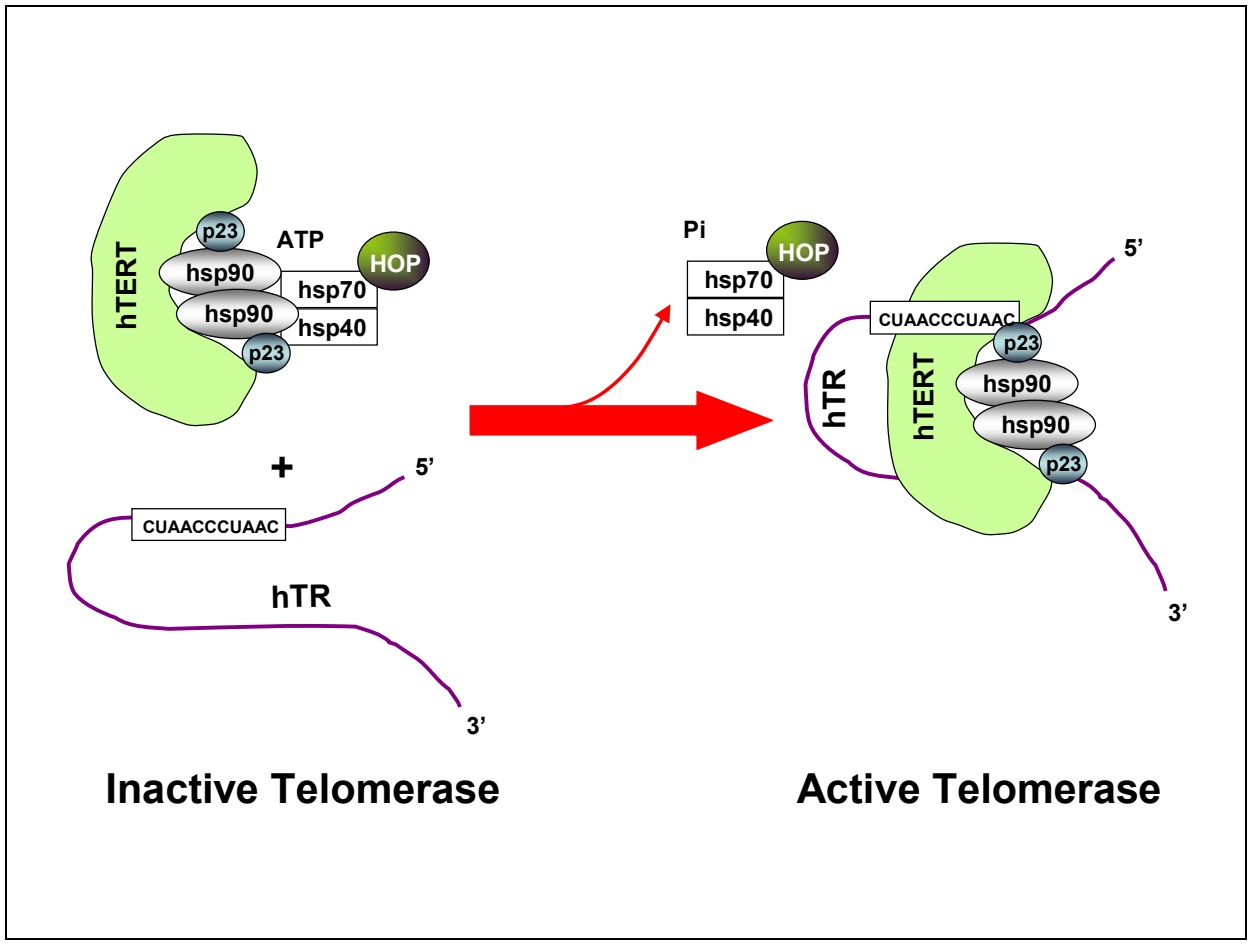

Figure 22: Assembly of telomerase. The assembly of the active form of the ribonucleoprotein enzyme telomerase has been shown to require the assistance of various chaperones. Hsp90 and p23 specifically aid in this process by mediating the joining of the hTERT catalytic subunit and its internal RNA template, hTR. As telomerase is folded into the active state, Hsp70, Hsp40, and HOP dissociate from the initial complex while Hsp90 and p23 remain stably associated with the final product. Adapted from Forsythe *et al*., 2001.

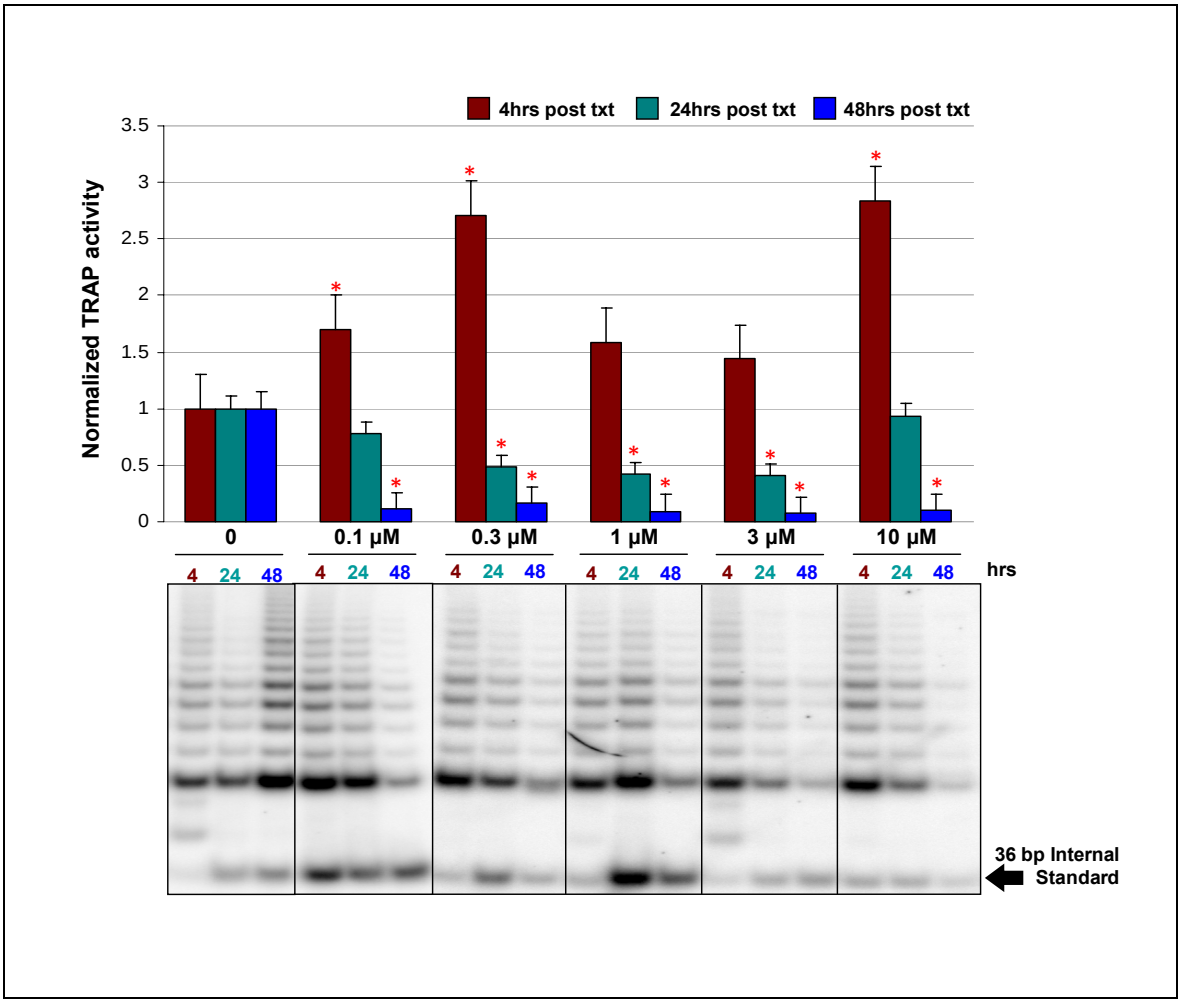

Figure 23: Radicicol-responsive telomerase activity. Breast cancer MCF7 cells were treated for 48 hrs with RAD at varying concentrations, including higher doses of 3 μM and 10 μM. For each RAD concentration, cells were harvested at 4 hr, 24 hr, and 48 hr post-treatment and subjected to analysis of TRAP activity. The PCR-based TRAP assay measures telomerase activity in comparison to the amplification of the 36 bp internal standard. The characteristic laddering effect reflects the variability in size of TRAP products. TRAP activity was quantitated and average values were normalized to untreated cells. Results representative of 3 individual experiments. Asterisks (*) denote significant changes ($p < 0.05$) in telomerase activity compared to no treatment.

activity is time-dependent. In general, 4 h post-treatment is associated with erratic telomerase activity, with only relatively lower RAD concentrations (0.1 μM and 0.3 μM) and the highest concentration (10 μM) eliciting significant changes. At 24 h post-treatment, middle range RAD concentrations produce significant reductions in TRAP activity, while at 48 h post-treatment, all RAD doses lead to considerable decreases in activity. It is important to note that although cell death is evident after treatment, only adherent cells were harvested for the TRAP assay (i.e. no floating cells).

Because MCF7 cells displayed great sensitivity in terms of growth inhibition and downregulation of telomerase activity to RAD treatment in the range of 0.1 μM to 10 μM, it is possible that these concentrations were too toxic for cell viability. In this case, long-term treatment with RAD may instead induce non-specific effects on cellular proliferation. In order to identify a working RAD concentration for future chronic studies, MCF7 cells were treated with lower doses of RAD, specifically, 0.01 μM and 0.03 μM. At these concentrations, MCF7 cells again display a dose-dependent growth decline at 24 h and 48 h post-treatment (Figure 24). Although cells are still in the log phase of growth (positive population doubling), proliferation rate nevertheless appreciably decreases in this lower RAD range. This is in contrast to the predominantly negative population doubling (death) at high RAD concentrations. Treatment with lower RAD doses also affects telomerase activity. At 0.03 μM, telomerase activity progressively declines over time, while treatment with 0.01 μM shows a transient effect on activity (Figure 25). Importantly, only treatment with 0.03 μM RAD significantly causes both a decline in cell growth without inducing toxicity-related cell death and a reduction in telomerase activity at all post-treatment times. Based on these collective negative effects, the RAD concentration of 0.03 μM was designated for chronic and combinational studies.

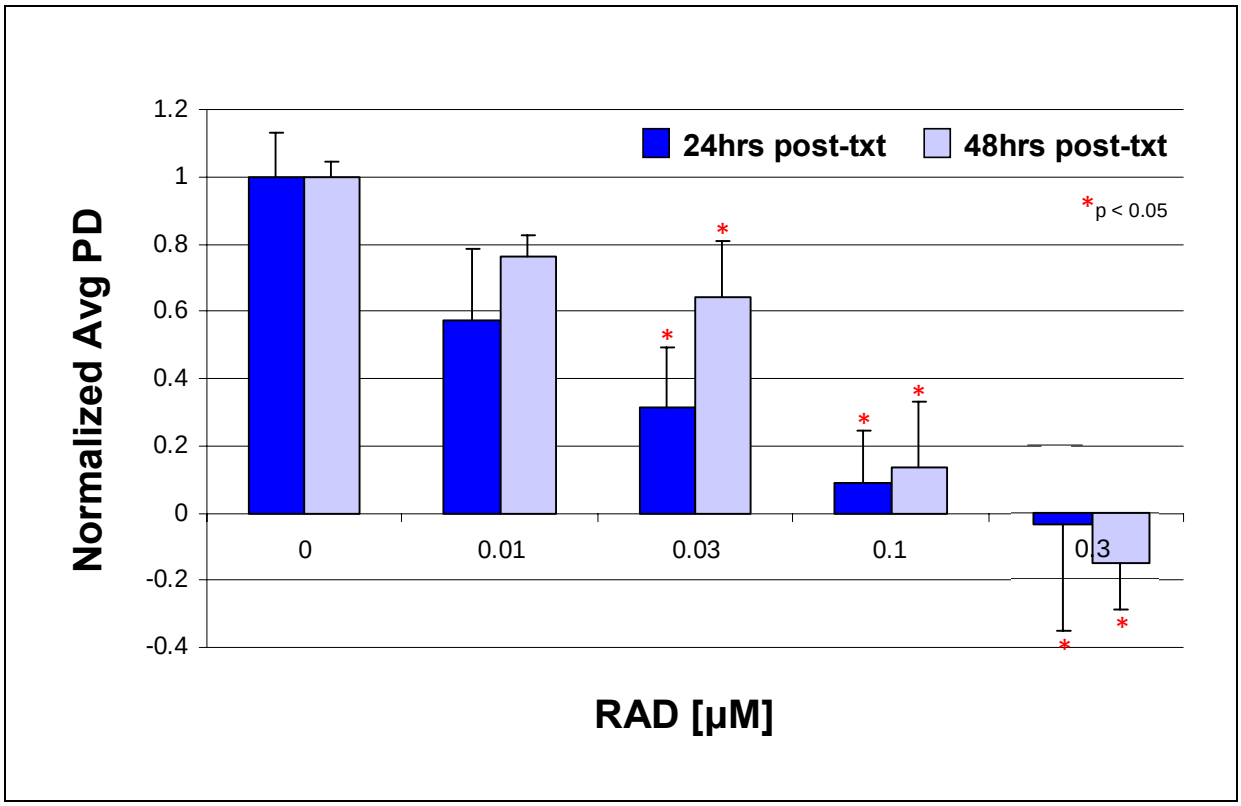

Figure 24: RAD-dependent cell growth at low RAD doses. Breast cancer MCF7 cells were treated with lower RAD concentrations for 48 hrs and harvested at 24 hr or 48 hr post-treatment. Even at very low concentrations, proliferation of MCF7 cells are negatively affected. Cells at each time point were counted in triplicate and population doubling (PD) calculated as described in the Methods section. MCF7 that were not treated served as the control and this PD was set to a value of 1, to which all other PDs were normalized. Results representative of 3 individual experiments. Asterisks (*) denote significant reduction ($p < 0.05$) in PD as compared to untreated cells.

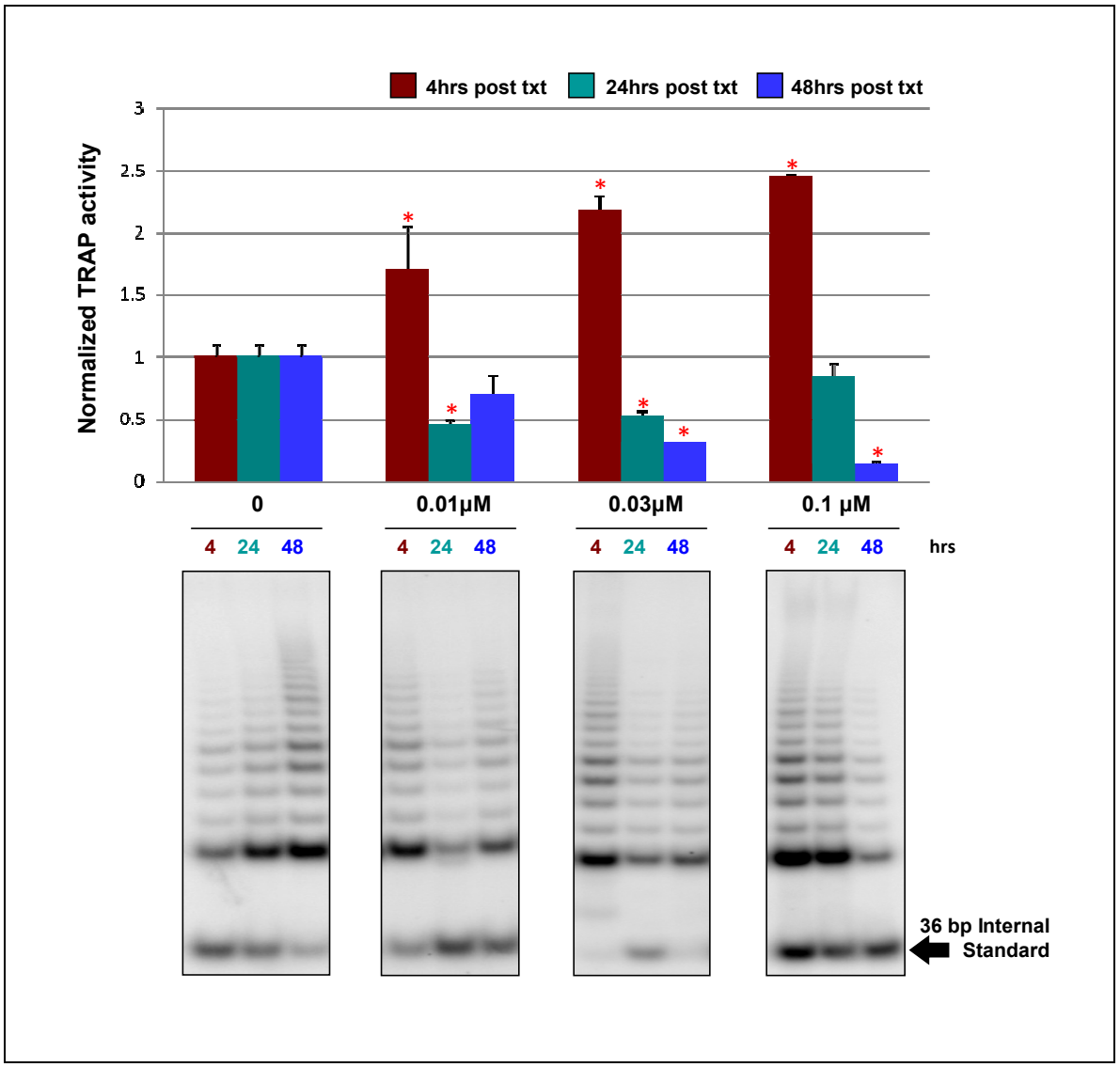

Figure 25: Telomerase activity declines at lower RAD concentrations. Breast cancer MCF7 cells were treated for 48 hrs with RAD at varying concentrations, including lower doses of 0.01 μM and 0.03 μM. For each RAD concentration, cells were harvested at 4 hr, 24 hr, and 48 hr post-treatment and subjected to analysis of TRAP activity. Again, the characteristic laddering effect was quantitated against the 36 bp internal standard and average values normalized to untreated cells. Results representative of 3 individual experiments. Asterisk (*) denotes significant changes ($p < 0.05$) in telomerase activity compared to no treatment.

4.2.2 RAD and Adr in combination more than additively alters growth properties.

Although effective in modulating cancer cell proliferation, Hsp90 inhibition alone may not be a practical course of treatment in combating breast cancer. The ability of RAD to act as an adjuvant or supplementary form of therapy was determined in combination studies with the established chemotherapeutic, Adriamycin. MCF7 cells were pretreated with 0.03 μM RAD for 48 hr, followed sequentially by acute treatment with a range of Adr concentrations, including 0.0075 μM, 0.025 μM, 0.075 μM, 0.25 μM, and 0.75 μM. At 2 d and 4 d after completion of this treatment series, cell growth was determined to be differentially affected.

For those cells treated with Adr alone, mean cell count decreases with increasing Adr concentration at both collection time points (Figure 26, black bars). MCF7 cells pretreated with 0.03 μM RAD display an even greater decline in average cell counts at both time points when compared to singly Adr-treated cells (Figure 26, grey bars). At 2 d post-treatment, cells display a significant reduction in cell number when pretreated with RAD in combination with Adr at 0.025 μM, 0.075 μM, and 0.25 μM (Figure 26A), while at 4 d, significant growth defects occur at 0.0075 μM, 0.025 μM, and 0.075 μM Adr, when compared against Adr only treated cells (Figure 26B). A comparison of growth at each concentration tested shows that 4 d cell counts are always less than 2 d cell counts. Interestingly at 4 d, the significant decreases in cell numbers upon RAD pretreatment at a given Adr concentration is greater than the effect of either agent acting independently, suggesting a more than additive response.

Examination of population doubling supports the observed change in cell numbers. For those cells treated with Adr only, population doubling generally decreases with increasing Adr concentration at both 2 d and 4 d post-treatment (Figure 27, black bars). Cells pretreated with RAD prior to initiation of Adr exposure display an even more pronounced growth reduction

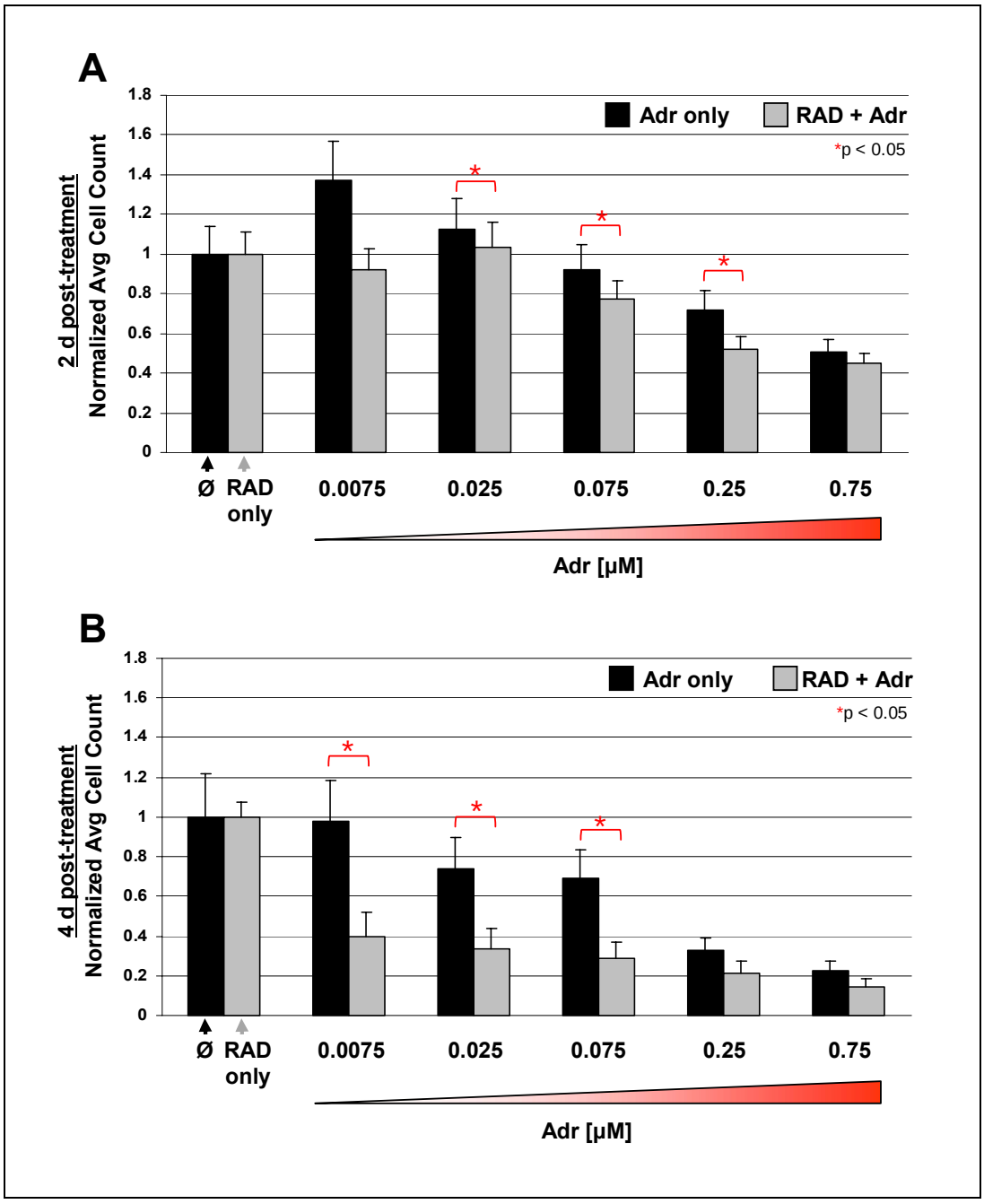

Figure 26: Average cell counts decrease in the presence of RAD pretreatment. MCF7 cells were either treated with Adr alone in increasing concentrations for 2 hr (black bars) or with 48 hr of 0.03 μM RAD pretreatment prior to initiating a 2 h Adr treatment (grey bars). Cells were harvested at 2 d (A) or 4 d (B) post-treatment and counted in triplicate. MCF7 cells that were not treated or only treated with RAD served as the control for Adr only or RAD + Adr, respectively. These PDs were set to a value of 1, to which all other PDs were normalized. Results representative of at least 3 experiments. Asterisks denote significant reduction ($p < 0.05$) in PD as compared to untreated or RAD only cells.

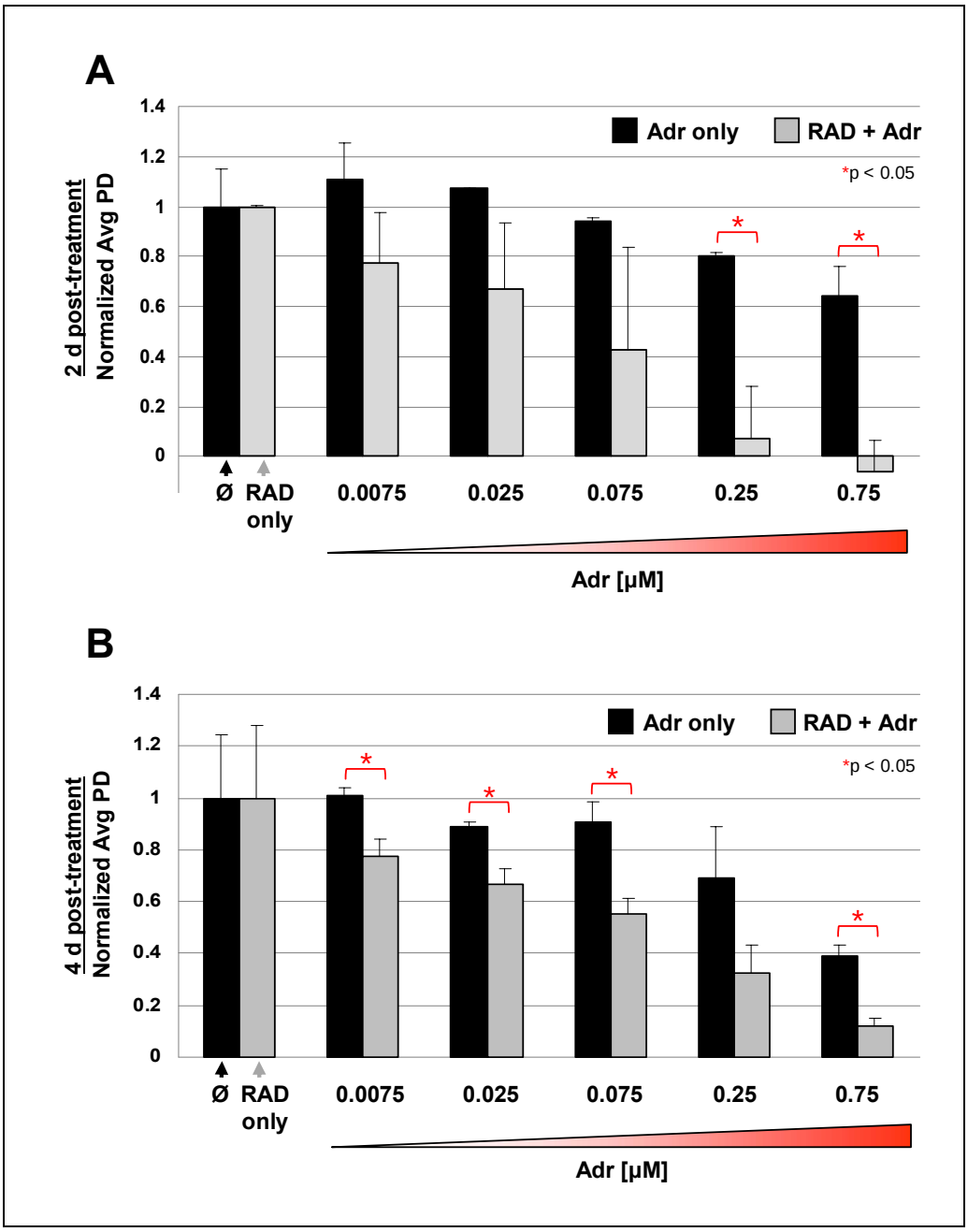

Figure 27: Greater decline in population doubling with RAD and Adr combination treatment. Breast cancer MCF7 cells were either acutely treated with increasing concentrations of Adr ranging from 0.0075 μM to 0.75 μM (black bars) or pretreated with 0.03 μM RAD for 48 hrs followed by acute Adr treatment in the same range (grey bars). Cells were harvested at 2 d (A) or 4 d (B) post-treatment, counted in triplicate and population doubling (PD) calculated. MCF7 cells that were not treated or only treated with RAD served as the control for Adr only or RAD + Adr, respectively. These PDs were set to a value of 1, to which all other PDs were normalized. Results representative of at least 3 experiments. Asterisks denote significant reduction ($p < 0.05$) in PD as compared to untreated or RAD only cells.

(Figure 27, grey bars). At 2 d, mean PD declines by 30%, 37%, and 55% when sequentially treated with RAD and Adr at 0.0075 μM, 0.025 μM, and 0.075 μM Adr, respectively, although these averages are not statistically different from Adr only treated cells (Figure 27A). However, RAD pretreatment followed by exposure to higher concentrations of Adr at 0.25 μM and 0.75 μM does significantly reduce cell growth by 91% and over 100%, respectively. At 4 d, RAD with all Adr combinations except 0.25 μM induces a significant reduction in population doubling compared to Adr alone (Figure 27B). It is notable that for both 2 d and 4 d post-treatment, pretreatment with RAD followed by higher Adr concentrations leads to a more than additive diminution of cell growth. Collectively, these cell count and population doubling data suggest that a more than additive, perhaps, synergistic effect may exist since growth is affected significantly more with RAD pretreatment than with either Adr or RAD alone.

4.2.3 RAD and Adr in combination affects cell fate and the expression of cell cycle-associated proteins and HSPs.

The transcription factor, p53, is so intimately linked to carcinogenesis that its role in modulating tumorigenic potential and the cellular response to DNA damage is indisputable. Because of its ability to regulate the cell cycle, we wanted to determine whether the observed growth alterations coincide with changes in p53 expression. MCF7 cells were again either treated with Adr alone using the same range of concentrations for 2 hrs or pretreated with RAD for 48 h. Acute treatment with Adr induces an appreciable upregulation of p53 total protein expression and a corresponding increase in the total protein levels of its downstream effector, $p21^{Waf1/Cip1}$ (Figure 28A). Pretreatment with RAD prior to Adr exposure also stimulates overexpression of p53 and $p21^{Waf1/Cip1}$, although the response is not as robust as in singly treated cells (Figure 28B).

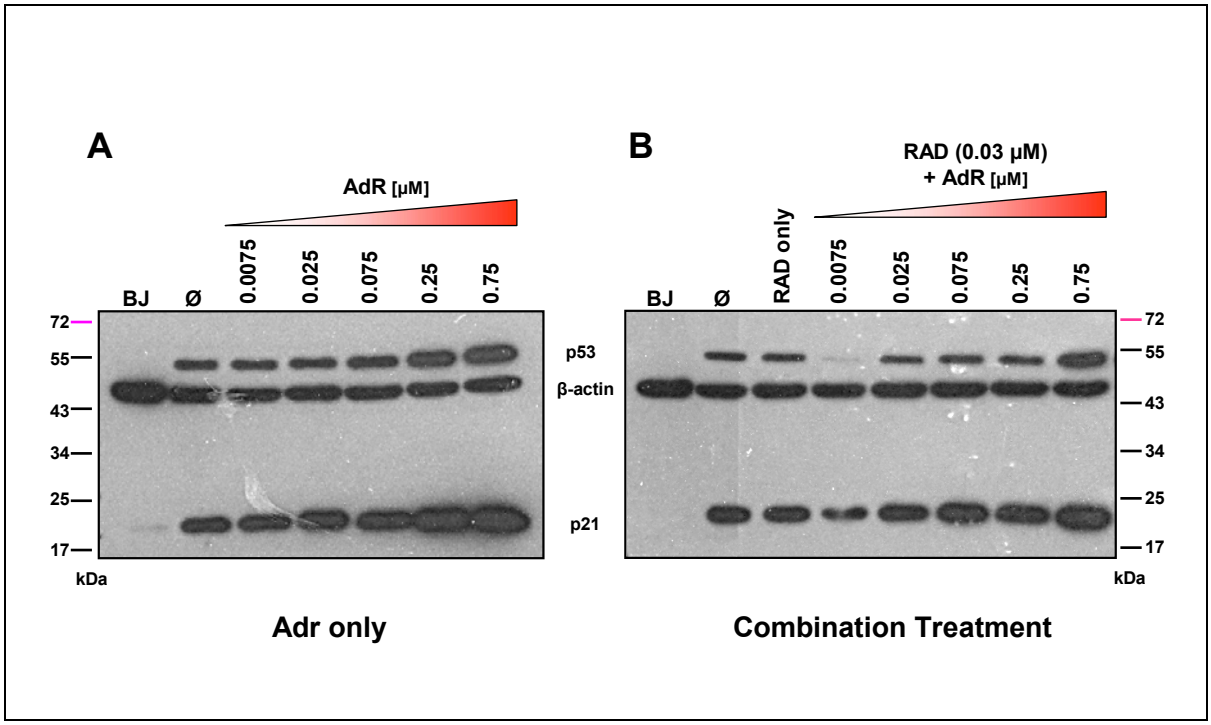

Figure 28: Induction of p53 and p21 upon single agent and combination treatments. MCF7 cells were either acutely treated with various concentrations of Adr (A), ranging from 0.0075 μM to 0.75 μM, or pretreated with 0.03 μM RAD for 48 hrs followed by acute Adr treatment in the same range (B). Cells were harvested at 4 d post-treatment and western analysis performed on 50 μg of total protein lysate. Immunblot was probed with anti-p53 and anti-p21 antibodies. β-actin served as the loading control. For both blots, lane 1 represents untreated normal fibroblasts and lane 2 is untreated MCF7 cells. In blot B, lane 3 represents RAD only treated MCF7 cells.

Upon closer inspection, single agent-treated cells display an elevation in $p21^{Waf1/Cip1}$ protein levels that is more dramatic with increasing Adr dose than the upregulation of p53 levels (Figure 29-30, black bars). Namely, p53 levels on average increase 23% with each successive increase in Adr dose, while $p21^{Waf1/Cip1}$ levels increase by 43%. A similar trend exists for RAD and Adr combination treated cells, as p53 levels increase by 31% and $p21^{Waf1/Cip1}$ levels increase by 37% with increasing Adr dose (Figure 29-30, blue bars).

Based on the finding that p53 and p21 protein levels increase in response to Hsp90 inhibition and that these changes coincide with growth aberrations, it was necessary to identify any corresponding effects on cell cycle regulatory proteins. Of these proteins, the cyclin-dependent kinase, Cdk4, in concert with cyclin D, controls the G1 to S phase transition, which is commonly deregulated in cancer (Deshpande *et al*., 2005). Adr singly treated MCF7 cells display reduced Cdk4 protein levels at 0.25 μM and an even greater decrease at 0.75 μM, compared to untreated cells (Figure 31). Pretreatment with 0.03 μM RAD followed by acute Adr treatment also results in a downregulation of Cdk4 protein expression (Figure 32). Compared to untreated MCF7 cells, treatment with RAD only induces a slight decrease in Cdk4 expression, which remains constant in MCF7 cells treated in combination with 0.0075 μM, 0.025 μM, and 0.075 μM. However, upon treatment with relatively higher Adr doses, 0.25 μM and 0.75 μM, there is an even greater reduction in Cdk4 protein levels. Furthermore, regardless of treatment, MCF7 cells consistently display enhanced Cdk4 levels when compared to normal BJ fibroblasts, which have an almost undetectable level of Cdk4. Thus, the overexpression of the cell cycle inhibitory proteins, p53 and p21, corresponds to a downregulation of the cell cycle stimulating factor, Cdk4, although this is likely unaffected by Hsp90 inhibition.

Since the Hsp90 chaperone machinery exists as a multiprotein complex, the next step was

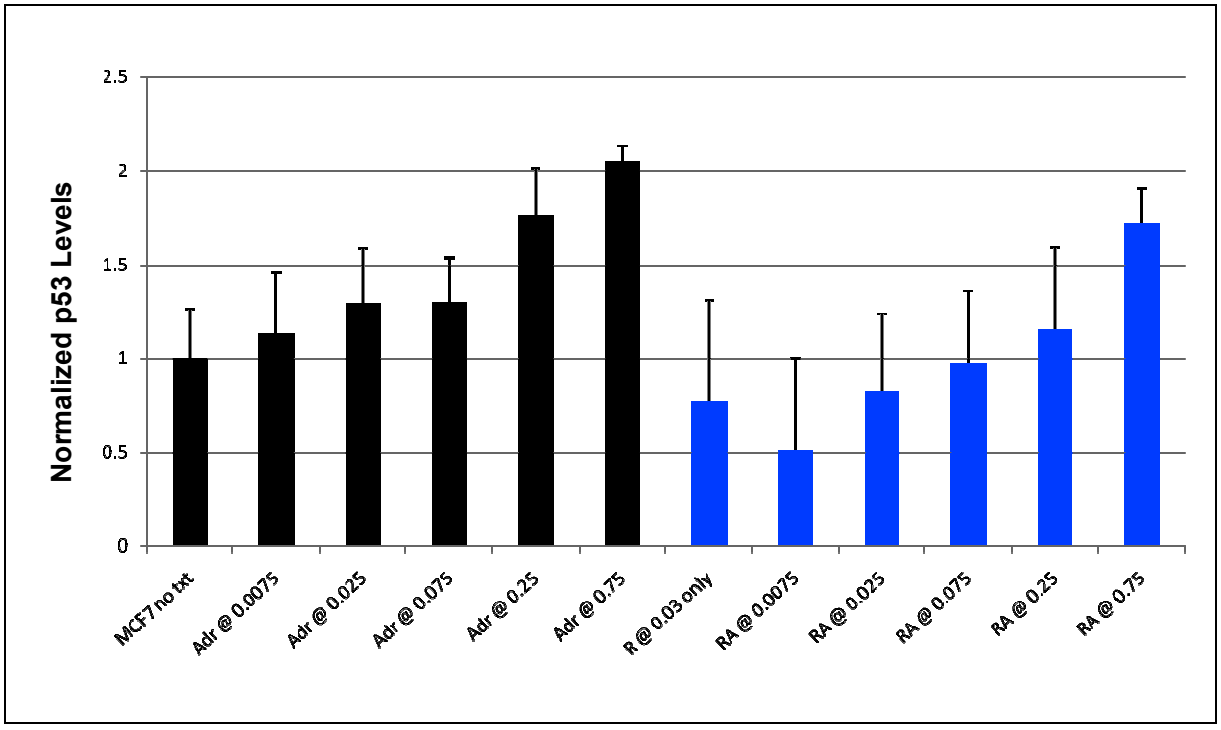

Figure 29: Greater induction of p53 upon Adr alone treatment. Quantitation of p53 levels in MCF7 cells treated with Adr alone (black bars) or in combination with RAD (blue bars). Western blots for p53 were ran three times and the average value calculated, designating untreated cells as the control. This p53 value was set to 1, to which all other values were normalized. The protein level of p53 is consistently higher in Adr only treated cells than in Adr and RAD treated cells at each specific Adr concentration.

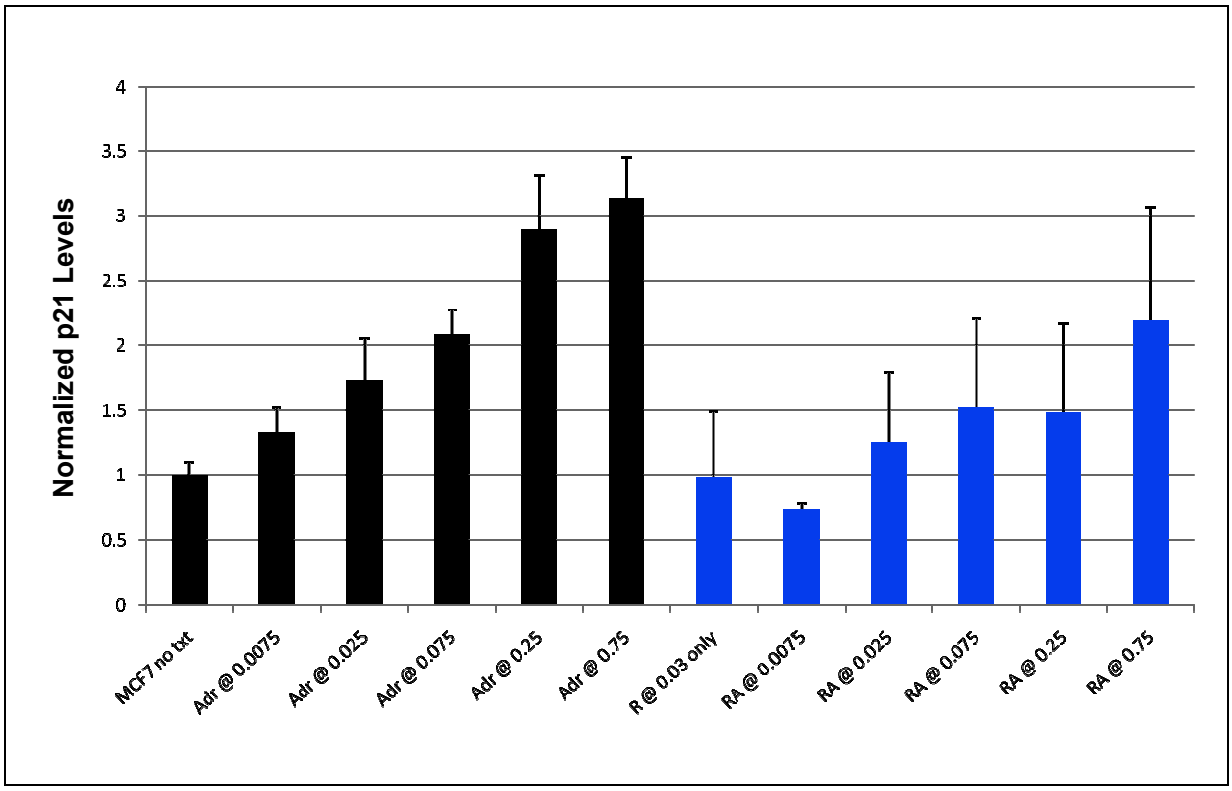

Figure 30: Greater induction of p21 levels upon Adr alone treatment. Quantitation of p21 levels in MCF7 cells treated with Adr alone (black bars) or in combination with RAD (blue bars). Western blots for p21 were ran three times and the average value calculated, designating untreated cells as the control. This p21 value was set to 1, to which all other values were normalized. The protein level of p21 is consistently higher in Adr only treated cells than in Adr and RAD treated cells at each specific Adr concentration. The levels of p21 are appreciably lower in Adr and RAD treated cells than in Adr alone cells. This differential expression is more dramatic than for p53.

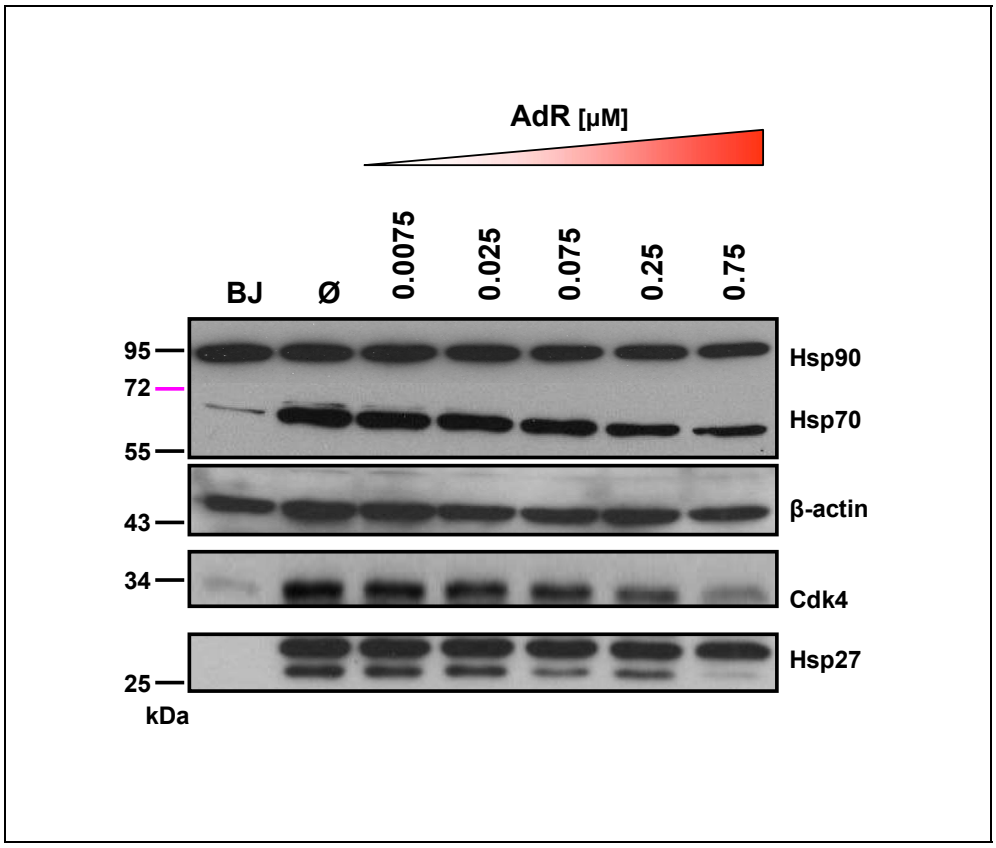

Figure 31: Expression of cochaperones and a cell cycle-regulatory protein in Adr treated cancer cells. Breast cancer cells were acutely treated with 0.0075 μM, 0.025 μM, 0.075 μM, 0.25 μM, and 0.75 μM Adr for 2 hrs. Cells were harvested at 4 d post-treatment and 50 μg of total protein lysate was subjected to western analysis. Immunoblot was probed with antibodies against Hsp90, Hsp70, Cdk4, and Hsp27. β-actin served as the loading control. Lane 1 represents untreated normal fibroblasts (BJ), lane 2 is untreated MCF7 cells, and lanes 3-7 are treated MCF7 cells.

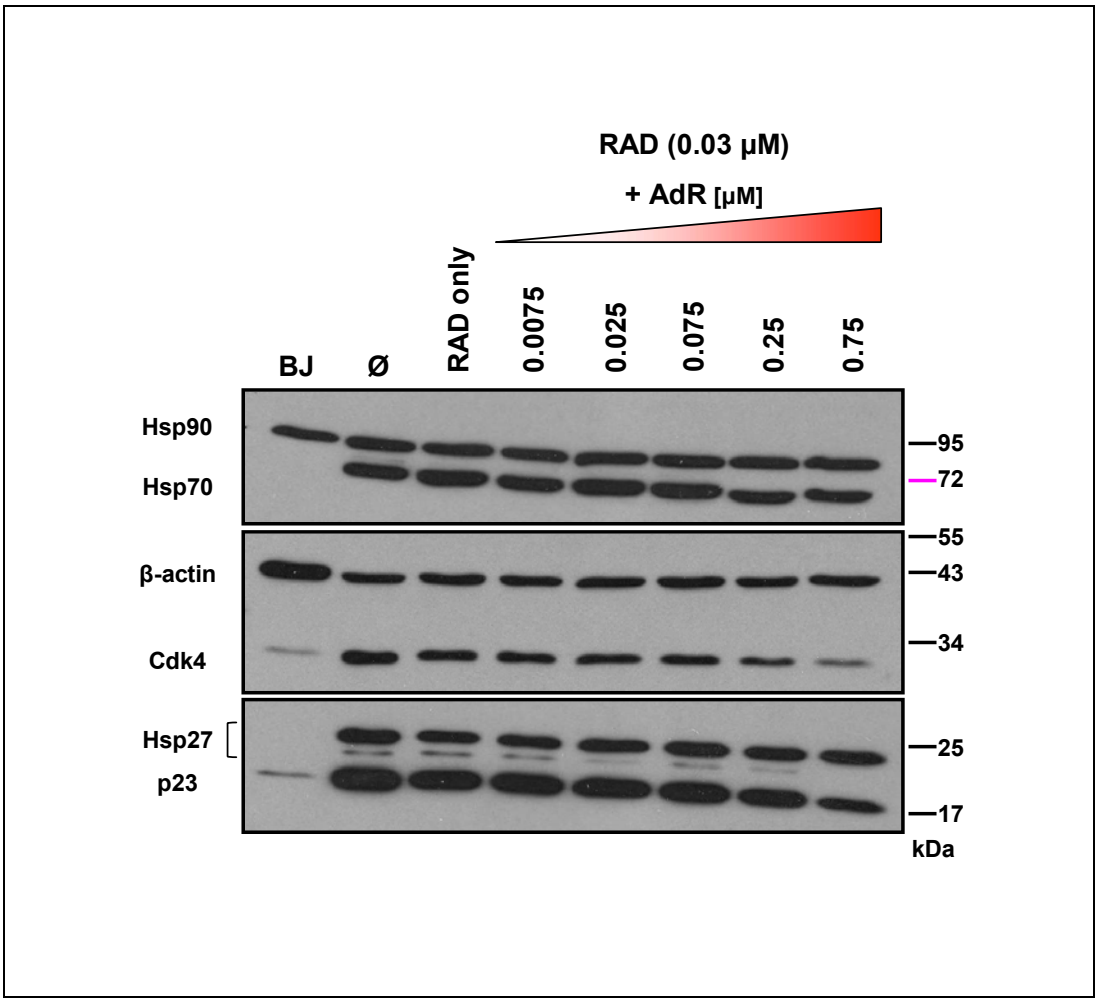

Figure 32: Expression of cochaperones and a cell cycle-regulatory protein in RAD and Adr treated cancer cells. Breast cancer cells were pretreated with 0.03 μM RAD for 48 hrs followed by treatment with 0.0075 μM, 0.025 μM, 0.075 μM, 0.25 μM, and 0.75 μM Adr for 2 hrs. Cells were harvested at 4 d post-treatment and 50 μg of total protein lysate was subjected to western analysis. Immunoblot was probed with antibodies against Hsp90, Hsp70, Cdk4, Hsp27, and p23. β-actin served as the loading control. Lane 1 represents untreated normal fibroblasts, lane 2 is untreated MCF7 cells, lane 3 represents RAD only treatment in MCF7 cells, and lanes 4-8 are RAD and Adr treated MCF7 cells.

to determine the effect of Hsp90 inhibition on the expression of these cofactors. As shown in Figures 31-32, Hsp90 is abundant in both normal and breast cancer cells and its protein expression is not affected by Adr or RAD treatments. However, expression of Hsp70 does appear to be affected with both single agent and combinational drugs. Treatment with Adr only leads to an appreciable downregulation of Hsp70 at 0.25 μM and 0.75 μM (Figure 31). Similarly, RAD pretreatment is also associated with a reduction in Hsp70 protein in combination with 0.25 μM and 0.75 μM Adr, although this reduction is not as robust (Figure 32). Although Hsp27 is not a component of the Hsp90 chaperone complex, its expression was also assessed because of its role as a major responder to cell stress. We show here that Hsp27 levels do not change greatly in either singly treated or combinationally treated cells. Taken together, protein levels of the Hsp90 co-chaperones, Hsp70 and p23, are moderately affected, but the level of the Hsp90 independently-acting chaperone, Hsp27, are not affected by Hsp90 inhibition.

4.2.4 Radicicol pretreatment elicits a stronger senescence response but no apoptotic response.

Because of the negative effect of RAD treatment on telomerase activity, we wanted to determine whether telomere length was also affected by Hsp90 inhibition. Genomic DNA was isolated from treated and untreated cells, thoroughly digested, and telomere fragments resolved on an agarose gel. The heterogeneity in length of telomere fragments is reflected in the smeared appearance of the TRF gel. According to the distribution of bands within each lane, there is no apparent difference in the range of telomere lengths between Adr treated and RAD pretreated cells (Figure 33). The telomere length in both treatment groups ranges between about 2.0 kb and less than 4.3 kb. However, it is important to recognize that this assay only assesses global

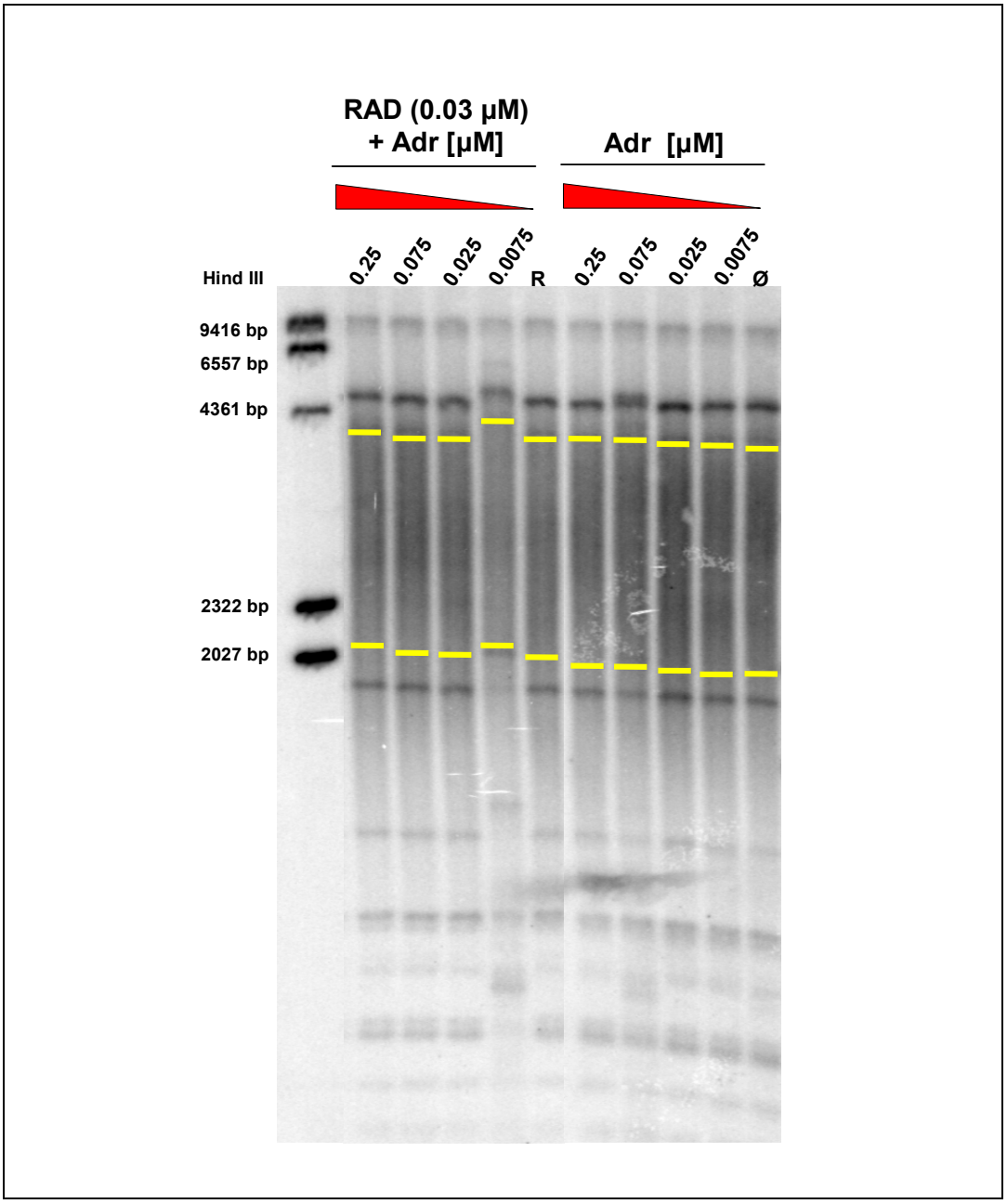

Figure 33: No change in overall telomere length upon drug treatment. Telomere length was assessed in MCF7 cells treated with Adr alone in a range of 0.0075 µM to 0.75 µM or in combination with 0.03 µM RAD. Genomic DNA from each sample was isolated, of which, 8-10 µg was digested and subjected to a TRF assay, which radiolabels telomeric ends using a G-rich telomere specific $(TTAGGG)_4$ probe. The Adr concentration of 0.75 µM was not able to be assessed due to lack of substantial DNA. The characteristic smeared appearance of the bands are a reflection of the heterogeneity in telomere length. The average range of telomere length is demarcated by yellow bars in each lane.

telomere length, accounting for the average telomere length in the cell, which does not exclude the possibility that chromosome-specific telomere length alterations may exist.

Although there were no changes in telomere length in both singly treated and combinationally treated cells compared to untreated cells, we wanted to assess whether a senescent phenotype existed in these cells. Due to the observed decrease in cell growth and population doubling, as well as the reduction in Cdk4 expression, it is possible that these cells are undergoing irreversible growth arrest in the absence of telomere shortening. Indeed, MCF7 cells treated with 0.075 μM and 0.75 μM Adr stain positively for senescence-associated β-galactosidase (SA-β-gal) activity (Figure 34C, E). Although many cells appear to be reactive to β-gal substrate (blue colored cells), they are not necessarily senescent. The criteria thus used are two-fold; cells must both be positively stained as well as display morphologic changes associated with the senescent phenotype. As denoted by the arrows, senescent cells assume a flattened appearance with a large nucleus to cytoplasm ratio. Proliferating MCF7 cells, in contrast, are much smaller and display a characteristic "cobblestone" shape. Based on these criteria, pretreatment with 0.03 μM RAD prior to Adr exposure similarly induces morphological changes and produces more SA-β-gal positive cells than with Adr alone (Figure 34D, F). Untreated cells also contain β-gal substrate reactive cells, but the morphology of these cells is not consistent with a senescent phenotype (Figure 34A). Quantitation of SA-β-gal activity shows an increase in the number of senescent cells with Adr as compared to untreated cells (Figure 35). At 0.075 μM Adr, there are approximately 1.5x more senescent cells, and at 0.75 μM, there is 3.35x more, when the number of untreated senescent cells is set to a value of 1. RAD only exposure induces 2.5x more senescent cells than untreated cells and this number increases when Adr is also added to the series, with 0.75 μM Adr eliciting more than 4x more positive cells. Furthermore, at 0.075

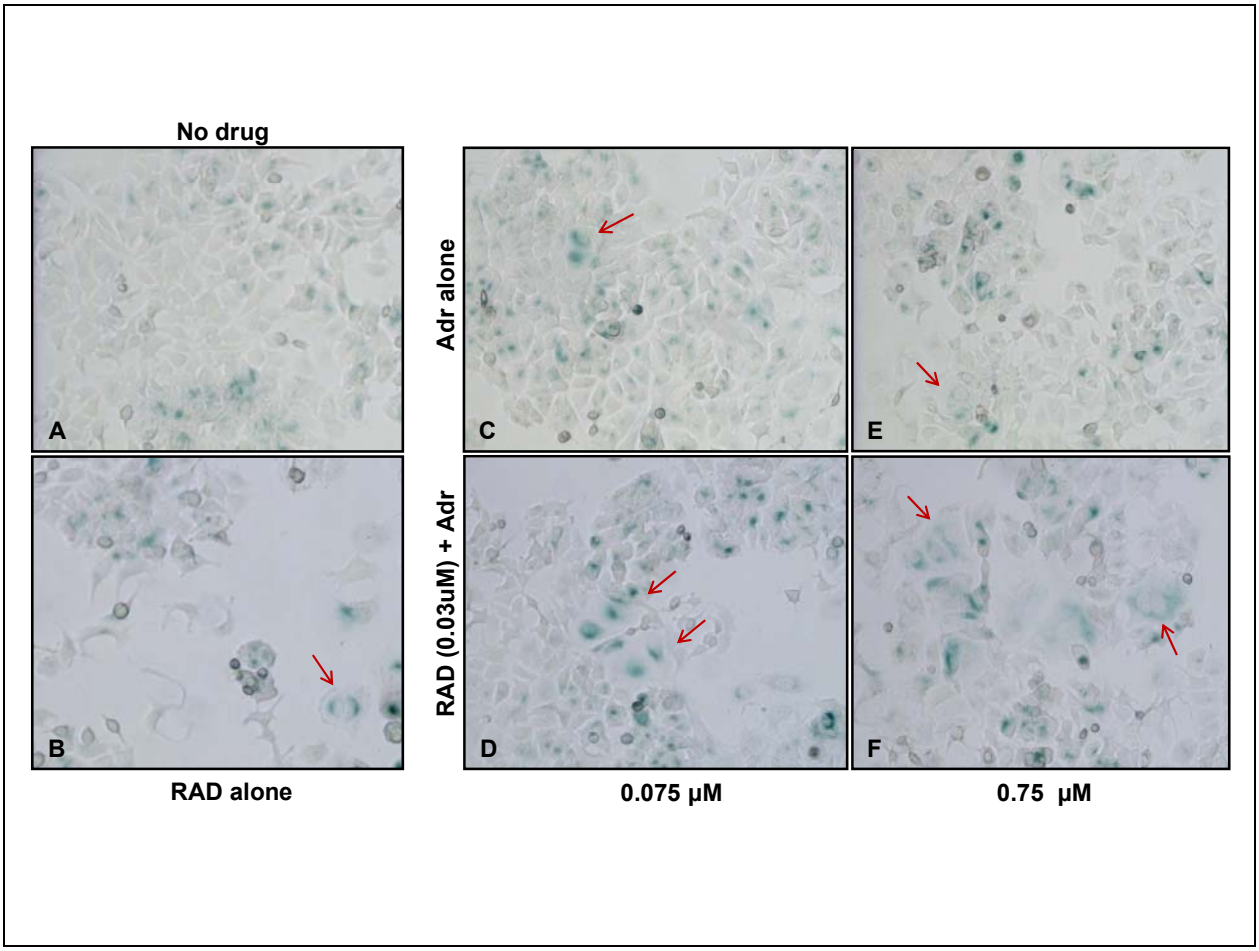

Figure 34: Drug treated cells exhibit positive senescence-associated β-gal staining. Breast cancer MCF7 cells were either acutely treated with 0.075 µM and 0.75 µM Adr for 2 hrs or pretreated with 0.03 µM RAD for 48 hrs followed by acute Adr treatment. At 2 d post-treatment, cells were fixed and stained for β-galactosidase activity, as a marker for senescence. Although untreated cells contain β-gal positive cells (A), the morphology of these cells is not consistent with senescence. Treatment with Adr (C, E) induces the appearance of senescent cells, as does treatment with RAD alone (B) and RAD + Adr (D, F). Arrows identify senescent cells based on positive staining and morphology. All images obtained at 40x.

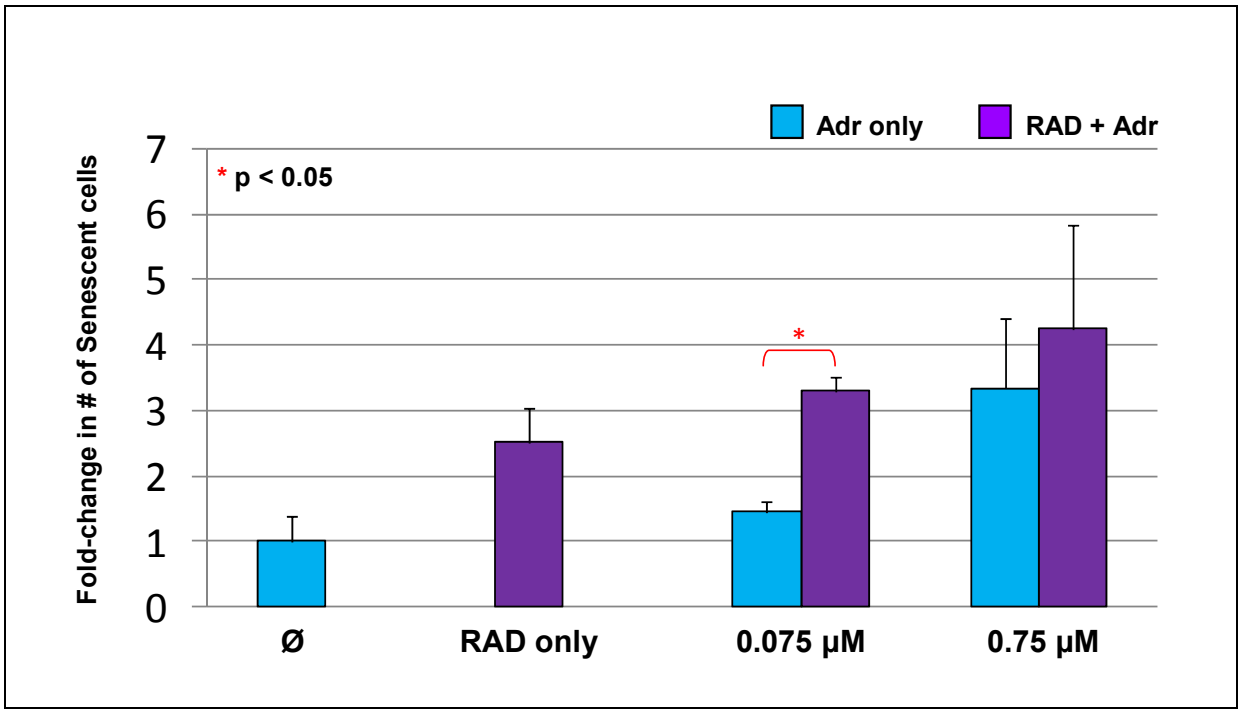

Figure 35: Increase in senescent cells upon treatment with RAD and Adr. Quantitation of β-gal activity in MCF7 cells acutely treated with Adr or pretreated with RAD. At 2 d post-treatment, cells were assessed for senescence-associated β-galactosidase expression based on both morphologic changes and positive staining. Three fields were counted for each treatment group. MCF7 cells not exposed to any drug served as the control to which all other counts were normalized. Asterisk (*) denotes significant change between Adr only treated and RAD pretreated cells ($p < 0.05$).

μM Adr, but not at 0.75 μM Adr, there is a significant difference in the number of senescent cells between Adr alone treated cells and RAD pretreated cells ($p < 0.0001$). Thus, Hsp90 inhibition appears to induce more moderate growth arrest when combined with a standard chemotherapeutic.

Because we observed a steady decline in cell growth as well as an upregulation of the cell-fate mediator, p53, with RAD and Adr treatments, we wanted to assess whether the increase in senescence was also associated with apoptosis. Apoptotic cells as measured by the TUNEL assay were largely undetectable with both Adr and RAD treatments, both singly and in combination (Figure 36). Representative images show only a basal level of activity, with only a few sporadic fields expressing TUNEL-positive cells. Specifically, treatment with 0.75 μM Adr alone is associated with the production of a few apoptotic cells, but this was a rare occurrence.

4.2.5 No change in p53 or p21 expression in MDA-MB231 cells.

Thus far, all experiments were performed using MCF7 breast cancer cells that, despite its abnormal karyotype, contain wild-type p53. As these cells show alterations in cell fate related proteins and Hsp90-related chaperone expression upon treatment, we wanted to determine whether these changes were dependent upon functional p53. In order to address this query, the highly metastatic MDA-MB 231 cell line, which expresses mutant p53 that possesses a missense mutation in the core DNA binding domain (van Slooten *et al*., 1999), was treated in an identical manner with Adr and RAD as MCF7 cells.

MDA cells treated acutely with Adr at any concentration (0.0075 μM, 0.025 μM, 0.075 μM, 0.25 μM, or 0.75 μM) do not show appreciable differences in p53 or p21 levels compared to untreated cells (Figure 37A). Similarly, pretreatment with 0.03 μM RAD followed by Adr

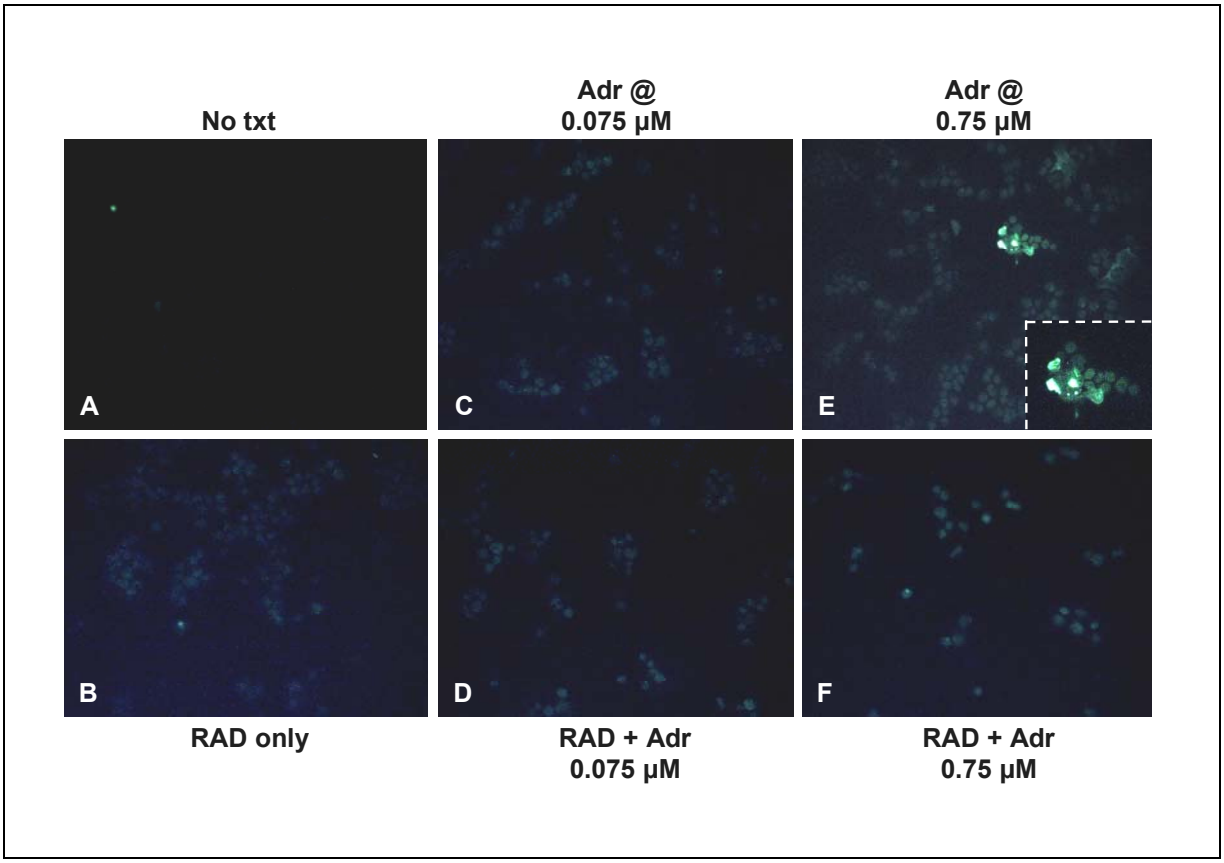

Figure 36: Apoptotic cells are undetectable upon RAD + Adr treatment. MCF7 cells were either acutely treated with 0.075 µM (C) and 0.75 µM (E) Adr for 2 hrs or pretreated with 0.03 µM RAD for 48 hrs followed by acute Adr treatment (D, F). Untreated cells are shown in (A) and RAD only cells in (B). Upon completion of the treatment series, cells were fixed and cytospun onto slides. The amount of apoptotic cells was assessed via the TUNEL assay, which detects DNA fragmentation by fluorescently labeling the nicked ends of nucleic acids. Inset in (E) shows nuclear localization of DNA fragments in apoptotic cells. All images taken at 40x.

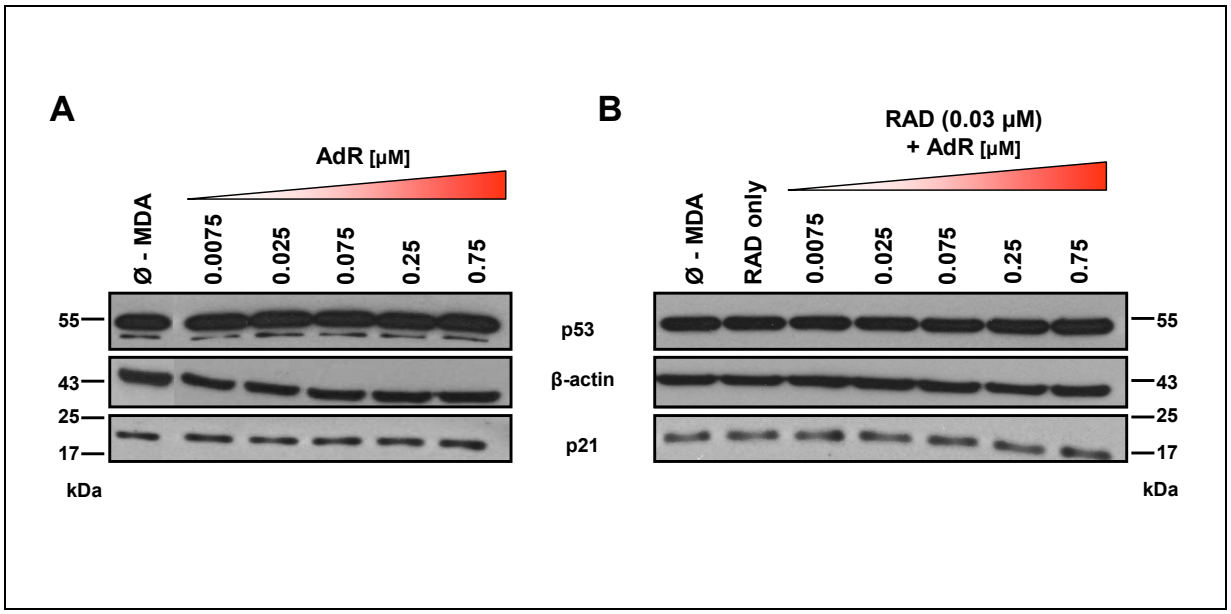

Figure 37: No change in p53 or p21 levels in single agent or combination treated MDA-MB231 cells. The mutant p53 containing MDA-MB 231 cell line was treated with either Adr alone in the range of 0.0075 μM to 0.75 μM for 2 hrs or pretreated with 0.03 μM RAD for 48 hrs followed by acute Adr treatment in the same range. At 4 d post-treatment, cells were harvested and 50 μg of total protein lysate was subjected to western analysis. Immunblots were probed with antibodies against total p53 and p21. β-actin served as the loading control.

treatment does not induce changes in total p53 or p21 protein levels (Figure 37B). Furthermore, both singly and combinationally treated cells do not display altered overall Hsp70 expression, as was evident in MCF7 cells. Unlike treated MCF7 cells, Hsp70 in treated MDA cells resolved as a doublet corresponding to 69 kDa and 72 kDa, of which the smaller isoform was more predominant in all cases. The expression of both the smaller and larger isoforms does not change with Adr treatment at any concentration as compared to untreated cells (Figure 38A). RAD pretreatment with Adr follow-up at various concentrations is also associated with consistently more expression of the smaller isoform (Figure 38B). Although it appears as though the larger isoform varies when RAD is present, this change is not appear to be significant. Finally, as expected, single and combination drug options do not affect Hsp90 protein expression. Collectively, these data suggest that the effects of Hsp90 inhibition on expression of cell fate related proteins and Hsp90 cycle co-chaperones are dependent upon the presence of functional p53.

4.2.6 CIS and TAX are associated with differential expression of cell fate proteins and HSPs.

In order to elucidate whether the alterations in cell fate related proteins, p53 and p21, and the Hsp90-associated co-chaperone, Hsp70, were dependent upon the mechanism of Adr, we sought to assesss the effect of other chemotherapeutics, including cisplatin and taxol. CIS, like Adr, is also a DNA damaging agent in that it forms unrepairable DNA cross-links. The mechanism of action of TAX, however, differs from that of Adr and CIS, since it acts as a microtubule-stabilizing agent. MCF7 cells were treated with either 0.1 μM CIS or 100 nM TAX for 24 hrs or pretreated with 0.03 μM RAD for 48 hrs followed sequentially by CIS or TAX treatment, respectively. At 4 hr, 24 hr, and 48 hr of treatment, cells were harvested and analyzed

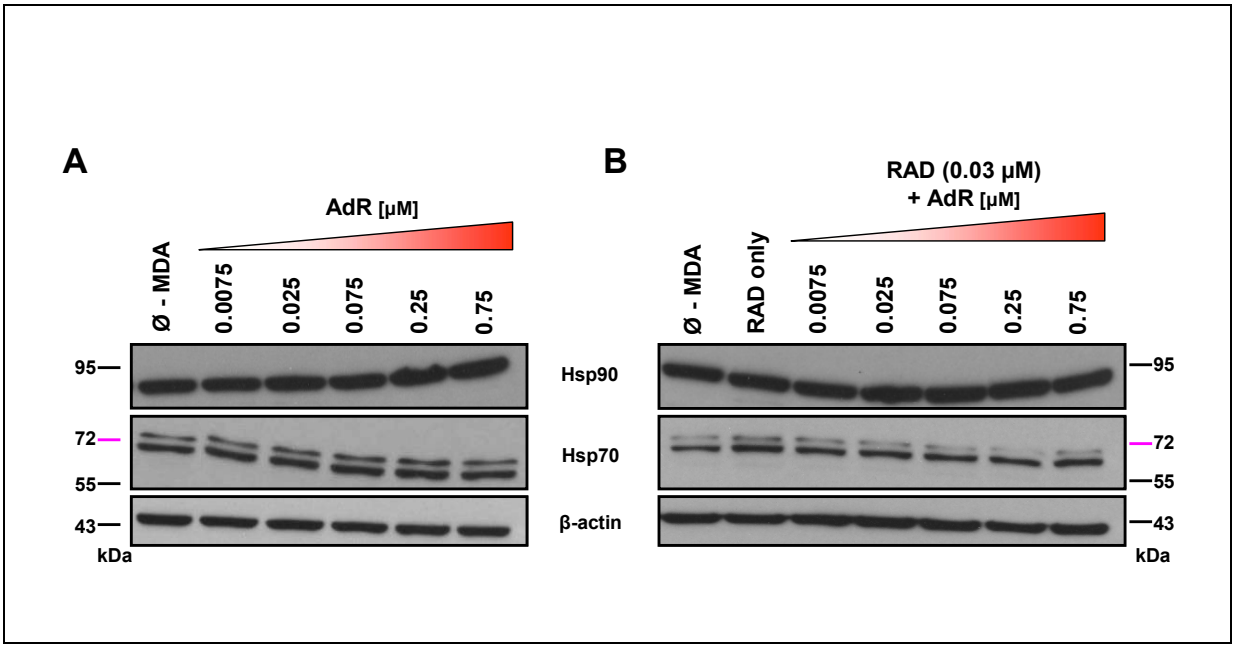

Figure 38: No change in chaperone expression in MDA-MB 231 cells upon Adr or RAD + Adr treatment. The MDA-MB 231 cell line was treated with either Adr alone in the range of 0.0075 μM to 0.75 μM for 2 hrs or pretreated with 0.03 μM RAD for 48 hrs followed by acute Adr treatment in the same range. Cells were harvested at 4 d post-treatment and 50 μg of total protein lysate was subjected to western analysis. Immunblots were probed with antibodies against Hsp90 and Hsp70. β-actin served as the loading control.

for Hsp90 client and co-chaperone expression.

Treatment with either drug alone or in combination with RAD has no effect on total Hsp90 protein levels (Figure 39). Cells in the CIS treatment group do not appear to be significantly different in p53 protein levels at any time point post-treatment (Figure 39A). As such, CIS singly treated cells at 4 hr, 24 hr, and 48 hr display p53 at levels similar to that of untreated MCF7 cells. Likewise, RAD pretreated cells with CIS follow-up present p53 levels comparable to that of RAD only treatment. The lack of change in protein expression between untreated, CIS only, RAD only, and RAD and CIS treated cells suggest that cisplatin does not exert its antitumor effects through p53. Despite the consistent p53 expression, levels of p21 do exhibit an appreciable alteration (Figure 39A). At 48 hr CIS treatment, p21 appears to be upregulated as compared to untreated cells and 4 hr or 24 hr harvest points. Pretreatment with RAD also induces a noticeable increase in p21 at 4 hr, 24 hr, and 48 hr as compared to both untreated and RAD only treated cells. These observations are clearly distinct from that seen with RAD and Adr treatment, which shows a corresponding increase in p21 with p53 upregulation. The data presented here thus suggest that CIS at 48 hr and RAD plus CIS in combination stimulates p21 induction independent of p53 activity.

TAX treatment with and without RAD elicits a similar response in terms of p53 and p21 expression as does treatment with Adr with and without RAD. However, although the concurrent increase p53 and p21 is parallel to that in Adr studies, the upregulation is much more robust with TAX treatment. Specifically, treatment with TAX alone elicits a large increase in p53 expression at 24 hr post-treatment, and this increase is even greater at 48 hr (Figure 39B). The level of p53 at 4 hr is comparable to that in untreated cells, so it appears that the amount of p53 induction is time-dependent. Likewise, RAD pretreatment followed by TAX also displays a time-dependent

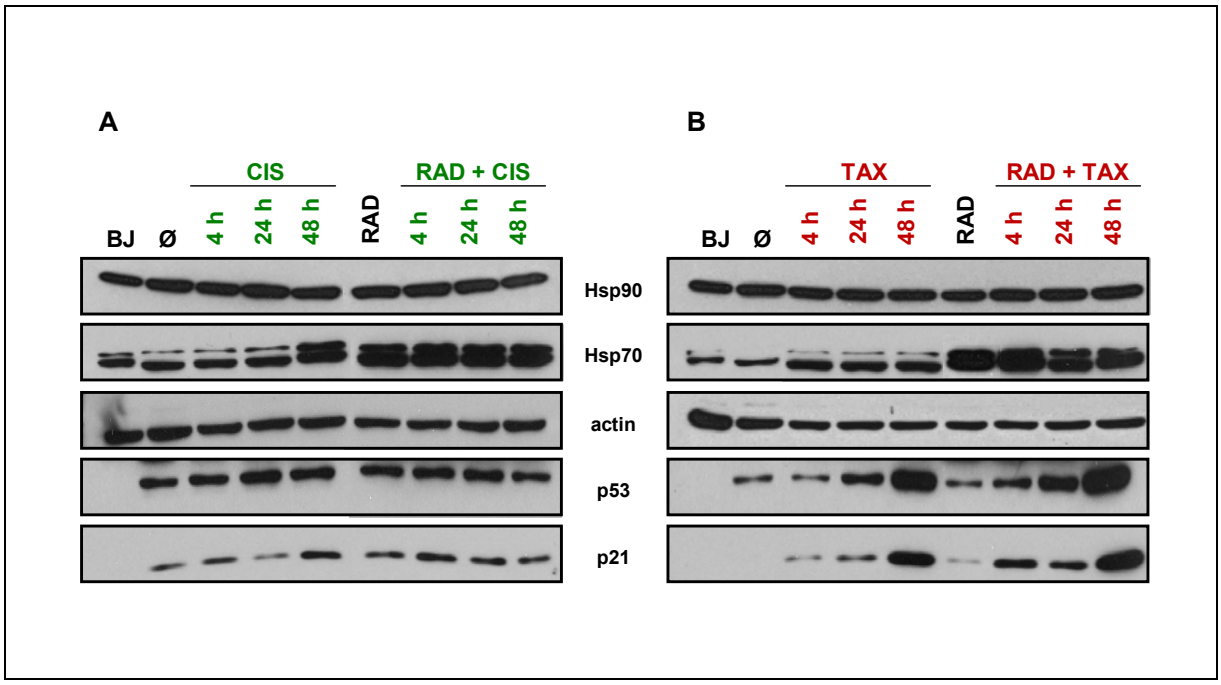

Figure 39: Differential expression of cell fate related proteins and the Hsp90-related co-chaperone after CIS or TAX treatment. MCF7 cells were treated in two different groups. In the CIS group (A), cells were either treated with 0.1 μM CIS for 24 hrs or pretreated with 0.3 μM RAD for 48 hrs followed by 24 hr of CIS. For the TAX group (B), cells were either treated with 100 nM TAX for 24 hrs or pretreated with 0.3 μM RAD followed by 24 hrs of TAX. Cells were harvested at 4 hr, 24 hr, and 48 hr of treatment and 50 μg total protein lysate subjected to western analysis. Immunoblot was probed with antibodies against Hsp90, Hsp70, p53, and p21. β-actin served as the loading control. For both blots, lane 1 represents untreated normal BJ fibroblasts, lane 2 is untreated MCF7 cancer cells, and lane 6 is 48 hr RAD only treated MCF7 cells.

upregulation of p53, though this increase is more dramatic at each time point compared to TAX only. Specifically, we observe an increase in p53 as early as 4 hr post initiation of treatment, and this upregulation gets progressively stronger over 24 hr and 48 hr. In addition to p53 changes, there are also clear differences in p21 expression. Namely, p21 levels increase according to p53 levels in both singly TAX treated and RAD pretreated cells (Figure 39B). While it is relatively low at 4 hr and 24 hr, p21 upregulation appears maximal at 48 hr post TAX alone treatment. Pretreatment with RAD also induces a p21 increase, but this increase is more robust since it is evident as early as 4 hr and is maintained at 24 hr. Again, the greatest induction occurs at 48 hr, and the level at this time point is generally equivalent to that seen at 48 hr in singly TAX treated cells. These TAX data indicate that the damage response triggered by TAX is mediated in a p53-dependent manner.

Because Hsp70 was shown to be relatively down-regulated in Adr treated cells, it was necessary to assess whether this decrease was drug specific. Unlike Adr treatment in MCF7 cells but akin to Adr exposure in MDA cells, CIS and TAX treatments produced a doublet band corresponding to Hsp70 when resolved. It is evident that the smaller 69 kDa isoform is constitutively present, as it is detectable in both normal BJ fibroblasts and untreated breast cancer cells (Figure 39). In the CIS only group, the larger 72 kDa isoform is strongly induced at 48 hr post-treatment, while its expression at 4 hr and 24 hr is nearly identical to untreated cells (Figure 39A). Pretreatment with RAD at all time points elicits a similarly strong induction of the larger isoform, which is also seen in RAD only cells. For the TAX only group, the larger Hsp70 form is minimally detectable, while the smaller constitutive form is predominant. RAD pretreatment again triggers a robust upregulation of the large Hsp70 form at all time points

(Figure 39B). Thus, CIS and TAX also affect expression of Hsp70, although this change was reflected in differential expression of its isoforms.

4.2.7 CIS and TAX affect Hsp90 client protein expression.

Since p53 upregulation was observed in CIS and TAX treated cells, we wanted to determine whether expression of Hsp90 client proteins involved in mediating a damage response was altered. The ubiquitous tyrosine kinase, c-Abl, was a logical query due to its role in both cell cycle arrest and apoptosis, and its implication in breast cancer aggressiveness (Lin and Arlinghaus, 2008). A comparison of CIS and TAX treated cells at 24 hr and 48 hr of treatment shows different expression of c-Abl depending on the drug used (Figure 40). Treatment with CIS only is associated with almost nonexistent c-Abl expression, as is treatment with RAD and CIS at 24 hr. However, at 48 hr, RAD and CIS combination treated cells display an increase in c-Abl expression. This finding is consistent with the role of c-Abl in responding specifically to DNA damage, which is produced as a consequence of CIS presence. Expression of c-Abl in cells treated with the microtubule damaging agent TAX is undetectable, which also supports the selectivity of response of this tyrosine kinase. Thus, only CIS upregulates c-Abl due to their compatibility in mediating and sensing DNA damage.

In addition to c-Abl, the expression of Cdk4 was also examined to determine whether cell cycle aberrations also exist with CIS and TAX treatments. Treatment with CIS alone or in combination with RAD does not appear to alter Cdk4 protein expression (Figure 40, lanes 3-5). The level of Cdk4 in these cases is comparable to that in RAD only treated and untreated MCF7 cells, suggesting that Hsp90 inhibition is not predisposing the cell to undergo growth arrest in response to CIS. On the other hand, TAX treatment does noticeably alter Cdk4 expression, such

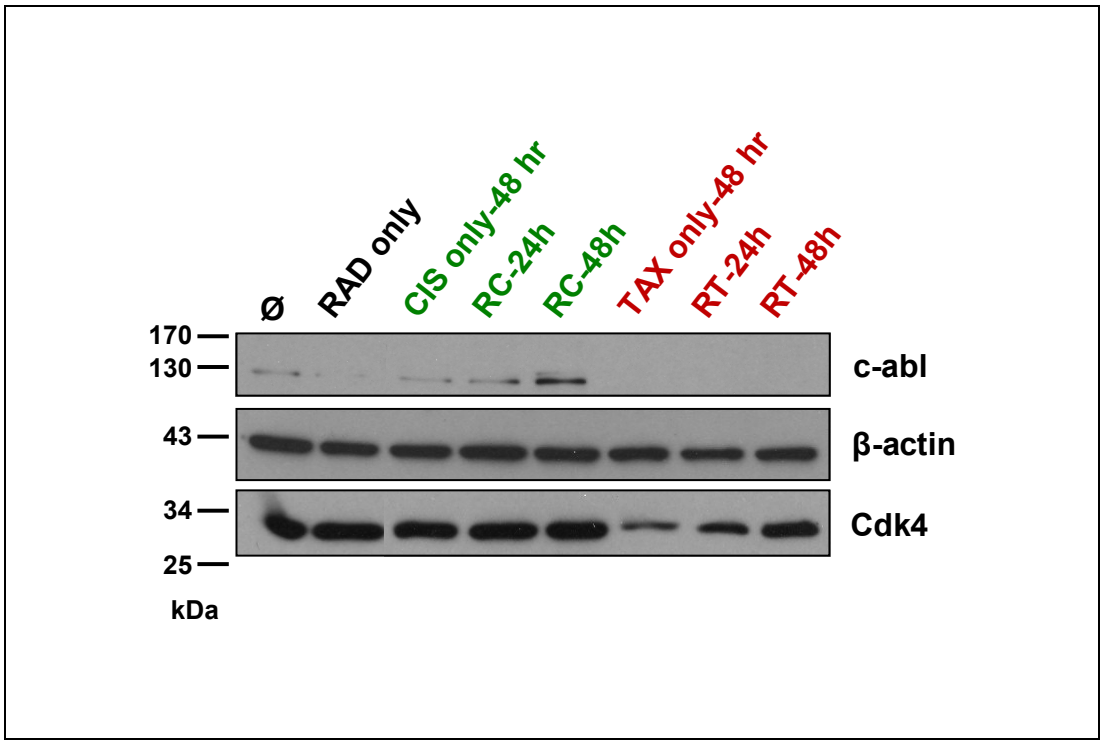

Figure 40: Altered expression of Hsp90 client proteins post CIS or TAX treatment. MCF7 cells were treated in two different groups. In the CIS group (A), cells were either treated with 0.1 μM CIS for 24 hrs or pretreated with 0.3 μM RAD for 48 hrs followed by 24 hr of CIS. For the TAX group (B), cells were either treated with 100 nM TAX for 24 hrs or pretreated with 0.3 μM RAD followed by 24 hrs of TAX. Upon completion of treatment, cells were harvested at 24 hr or 48 hr and 50 μg total protein lysate subjected to western analysis. Immunoblot was probed with antibodies against c-Abl and cdk4. β-actin served as the loading control. Lane 1 represents untreated MCF7 cancer cells, lane 2 is 48 hr RAD only treated MCF7 cells, lane 3 is 48 hr CIS only treated MCF7 cells, and lane 6 is 48 hr TAX only treated MCF7 cells.

that there is a reduced level with TAX alone (Figure 40, lanes 6-8). RAD pretreatment at 24 hr post-treatment is also associated with a reduction in Cdk4 as compared to RAD only cells. However, at 48 hr with RAD and TAX, the level of Cdk4 is similar to that of RAD only, suggesting that TAX increases Hsp90-induced Cdk4 degradation which is alleviated by RAD treatment.

4.2.8 CIS and TAX induce apoptotic cell death.

In order to determine whether the mechanism of action of CIS and TAX affects cellular fate, we assessed the amount of cell death in drug treated cells. In particular, we wanted to determine whether CIS elicits a response similar to Adr since they are both DNA damaging agents and whether TAX sends the cell down a different path. MCF7 cells were treated with 0.03 μM RAD, 0.1 μM CIS, or in combination and cell growth analyzed at 4, 24, and 48 hr post initiation of treatment. Treated cells in these groups generally retain the morphology of untreated cells, displaying the characteristic cobblestone shape (Figure 41). However, RAD pretreatment leads to the appearance of detached cells, albeit at a low frequency, represented by rounded, "glowing" structures. The emergence of a small population of senescent cells is also present, as denoted by the large, flattened, and irregular shape of these cells. When quantified, the extent of CIS-induced cell death does not apparently differ when cells are pretreated with RAD (compare CIS only versus RAD plus CIS at each time point), since there is no appreciable difference in the number of detached cells (Figure 42). For CIS only treated cells, while 4 hr is associated with negligible cell detachment, both 24 hr and 48 hr post-treatment induces about 1.4% cell death, as compared to untreated cells, which also show negligible cell detachment. While RAD alone produces about 0.96% cell death, pretreated cells in combination with CIS are associated with

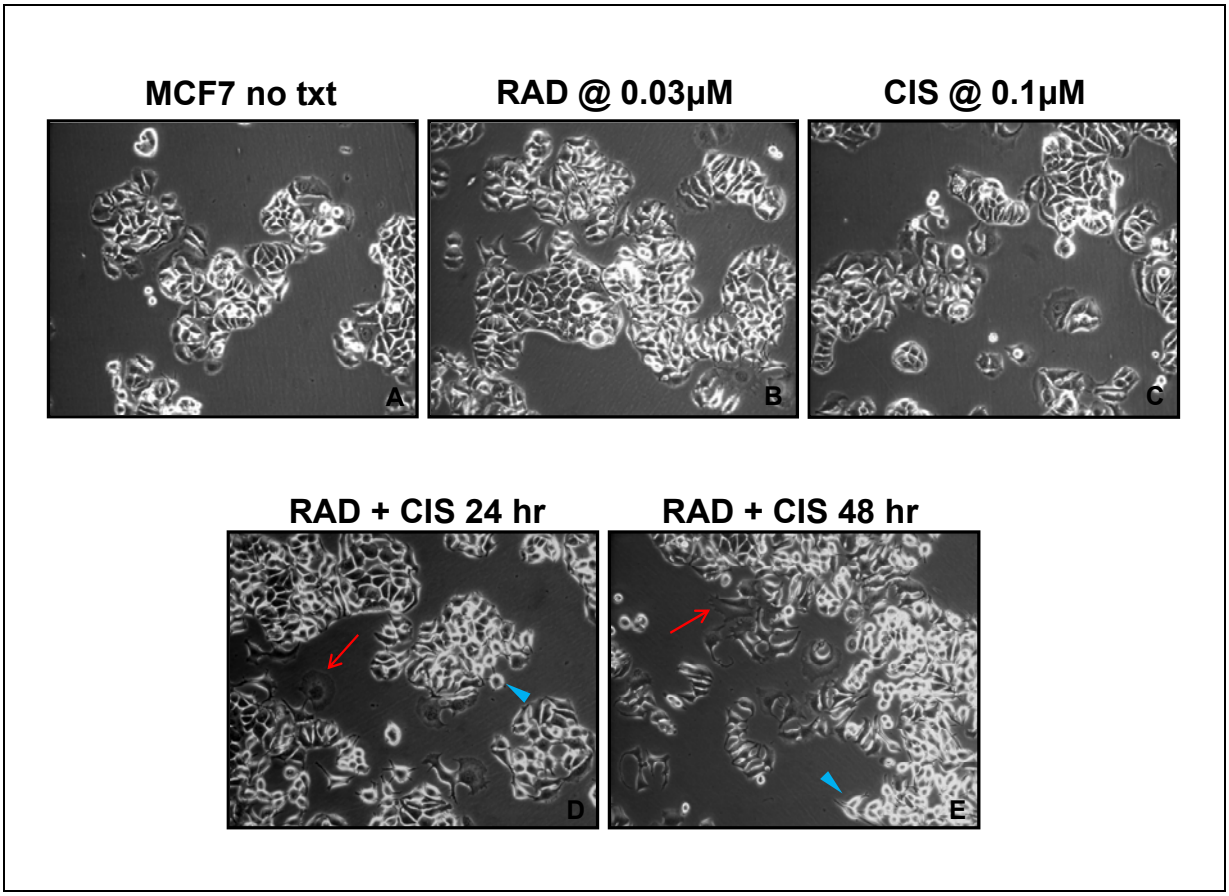

Figure 41: Small percentage of morphological cell death in response to treatment with Cisplatin. Breast cancer MCF7 cells were treated with either 0.03 μM RAD (B), 0.1 μM CIS (C), or with a combination of RAD and CIS (D, E). Phase contrast images of adherent and non-adherent cells were taken at 24 hr and 48 hr post initiation of combination treatment. CIS induces detachment in a small percentage of cells at 24 hr and this amount increases by 48 hrs. Untreated (A) and the majority of RAD singly-treated cells remain adherent. Red arrows and blue arrowheads denote examples of senescent cells and dead cells, respectively. All images taken at 40x.

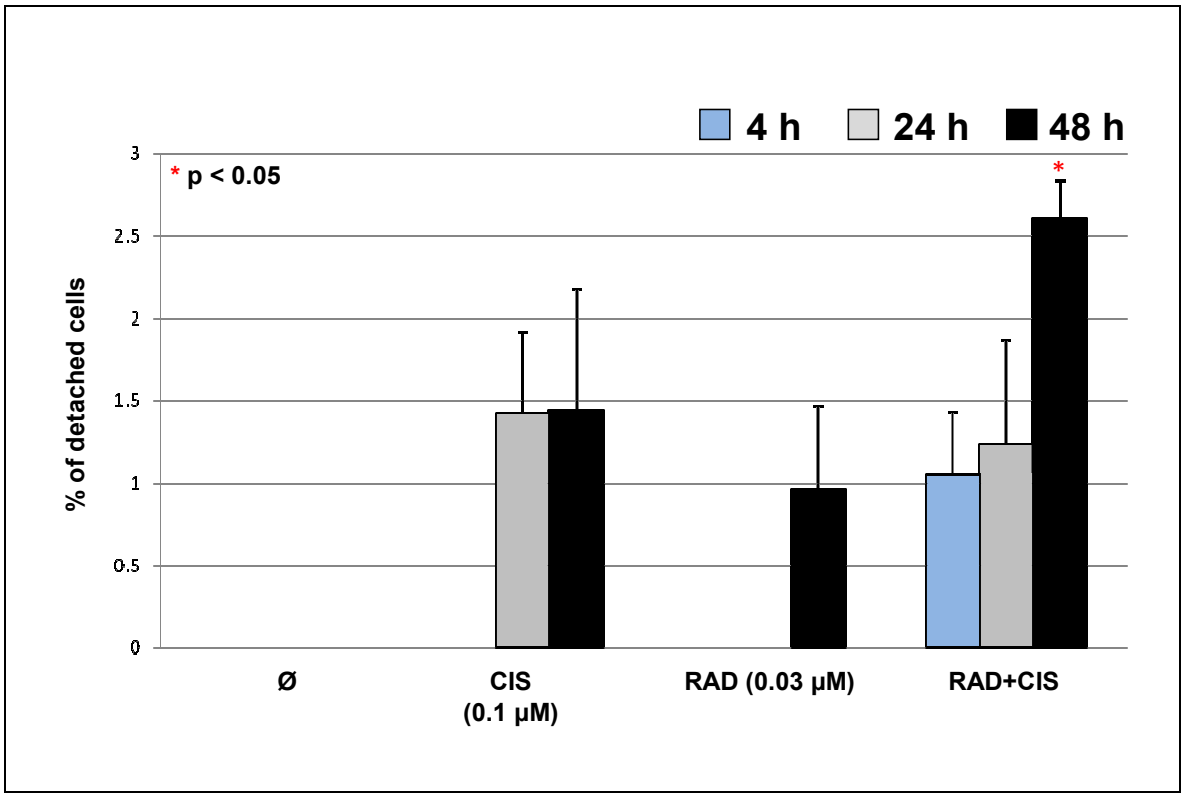

Figure 42: Cell death upon CIS treatment. MCF7 cells were either treated with 0.1 µM CIS alone or pretreated for 48 hrs with 0.03 µM RAD prior to CIS treatment. Cells were harvested at 4 h, 24 h, and 48 h of treatment and both adherent and non-adherent cells collected and counted in triplicate. Percentage of detached (floating) cells were calculated using non-treated cells as the control to which all other counts were normalized. A percentage of 0% represents a negligible number of dead cells. Significant difference ($p < 0.05$) between RAD only and RAD + CIS at 48 hr is denoted by the asterisk (*).

detectable cell death at 4 hr. At this time point, there are about 1.1% dead cells and this percentage increases over time, to 2.6% at 48 hr. The only significant difference in percentage of dead cells occurs between RAD only treated cells and RAD + CIS treated cells at 48 hr ($p = 0.007$), which produces a more than additive effect on the production dead cells. The lack of difference between CIS treatment alone and in combination with RAD is supported by TUNEL data, which shows no major change in the amount of apoptotic cells between CIS alone and RAD + CIS (Figure 43). Thus, RAD pretreatment with 0.1 μM CIS follow-up does not induce significantly more cell death than CIS singly treated cells.

In contrast, treatment with TAX alone and in combination with RAD induces widespread cell death in the form of cell detachment (Figure 44). MCF7 cells were treated with 0.03 μM RAD, 100 nM TAX, or in combination and cell growth analyzed at 4, 24, and 48 hr post initiation of treatment. It is evident that the majority of cells that are treated with TAX alone undergo considerable detachment from each other and the surface of the plate. Similarly, RAD pretreatment also massively induces the appearance of non-adherent cells, while the vast majority of those cells that remain adherent display altered morphology reminiscent of senescent cells. Although these morphologically distinct cells are also present with CIS treatment, TAX is associated with a great increase in incidence of these cells. When quantified, TAX single treatment leads to 12.2% cell death in the form of detached cells at 24 hr and 23.6% cell death at 48 hr, which is almost a two-fold increase over 24 hr (Figure 45). Pretreatment with RAD leads to the emergence of a minute fraction of dead cells at 4 hr, but this percentage increases by 14-times to 8.4% at 24 hr and by 39-times to 23.6% at 48 hr. These fold increases may be initially misleading in that a comparison of TAX alone and RAD/TAX at either 24 hr or 48 hr does not produce significant differences in the number of non-adherent cells, as supported by evidence

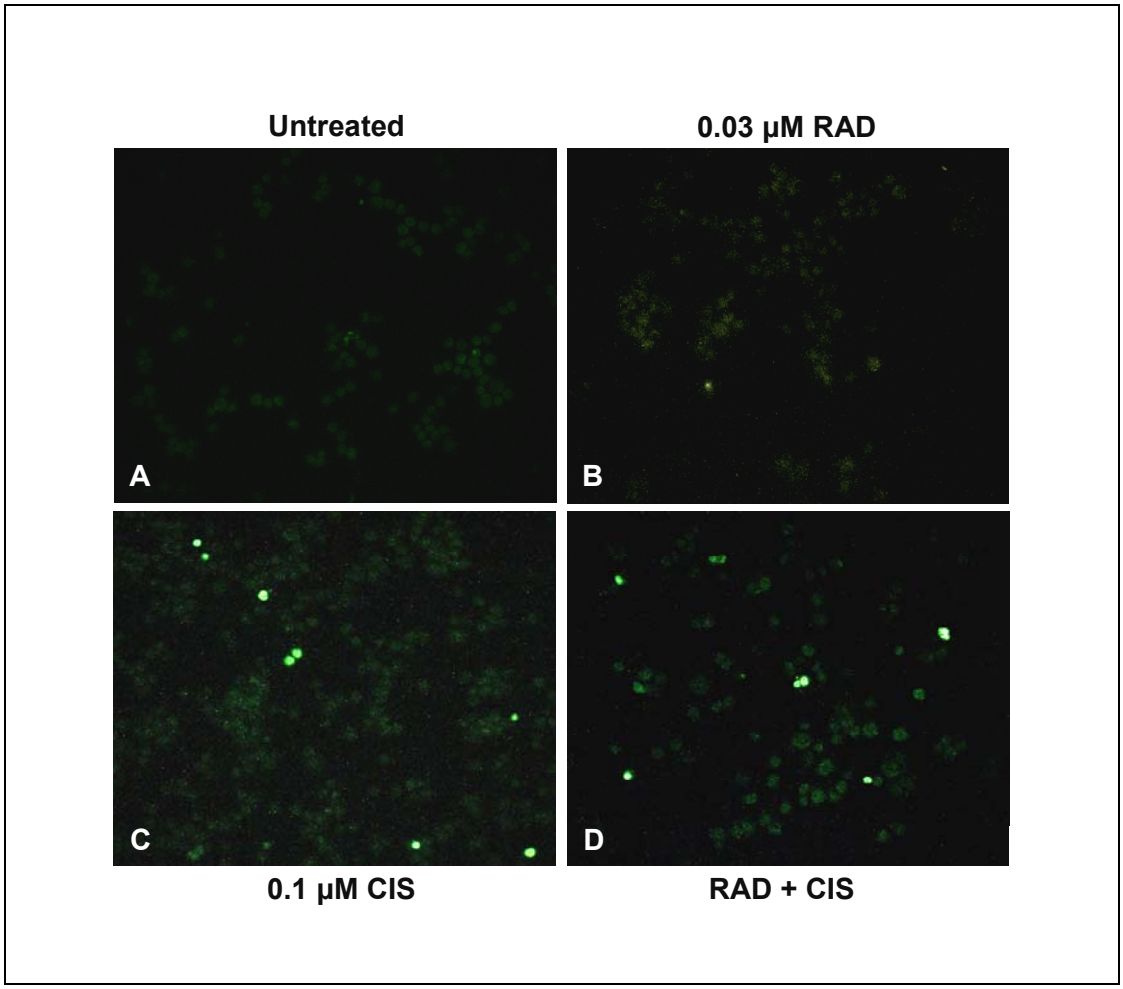

Figure 43: Indiscernible change in apoptotic cells between CIS alone or with RAD pretreatment. MCF7 cells were treated with 0.1 μM CIS alone for 24 hr (C) or in combination with 48 hr pretreatment with 0.03 μM RAD (D). Upon completion of treatment series, cells were fixed and processed for the TUNEL assay. Apoptotic cells are represented by the visibly green nuclear staining. Untreated cells (A) and RAD only treated cells (B) have only a background level of activity, while CIS and RAD/CIS have detectable apoptotic cells. All images taken at 40x.

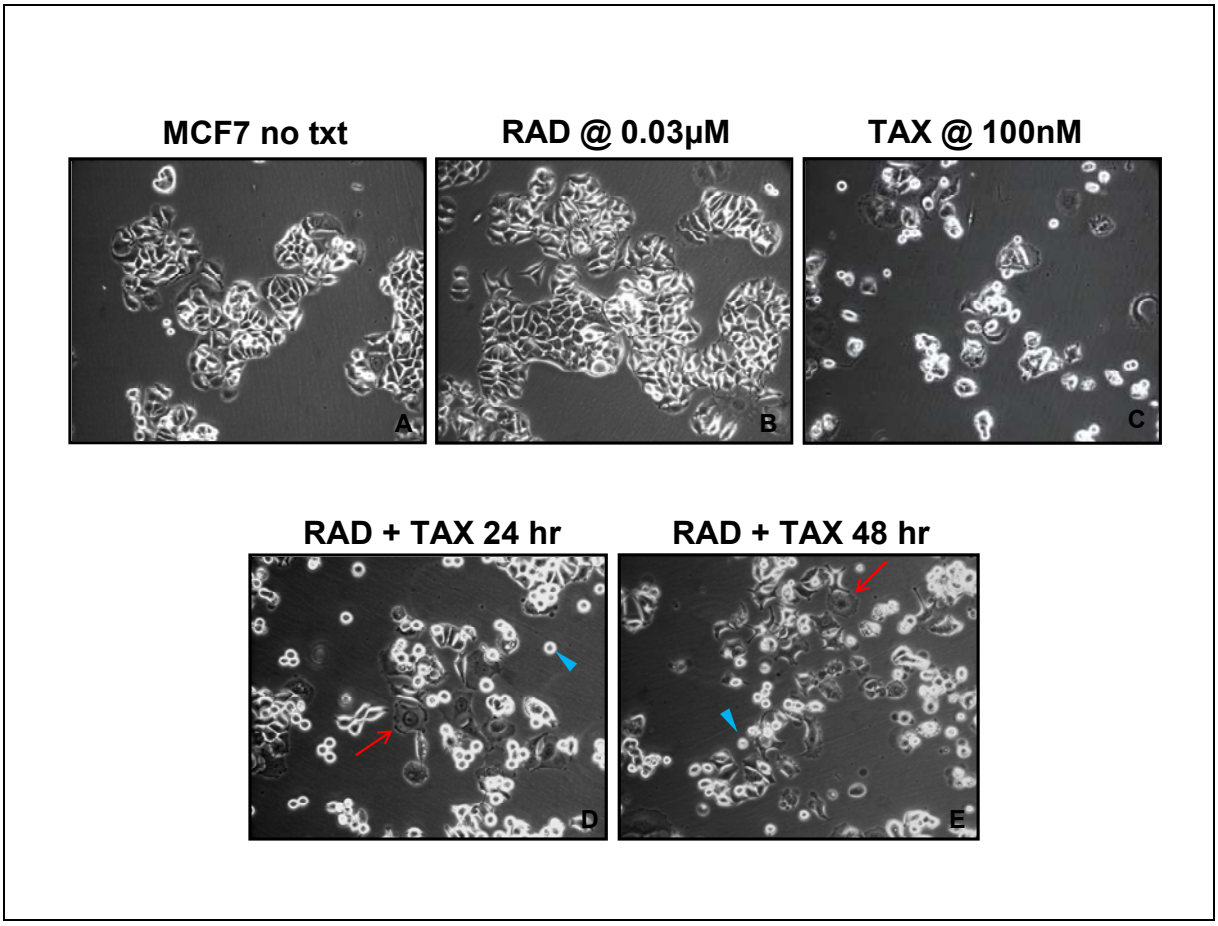

Figure 44: Massive morphological cell death occurs in response to treatment with Taxol. Breast cancer MCF7 cells were treated with either 0.03 μM RAD (B), 100 nM TAX (C), or with a combination of RAD and TAX (D, E). Phase contrast images of adherent and non-adherent cells were taken at 24 hr and 48 hr post initiation of combination treatment. TAX alone and in combination with RAD induces the detachment of the majority of cells at 24 and 48 hrs. Untreated (A) and the majority of RAD singly-treated cells remain adherent. Red arrows and blue arrowheads denote examples of senescent cells and dead cells, respectively. All images taken at 40x.

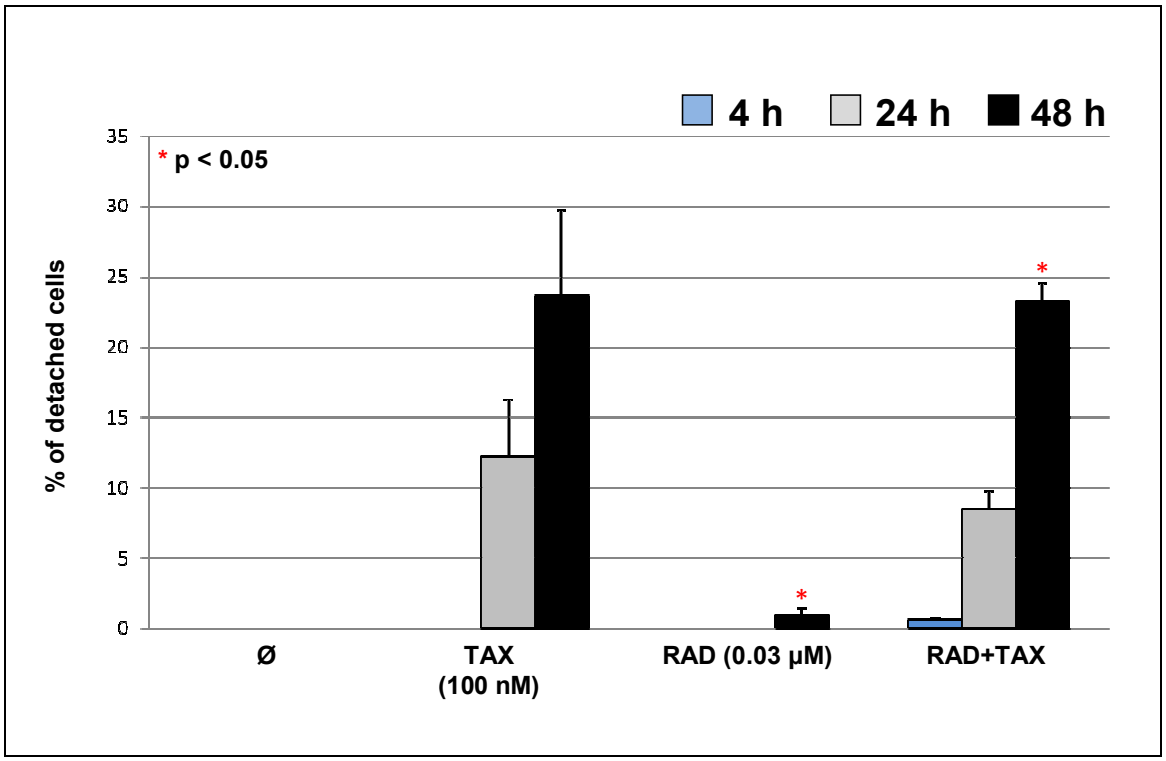

Figure 45: Greater cell death upon TAX treatment. MCF7 cells were either treated with 100 nM TAX alone or pretreated for 48 hrs with 0.03 µM RAD prior to TAX treatment. Cells were harvested at 4 h, 24 h, and 48 h of treatment and both adherent and non-adherent cells collected and counted in triplicate. Percentage of detached (floating) cells were calculated using non-treated cells as the control to which all other counts were normalized. A percentage of 0% represents a negligible number of dead cells. Significant differences ($p < 0.05$) between RAD only and TAX only at 48 hr and between RAD only and RAD + TAX at 48 hr are denoted by asterisks (*).

from the TUNEL stain (Figure 46). The only significant differences that do emerge exist between RAD only and RAD/TAX at 48 hr ($p < 0.001$) and between RAD only and TAX only at 48 hr ($p = 0.003$), which only suggests that TAX sensitizes MCF7 cells to RAD. These data indicate that RAD pretreatment does not appreciably affect the emergence of dead cells upon 100 nM TAX treatment such that the appearance of non-adherent cells is mainly due to the response to TAX.

4.2.9 TAM treatment affects cellular proliferation and p53/p21 expression.

As shown in previous sections, RAD treatment alone and as a pretreatment in combination with Adr evokes a significant reduction in cell proliferation. This decline in cell growth was also shown to be associated with an upregulation of p53 and p21. These changes in cell fate related proteins were evident in wild-type p53 MCF7 cells but were not recapitulated in mutant p53-containing MDA-MB 231 cells. In addition to possessing a different p53 status, MCF7 and MDA cells also differ in the status of other factors, including ER and PR, and so may elicit cellular responses due to their inherently distinct genotypes. In order to investigate the significance of the association of high Hsp90 levels and ER negative breast cancer, we wanted to compare MCF7 cells against an appropriate cognate cell.

TAM, as an ER antagonist, was used at a concentration of 1 μM to block ER activity in ER (+) MCF7 cells. TAM treated and untreated cells were then acutely treated with Adr alone or in combination with RAD. When compared against untreated cells, treatment with TAM alone elicits a 43% decrease in cell growth, which is even less than that observed with Adr single treatment at 0.75 μM at 2 d (see Figure 27). TAM in combination with Adr at increasing concentrations shows a trend towards decreased cell growth, which is significantly different than

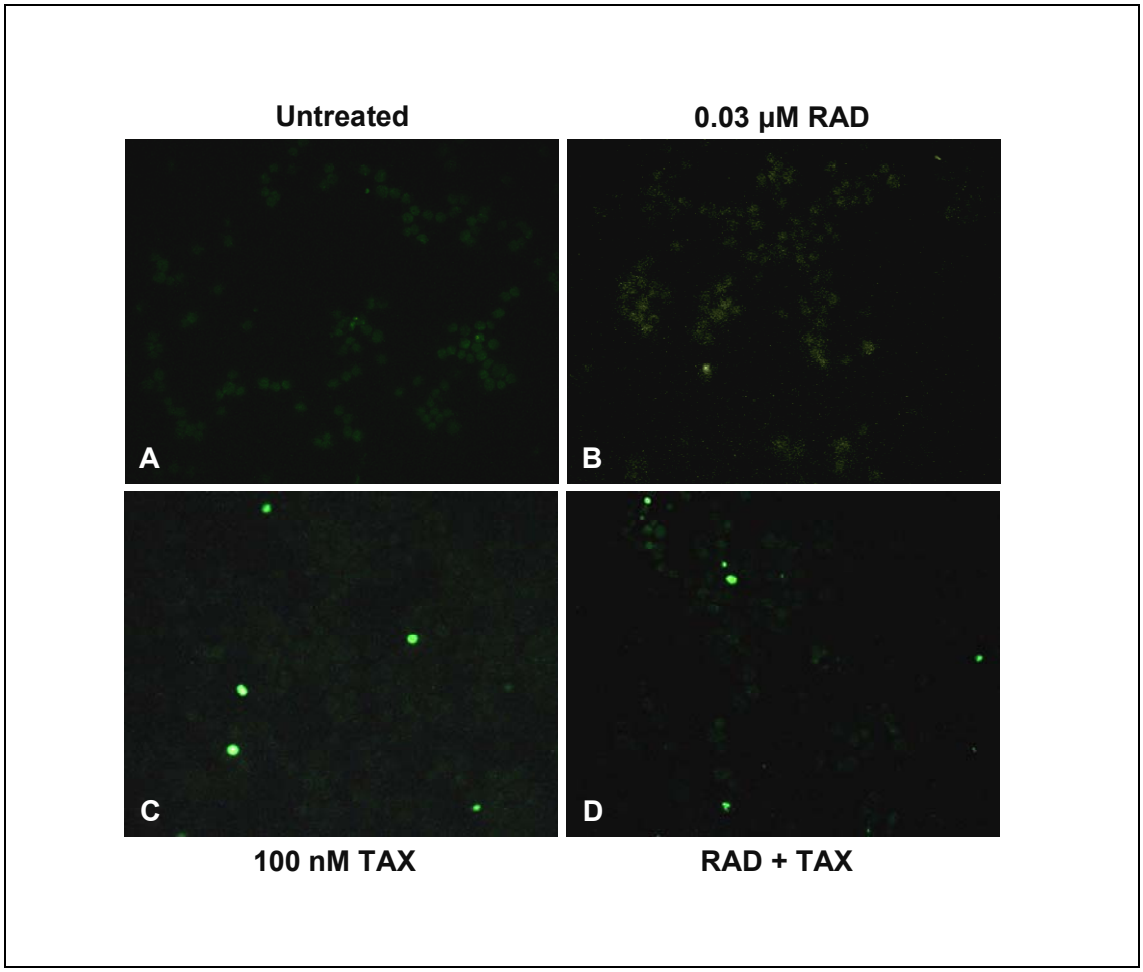

Figure 46: Apoptotic cell emergence not affected by RAD pretreatment with TAX. MCF7 cells were treated with 100 nM TAX alone for 24 hr (C) or in combination with 48 hr pretreatment with 0.03 μM RAD (D). Upon completion of treatment series, cells were fixed and processed for the TUNEL assay. Apoptotic cells are represented by the visibly green nuclear staining. Untreated cells (A) and RAD only treated cells (B) have only a background level of activity, while TAX and RAD/TAX have detectable apoptotic cells. All images taken at 40x.

untreated cell growth at all Adr doses (Figure 47, compare blue bar against black bars). RAD pretreatment with TAM alone follow-up leads to a 44% reduction in growth compared to RAD only (Figure 47, compare green bar against first grey bar). When Adr is added to this series, the decline in population doubling is even more apparent with increasing Adr dose. More notably, significant proliferation differences emerge between the TAM + Adr and TAM + RAD + Adr series. At Adr concentrations of 0.025 μM, 0.25 μM, and 0.75 μM, RAD pretreated cells have undergone significantly fewer PDs than TAM alone, suggesting that inhibition of Hsp90 acts in concert with ER antagonism. Taken together, these data indicate that blocking ER signaling does negatively affect cellular proliferation, although it appears to be more additive than synergistic.

Since we observe a decline in cell growth upon TAM treatment with RAD and Adr, we wanted to determine whether expression of p53 and p21 were also affected as they are by RAD and Adr together. ER antagonism by TAM apparently drastically diminishes p53 protein expression, regardless of whether Adr is present or not (compare lane 3 to lanes 4-8, Figure 48A), and TAM suppresses the Adr-induced p53 stabilization. However, expression of p21 does not seem to be affected since its protein levels remain constant throughout the TAM/Adr series and is comparable to that of untreated MCF7 cells. Despite the lack of change in p21, which mediates inhibition of Cdk4-dependent cell cycle progression, the protein level of Cdk4 is nevertheless markedly reduced. Likewise, TAM in combination with both RAD and Adr produces a considerable decrease in p53 expression compared to untreated and RAD alone treated cells (Figure 48B). The expression of p21 remains unchanged in this treatment series at 0.0075 μM and 0.025 μM Adr since levels are equivalent to that of TAM/RAD, RAD only, and untreated. However, at 0.075 μM, 0.25 μM, and 0.75 μM Adr, p21 substantially decreases. There is also an observable reduction in Cdk4 expression, similar to that of the TAM/Adr series.

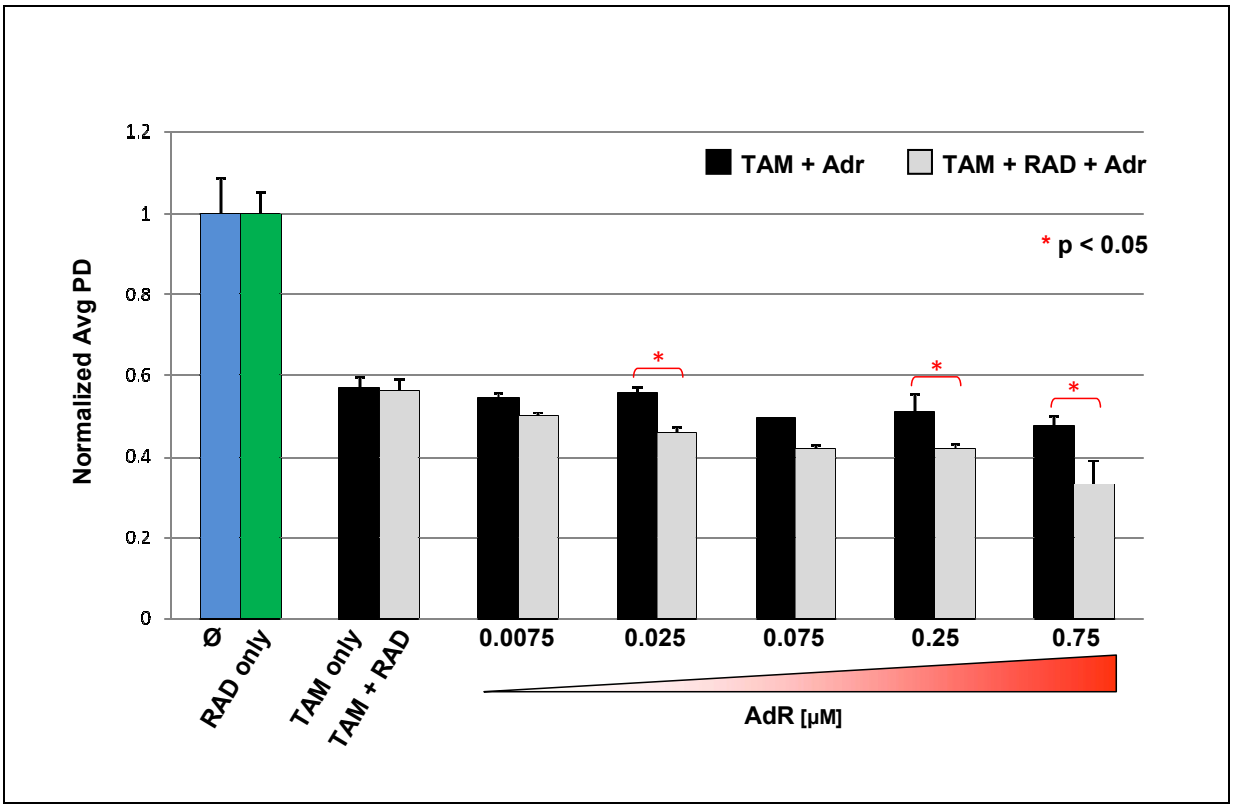

Figure 47: Cell growth declines in response to tamoxifen treatment. MCF7 cells were treated with 1 μM TAM for 24 hr. Cells were then either acutely treated with Adr alone ("TAM + Adr", black bars) at various concentrations, ranging from 0.0075 μM to 0.75 μM, or pretreated for 48 hrs with 0.03 μM RAD followed by Adr treatment at the same range ("TAM + RAD + Adr", grey bars). Upon completion of drug treatments, cells were harvested and counted in triplicate. MCF7 cells without drug exposure (blue bar) and RAD only treated cells (green bar) served as controls to which all other population doublings for TAM + Adr or TAM + RAD + Adr, respectively, were normalized. Asterisks (*) denote significant changes ($p < 0.05$) between TAM + Adr and TAM + RAD + Adr at the indicated Adr concentration.

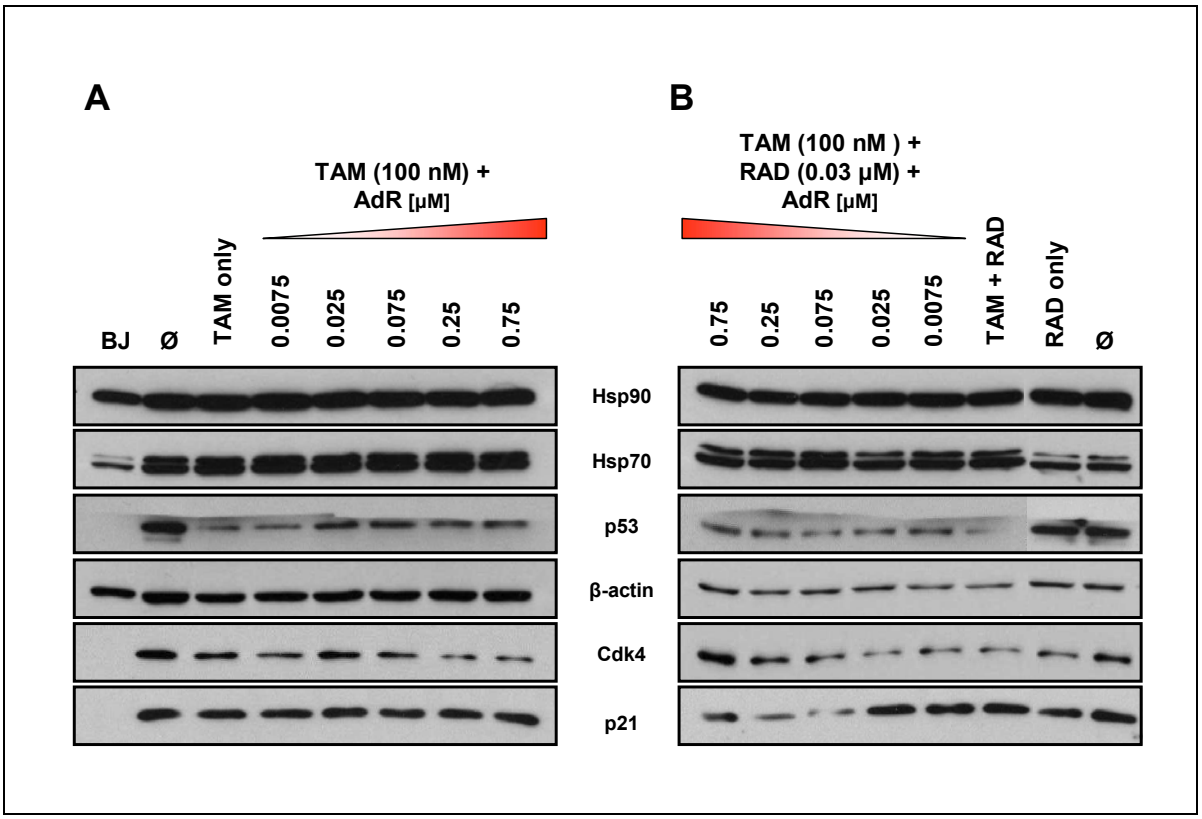

Figure 48: Decreased expression of cell fate related proteins with TAM treatment. MCF7 cells were treated with 1 μM TAM for 24 hr. Cells were then either acutely treated with Adr alone ("TAM + Adr", A) at various concentrations, ranging from 0.0075 μM to 0.75 μM, or pretreated for 48 hrs with 0.03 μM RAD followed by Adr treatment at the same range ("TAM + RAD + Adr", B). Upon completion of treatment, cells were harvested and 50 μg of total lysate was subjected to western analysis. Immunoblot was probed with antibodies against Hsp90, Hsp70, p53, Cdk4, and p21. β-actin served as the loading control. Normal fibroblasts are represented by "BJ" and untreated MCF7 cells by "Ø".

Unexpectedly, it appears that 0.75 μM Adr in conjuction with TAM and RAD is associated with an upregulation of Cdk4, but this could be a spurious finding.

Furthermore, expression of the Hsp90 cycle-associated co-chaperone, Hsp70 was assessed to identify consequences of ER antagonism on other heat shock proteins. Within each treatment series, TAM/Adr or TAM/RAD/Adr, Hsp70 expression does not greatly differ with increasing Adr concentration (Figure 48). Both the smaller 69 kDa and the larger 72 kDa forms abundantly exist. Initial assessment of Hsp70 in the TAM/RAD/Adr series suggests relatively lower expression of the larger form, but this is in fact due to reduced protein content, as shown by β-actin levels. Finally, TAM treatment is does not appear to be associated with any affect on Hsp90 expression in any case. Collectively, TAM data imply that blockade of ER signaling negatively affects p53 and Cdk4 expression and that the presence of RAD causes a decrease in p21 levels and a stabilization of Cdk4 with TAM and high Adr concentration.

Chapter 5

Discussion

5.1 Preface

Since the war on cancer was declared by President Nixon in 1971, many advances have been made in understanding breast cancer biology mechanisms and developing practical treatments. Although a wide array of therapeutic options are currently available and improvements continually made, cancer prevalence is on the rise and drug resistance remains a major challenge in successful disease elimination. Targeted therapies directed at specific molecules or signaling pathways have become increasingly prominent, but cancer cells nevertheless manage to evade complete eradication by utilizing alternative mechanisms of survival. These properties highlight the inherent genomic instability and adaptiveness of cancer cells. In order to address the deregulation of multiple routes of tumorigenesis, Hsp90 inhibition has evolved as an attractive method of simultaneously targeting a variety of pathways. Hence, indirect targeting of client proteins for degradation or inactivation via Hsp90 inhibition has a promising future in the treatment of cancer.

5.2 Differential expression of Hsp90 and p23 in breast cancer

The results presented in the immunostaining study offer considerable insight into the importance of chaperones in breast cancer and demonstrate the utility of tissue arrays. The use of CBCTR tissue arrays with both benign and malignant breast tissues embedded on individual slides provides a powerful tool with great analytical and statistical power, allowing for the simultaneous examination of disease stages from a variety of specimens relevant to the breast.

Notably, their experimentally uniform nature allows for reliable data analysis and less variability, both of which are advantages for any study. Each tissue microarray contained hundreds of cores including 23 normal breast specimens, 10-11 DCIS, 79-80 invasive cores, and 9 duplicate cell lines representing the breast, prostate, kidney, colon, and endometrium. The robustness of this study is certain, since normal and DCIS tissues were analyzed alongside invasive carcinomas. Additionally, the use of breast tissue specimens as an initial means of analysis allows for a more applicable translation into a clinical setting. Furthermore, the method of collection of immunoreactivity scores prevents any bias from forming, thus eliminating the possibility of data skewing. This is evident for Hsp90 and p23 immunostaining since inter-rater agreement was high in both cases.

Since Hsp90 exists as an abundant and ubiquitous cellular protein, it is not surprising that Hsp90 protein expression is highly detectable in normal mammary epithelial cell strains, immortal cells, and breast cancer cell lines. We found a significant increase in total cellular levels of Hsp90 in tumor cell lines as compared to mortal, non-tumorigenic lines. Tissue array data supports this finding as evident by an increase in the average immunostaining score for cytoplasmic Hsp90. Overall, normal breast tissue express less total Hsp90 in the cytoplasm than DCIS and invasive carcinomas. These findings are in line with previous reports of increased expression of both total Hsp90 and Hsp90α in tumor cells compared to normal cells (Pick *et al*., 2007; Yano *et al*., 1996, 1999). In addition to breast cancer, overexpression of Hsp90 mRNA or protein has also been reported in leukemia, gliomas, and ovarian, endometrial, and pancreatic cancers (Xiao *et al*., 1996; Strik *et al*., 2000; Nanbu *et al*., 1996; Mileo *et al*., 1990; Ogata *et al*., 2000). Although the mechanism driving this Hsp90 upregulation needs clarification, it is possible that the inherently "stressful" conditions of the tumor microenvironment, including low glucose,

low intra- and extra-cellular pH, and hypoxia (Laderoute *et al*., 2006; Lee *et al*., 2008; Qing and Simon, 2009) are favorable for Hsp90 induction. Furthermore, the accumulation of mutant oncoproteins during cancer establishment may trigger Hsp90 upregulation in response to the presence of these misfolded or conformationally altered proteins. Thus, the increase in Hsp90 in cancer cells is likely related to the induction of the heat shock response, mediated by heat shock transcription factors such as HSF1 (Shamovsky and Nudler, 2008). The HSF1 protein is normally sequestered by Hsp70/Hsp40 in an inactive state, but upon heat shock, it is released from this complex and trimerizes to gain activity. These actions cause the subsequent binding of HSF1 to DNA elements that promote the transcription of HSPs. In the context of this study, it is possible that the tumor environment is triggering a heat shock response involving the activation of HSF1, which then stimulates Hsp90 upregulation.

Expression of Hsp90 in the nucleus, however, is lower for all disease types and does not significantly vary between the three disease states. This predominantly cytoplasmic localization has also been similarly reported in lobular neoplasia of the breast (Zagouri *et al*., 2008). Despite the generally weak nuclear Hsp90 expression, it is notable that only invasive carcinomas contain a subset of specimens that stain intensely in the nucleus. Nevertheless, the dual localization of Hsp90 is consistent with previous studies that report localization of Hsp90 in both the nucleus and cytoplasm of breast cancer tissue (Yano *et al*., 1996). Future breast cancer therapy could be designed to take advantage of this nuclear localization of Hsp90. In fact, many Hsp90 targets require its association for entry into the nucleus, including mutant steroid receptors (Kang *et al*., 1994) and fibroblast growth factors (Wesche *et al*., 2006). Thus, treatments that exploit a nucleus-targeted approach to blocking Hsp90 function could potentially be more effective in

both delivery and eliciting a response in advanced breast cancers that are more difficult to treat with conventional therapies.

Although p23 total protein expression was shown to increase in cell culture as pre-immortal HME cells progressed toward immortality and also in breast cancer cell lines, this observation was not reproducible in clinical specimens. In fact, p23 expression decreases when comparing normal versus DCIS versus invasive breast carcinomas, suggesting an inverse relationship between p23 expression and breast cancer progression. Thus, it appears that as malignancy increases, p23 expression decreases. The significance of this observation is unclear, since studies involving p23 function in cancer mostly focus on its role in estrogen receptor signaling. It is known that p23 preferentially interacts with Hsp90 in the ATP-bound state (Sullivan *et al*., 2002), but the mechanism of action of this co-chaperone remains to be elucidated. One report suggests that mutant p23 (which affects ER signaling, but still binds Hsp90) antagonizes Hsp90 function under heat shock conditions, suggesting that Hsp90 is actually sequestered by p23 under cellular stress (Oxelmark *et al*., 2003).

The opposing results found in our cultured systems and clinical specimens related to p23 expression reflect the presence of inherent differences between these two models, highlighting the fact that *in vitro* data is not always a true representation of nature. Based on this idea, we find that nuclear Hsp90 is greater in established cell lines than nuclear expression in DCIS and invasive breast tissue. Similarly, cytoplasmic Hsp90 is also greater in cancer cell lines than cytoplasmic Hsp90 in the same tissue specimens. These findings also extend to p23 nuclear and cytoplasmic locations, indicating that chaperone expression is innately higher in artificial systems. These differences reflect the dissimilarity of cell lines and *in vivo* tumors (Lerescu *et*

al., 2008) and may be indicative of the accumulation of alterations due to continuous culture and growth in an isolated environment.

Since invasive carcinomas displayed highly variable Hsp90 and p23 immunostaining, we explored the possibility that chaperone expression in these heterogeneous cores may correlate with other breast cancer-associated factors. In order to describe the extent or severity of a particular breast cancer, the TNM system has delineated specific criteria for grouping cancers and has been a standard method of uniformly grading breast cancers to allow meaningful comparisons (Escobar *et al*., 2006). This system takes into account the tumor-node-metastasis stage of a particular cancer by assigning categorical numbers describing the size of the tumor (TX, Tis, T0-T4), the involvement of lymph nodes (NX, N0-N4), and the presence of metastases (MX, M0-M1).[5] Using these guidelines, a higher T, N, and M number signifies a more advanced tumor. The TNM score also serves as a predictive marker for response to therapy and as such, provides prognostic information. Accordingly, we discovered that a positive correlation exists between nuclear Hsp90 and TNM stage, such that higher Hsp90 in invasive breast carcinomas was associated with a higher TNM grade. This finding suggests that elevated nuclear Hsp90 may be an indicator or marker of severity and may identify those cancers that are more likely to metastasize.

Since the majority of breast cancers are estrogen-dependent (Bai and Gust, 2009), it was necessary to address whether chaperones were associated with the presence or absence of steroid hormone receptors, specifically the estrogen and progesterone receptors. Additionally, since ER and PR use the Hsp90 machinery for maturation, it would be logical to address whether the status of these receptors is altered upon Hsp90 and/or p23 upregulation. As a summary of receptor status, less than a third and less than half of all invasive carcinomas included in our

[5] http://ccm.ucdavis.edu/bcancercd/311/tnm_staging.html

tissue arrays are ER or PR negative, respectively, which is in line with the general observation that ER and PR are present in the majority of breast cancers. Of note is the fact that more advanced and/or recurrent breast cancers that are originally ER positive eventually lose ER expression through various mechanisms, including epigenetic ones, thus obviating any response to endocrine therapy (Kuukasjärvi *et al*. 1996; Jensen and Jordan, 2003; Schiff *et al*., 2003; Leu *et al*., 2004). Similar observations have been reported for PR, which is positively regulated by ER, in that loss of PR expression coincides with the onset of tamoxifen resistance (Gross *et al*., 1984) together with an increase in tumor aggressiveness and a decrease in survival rate (Balleine *et al*., 1999). The mechanisms for loss of PR are also variable and include the presence of nonfunctional ER and hypermethylation of the PR promoter (Horwitz and McGuire, 1978; Lapidus *et al*., 1996).

Breast cancer progression studies involving Hsp90 and ER are less defined, but we find here that higher Hsp90 expression is tightly associated with ER negativity. In identifying a negative correlation between cytoplasmic Hsp90 and ER status, it appears that higher chaperone levels are associated with the loss of ER expression and the development of more aggressive breast cancers. Because ER is also a key prognostic marker for early breast cancer outcome (Martín, 2006; Rhee *et al*., 2008), as opposed to advanced stages where ER is weakly informative, it is indicative that high Hsp90 is associated with those cancers that have a poorer prognosis. Furthermore, since ER is a client protein of Hsp90, it may be possible that the upregulation of Hsp90 in invasive carcinomas is hyperactively reducing ER stability by targeting it for degradation, which contributes to loss of receptor expression. The finding presented here is contrary to a previous study, which reported the lack of any correlation between Hsp90 and ER; however, this previous study only examined lobular neoplasia *in situ* and adjacent normal tissue

(Zagouri *et al*., 2008). Indeed, it has been found that higher Hsp90 expression is significantly associated with decreased survival over 10 years in breast cancer patients (Pick *et al*., 2007), implying that increased Hsp90 levels may affect response to treatment. In our study, although no significant correlation emerged between Hsp90 and PR, which is also a prognostic marker in breast cancer, it has been shown that PR requires more Hsp90 for stabilization and activity than ER, which would suggest that elevated Hsp90 may lead to hyperactive PR rather than degradation (Felts *et al*., 2007). As an extension of our hormone receptor analysis, we sought to determine whether any relationship exists between TNM score and ER/PR status. Consistent with previous reviews (Cui *et al*., 2005), we found that those cancers that are ER or PR negative also exist at a higher TNM stage. It is evident that a change in hormone receptor status over the natural course of the disease corresponds to more advanced cancers.

Despite the lack of a significant relationship between p23 and TNM stage, there was a positive correlation with ER and PR. The significant correlation to ER in malignant cancers supports other reports proposing that upregulation of p23 in an ER-positive tumor setting may impart a greater invasive potential (Oxelmark *et al*., 2006). The co-chaperone p23 may act as a positive regulator of ER signaling in the presence of Hsp90 and thus affect ligand binding and subsequently, the transcriptional activity of this receptor (Oxelmark *et al*., 2003). Our results showing that p23 positively correlates with ER presence support these previous studies. In fact, a decline in p23's association with the ER complex during progression increases the likelihood that ER is targeted for Hsp90-mediated proteasomal degradation. Thus, the development of more aggressive cancers may be influenced by p23 in ER positive cancers, while ER negative cancers may be less affected by p23 upregulation. In terms of PR, we observed a significant positive correlation between p23 expression and PR presence, which is supported by the dependence of

PR stability and maturation on Hsp90 co-chaperones, such as p23 (Felts *et al*., 2007). Thus, high p23 expression positively regulates ER signaling, which in turn upregulates PR expression. Taken together, there appears to be a differential association of chaperones with clinical parameters that seemingly influences the prognosis of disease.

The HER2/neu receptor, which is a member of the epidermal growth factor family, mediates signaling of growth and differentiation, and is thus also highly implicated in establishing or maintaining the pathogenesis of breast cancer. It is overexpressed in 20-30% of all breast cancers, and as such, is useful as a prognostic marker since its expression is associated with poorly differentiated and more aggressive breast cancers (Slamon *et al*., 1987). Indeed, HER2/neu positive lymph node-negative patients show significantly decreased disease-free and overall survival over 10 years (Choi *et al*., 2009). Due to various study limitations, we were not able to assess correlative HER2/neu protein expression with Hsp90 or p23 in our tissue arrays. It is possible that since HER2/neu overexpression is significantly associated with ER and PR negativity (Choi *et al*., 2009), Hsp90 expression may be higher while p23 may be reduced in these tumors.

5.3 Client-bound and free forms of Hsp90 co-exist in cancer cells.

The upregulation of Hsp90 expression has been reported to be associated with functional or mechanistic differences between normal and transformed cells. One published study reported that Hsp90 in cancer cells has been found predominantly in an activated form bound to its client proteins, while most normal cells have uncomplexed Hsp90 (Kamal *et al*., 2003). Furthermore, they show that Hsp90 in cancer cells has a higher affinity for Hsp90 inhibitors compared to normal cells, thus providing tumor selectivity via an unknown mechanism (Kamal *et al*., 2003).

These observations suggest that Hsp90 in stressful conditions (as in tumor cells) exists in a highly activated state as a multiprotein complex capable of supporting the transformed phenotype (Chiosis and Neckers, 2006). Normal cells must then maintain Hsp90 in an inactive state that undergoes more dynamic interactions with client partners. Thus, the balance between activated and latent Hsp90 must be tipped in favor of multichaperone assembly in order for transformation to occur or progress.

Together, these data have provided a global rationale for Hsp90 inhibition; yet, our highly reproducible results contradict those previous observations, showing that Hsp90, while increased in high grade breast tumors over normal cells, is maintained in both a free and a bound state in normal, immortal, and tumor cells. Thus, based on both *in vivo* observations and *in vitro* data, it appears that while cancer cells exhibit upregulated Hsp90 expression, the heightened formation of client-bound complexes may not be exclusive for tumor cells and may therefore be dependent on increased Hsp90 levels, which could in turn drive the observed increased detectable association with clientele. Given this finding, the significance of Hsp90 inhibition is more importantly related to its localization and increased expression, rather than its client-bound or -unbound state. Hence, Hsp90 inhibition remains a promising field of research, with analogs of geldanamicin already in later phases of clinical trials.

The results of this study have provided a framework on which to study the biological significance of Hsp90 and p23 in breast cancer progression and the utility of chaperone inhibition as a breast cancer therapy. In summary, chaperone protein levels are differentially expressed in normal breast cells versus invasive breast carcinomas, and that this differential expression is based on cancer staging, rather than alterations in the Hsp90/client protein binding status. To our knowledge, this is the first comprehensive study examining Hsp90 and p23

proteins in terms of both expression and cellular compartmentalization. Examination of the role of p23 has determined that this co-chaperone has minimal correlation to breast cancer progression *per se*, but rather acts to influence ER signaling in established cancers. More importantly, we find that Hsp90 levels increase significantly in the nucleus of metastatic breast tumors, correlating with a higher TNM stage and ER negativity. Because of this relationship, it is feasible then that future breast cancer therapy could be designed to exploit a nucleus-targeted approach to blocking Hsp90 function and thus improve both delivery and response. These results have not only confirmed the upregulation of Hsp90 protein levels in cancer cells but have also implicated a relationship between this chaperone and prognostic parameters in breast cancer. Thus, Hsp90 is certainly an important regulator during breast cancer progression, and based on our results, its role in chaperoning oncogenic client proteins coupled to its linkage with clinical markers is clear.

5. 4 Radicicol, alone and in combination, affects cellular proliferation

The chaperone Hsp90 is designated as a member of a new GHKL superfamily of proteins that are ATP-dependent. This family of proteins varies in their functions and primary sequence, but do share a unique ATP-binding motif, termed the Bergerat fold (Dutta and Inouye, 2000). Since radicicol directly interacts with Hsp90 via this fold, this inhibitor is able is modulate the chaperoning activities of Hsp90. In fact, RAD has a higher affinity for Hsp90, competes with GA for binding in the N-terminal domain (Schulte *et al*., 1998a), and is effective in GA-resistant cells (Chiosis *et al*., 2003). Furthermore, RAD is not associated with hepatotoxicity as seen with GA treatment, is more potent in terms of blocking ATPase activity, and prevents the association of the co-chaperone p23 with Hsp90 (Yamamoto *et al*., 2003; Roe *et al*., 1999). In cancer cells,

RAD has been shown to affect the level of Hsp90 client proteins involved in cell signaling (Schulte *et al*., 1998a). The major drawback for RAD is its lack of *in vivo* efficacy, which could be overcome with appropriate delivery mechanisms.

Since Hsp90 affects the maturation of client proteins that are involved in the cell cycle, examining cell growth was a logical start to delving into the cellular response to RAD. We have shown here that RAD does elicit a robust decline in proliferation and this effect is noticeable even at lower RAD concentrations. It is possible that RAD is acting on key factors that modulate progression through the cell cycle. Studies have shown that RAD inhibits the activity of human topoisomerase II, which aids in unwinding DNA during replication (Gadelle *et al*., 2006). Because MCF7 cells respond to RAD at a lower concentration, it is possible that breast cancer cells are more sensitive to Hsp90 inhibition than prostate cancer cells (Compton *et al*., 2006), which show responsiveness at a much higher (10-fold) RAD concentration.

RAD pretreatment in combination with Adr elicits an even greater reduction in cell growth when compared to Adr singly treated cells. At each Adr concentration, the decrease in population doubling with RAD pretreatment is more than the combined effects of RAD alone and Adr alone. These results indicate that RAD plus Adr produces a greater than additive effect on cell growth, rather, it suggests a more synergistic response. As such, RAD pretreatment appears to be sensitizing breast cancer cells to the damaging effects of Adr, culminating in a more potent growth inhibition. Substantiating this finding, RAD has been shown to induce radiosensitization as evidenced by an increase in cell death and the degradation of Her2/neu, which is responsible for mediating cell growth signaling (Harashima *et al*., 2005). Additionally important is the finding that since low Adr concentrations in combination with RAD is able to

significantly reduce cell growth, it is possible to treat breast cancer using a less toxic chemotherapeutic dosage when combined with a pretreatment agent.

Unlike RAD plus Adr treatment, which was associated with negligible cell death, RAD plus CIS or TAX did cause an increase in cell death. As assessed by the number of non-adherent cells, treatment with RAD plus CIS caused a significant increase in dead cells as compared to treatment with RAD alone at the longest treatment period. The average number of CIS induced dead cells was also less than combination treatment but it was not statistically significant. Considering average numbers, the combination of RAD and CIS (2.6%) is associated with slightly more dead cells than the simple addition of RAD only (0.96%) and CIS only (1.4%) treated cells (0.96% + 1.4% = 2.4%). It is necessary to point out that although non-adherent cells appear upon RAD and CIS combination treatment, the percentages of dead cells are still considerably low. RAD pretreatment with TAX greatly induces the appearance of non-adherent cells, displaying percentages more than nine times that of RAD plus CIS at the longest treatment time, but this increase is comparable to that of TAX alone. Again, the number of dead cells with RAD plus TAX was significantly different than with RAD alone. Thus, Hsp90 inhibition does not appear to be sensitizing CIS or TAX treated cells to cell death.

Tamoxifen acts as an ER antagonist, such that it recognizes and binds at the same site as the normal ligand, estradiol, but is believed to prohibit functional signaling beyond this receptor. At a concentration of 1 μM, TAM was shown to negatively affect cellular proliferation in ER-positive MCF7 cells. When compared to MCF7 with intact ER activity (RAD plus Adr), TAM plus RAD plus Adr treated cells display even more reduced cell growth at lower Adr concentrations. It is apparent that blocking ER activity is eliciting a stronger negative proliferative response in breast cancer cells. Furthermore, since the estrogen receptor is also a

client protein of Hsp90 whose activity triggers proliferation signals (Björnström and Sjöberg, 2005), inhibition of Hsp90 may be leading to ER degradation. Indeed, RAD represses ER activation of ERE-responsive target genes and contributes to a ubiquitination and subsequent degradation of ERα (Lee *et al*., 2002). Thus, prior blockade of ER activity combined with inhibition of Hsp90 chaperoning activities on ER may collectively contribute to decreased cell growth.

5.5 Telomerase activity decreases in response to RAD

As an Hsp90 client protein that is involved in immortalization and conversion to the transformed phenotype, telomerase is upregulated in the majority of human cancers and is associated with more aggressive breast cancers (Bieche *et al*., 2000). Minimally composed of the catalytic hTERT subunit and the internal RNA template, hTR, telomerase maintains telomere length and provides for an unlimited replication potential. The stable association of Hsp90 and p23 with the functional telomerase enzyme is an uncommon occurrence for chaperones (Forsythe *et al*., 2001), since chaperones generally interact dynamically with their clientele (Banerji, 2009). The interaction between Hsp90 and its client protein telomerase, in this case, is more than a transient process and may provide functional insight into this reverse transcriptase.

It has been proposed that the continued association of Hsp90 and p23 is required to maintain the proper conformation of telomerase during translocation of the enzyme as hTR binds and unbinds telomeric sequence (Forsythe *et al*., 2001). We present here that Hsp90 inhibition effectively reduces telomerase activity in a time-dependent manner. It is possible that RAD is blocking the chaperoning function of Hsp90 on telomerase, which may lead to reduced assembly or less stability and thus less activity. This decrease in telomerase activity has been reported in

other studies involving both RAD and other Hsp90 inhibitor classes (Nakai *et al*., 2006; Donnelly and Blagg, 2008). It is notable that 0.03 μM RAD alone induces a decline in telomerase activity that coincides with a reduction in cell proliferation, such that RAD only treated cells display a 70% reduction in cell growth at 2 d and a 35% reduction at 4 d compared to untreated cells. In this respect, the decrease in telomerase activity may be alleviating telomere maintenance in these cancer cells, leading to the lack of proliferation. As supporting evidence, inhibition of telomerase activity is associated with growth inhibition and reduction in telomere length in myeloma cells (Shammas *et al*., 2004).

In this respect, the decline in telomerase activity upon Hsp90 inhibition could be due to a lack of telomerase assembly, a lack of telomere binding, the absence of catalytic hTERT activity, or telomerase degradation. Firstly, inhibition of Hsp90 may prevent the association of the catalytic subunit with the internal RNA subunit, and thus prevent proper assembly of telomerase. Alternatively, it is possible that Hsp90 inhibition exerts its effect on telomerase activity by preventing the reassembly of hTERT and hTR following translocation to the next telomeric tract. Secondly, Hsp90 could aid in substrate recognition by telomerase, such that inhibition of Hsp90 activity subsequently leads to an inability of telomerase to bind telomeres. Thirdly, it may be possible that hTERT and hTR are able to associate, but inhibition of Hsp90 prevents functional activity of the assembled complex. Finally, telomerase degradation via the proteasomal pathway has been observed in lung carcinoma cells treated with GA in a time- and dose-dependent manner (Kim *et al*., 2005). Our lab has corroborated this finding in prostate cancer cells, showing that cells transfected with GFPhTERT show a time- and dose-dependent decline in fluorescence upon RAD treatment that is able to be blocked by a proteasome inhibitor (Nguyen and Holt, unpublished observations).

5.6 p53, p21, and cell cycle regulation

The tumor suppressor protein, p53, has been associated with malignant transformation since it is frequently mutated in cancer. Long considered the guardian of the genome, p53's essential role in mediating cell cycle arrest, senescence, and apoptosis in response to DNA damage is well documented (Vasquez *et al*., 2008). Mutant p53 is dependent upon the chaperoning ability of the Hsp90 machinery in order to remain in a stable conformation, supported by structural studies that reveal the presence of the unfolded form of p53 in association with Hsp90 (Rudiger *et al*., 2002). Abrogation of functional Hsp90 by geldanamycin leads to a reduction in mutant p53 most likely through destabilization of the improperly folded form of p53 (Blagosklonny *et al*., 1996).

Deregulation of the cell cycle is a fundamental factor contributing to the persistence of the cancer phenotype. By gaining the ability to continuously proliferate, tumor cells can proceed through the cell cycle unchecked due to their insensitivity to inhibitory signals and regulatory controls (Deshpande *et al*., 2005). As explained in detail in the introduction, upon DNA damage, wild-type p53 primarily signals via the cyclin-dependent kinase inhibitor, $p21^{Waf1/Cip1}$, which triggers G1/S phase cell cycle arrest (Cadwell and Zambetti¸ 2001). p21 physically associates with and is able to inhibit the activity of cyclin D-Cdk4 complexes, which normally guide progression through the G1/S restriction point upon stimulation by mitogenic signals (LaBaer *et al*., 1997).

Although it acts as the standard breast cancer cell line in basic research, MCF7 cells (here obtained from ATCC) carry a highly complex karyotype, containing between 64-83 chromosomes with various chromosome-specific duplications and deletions (Wenger *et al*., 2004). For most studies, proliferating (young) BJ foreskin fibroblasts were included as the

standard “normal” cell line to which breast cancer cells were compared. These fibroblasts were maintained and used at population doublings in the range of approximately PD 30 to PD 45, which is well below the onset of senescence in the range of PD 80-100 (Keys *et al*., 2004; Sitte *et al*., 2001). Of note, the levels of p53 and p21 in normal BJ fibroblasts are consistently very low to undetectable by western blotting at low protein concentration, suggesting that under normal conditions, the tumor suppressor protein p53 and its downstream target p21 remain in a latent state. Hence, normal cells are subject to growth regulatory controls, while cancer cells display enhanced cell cycle progression and hyperactivation of cyclin-Cdk complexes (Ortega *et al*., 2002). This cell cycle deregulation exists in sporadic breast carcinomas, in which Cdk4 gene amplification and high Cdk4 protein expression has been associated with an increase in proliferative index (An *et al*., 1999).

The decline in cell growth with the concurrent upregulation of p53 and p21 upon treatment with Adr alone and with RAD plus Adr support the role of these proteins in negative regulation of the cell cycle. RAD plus Adr induces p53 and p21 to a lesser extent than Adr alone, indicating that MCF7 cells are being sensitized by Hsp90 inhibition. In other words, the combination of RAD plus Adr evokes a pronounced decline in cell growth (more so than with Adr alone) but elicits less DNA damage. The less severe damage response could then be interpreted as a clinical advantage since it would be associated with less cytotoxicity. Additionally, both Adr alone and RAD with acute Adr treatment leads to a decrease in Cdk4 levels, such that the highest Adr concentration corresponds to the greatest induction of p53 and p21 and the lowest reduction of Cdk4. The notable decline in Cdk4 is indicative of a blockade in cell cycle progression, which leads to growth arrest manifested as decreased cell growth. Indeed, it has been established that in cells with wild-type p53, Cdk4 down regulation in the presence of

TGF-β coincides with G1 growth arrest (Ewen, 1996). Furthermore, since Cdk4 is also a client protein of Hsp90, the observed Cdk4 reduction could also reflect the consequence of Hsp90 inhibition. In this manner, RAD may cause the degradation of Hsp90-associated Cdk4. Finally, mutant p53 MDA-MB231 cells do not display alterations in p53 or p21 protein expression upon Adr or RAD plus Adr treatments, suggesting that the results noted in MCF7 cells may be p53-dependent. Taken together, cell growth aberrations are likely the culmination of both p53- and p21-induced arrest at the transition point between G1 and S phases, as well as the potential degradation of cell cycle regulatory proteins upon RAD and Adr treatment.

In order to elucidate whether the alterations in cell fate-related proteins, p53 and p21, were dependent upon the mechanism of action related to Adr, we sought to assess the effect of other chemotherapeutics, including cisplatin and taxol. CIS, like Adr, is also a DNA damaging agent in that it forms unrepairable DNA cross-links. While Adr inhibits DNA unwinding by topoisomerase II, CIS acts by prohibiting further progression by RNA polymerase II, creating stalled complexes that are ineffectively resolved. The mechanism of action of TAX, however, differs from that of Adr and CIS, since it acts as a microtubule-stabilizing agent. In this manner, the metaphase to anaphase transition is blocked due to the absence of the required microtubule depolymerization. Despite the different mechanisms, CIS and TAX both typically influence cell fate by sending cells down an apoptotic pathway.

In our study, treatment with CIS over 48 hr results in a slight upregulation of p21 without a concurrent increase in p53 upon CIS treatment alone and more evidently, in conjunction with RAD. Although no detectable change occurs in p53 protein levels over this time period, it may be possible that p53 is transiently induced early (< 4 hr) upon CIS treatment. Nevertheless, these data indicate that p53-independent mechanisms exist to stimulate p21 activation or expression in

response to CIS. It is notable that CIS alone at 48 hr induces a similar level of p21 expression as does RAD and CIS at 4 hr. Unlike RAD and Adr combination treatments, treatments with CIS do not induce any significant changes in Cdk4 expression. It may be possible that p21 levels must reach a threshold level not attained in our CIS studies in order to exert an inhibitory effect on Cdk4. Nevertheless, it is possible that inhibition of Hsp90 is sensitizing cells to be more responsive to CIS in terms of cell fate mediator expression. In other words, RAD pretreatment could be eliciting a damage response earlier than with CIS alone, which may have therapeutic implications. Breast cancer cells could be treated for a shorter period of time if first applied with RAD, thus limiting off target effects while maximizing antitumor responses.

Treatment with TAX alone or with RAD plus TAX produces an extreme upregulation of p53 protein levels, potentially reflecting increased protein stability, and a corresponding increase in p21 that appears to be time-dependent. A closer inspection shows that RAD pretreatment elicits an increase in p53 and p21 earlier than with TAX alone. Similar to CIS treated cells, RAD may be sensitizing cells to be more responsive to TAX in terms of cell fate protein induction. TAX, as a microtubule stabilizing agent, blocks the G2 to M phase transition but is also associated with a down regulation of Cdk4 (Yoo *et al*., 1998). This decrease subsequently leads to a blockade in the G1 to S phase transition, thus inducing cell cycle arrest at this stage. Our observation that Cdk4 is reduced upon treatment with TAX alone is consistent with this previous finding, yet the significance of why RAD pretreatment subsequently increases Cdk4 expression remains unclear.

Treatment with TAM in conjunction with Adr leads to a marked decrease in p53, without a concurrent decrease in p21. Similarly TAM + RAD + Adr (TRA) treated cells also display decreased p53 comparable to that of TAM + Adr (TA) treated cells, suggesting that TAM is the

key factor driving p53 reduction. It has been reported that ER activity is regulated by wild-type p53, signifying concordance between ER and p53 expression (Shirley *et al*., 2009), but it is unclear whether abolition of ER activity in turn affects p53 expression. Unlike that of TA cells, TRA cells exhibit reductions in p21 at the highest Adr concentrations, indicating that RAD pretreatment may only be effective at higher doses of Adr, and thus would not be a good method of sensitization. Both TA and TRA treated cells display reduced Cdk4 protein levels in the absence of p21 upregulation, suggesting that TAM is modulating Cdk4 inhibition via a different cyclin-dependent kinase inhibitor, such as p16.

5.7 Radicicol affects co-chaperones of the Hsp90 cycle

Upon proteotoxic damage, the main responders, Hsp70 and Hsp27, are strongly induced. The ATP-dependent chaperone Hsp70 is able to act both independently of and in concert with Hsp90. When utilized for the Hsp90 machinery, Hsp70 acts as a co-chaperone to recruit client proteins for the Hsp90 cycle (Morishima *et al*., 2000). This co-chaperone has been shown to include various isoforms, otherwise considered different members of the Hsp70 family. Our data suggest that a constitutive and inducible form exist and that they are differentially expressed depending upon the type of drug treatment. The smaller 69 kDa form is seen in all cells, treated or not, and so appears to represent constitutive Hsp70 found under basal conditions, while the larger 72 kDa form seems to be inducible. The ATP-independent chaperone, Hsp27, exerts its protective function autonomously since it is not a component of the Hsp90 cycle.

Adr single treatment induces an appreciable reduction in Hsp70 while RAD plus Adr only produces a slight decrease. This observation further supports the presence of sensitization since the heat shock response is less stimulated due to less stress on the cell upon RAD

pretreatment. Although treatment with AdR and RAD plus Adr did not affect total protein levels of Hsp27, this chaperone has also been implicated in cell survival (Landry *et al*., 1989). For instance, overexpression of Hsp27 blocks apoptosis by preventing caspase activation in leukemic cells treated with etoposide, an inhibitor of topoisomerase II (Garrido *et al*., 1999). Thus, the Hsp90-related chaperone, Hsp70, is affected by RAD, but not the Hsp90-independent chaperone, Hsp27.

RAD pretreatment with Adr follow-up also led to an appreciable decrease in p23 levels at the highest Adr concentration (0.75 μM). This decline may be related to the role of p23 as both a member of the Hsp90 machinery and as an independent chaperone. Since p23 stabilizes the ATP-bound form of Hsp90, it is likely that treatment with radicicol prevents this association, as reported with GA treatment. In support of this notion, p23 was found to be cleaved by caspase 3 and 7 upon GA treatment in cancer cells (Gausdal *et al*., 2004), and in apoptotic cells, this cleavage occurred at the C-terminal end creating a truncated p23 that was then directed towards degradation in a proteasome-dependent manner (Mollerup and Berchtold, 2005). RAD pretreatment may be eliciting the same effect and causing the degradation of p23 via the proteasomal pathway. Since p23 also has chaperoning activity independent of Hsp90 (Freeman *et al*., 1996), RAD and Adr in combination may be blocking this additional function. Furthermore, overexpression of p23 has been shown to be associated with the development of resistance to Hsp90 inhibitors. In corroborating studies, p23 overexpression reduced the inhibitory activity of RAD (Cox and Miller, 2003), while p23 reduction increased susceptibility to Hsp90 inhibition (Forafonov *et al*., 2008). Extended to our data, RAD pretreatment may lead to a p23 decrease when treated in combination with 0.75 μM Adr, causing destabilization of the ATP-bound form of Hsp90, which consequently negatively affects Hp90 activity on clientele.

Inhibition of Hsp90 prior to CIS or TAX treatment, as well as CIS alone at 48 hr, is associated with an upregulation of the inducible 72 kDa form of Hsp70. Likewise, RAD plus TAX treated cells also induce the larger Hsp70 form. Since this form is only barely detectable at earlier CIS only time points and at all TAX only time points, it may be that Hsp90 inhibition is stimulating a more robust heat shock response from other chaperones. In other words, Hsp70 may be upregulated in response to the lack of Hsp90 activity. This is supported by the finding that RAD alone treatment elicits the same upregulation of the inducible Hsp70 form, suggesting that RAD is not sensitizing cells to CIS or TAX treatments in terms of co-chaperone expression. Treatment with the TAM plus Adr series does not considerably affect Hsp70 expression, while the TRA series does seem to show a small increase in the inducible Hsp70 form when compared against RAD only, again suggesting that RAD may be provoking the stress response of other chaperones in the context of Hsp90 inactivity.

5.8 Expression of c-Abl is altered in response to CIS but not TAX

The c-Abl tyrosine kinase is an Hsp90 client protein that is ubiquitously expressed in all tissues and aids in the regulation of cellular proliferation, cell survival, cell migration, and influences cell fate decisions (Lin and Arlinghaus, 2008). Nuclear c-Abl is activated by DNA damage, which in turn initiates an apoptotic response, while cytoplasmic c-Abl is involved in signal transduction and is thus believed to be the oncogenic form (Wang, 2000). Although mostly known for its role as part of the bcr-abl fusion protein found in chronic myeloid leukemia, c-Abl activation also exists in solid tumors, including breast cancer. Previous studies have reported that c-Abl can be stimulated by ErbB2 signaling, which has been shown to be constitutively active in breast cancer (Plattner *et al*., 1999). Activated c-Abl can promote

invasion in breast cancer cells, such that treatment with imatinib mesylate (Gleevec), a c-Abl kinase inhibitor, in a highly metastatic breast cancer cell line reduces the size and incidence of colony formation (Srinivasan and Plattner, 2006; Srinivasan *et al*., 2008).

We present here that RAD plus TAX does not stimulate c-Abl production, while RAD in combination with CIS only modestly induces an increase in protein levels. This suggests that the difference in c-Abl expression is likely due to the presence of either CIS, a DNA damaging agent, or TAX, a microtubule stabilization agent, but not RAD. It would be interesting to assess the activity of this tyrosine kinase in terms of its ability to interact with and activate signaling molecules and apoptotic mediators. In this respect, CIS may be activating the kinase function in MCF7 cells while c-abl remains dormant in TAX treated cells.

5.9 Induction of senescence or apoptosis

The observed increase in senescence in RAD pretreated cells corresponds to the decrease in telomerase activity over time. It is believed that overcoming proliferative boundaries involves the upregulation of telomerase and the subsequent maintenance of telomere length (Shay and Wright, 1996). Through inhibition of Hsp90, we were not only able to reduce telomerase activity but also induce a senescent phenotype. However, no observable changes in telomere length were noted, which contradicts the idea that replicative senescence is universally associated with telomere shortening. Rather, the range of telomere length is consistently between 2.0 kb and about 4.0 kb, regardless of treatment or no treatment, with is in line with previous findings reporting an average telomere length of 3.5 kb in MCF7 cells (Elmore *et al*., 2002). As such, the change in telomerase activity may not be associated with telomere length, since a previous study has shown that telomerase activity does not foretell telomere length (Savre-Train *et al*., 2000).

The lack of telomere length changes may also point to the limitation of the TRF assay, which assesses global length alterations such that chromosome-specific changes are not readily detectable. It is possible that telomere length regulation and restriction of proliferative capacity is mediated by alterations at specific chromosome ends rather than by the overall shortening of all telomeres. In theory, because human telomere length varies greatly, the shortest telomere should govern proliferative life span (Lansdorp *et al*., 1996). In support of the chromosome-specific proliferation restriction, the Xp chromosome reportedly maintains its length while all other telomeres shorten, and the active Xp undergoes shortening at a slower rate than inactive Xp (Hao and Tan, 2001; Marten *et al*., 2000; Surralles *et al*., 1999). Similarly, the telomeres of chromosome 17q are shorter than global telomere lengths in DCIS and breast carcinoma tissue, while chromosome 9p telomere length is shorter in breast cancer patients than unaffected controls (Rashid-Kolvear *et al*., 2007; Zheng *et al*., 2009).

Despite the lack of replicative senescence, accelerated senescence induced in response to chemotherapeutics may exist. Cells undergoing this type of senescence share morphological and biochemical similarities to those undergoing replicative senescence (Gewirtz *et al*., 2008). Senescence in RAD and Adr treated cells was assessed by β-galactosidase staining which works optimally at pH 6.0. Initially believed to be an isoform of the lysosomal β-galactosidase, recent studies report that this enzyme is in fact lysosomal β-galactosidase, and its accumulation is a reflection of increased lysosomal mass, which is present in senescent cells (Kurz *et al*., 2000). Although the β-gal enzyme is not directly related to senescence, cells undergoing growth arrest uniformly express its activity, while proliferating or young cells do not contain detectable activity. Despite its seemingly arbitrary designation, it is an accepted and widely used marker of the senescence phenotype in the absence of an alternative method of detection (Coates, 2002;

Dimri *et al*., 1995). As a cautionary statement, normal cells also display positive SA-β-gal activity depending on the temperature and incubation time with β-gal substrate, so additional parameters must be applied to assess a genuine senescence response.

Our observation that the population of senescent cells increases upon drug treatment is consistent with the upregulation of p53, which has been reported in other studies (Wynford-Thomas, 1999). The increase in p53 and p21 expression after both Adr treatment and Hsp90 inhibition triggers the cell to cease cell division and may in turn lead to growth arrest. However, p53 and p21 are not exclusive to growth arrest induction since they also participate in quiescence, differentiation, and apoptosis. Indeed, activation of senescence and apoptotic programs via p53 are critical tumor suppressor mechanisms that prevent malignant transformation (Rodier *et al*., 2007).

As p53 is also intricately involved in transducing an apoptotic signal in response to DNA damage, apoptotic cell death was assessed upon RAD pretreatment. We observe no outstanding differences between Adr singly treated cells and RAD pretreated cells, suggesting that Hsp90 inhibition does not predispose MCF7 breast cancer cells to apoptosis. The lack of apoptotic cells may be related to the unchanged expression of Hsp27, which has the ability to abrogate apoptosis (Garrido *et al*., 2006). Taken together with the cell growth data, it appears that RAD pretreatment with Adr follow-up does not primarily stimulate an apoptotic response. However, it is also important to recognize that MCF7 cells lack functional caspase 3, which is a key effector of the apoptotic response and a valid biochemical marker of apoptosis (Abu-Qare *et al*., 2001). In support of this role of caspase 3, MCF7 cells are reportedly resistant to radiation-induced apoptosis in the absence of caspase 3, but are observed to activate caspase 9 and undergo apoptosis upon reintroduction of caspase 3 (Essmann *et al*., 2004). Thus, in our study,

undetectable apoptosis in RAD plus Adr treated MCF7 cells may in part be attributed to the absence of activated caspase 3.

On the other hand, RAD in combination with 0.1 μM CIS or 100 nM TAX does lead to the emergence of apoptotic cells. CIS and TAX exert their actions through both the mitochondrial (intrinsic) and death receptor mediated (extrinsic) apoptotic pathways (Fulda and Debatin, 2006). We show here that RAD plus CIS is associated with more apoptotic cells than RAD alone, as supported by the difference in the number of non-adherent cells. However, the percentage of non-adherent cells between RAD plus CIS and CIS alone treated cells do not significantly differ at either 24 hr or 48 hr, which is also shown by the lack of difference in the amount of apoptotic cells. Similar observations were found for TAX studies, in that RAD plus TAX induced apoptotic cell death to the same extent as TAX only treated cells. Based on this data, it appears that Hsp90 inhibition is not sensitizing cells to be more responsive to CIS or TAX sequential treatment in terms of apoptotic death induction. Perhaps lower drug concentrations may produce more sensitivity to RAD pretreatment and lead to synergistic effects on apoptosis. As such, non-apoptotic cell death (necrosis, autophagy, mitotic catastrophe) may be present, but undetectable, since drug dosage may affect the type of cell death (Fulda and Debatin, 2006).

5.10 Perspective

In summary, the results presented herein highlight the utility of Hsp90 inhibition on abrogation of cellular proliferation, a key aspect of any cancer. Expression of cell fate related proteins and those involved in regulation of the cell cycle, as well as co-chaperones and Hsp90 client proteins, are differentially affected depending on the drug used. In conclusion, the overall

study has presented both descriptive and informative data suggestive of mechanistic differences regarding the role of Hsp90 in breast cancer progression. Higher Hsp90 expression is present in invasive breast carcinomas as compared to normal breast tissue, and this upregulation corresponds to loss of ER expression and advanced disease stage. Inhibition of Hsp90 through the action of radicicol appears to be a valid method to combat breast cancer, especially in terms of cellular proliferation and expression of Hsp90-related oncogenic proteins. Thus, Hsp90 clearly plays an active role in breast cancer progression and maintenance such that inhibition of Hsp90 elicts a robust response to certain chemotherapies more so than others. The future will surely reveal exciting advances in the comprehension of Hsp90 inhibition and advantages of its use in cancer therapy.

List of References

References Cited

Abukhdeir AM and Park BH. 2008. p21 and p27: roles in carcinogenesis and drug resistance. *Expert Rev Mol Med*. 10: 1-15.

Abu-Qare AW and Abou-Donia MB. 2001. Biomarkers of apoptosis: release of cytochrome c, activation of caspase-3, induction of 8-hydroxy-2'-deoxyguanosine, increased 3-nitrotyrosine, and alteration of p53 gene. *J Toxicol Environ Heath B Crit Rev*. 4: 313-332.

Agrawal A, Gutteridge E, Gee JM, Nicholson RI, Robertson JF. 2005. Overview of tyrosine kinase inhibitors in clinical breast cancer. *Endocr Relat Cancer*. 12 (Suppl): S135-S144.

Akalin A, Elmore, LW, Forsythe HL, Amaker BA, McCollum ED, Nelson PS, Ware JL, Holt SE. 2001. A novel mechanism for chaperone-mediated telomerase regulation during prostate cancer progression. *Cancer Research*. 61: 4791-4796.

Akashi M and Koeffler HP. 1998. Li-Fraumeni syndrome and the role of the p53 tumor suppressor gene in cancer susceptibility. *Clin Obstet Gynecol*. 41: 172-199.

Algeciras-Schimnich A, O'Kane DJ, Snozek CL. 2008. Pharmacogenomics of tamoxifen and irinotecan therapies. *Clin Lab Med*. 28: 553-567.

Allday MJ, Inman GJ, Crawford DH, Farrell PJ. 1995. DNA damage in human B cells can induce apoptosis, proceeding from G1/S when p53 is transactivation competent and G2/M when it is transactivation defective. *EMBO J*. 14: 4994-5005.

Alsner J, Yilmaz M, Guldberg P, Hansen LL, Overgaard J. 2000. Heterogeneity in the clinical phenotype of TP53 mutations in breast cancer patients. *Clin Cancer Res*. 6: 3923-3931.

An HX, Beckmann MW, Reifenberger G, Bender HG, Niederacher D. 1999. Gene amplification and overexpression of CDK4 in sporadic breast carcinomas is associated with high tumor cell proliferation. *Am J Pathol*. 154: 113-118.

Angele S, Treilleux I, Taniere P, Martel-Planche G, Vuillaume M, Bailly C, Bremond A, Montesano R, Hall J. 2000. Abnormal expression of the ATM and TP53 genes in sporadic breast carcinomas. *Clin Cancer Res*. 6: 3536-3544.

Anthoney DA, McIlwrath AJ, Gallagher WM, Edlin AR, Brown R. 1996. Microsatellite instability, apoptosis, and loss of p53 function in drug-resistant tumor cells. *Cancer Res*. 56: 1374-1381.

Argon Y and Simen BB. 1999. GRP94, an ER chaperone with protein and peptide binding properties. *Semin Cell Dev Biol*. 10: 495-505.

Artandi SE and Attardi LD. 2005. Pathways connecting telomeres and p53 in senescence, apoptosis, and cancer. *Biochemical and Biophysical Research Communications*. 331: 881-890.

Aubert G and Lansdorp PM. 2008. Telomeres and aging. *Physiol Rev*. 88: 557-579.

Bachur NR, Johnson R, Yu F, Hickey R, Applegren N, Malkas L. 1993. Antihelicase action of DNA-binding anticancer agents: relationship to guanosine-cytidine intercalator binding. *Mol Pharmacol*. 44: 1064-1069.

Bai A and Gust R. 2009. Breast Cancer, Estrogen Receptor and Ligands. *Arch Pharm Chem Life Sci*., 342: 133-149.

Balleine RL, Earl MJ, Greenberg ML, Clarke CL. 1999. Absence of progesterone receptor associated with secondary breast cancer in postmenopausal women. *Br J Cancer*. 79: 1564-1571.

Banerji U. 2009. Heat shock protein 90 as a drug target: some like it hot. *Clin Cancer Res*. 15: 9-14.

Banerji U, Walton M, Raynaud F, Grimshaw R, Kelland L, Valenti M, Judson I, Workman P. 2005. Pharmacokinetic-pharmacodynamic relationships for the heat shock protein 90 molecular chaperone inhibitor 17-allylamino, 17-demethoxygeldanamycin in human ovarian cancer xenograft models. *Clin Cancer Res*. 11: 7023-7032.

Bartek J and Lukas J. 2001. Mammalian G1- and S-phase checkpoints in response to DNA damage. *Curr Opin Cell Biol*. 13:738-747.

Bartek J and Lukas J. 2007. DNA damage checkpoints: from initiation to recovery or adaptation. *Current Opinion in Cell Biology*. 19: 1-8.

Baykal A, Rosen D, Zhou C, Liu J, Sahin AA. 2004. Telomerase in Breast Cancer. *Adv Anat Pathol*. 11: 262-268.

Becker B, Multhoff G, Farkas B, Wild PJ, Landthaler M, Stolz W, Vogt T. 2004. Induction of Hsp90 protein expression in malignant melanomas and melanoma metastases. *Exp Derm*. 13: 27-32.

Beliakoff J, Whitesell L. 2004. Hsp90: an emerging target for breast cancer therapy. *Anti-Cancer Drugs*. 15: 651-662.

Bendre M, Gaddy D, Nicholas RW, Suva LJ. 2003. Breast cancer metastasis to the bone: it is not all about PTHrP. *Clin Orthop Relat Res*. 415: S39-45.

Benson JR, Jatoi I, Keisch M, Esteva FJ, Makris A, Jordan VC. 2009. Early breast cancer. *Lancet*. 373: 1463-1479.

Berrieman HK, Lind MJ, Cawkwell L. 2004. Do beta-tubulin mutations have a role in resistance to chemotherapy? *Lancet Oncol*. 5:158-164.

Bhattacharyya MK and Lustig AJ. 2006. Telomere dynamics in genome stability. *Trends in Biochemical Sciences*. 31: 114-122.

Bieche I, Nogues C, Paradis V, Olivi R, Bedossa P, Lidereau R, Vidaud M. 2000. Quantitation of hTERT gene expression in sporadic breast tumors with a real-time reverse transcription-polymerase chain reaction assay. *Clin Cancer Res*. 6: 452-459.

Björnström L and Sjöberg M. 2005. Mechanisms of estrogen receptor signaling: convergence of genomic and nongenomic actions on target genes. *Mol Endocrinol*. 19: 833-842.

Blagosklonny MV, Toretsky J, Bohen S, Neckers L. 1996. Mutant conformation of p53 translated in vitro or in vivo requires functional Hsp90. *Proc Natl Acad Sci USA*. 93: 8379-8383.

Bracher A and Hartl FU. 2006. Hsp90 structure: when two ends meet. *Nat Struct Mol Biol*. 13: 478-480.

Bradshaw PS, Stavropoulous DJ, Meyn MS. 2005. Human telomeric protein TRF2 associates with genomic double-strand breaks as an early response to DNA damage. *Nature Genetics*. 37: 193-197.

Brown MA, Zhu L, Schmidt C, Tucker PW. 2007. Hsp90-from signal transduction to cell transformation. *Biochem Biophys Res Commun*. 363: 241-246.

Bryan TM, Englezou A, Dalla-Pozza L, Dunham MA, Reddel RR. 1997. Evidence for an alternative mechanism for maintaining telomere length in human tumors and tumor-derived cell lines. *Nat Med.* 3: 1271-1274.

Buchner J. 1999. Hsp90 & Co. – a holding for folding. *Trends Biochem Sci*. 24: 136-141.

Burkhart CA, Kavallaris M, Horwitz SB. 2001. The role of beta-tubulin isotypes in resistance to antimitotic drugs. *Biochim Biophys Acta*. 1471: O1-O9.

Cadwell C and Zambetti GP. 2001. The effects of wild-type p53 tumor suppressor activity and mutant p53 gain-of-function on cell growth. *Gene*. 277: 15-30.

Callén E and Surrallés J. 2004. Telomere dysfunction in genome instability syndromes. *Mutation Research*. 567: 85-104.

Caplan AJ. 2003. What is a co-chaperone? *Cell Stress Chaperones*. 8: 105-107.

Cardillo MR, Sale P, Di Silverio F. 2000. Heat shock protein-90, IL-6 and IL-10 in bladder cancer. *Anticancer Res*. 20:4579-4583.

Carey LA, Hedican CA, Henderson GS, Umbricht CB, Dome JS, Varon D, Sukumar S. 1998. Careful histological confirmation and microdissection reveal telomerase activity in otherwise telomerase-negative breast cancers. *Clin Cancer Res*. 4: 435-440.

Castedo M, Perfettini JL, Roumier T, Valent A, Raslova H, Yakushijin K, Horne D, Feunteun J, Lenoir G, Medema R, Vainchenker W, Kroemer G. 2004. Mitotic catastrophe constitutes a special case of apoptosis whose suppression entails aneuploidy. *Oncogene*. 23: 4362-4370.

Chang Z. 2009. Posttranslational modulation of the biological activities of molecular chaperones. *Sci China C Life Sci*. 52: 515-520.

Chen GG, Zeng Q, Tse G. 2008. Estrogen and its receptors in cancer. *Medicinal Research Reviews*. 28: 954-974.

Cheung KM, Matthews TP, James K, Rowlands MG, Boxall KJ, Sharp SY, Maloney A, Roe SM, Prodromou C, Pearl LH, Aherne GW, McDonald E, Workman P. 2005. The identification, synthesis, protein crystal structure and in vitro biochemical evaluation of a new 3,4-diarylpyrazole class of Hsp90 inhibitors. *Bioorg Med Chem Lett*. 15: 3338-3343.

Chin L, Pomerantz J, DePinho RA. 1998. The INK4a/ARF tumor suppressor gene: one gene-two products-two pathways. *Trends Biochem Sci*. 23: 291-296.

Chiosis G. 2006. Targeting chaperones in transformed systems-A focus on Hsp90 and cancer. *Expert Opin Ther Targets*. 10: 37-50.

Chiosis G, Huezo H, Rosen N, Minmaugh E, Whitesell L, Neckers L. 2003 17AAG: low target binding affinity and potent cell activity – finding an explanation. *Mol Cancer Ther*. 2: 123-129.

Chiosis G, Lucas B, Huezo H, Solit D, Basso A, Rosen N. 2003. Development of purine-scaffold small molecule inhibitors of Hsp90. *Curr Cancer Drug Targets*. 3: 371-376.

Chiosis G and Neckers L. 2006. Tumor selectivity of Hsp90 inhibitors: the explanation remains elusive. *ACS Chem Biol*. 1: 279-284.

Choi YH, Ahn JH, Kim SB, Jung KH, Gong GY, Kim MJ, Son BH, Ahn SH, Kim WK. 2009. Tissue microarray-based study of patients with lymph node-negative breast cancer shows that HER2/neu overexpression is an important predictive marker of poor prognosis. *Ann Oncol*. Epub ahead of print.

Christman SA, Kong BW, Landry MM, Kim H, Foster DN. 2006. Contributions of differential p53 expression in the spontaneous immortalization of a chicken embryo fibroblast cell line. *BMC Cell Biol*. 7: 27-38.

Clark GM, Osborne CK, Levitt D, Wu F, Kim NW. 1997. Telomerase activity and survival of patients with node-positive breast cancer. *J Natl Cancer Inst*. 89: 1874-1881.

Coates PJ. 2002. Markers of senescence? *J Pathol*. 196: 371-373.

Cohen SB, Graham ME, Lovrecz GO, Bache N, Robinson PJ, Reddel RR. 2007. Protein composition of catalytically active human telomerase from immortal cells. *Science*. 315: 1850-1853.

Compton SA, Elmore LW, Haydu K, Jackson-Cook CK, Holt SE. 2006. Induction of nitric oxide synthase-dependent telomere shortening after functional inhibition of Hsp90 in human tumor cells. *Mol Cell Biol*. 26: 1452-1462.

Corda Y, Job C, Anin MF, Leng M, Job D. 1991. Transcription by eukaryotic and prokaryotic RNA polymerases of DNA modified at a d(GG) or a d(AG) site by the antitumor drug cis-diamminedichloroplatinum(II). *Biochemistry*. 30: 222-230.

Couzin J. 2003. Tracing the steps of metastasis, cancer's menacing ballet. *Science*. 299: 1002-1006.

Cox MB and Miller III CA. 2003. Pharmacological and genetic analysis of 90-kDa heat shock protein isoprotein-aryl hydrocarbon receptor complexes. *Mol Pharmacol*. 64: 1549-1556.

Crewe HK, Notley LM, Wunsch RM, Lennard MS, Gillam EM. 2002. Metabolism of tamoxifen by recombinant human cytochrome P450 enzymes: formation of the 4-hydroxy, 4'-hydroxy and N-desmethyl metabolites and isomerization of trans-4-hydroxytamoxifen. *Drug Metab Dispos*. 30: 869-874.

Csermely P, Schnaider T, Soti C, Prohaszka Z, Nardai G. 1998. The 90-kDa Molecular Chaperone Family: Structure, Function, and Clinical Applications. A Comprehensive Review. *Pharmacol Ther*. 79: 129-168.

Cui X, Schiff R, Arpino G, Osborne CK, Lee AV. 2005. Biology of progesterone receptor loss in breast cancer and its implications for endocrine therapy. *J Clin Oncol*. 23: 7721-7735.

Cullinane C, Cutts SM, Panousis C, Phillips DR. 2000. Interstrand cross-linking by adriamycin in nuclear and mitochondrial DNA of MCF7 cells. *Nucleic Acids Res*. 28: 1019-1025.

Dai C, Whitesell L. 2005. HSP90: A Rising Star on the Horizon of Anticancer Targets. *Future Oncol*. 1: 529-540.

Daniel S, Bradley G, Longshaw VM, Söti C, Csermely P, Blatch GL. 2008. Nuclear translocation of the phosphoprotein Hop (Hsp70/Hsp90 organizing protein) occurs under heat shock, and its proposed nuclear localization signal is involved in Hsp90 binding. *Biochim Biophys Acta*. 1783: 1003-1014.

De Boeck G, Forsyth RG, Praet M, Hogendoorn PC. 2009. Telomere-associated proteins: cross-talk between telomere maintenance and telomere-lengthening mechanisms. *J Pathol*. 217: 327-344.

DeBoer C, Meulman PA, Wnuk RJ, Peterson DH. 1970. Geldanamycin, a new antibiotic. *J Antibiot*. 23: 442-447.

de Lange T. 2005. Shelterin: the protein complex that shapes and safeguards human telomeres. *Genes and Development*. 19: 2100-2110.

Delmotte P and Delmotte-Plaque J. 1953. A new antifungal substance of fungal origin. *Nature*. 171: 344.

Deng C, Zhang P, Harper JW, Elledge SJ, Leder P. 1995. Mice lacking p21CIP/WAF1 undergo normal development, but are defective in G1 checkpoint control. *Cell*. 82: 675-684.

Deng Y and Chang S. 2007. Role of telomeres and telomerase in genomic instability, senescence, and cancer. *Laboratory Investigation*. 87: 1071-1076.

Deshpande A, Sicinski P, Hinds PW. 2005. Cyclins and cdks in development and cancer: a perspective. *Oncogene*. 24: 2909-2915.

DeVita V.T., Hellman,S. and Rosenberg,S.A. 1993. *Cancer Principles and Practice in Oncology*, 4th Edn, Vols 1 and 2. J.B. Lippincott, Philadelphia, PA.

Di Cosimo S and Baselga J. 2008. Targeted therapies in breast cancer: where are we now? *Eur J Cancer*. 44: 2781-2790.

Diehl MC, Elmore LW, Holt SE. 2009. In Hiyama K (ed). Telomere Dysfunction and the DNA Damage Response. *Telomeres and Telomerase in Cancer: Cancer Drug Discovery and Development*. Totowa, NJ: Humana Press. (pp.87-125).

Dimri GP, Lee X, Basile G, Acosta M, Scott G, Roskelley C, Medrano EE, Linskens M, Rubelj I, Pereira-Smith O, Peacocke M, Campisi J. 1995. A biomarker that identifies senescent human cells in culture and in aging skin in vivo. *Proc Natl Acad Sci USA*. 92: 9363-9367.

Dittmar T, Husemann A, Schewe Y, Nofer JR, Niggemann B, Zänker KS, Brandt BH. 2002. Induction of cancer cell migration by epidermal growth factor is initiated by specific phosphorylation of tyrosine 1248 of c-erbB-2 receptor via EGFR. *FASEB J*. 16: 1823-1825.

Dollins DE, Warren JJ, Immormino RM, Gewirth DT. 2007. Structures of GRP94-nucleotide complexes reveal mechanistic differences between the Hsp90 chaperones. *Mol Cell*. 28: 41-56.

Donnelly A and Blagg BS. 2008. Novobiocin and additional inhibitors of the Hsp90 C-terminal nucleotide-binding pocket. *Curr Med Chem*. 15: 2702-2717.

Downing KH and Nogales E. 1999. Crystallographic structure of tubulin: implications for dynamic and drug binding. *Cell Struct Funct*. 24: 269-275.

Dowsett M, Daffada A, Chan CM, Johnston SR. 1997. Oestrogen receptor mutants and variants in breast cancer. *Eur J Cancer*. 33: 1177-1183.

Dorssers LC, Van der Flier S, Brinkman A, van Agthoven T, Veldscholte J, Berns EM, Beex LV, Foekens JA. 2001. Tamoxifen resistance in breast cancer: elucidating mechanisms. *Drugs*. 61: 1721-1733.

Doyle LA, Yang W, Abruzzo LV, Krogman T, Gao Y, Rishi AK, Ross DD. 1998. A multidrug resistance transporter from human MCF7 breast cancer cells. *Proc Natl Acad Sci USA*. 95: 15665-15670.

Dutta R and Inouye M. 2000. GHKL, an emergent ATPase/kinase superfamily. *Trends Biochem Sci*. 25: 24-28.

Eiseman JL, Lan J, Lagattuta TF, Hamburger DR, Joseph E, Covey JM, Egorin MJ. 2005. Pharmacokinetics and pharmacodynamics of 17-demethoxy 17-[[(2-dimethylamino)ethyl]amino]geldanamycin (17DMAG, NSC 707545) in C.B-17 SCID mice bearing MDA-MB-231 human breast cancer xenografts. *Cancer Chemother Pharmacol*. 55: 21-32.

Eleuteri AM, Cuccioloni M, Bellesi J, Lupidi G, Fioretti E, Angeletti M. 2002. Interaction of Hsp90 with 20S proteasome: thermodynamic and kinetic characterization. *Proteins: Struc Funct Genet*. 48: 169-177.

Elmore LW, Forsythe R, Forsythe H, Bright T, Nasim S, Endo K, Holt SE. 2008. Overexpression of telomerase-associated chaperone proteins in prostatic intraepithelial neoplasia and carcinomas. *Oncology Reports*. 20: 613-617.

Elmore LW, Rehder CW, Di X, McChesney PA, Jackson-Cook CK, Gewirtz DA, Holt SE. 2002. Adriamycin-induced senescence in breast tumor cells involves functional p53 and telomere dysfunction. *J Biol Chem*. 277: 35509-35515.

Escobar PF, Patrick RJ, Rybicki LA, Weng DE, Crowe JP. 2006. The 2003 Revised TNM Staging System for Breast Cancer: Results of Stage Re-classification on Survival and Future Comparisons among Stage Groups. *Annals of Surgical Oncology*. 14: 143-147.

Essmann F, Engels IH, Totzke G, Schulze-Osthof K, Jänicke RU. 2004. Apoptosis resistance of MCF7 breast carcinoma cells to ionizing radiation is independent of p53 and cell cycle control but caused by the lack of caspase-3 and a caffeine-inhibitable event. *Cancer Res*. 64: 7065-7072.

Ewen ME. 1996. P53-dependent repression of cdk4 synthesis in transforming growth factor-β-induced G1 cell cycle arrest. *J Lab Clin Med*. 128: 355-360.

Faneyte IF, Kristel PM, Maliepaard M, Scheffer GL, Scheper RJ, Schellens JH, van de Vijver MJ. 2002. Expression of the breast cancer resistance protein in breast cancer. *Clin Cancer Res*. 8: 1068-1074.

Farraway JJ. 2006. Extending the linear model with R. *J R Stat Soc Ser A Stat Soc*. 169: 1008.

Fedi P, Kimmelman A, Aaronson SA. 2000. In Bast RC, Kufe DW, Pollock RE, Weichselbaum RR, Holland JF, Frei E, and Gansler TS (eds). *Cancer Medicine*. Section 1: Cancer Biology. Ontario, Canada: BC Decker.

Feinstein E, Canaani E, Weiner LM. 1993. Dependence of nucleic acid degradation on in situ free-radical production by adriamycin. *Biochemistry*. 32: 13156-13161.

Feldser DM, Hackett JA, Greider CW. 2003. Telomere dysfunction and the initiation of genome instability. *Nat Rev Cancer*. 3: 4-6.

Felts SJ. Karnitz LM, Toft DO. 2007. Functioning of the Hsp90 machine in chaperoning checkpoint kinase 1 (Chk1) and the progesterone receptor (PR). *Cell Stress Chaperones*. 12: 353-363.

Felts SJ, Owen BA, Nguyen P, Trepel J, Donner DB, Toft DO. 2000. The hsp90-related protein TRAP1 is a mitochondrial protein with distinct functional properties. *J Biol Chem*. 275: 3305-3312.

Ferrarini M, Heltai S, Zocchi MR, Rugarli C. 1992. Unusual expression and localization of heat-shock proteins in human tumor cells. *Int J Cancer*. 51: 613-619.

Ferrer-Soler L, Vasquez-Martin A, Brunet J, Menendez JA, De Llorens R, Colomer R. 2007. An update of the mechanisms of resistance to EGFR-tyrosine kinase inhibitors in breast cancer: Gefitinib (Iressa)-induced changes in the expression and nucleo-cytoplasmic trafficking of HER-ligands (Review). *Int J Mol Med*. 20: 3-10.

Finlay C. 1992. p53 loss of function: implications for the processes of immortalization and tumorigenesis. *BioEssays*. 14: 557-560.

Fisher B, Jeong HJ, Anderson S, Bryant J, Fisher ER, Wolmark N. 2002. Twenty-five year follow-up of a randomized trial comparing radical mastectomy, total mastectomy, and total mastectomy followed by irradiation. *N Engl J Med*. 347: 567-575.

Fisher B, Redmond C. Wickerham D, Bowman D, Schipper H, Wolmark N, Sass R, Fisher E, Jochimsen P, Legault-Poisson S. 1989. Doxorubicin-containing regimens for the treatment of stage II breast cancer: the National Surgical Adjuvant Breast and Bowel Project experience. *J Clin Oncol*. **7:** 572–582.

Forafonov F, Toogun OA, Grad I, Suslova E, Freeman BC, Picard D. 2008. p23/Sba1p protects against Hsp90 inhibitors independently of its intrinsic chaperone activity. *Mol Cell Biol*. 28: 3446-3456.

Fornari FA, Randolph JK, Yalowich JC, Ritke MK, Gewirtz DA. 1994. Interference by doxorubicin with DNA unwinding in MCF-7 breast tumor cells. *Mol Pharmacol*. 45: 649-656.

Forsythe HL, Jarvis JL, Turner JW, Elmore LW, Holt SE. 2001. Stable association of hsp90 and p23, but not hsp70, with active human telomerase. *J Biol Chem*. 276: 15571-15574.

Freeman BC, Toft DO, Morimoto RI. 1996. Molecular chaperone machines: chaperone activities of the cyclophilin Cyp-40 and the steroid aporeceptor-associated protein p23. *Science*. 274: 1718-1720.

Freeman BC and Yamamoto KR. 2002. Disassembly of transcriptional regulatory complexes by molecular chaperones. *Science*. 296: 2232-2235.

Fulda S. 2008. Tumor resistance to apoptosis. *Int J Cancer*. 124: 511-515.

Fulda S and Debatin KM. 2006. Extrinsic versus intrinsic apoptosis pathways in anticancer chemotherapy. *Oncogene*. 25: 4798-4811.

Fynan TM and Reiss M. 1993. Resistance to inhibition of cell growth by transforming growth factor-β and its role in oncogenesis. *Crit Rev Oncog*. 4: 493-540.

Gadelle D, Graille M, Forterre P. 2006. The Hsp90 and DNA topoisomerase VI inhibitor radicicol also inhibits human type II DNA topoisomerase. *Biochem Pharmacol*. 72: 1207-1216.

Garrido C, Bruey JM, Fromentin A, Hammann A, Arrigo AP, Solary E. 1999. HSP27 inhibits cytochrome c-dependent activation of procaspase-9. *FASEB J*. 13: 2061-2070.

Garrido C, Brunet M, Didelot C, Zermati Y, Schmitt E, Kroemer G. 2006. Heat shock proteins 27 and 70. *Cell Cycle*. 5: 2592-26001.

Gasco M, Shami S, Crook T. 2002. The p53 pathway in breast cancer. *Breast Cancer Research*. 4: 70-76.

Gausal G, Gjertsen BT, Fladmark KE, Demol H, Vandekerckhove J, Doskeland SO. 2004. Caspase-dependent, geldanamycin-enhanced cleavage of co-chaperone p23 in leukemic apoptosis. *Leukemia*. 18: 1989-1996.

Gelasco A and Lippard SJ. 1998. NMR solution structure of a DNA dodecamer duplex containing a cis-diammineplatinum(II) d(GpG) intrastrand cross-link, the major adduct of the anticancer drug cisplatin. *Biochemistry*. 37: 9230-9239.

Geng X, Yang ZQ, Danishefsky SJ. 2004. Synthetic development of radicicol and cycloproparadicicol: highly promising anticancer agents targeting Hsp90. *Synletti*. 8: 1325-1333.

Gewirtz DA. 1999. A critical evaluation of the mechanisms of action proposed for the antitumor effects of the anthracycline antibiotics Adriamycin and Daunorubicin. *Biochemical Pharmacology*. 57: 727-741.

Gewirtz DA, Holt SE, Elmore LW. 2008. Accelerated senescence: an emerging role in tumor cell response to chemotherapy and radiation. *Biochem Pharmacol*. 76: 947-957.

Geyer CE, Forster J, Lindquist D, Chan S, Romieu CG, Pienkowski T, Jagiello-Gruszfeld A, Crown J, Chan A, Kaufman B, Skarlos D, Campone M, Davidson N, Berger M, Oliva C, Rubin SD, Stein S, Cameron D. 2006. Lapatinib plus capecitabine for HER2-positive advanced breast cancer. *N Engl J Med*. 355: 2733-2743.

Goetz MP, Toft DO, Ames MM, Erlichman C. 2003. The Hsp90 chaperone complex as a novel target for cancer therapy. *Ann Oncol*. 14: 1169-1176.

Goncalves A, Braguer D, Kamath D, Martello L, Briand D, Horwitz S, Wilson L, Jordan MA. 2001. Resistance to taxol in lung cancer cells associated with increased microtubule dynamics. *Proc. Natl Acad Sci USA*. 98: 11737-11742.

Gong JG, Costanzo A, Yang HQ, Melino G, Kaelin WG Jr, Levrero M, Wang JY. 1999. The tyrosine kinase c-Abl regulates p73 in apoptotic response to cisplatin-induced DNA damage. *Nature*. 399: 806-809.

Greenblatt MS, Chappuis PO, Bond JP, Hamel N, Foulkes WD. 2001. TP53 mutations in breast cancer associated with BRCA1 or BRCA2 germ-line mutations: distinctive spectrum and structural distribution. *Cancer Res*. 61: 4092-4097.

Greider CW and Blackburn EH. 1985. Identification of a specific telomere terminal transferase activity in Tetrahymena extracts. *Cell*. 43: 405-413.

Griffith JD, Comeau L, Rosenfield S, Stansel RM, Bianchi A, Moss H, de Lange T. 1999. Mammalian telomeres end in a large duplex loop. *Cell.* 97: 503-514.

Gross GE, Clark GM, Chamness GC, McGuire WL. 1984. Multiple progesterone receptor assays in human breast cancer. *Cancer Res*. 44: 836-840.

Hadden MK, Lubbers DJ, Blagg BS. 2006. Geldanamycin, radicicol, and chimeric inhibitors of the Hsp90 N-terminal ATP binding site. *Curr Top Med Chem*. 6: 1173-1182.

Hainzl O, Lapina MC, Buchner J, Richter K. 2009. The charged linker region is an important regulator of Hsp90 function. *J Biol Chem*. Epub ahead of print.

Hanahan D and Folkman J. 1996. Patterns and emerging mechanisms of the angiogenic switch during tumorigenesis. *Cell*. 86: 353-364.

Hanahan D and Weinberg RA. 2000. The Hallmarks of Cancer. *Cell*. 100: 57-70.

Hao YH and Tan Z. 2001. Telomeres at the chromosome X(p) might be critical in limiting the proliferative potential of human cells. *Exp Gerontol*. 36: 1639-1647.

Harashima K, Akimoto T, Nonaka T, Tsuzuki K, Mitsuhashi N, Nakano T. 2005. Heat shock protein 90 (Hsp90) chaperone complex inhibitor, radicicol, potentiated radiation-induced cell killing in a hormone-sensitive prostate cancer cell line through degradation of the androgen receptor. *Int J Radiat Biol*. 81: 63-76.

Harrison JC and Haber JE. 2006. Surviving the breakup: the DNA damage checkpoint. *Annu Rev Genet.* 40: 209-235.

Hayflick L. 2000. The illusion of cell immortality. *Br J Cancer.* 83: 841-846.

Hayflick L and Moorhead PS. 1961. The serial cultivation of human diploid cell strains. *Exp Cell Res.* 25: 585–621.

He H, Zatorska D, Kim J, Aguirre J, Llauger L, She Y, Wu N, Immormino RM, Gewirth DT, Chiosis G. 2006. Identification of potent water-soluble purine-scaffold inhibitors of the heat shock protein 90. *J Med Chem*. 49: 381-390.

Hemann MT, Hackett J, Ijpma A, Greider CW. 2000. Telomere length, telomere-binding proteins, and DNA damage signaling. *Cold Spring Harbor Symposia on Quantitative Biology*. 65: 275-279.

Henderson IC, Berry DA, Demetri GD, Cirrincione CT, Goldstein LJ, Martino S, Ingle JN, Cooper MR, Hayes DF, Tkaczuk KH, Fleming G, Holland JF, Duggan DB, Carpenter JT, Frei III E, Schilsky RL, Wood WC, Muss HB, Norton L. 2003. Improved outcomes from adding sequential paclitaxel but not from escalating doxorubicin dose in an adjuvant chemotherapy regimen for patients with node-positive primary breast cancer. *J Clin Oncol*. 21: 976-983.

Henson JD, Neumann AA, Yeager TR, Reddel RR. 2002. Alternative lengthening of telomeres in mammalian cells. *Oncogene*. 21: 598-610.

Herbert BS, Wright WE, Shay JW. 2001. Telomerase and breast cancer. *Breast Cancer Res*. 3: 146-149.

Hernandez MP, Sullivan WP, Toft DO. 2002. The assembly and intermolecular properties of the hsp70-Hop-hsp90 molecular chaperone complex. *J Biol Chem*. 277: 38294-38304.

Herskind C and Rodemann HP. 2000. Spontaneous and radiation-induced differentiation of fibroblasts. *Exp Gerontol.* 35: 747-755.

Herynk MH and Fuqua SAW. 2004. Estrogen receptor mutations in human disease. *Endocr Rev*. 25: 869-898.

Hickey E, Brandon SE, Smale G, Lloyd D, Weber LA. 1989. Sequence and regulation of a gene encoding a human 89-kilodalton heat shock protein. *Mol Cell Biol*. 9: 2615-2626.

Holt SE and Shay JW. 1999. Role of Telomerase in Cellular Proliferation and Cancer. *Journal of Cellular Physiology*.180: 10-8.

Holt SE, Shay JW, Wright WE. 1996. Refining the telomere-telomerase hypothesis of aging and cancer. *Nat Biotechnol*. 14: 836-839.

Holt SE, Aisner DL, Baur J, Tesmer VM, Dy M, Ouellette M, Trager JB, Morin GB, Toft JW, Wright WE, White MA. 1999. Functional requirement of p23 and Hsp90 in telomerase complexes. *Genes Dev*. 13: 817-826.

Honore S, Pasquier E, Braguer D. 2005. Understanding microtubule dynamics for improved cancer therapy. *Cell Mol Life Sci.* 62: 3039-3056.

Hoos A, Hepp HH, Kaul S, Ahlert T, Bastert G, Wallweiner D. 1998. Telomerase activity correlates with tumor aggressiveness and reflects therapy effect in breast cancer. *Int J Cancer*. 79: 8-12.

Horwitz KB and McGuire WL. 1978. Estrogen control of progesterone receptor in human breast cancer. *J Biol Chem*. 253: 2223-2228.

Hsiao SJ and Smith S. 2008. Tankyrase function at telomeres, spindle poles, and beyond. *Biochimie*. 90: 83-92.

Huang GC, Hobbs S, Walton M, Epstein RJ. 2002. Dominant negative knockout of p53 abolishes ErbB2-dependent apoptosis and permits growth acceleration in human breast cancer cells. *Br J Cancer*. 86: 1104-1109.

Huang JC, Zamble DB, Reardon JT, Lippard SJ, Sancar A. 1994. HMG-domain proteins specifically inhibit the repair of the major DNA adduct of the anticancer drug cisplatin by human excision nuclease. *Proc Natl Acad Sci USA*. 91: 10394-10398.

Irwin M, Marin MC, Phillips AC, Seelan RS, Smith DI, Liu W, Flores ER, Tsai KY, Jacks T, Vousden KH, Kaelin WG Jr. 2000. Role for the p53 homologue p73 in E2F-1-induced apoptosis. *Nature.* 407: 645-648.

Itoh H, Ogura M, Komatsuda A, Wakui H, Miura AB, Tashima Y. 1999. A novel chaperone-activity-reducing mechanism of the 90-kDa molecular chaperone Hsp90. *Biochem J*. 343: 697-703.

Jameel A, Skilton RA, Cambell Ta, Chander SK, Coombes RC, Luqmani YA. 1992. Clinical and biological significance of HSP89 alpha in human breast cancer. *Int J Cancer*. 50: 409-415.

Jensen EV and Jordan VC. 2003. The estrogen receptor: a model for molecular medicine. *Clin Cancer Res*. 9: 1980-1989.

Johnston SR, Lu B, Dowsett M, Liang X, Kaufmann M, Scott GK, Osborne CK, Benz CC. 1997. Comparison of estrogen receptor DNA binding in untreated and acquired antiestrogen-resistant human breas cancers. *Cancer Res*. 57: 3723-3727.

Johnston SR, Saccani-Jott G, Smith IE, Salter J, Newby J, Coppen M, Ebbs SR, Dowsett M. 1995. Changes in estrogen receptor, progesterone receptor, and pS2 expression in tamoxifen-resistant human breast cancer. *Cancer Res*. 55: 3331-3338.

Jones KR, Elmore LW, Jackson-Cook C, Demasters G, Povirk LF, Holt SE, Gewirtz DA. 2005. p53-Dependent accelerated senescence induced by ionizing radiation in breast tumour cells. *Int. J. Radiat. Biol*. 81: 445-458.

Jordan MA and Wilson L. 2004. Microtubules as a target for anticancer drugs. *Nat Rev Cancer*. 4: 253-265.

Jordan P and Carmo-Fonseca M. 2000. Molecular mechanisms involved in cisplatin cytotoxicity. *Cell Mol Life Sci*. 57: 1229-1235.

Kaelin WG. 1999. The emerging p53 gene family. *J. Natl Cancer Institute*. 91: 594–598.

Kamal A, Thao L, Sensintaffar J, Zhang L, Boehm MF, Fritz LC, Burrows FJ. 2003. A high-affinity conformation of Hsp90 confers tumour selectivity on Hsp90 inhibitors. *Nature*. 425: 407-410.

Kang KI, Devin J, Cadepond F, Jibard N, Guiochon-Mantel A, Baulieu E, Catelli M. 1994. *In vivo* functional protein-protein interaction: nuclear targeted hsp90 shifts cytoplasmic steroid receptor mutants into the nucleus. *Proc Natl Acad Sci USA*. 91: 340-344.

Kanoh J and Ishikawa F. 2003. Composition and conservation of the telomeric complex. *Cellular and Molecular Life Sciences*. 60: 2295-2302.

Karlseder J, Broccoli D, Dai Y, Hardy S, de Lange T. 1999. p53- and ATM-dependent apoptosis induced by telomeres lacking TRF2. *Science*. 283: 1321-1325.

Karlseder J, Smogorsewska A, de Lange T. 2002. Senescence induced by altered telomere state, not telomere loss. *Science*. 295: 2446-2449.

Karlseder J. 2003. Telomere repeat binding factors: keeping the ends in check. *Cancer Letters*. 194: 189-197.

Karnik PS, Kulkarni S, Liu XP, Budd GT, Bukowski RM. 1994. Estrogen receptor mutations in tamoxifen-resistant breast cancer. *Cancer Res*. 54: 349-353.

Kastan Mb, Zhan Q, el-Deiry WS, Carrier F, Jacks T, Walsh WV, Plunkett BS, Vogelstein B, Fornace Jr, AJ. 1992. A mammalian cell cycle checkpoint pathway utilizing p53 and GADD45 is defective in ataxia-telangiectasia. *Cell*. 71: 587-597.

Kato S, Endoh H, Masuhiro Y, Kitamoto T, Uchiyama S, Sasaki H, Masushige S, Gotoh Y, Nishida E , Kawashima H. Metzger D, Chambon P. 1995. Activation of the estrogen receptor through phosphorylation by mitogen-activated protein kinase. *Science*. 270: 1491-1494.

Kato S, Morita T, Takenaka T, Kato M, Hirano A, Herz F, Ohama E. 1995. Stress-response (heat-shock) protein 90 expression in tumors of the central nervous system: an immunohistochemical study. *Acta Neuropathol*. 89: 184-188.

Keogh MC, Kim JA, Downey M, Fillingham J, Chowdhury D, Harrison JC, Onishi M, Datta N, Galicia S, Emili A, Lieberman J, Shen X, Buratowski S, Haber JE, Durocher D, Greenblatt JF, Krogan NJ. 2006. A phosphatase complex that dephosphorylates γH2AX regulates DNA damage checkpoint recovery. *Nature.* 439: 497-501.

Keys B, Serra V, Saretzki G, von Zglinicki T. 2004. Telomere shortening in human fibroblasts is not dependent on the size of the telomeric-3'-overhang. *Aging Cell*. 3: 103-109.

Khazaie K, Schirrmacher V, Lichtner RB. 1993. EGF receptor in neoplasia and metastasis. *Cancer Metastasis Rev*. 12: 255-274.

Kim JH, Park SM, Kang MR, Oh SY, Lee TH, Muller MT, Chung IK. 2005. Ubiquitin ligase MKRN1 modulates telomere length homeostasis through a proteolysis of hTERT. *Genes Dev*. 19: 776-781.

Kim NW, Piatyszek MA, Prowse KR, Harley CB, West MD, Ho PL, Coviello GM, Wright WE, Weinrich SL, Shay JW. 1994. Specific association of human telomerase activity with immortal cells and cancer. *Science*. 266: 2011-2015.

Knoblauch R and Garabedian MJ. 1999. Role for Hsp90-associated cochaperone p23 in estrogen receptor signal transduction. *Mol Cell Biol.* 19: 3748-3759.

Krebs J, Saramaslani P, Caduff R. 2002. ALG-2: a Ca^{2+}-binding modulator protein involved in cell proliferation and in cell death. *Biochim Biophys Acta*. 1600: 68-73.

Kurahashi T, Miyake H, Hara I, Fujisawa M. 2005. Expression of Major Heat Shock Proteins in Prostate Cancer: Correlation with Clinicopathological Outcomes in Patients Undergoing Radical Prostatectomy. 177: 757-761.

Kurebayashi J. 2001. Biological and clinical significance of HER2 overexpression in breast cancer. *Breast Cancer*. 8: 45-51.

Kurz DJ, Decary S, Hong Y, Erusalimsky JD. 2000. Senescence-associated (beta) galactosidase reflects an increase in lysosomal mass during replicative ageing of human endothelial cells. *J Cell Sci*. 113: 3613-3622.

Kuukasjärvi T, Kononen J, Helin H, Holli K, Isola J. 1996. Loss of estrogen receptor in recurrent breast cancer is associated with poor response to endocrine therapy. *J Clin Oncol*. 14: 2584-2589.

Kwon HJ, Yoshida M, Abe K, Horinouchi S, Beppu T. 1992a. Radicicol, an agent inducing the reversal of transformed phenotypes of src-transformed fibroblasts. *Biosci Biotechnol Biochem*. 56: 538-539.

Kwon HJ, Yoshida M, Fukui Y, Horinouchi S, Beppu T. 1992b. Potent and specific inhibition of p60v-src protein kinase both in vivo and in vitro by radicicol. *Cancer Res*. 52: 6926-6930.

LaBaer J, Garrett MD, Stevenson LF, Slingerland JM, Sandhu C, Chou HS, Fattaey A, Harlow E. 1997. New functional activities for the p12 family of CDK inhibitors *Genes Dev*. 11: 847-862.

Lacroix M, Toillon RA, Leclercq G. 2006. p53 and breast cancer, an update. *Endocine-Related Cancer*., 13: 293-325.

Laderoute KR, Amin K, Caloagan MJ, Knapp M, Le T, Orduna J, Foretz M, Viollet B. 2006. 5'-AMP-activated protein kinase (AMPK) is induced by low oxygen and glucose deprivation conditions found in solid tumor microenvironments. *Mol Cell Biol*. 26: 5336-5347.

Landry J, Chrétien P, Lambert H, Hickey E, Weber LA. 1989. Heat shock resistance conferred by expression of the human HSP27 gene in rodent cells. *J Cell Biol*. 109: 7-15.

Lane DP and Crawford LV. 1979. T antigen is bound to a host protein in SV40-transformed cells. *Nature*. 178: 267-263.

Lansdorp PM, Verwoerd NP, van de Rijke FM, Dragowska V, Little MT, Dirks RW, Raap AK, Tanke HJ. 1996. Heterogeneity in telomere length of human chromosomes. *Hum Mol Genet*. 5: 685-691.

Lapidus RG, Ferguson AT, Ottaviano YL, Parl FF, Smith HS, Weitzman SA, Baylin SB, Issa JP, Davidson NE. 1996. Methylation of estrogen and progesterone receptor gene 5' CpG islands correlates with lack of estrogen and progesterone receptor gene expression in breast tumors. *Clin Cancer Res*. 2: 805-810.

Lee ES, Gao Z, Bae YH. 2008. Recent progress in tumo pH targeting nanotechnology. *J Control Release*. 132: 164-170.

Lee MO, Kim EO, Kwon HJ, Kim YM, Kang HJ, Kang H, Lee JE. 2002. Radicicol suppresses the transcriptional function of the estrogen receptor by suppressing the stabilization of the receptor by heat shock protein 90. *Mol Cell Endocrin*. 188: 47-54.

Lei M, Zaug AJ, Podell ER, Cech TR. 2005. Switching human telomerase on and off with hPOT1 protein in vitro. *J Biol Chem*. 280: 20449-20456.

Lerescu L, Tucureanu C, Caras I, Neagu S, Melinceanu L, Sălăgeanu A. 2008. Primary cell culture of human adenocarcinomas-practical considerations. *Roum Arch Microbiol Immunol*. 67: 55-66.

Leu YW, Yan PS, Fan M, Jin VX, Liu JC, Curran EM, Welshons WV, Wei SH, Davuluri RV, Plass C, Nephew KP, Huang TH. 2004. Loss of estrogen receptor signaling triggers epigenetic silencing of downstream targets in breast cancer. *Cancer Res*. 64: 8184-8192.

Lewis JS and Jordan VC. 2005. Selective estrogen receptor modulators (SERMs): mechanisms of anticarcinogenesis and drug resistance. *Mutat Res*. 591: 247-263.

Lin J and Arlinghaus R. 2008. Activated c-Abl tyrosine kinase in malignant solid tumors. *Oncogene*. 27: 4385-4391.

Lin KW and Yan J. 2005. The Telomere Length Dynamic and Methods of its Assessment. *J Cell Mol Med*. 9: 977-989.

Lindquist S and Craig EA. 1988. The heat shock proteins. *Ann Rev Genet*. 22: 631-637.

Loayza D and de Lange T. 2003. POT1 as a terminal transducer of TRF1 telomere length control. *Nature*. 423: 1013-1018.

Lønning E and Lien EA. 1995. Mechanisms of action of endocrine treatment in breast cancer. *Crit Rev Oncol Hematol*. 21: 158-193.

Maass N, Teffner M, Rosel F, Pawaresch R, Jonat W, Nagasaki K, Rudoph P. 2001. Decline in the expression of the serine proteinase inhibitor maspin is associated with tumour progression in ductal carcinomas of the breast. *J Pathol*. 195: 321-326.

Marcu MG, Chadli A, Bouhouche I, Catelli M, Neckers LM. 2000a. The heat shock protein 90 antagonist novobiocin interacts with a previously unrecognized ATP-binding domain in the carboxyl terminus of the chaperone. *J Biol Chem*. 275: 37181-37186.

Marcu MG, Schulte TW, Neckers L. 2000b. Novobiocin and related coumarins and depletion of heat shock protein 90-dependent signaling proteins. *J Natl Cancer Inst*. 92: 242-248.

Marques C, Guo W, Pereira P, Taylor A, Patterson C, Evans PC, Shang F. 2006. The triage of damaged proteins: degradation by the ubiquitin-proteasome pathway or repair by molecular chaperones. *FASEB J*. 20: 741-743.

Martens UM, Chavez EA, Poon SS, Schmoor C, Lansdorp PM. 2000. Accumulation of short telomeres in human fibroblasts prior to replicative senescence. *Exp Cell Res*. 256: 291-299.

Martín M. 2001. Platinum compounds in the treatment of advanced breast cancer. *Clin Breast Cancer*. 2: 190-208.

Martín M. 2006. Molecular biology of breast cancer. *Clin Transl Oncol*. 8: 7-14.

Martínez-Ruiz A, Villaneuva L, González de Orduña C, López-Ferrer D, Higueras MA, Tarín C, Rodríguez-Crespo I, Vásquez J, Lamas S. 2005. S-nitrosylation of Hsp90 promotes the inhibition of its ATPase and endothelial nitric oxide synthase regulatory activities. *Proc Natl Acad Sci USA*. 102: 8525-8530.

Masuda H, Miller C, Koeffler HP, Battifora H, Cline MJ. 1987. Rearrangement of the p53 gene in human osteogenic sarcomas. *Proc Natl Acad Sci*. 84: 7716-7719.

Matulić M, Sopta M, Rubelj I. 2007. Telomere dynamics: the means to an end. *Cell Prolif*. 40: 462-474.

Mazzocca A and Carloni V. 2009. The Metastatic Process: Methodological Advances and Pharmacological Challenges. *Curr Med Chem*. 16: 1704-1717.

McGowan CH and Russell P. 2004. The DNA damage response: sensing and signaling. *Current Opinion in Cell Biology*. 6: 629-633.

McGrogan BT, Gilmartin B, Carney DN, McCann A. 2007. Taxanes, microtubules, and chemoresistant breast cancer. *Biochim Biophys Acta*. 1785: 96-132.

Meeker AK, Hicks JL, Gabrielson E, Strauss WM, De Marzo AM, Argani P. 2004a. Telomere shortening occurs in subsets of normal breast epithelium as well as in situ and invasive carcinoma. *Am J Path*. 164: 925-935.

Meeker AK, Hicks JL, Iacobuzio-Donahue CA, Montgomery EA, Westra WH, Chan TY, Ronnett BM, De Marzo AM. 2004b. Telomere length abnormalities occur early in the initiation of epithelial carcinogenesis. *Clinical Cancer Research*. 10: 3317-3326.

Meijer-van Gelder ME, Look MP, Peters HA, Schmitt M, Brünner N, Harbeck N, Klijn JG, Foekens JA. 2004.Urokinase-type plasminogen activator system in breast cancer: association with tamoxifen therapy in recurrent disease. *Cancer Res*. 64: 4563-4568.

Meyer P, Prodromou C, Hu B, Vaughan C, Roe SM, Panaretou B, Piper PW, Pearl LH.2003. Structural and functional analysis of the middle segment of hsp90: implications for ATP hydrolysis and client protein and cochaperone interactions. *Mol Cell*. 11: 647-658.

Mileo AM, Fanuele M, Battaglia F, Scambia G, Benedetti-Panici P, Mancuso S, Ferrini U. 1990. Selective over-expression of mRNA coding for 90-kDa stress protein in human ovarian cancer. *Anticancer Res*. 10: 903-906.

Miller K, Rosen LS, Modi S, Schneider B, Roy J, Chap L, Paulsen M, Kersey K, Hannah A, Hudis C. 2007. Phase I trial of alvespimycin (KOS-1022; 17-DMAG) and trastuzumab (T). ASCO Annual Meeting Proceedings, Supplement. *J Clin Oncol*. 25: 1115.

Mitchison TJ and Kirschner M. 1984. Dynamic instability of microtubule growth. *Nature*. 312: 237-242.

Modi S, Stopeck AT, Gordon MS, Mendelson D, Solit DB, Bagatell R, Ma W, Wheler J, Rosen N, Norton L, Cropp GF, Johnson RG, Hannah AL, Hudis CA. 2007. Combination of trastuzumab and tanespimycin (17-AAG, KOS-953) is safe and active in trastuzumab-refractory HER-2 overexpressing breast cancer: a phase I dose-escalation study. *J Clin Oncol*. 25: 5410-5417.

Mokbel KM, Parris CN, Ghilchik M, Amerasinghe CN, Newbold RF. 2000. Telomerase activity and lymphovascular invasion in breast cancer. *Eur J Surg Oncol*. 26: 30-33.

Moll UM, Riou G, Levine AJ. 1992. Two distinct mechanism alter p53 in breast cancer: mutation and nuclear exclusion. *Proc Natl Acad Sci USA*. 89: 7262-7266.

Mollerup J and Berchtold MW. 2005. The co-chaperone p23 is degraded by caspases and the proteasome during apoptosis. *FEBS Lett*. 579: 4187-4192.

Mollerup J, Krogh TN, Nielson PF, Berchtold MW. 2003. Properties of the co-chaperone protein p23 erroneously attributed to ALG-2 (apoptosis-linked gene 2). *FEBS Lett*. 555: 478-482.

Morishima Y, Murphy PJ, Li DP, Sanchez ER, Pratt WB. 2000. Stepwise assembly of a glucocorticoid receptor-hsp90 heterocomplex resolves two sequential ATP-dependent events involving first hsp70 and then hsp90 in opening of the steroid binding pocket. *J Biol Chem*. 275: 18054-18060.

Moss T and Stefanovsky VY. 1995. Promotion and regulation of ribosomal transcription in eukaryotes by RNA polymerase I. *Prog Nucleic Acid Res Mol Biol*. 50: 25-66.

Mosser DD and Morimoto RI. 2004. Molecular chaperones and the stress of oncogenesis. *Oncogene*. 23: 2907-2918.

Mueller C, Riese U, Kosmehl H, Dahse R, Claussen U, Ernst G. 2002. Telomerase activity in microdissected human breast cancer tissues: association with p53, p21, and outcome. *Int J Oncol*. 20: 385-390.

Muggia F. 2009. Platinum compounds 30 years after the introduction of cisplatin: implications for the treatment of ovarian cancer. *Gynecol Oncol*. 112: 275-281.

Müller V, Witzel I, Lück HJ, Köhler G, von Minckwitz G, Möbus V, Sattler D, Wilczak W, Löning T, Jänicke F, Pantel K, Thomssen C. 2004. Prognostic and predictive impact of the HER-2/neu extracellular domain (ECD) in the serum of patients treated with chemotherapy for metastatic breast cancer. *Breast Cancer Res Treat*. 86: 9-18.

Murphy GP, Lawrence Jr W and Lenhard RE (eds.). 1995. *American Society Textbook of Clinical Oncology*. 2nd Edn. American Cancer Society, Atlanta, GA.

Nakai R, Ishida H, Asai A, Ogawa H, Yamamoto Y, Kawasaki H, Akinaga S, Mizukami T, Yamashita Y. 2006. Telomerase inhibibitors identified by a forward chemical genetics approach using a yeast strain with shortened telomere length. *Chem Biol*. 13: 183-190.

Nanbu K, Konishi I, Komatsu T, Mandai M, Yamamoto S, Kuroda H, Koshiyama M, Mori T. 1996. Expression of heat shock porteins HSP70 and HSP90 in endometrial carcinomas. Correlation with clinicopathology, sex steroid receptor status, and p53 protein expression. *Cancer*. 77: 330-338.

Narita M, Nũnez S, Heard E, Narita M, Lin AW, Hearn SA, Spector DL, Hannon GJ, Lowe SW. 2003. Rb-mediated heterochromatin formation and silencing of E2F target genes during cellular senescence. *Cell.* 113: 703-716.

Neckers L. 2000. Effects of geldanamycin and other naturally occurring small molecule antagonists of heat shock protein 90 on HER2 protein expression. *Breast Dis*. 11: 49-59.

Neckers L. 2006. Using natural product inhibitors to validate Hsp90 as a molecular target in cancer. *Curr Top Med Chem*. 6: 1163-1171.

Neidle S and Parkinson GN. 2003. The structure of telomeric DNA. *Curr Opin Structural Biol*. 13: 275-283.

Nemoto T, Ohara-Nemoto Y, Takagi T, Yokoyama K. 1995. Mechanism of dimer formation of the 90-kDa heat-sock protein. *Eur J Biochem*. 233: 1-8.

Niida H, Shinkai Y, Hande MP, Matsumoto T, Takehara S, Tachibana M, Oshimura M, Lansdorp PM, Furuichi Y. 2000. Telomere maintenance in telomerase-deficient mouse embryonic stem cells: characterization of an amplified telomeric DNA. *Mol Cell Biol.* 20: 4115-4127.

Nijjar T, Bassett E, Garbe J, Takenaka Y, Stampfer MR, Gilley D, Yaswen P. 2005. Accumulation and altered localization of telomere-associated protein TRF2 in immortally transformed and tumor-derived human breast cells. *Oncogene*. 24: 3369-3376.

Ning H, Li TT, Zhao L, Li T, Li J, Liu J, Liu Z, Fan D. 2006. TRF2 Promotes Multidrug Resistance in Gastric Cancer Cells. *Cancer Biology and Therapy*. 5: 950-956.

Normanno N, De Luca A, Bianco C, Strizzi L, Mancino M, Maiello MR, Carotenuto A, De Feo G, Caponigro F, Salomon DS. 2006. Epidermal growth factor receptor (EGFR) signaling in cancer. *Gene*. 366: 2-16.

Ogata M, Naito Z, Tanaka S, Moriyama Y, Asano G. 2000. Overexpression and localization of heat shock proteins mRNA in pancreatic carcinoma. *J Nippon Med Sch*. 67: 177-185.

Ortega S, Malumbres M, Barbacid M. 2002. Cylcin D-dependent kinases, INK4 inhibitors, and cancer. *Biochim Biophys Acta*. 1602: 73-87.

Osborne CK, Boldt DH, Clark GM, Trent JM. 1983. Effects of tamoxifen on human breast cancer cell cycle kinetics: accumulation of cells in early G1 phase. *Cancer Res*. 43: 3583-3585.

Oxelmark E, Knoblauch R, Arnal S, Su LF, Schapira M, Garabedian MJ. 2003. Genetic dissection of p23, an Hsp90 cochaperone, reveals a distinct surface involved in estrogen receptor signaling. *J Biol Chem*. 278: 36547-36555.

Oxelmark E, Roth JM, Brooks PC, Braunstein SE, Schneider RJ, Garabedian MJ. 2006. The cochaperone p23 differentially regulates estrogen receptor target genes and promotes tumor cell adhesion and invasion. *Mol Cell Biol.* 26: 5205-5213.

Pacey S, Banerji U, Judson I, Workman P. 2006. Hsp90 inhibitors in the clinic. *HEP*. 172: 331-358.

Pearce ST and Jordan VC. 2004. The biological role of estrogen receptors alpha and beta in cancer. *Crit Rev Oncol Hematol*. 50: 3-22.

Pearl LH and Prodromou C. 2006. Structure and mechanism of the Hsp90 molecular chaperone machinery. *Annu Rev Biochem*. 75: 271-294.

Pearl LH, Prodromou C, Workman P. 2008. The Hsp90 molecular chaperone: an open and shut case for treatment. *Biochem J*. 410: 439-453.

Perry RR, Kang Y, Greaves B. 1995. Effects of tamoxifen on growth and apoptosis of estrogen-dependent and –independent human breast cancer cells. *Ann Surg Oncol*. 2: 238-245.

Pharaoh PD, Day NE, Caldas C. 1999. Somatic mutations in the p53 gene and prognosis in breast cancer: a meta-analysis. *Br J Cancer*. 80: 1968-1973.

Picard D. 2006. Chaperoning Steroid Hormone Action. *Trends in Endo and Meta*. 17: 229-235.

Pick E, Kluger Y, Giltnane JM, Moeder C, Camp RL, Rimm DL, Kluger HM. 2007. High HSP90 Expression is Associated with Decreased Survival in Breast Cancer. *Cancer Research*. 67: 2932-2937.

Pietras RJ. 2006. Biologic basis of sequential and combination therapies for hormone-responsive breast cancer. *The Oncologist*. 11: 704-717.

Plattner R, Kadlec L, DeMali K, Kazlauskas A, Pendergast A. 1999. c-Abl is activated by growth factors and Src family kinases and has a role in the cellular response to PDGF. *Genes Dev*. 13: 2400-2411.

Pommier Y, Sordet O, Antony S, Hayward RL, Kohn KW. 2004. Apoptosis defects and chemotherapy resistance: molecular interaction maps and networks. *Oncogene*. 23: 2934-2949.

Pratt WB and Toft DO. 2003. Regulation of signaling protein function and trafficking by the hsp90/hsp70-based chaperone machinery. *Exp Biol Med (Maywood)*. 228: 111-133.

Prodromou C and Pearl LH. 2003. Structural and functional relationships of Hsp90. *Curr Cancer Drug Targets*. 3: 301-323.

Prodromou C, Roe SM, O'Brien R. Ladbury JE, Piper PW, Pearl LH. 1997. Identification and structural characterization of the ATP/ADP-binding site in the Hsp90 molecular chaperone. *Cell*. 90: 65-75.

Prost S. 1995. Mechanisms of resistance to topoisomerases poisons. *Gen Pharmacol*. 26: 1773-1784.

Putti T, El-Rehim DM, Rakha EA, Paish CE, Lee A, Pinder SE, Ellis IO. 2005. Estrogen receptor-negative breast carcinomas: a review of morphology and immunophenotypical analysis. *Modern Pathology*. 18: 26-35.

Qing G and Simon MC. 2009. Hypoxia inducible factor-2-alpha: a critical mediator of aggressive tumor phenotypes. *Curr Opin Genet Dev*. 19: 60-66.

Rashid-Kolvear F, Pintilie M, Done SJ. 2007. Telomere length on chromosome 17q shortens more than global telomere length in the development of breast cancer. *Neoplasia*. 9: 265-270.

Reddel RR and Bryan TM. 2003. Alternative lengthening of telomeres: dangerous road less travelled. *Lancet*. 361: 1840–1841.

Rhee J, Han SW, Oh DY, Kim JH, Im SA, Han W, Park IA, Noh DY, Bang YJ, Kim TY. 2008. The clinicopathologic characteristics and prognostic significance of triple-negativity in node-negative breast cancer. *BMC Cancer*. 23:307-314.

Rhodes D. 2006. The Structural Biology of Telomeres. In de Lange T, Lundblad V, Blackburn E (eds). *Telomeres*, 2nd ed. Cold Spring Harbor, NY: Cold Spring Harbor Laboratory Press. (pp. 317-343).

Riggs DL, Cox MB, Cheung-Flynn J. Prapapanich V, Carrigan PE, Smith DF. 2004. Functional specificity of co-chaperone interactions with Hsp90 client proteins. *Crit Rev Biochem Mol Biol*. 39: 279-295.

Ring AE and Ellis PA. 2005. Taxanes in the treatment of early breast cancer. *Cancer Treat Rev*. 31: 618-627.

Ritossa F. 1962. A new puffing pattern induced by temperature shock and DNP in *Drosophila*. *Experientia*. 18: 571-576.

Robles SJ and Adami GR. 1998. Agents that cause DNA double strand breaks lead to p16INK4a enrichment and the premature senescence of normal fibroblasts. *Oncogene.* 16:1113-1123.

Rodier F, Campisi J, Bhaumik D. 2007. Two faces of p53: aging and tumor suppression. *Nucleic Acids Res*. 35: 7475-7484.

Roe SM, Prodromou C, O'Brien R, Ladbury JE, Piper PW, Pearl LH. 1999. Structural basis for inhibition of the Hsp90 molecular chaperone by the antitumor antibiotics radicicol and geldanamycin. *J Med Chem*. 42: 260-266.

Romanucci M, Marinelli A, Sarli G, Della Salda L. 2006. Heat shock protein expression in canine malignant mammary tumors. *BMC Cancer*. 6: 171-182.

Rosenberg B, van Camp L, Krigas T. 1965. Inhibition of cell division in *Escherichia coli* by electrolysis products from a platinum electrode. *Nature*. 205: 698-699.

Rosenhagen MC, Soti C, Schmidt U, Wochnik GM, Hartl FU, Holsboer F, Young JC, Rein T. 2003. The heat shock protein 90-targeting drug cisplatin selectively inhibits steroid receptor activation. *Mol Endocrinol*. 17: 1991-2001.

Rudiger S, Freund SM, Veprintsev DB, Fersht AR. 2002. CRINEPT-TROSY NMR reveals p53 core domain bound in an unfolded form to the chaperone Hsp90. *Proc Natl Acad Sci USA*. 99: 11085-11090.

Samphao S, Eremin JM, El-Sheemy M, Eremin O. 2009. Treatment of established breast cancer in post-menopausal women: role of aromatase inhibitors. *Surgeon*. 7: 42-55.

Sarto C, Binz PA, Mocarelli P. 2000. Heat shock proteins in human cancer. E*lectrophoresis*. 21: 1218-1226.

Sausville EA. 2003. Clinical development of 17-allyamino, 17-demethoxy geldanamycin. *Curr Cancer Drug Targets*. 3: 377-383.

Savre-Train I, Gollahon LS, Holt SE. 2000. Clonal heterogeneity in telomerase activity and telomere length in tumor-derived cell lines. *Proc Soc Exp Biol Med*. 223: 379-388.

Scheibel T, Weikl T, Buchner J. 1998. Two chaperones sites in Hsp90 differing in substrate specificity and ATP hydrolysis. *Proc Natl Acad Sci USA*. 95: 1495-1499.

Scheibel T, Siegmund HI, Jaenicke R, Ganz P, Lilie H, Buchner J. 1999. The charged region of Hsp90 modulates the function of the N-Terminal domain. *Proc Natl Acad Sci USA*. 96: 1297-1302.

Schiff R, Massarweh S, Shou J, Osborne CK. 2003. Breast cancer endocrine resistance: how growth factor signaling and estrogen receptor coregulators modulate response. *Clin Cancer Res*. 9: 447s-454s.

Schlessinger J. 2004. Common and distinct elements in cellular signaling via EGF and FGF receptors. *Science*. 306: 1506-1507.

Schulte TW, Akinaga S, Soga S, Sullivan W, Stensgard B, Toft D, Neckers LM. 1998a. Antibiotic radicicol binds to the N-terminal domain of Hsp90 and shares important biological activities with geldanamycin. *Cell Stress Chaperones*. 3: 100-108.

Schulte TW and Neckers LM. 1998b. The benzoquinone ansamycin 17-allyamino, 17-demethoxy geldanamycin binds to Hsp90 and shares important biological activities with geldanamycin. *Cancer Chemother Pharmacol*. 42: 273-279.

Schwartz AL, Ciechanover A. 2009. Targeting proteins for destruction by the ubiquitin system: implications for human pathobiology. *Annu Rev Pharmacol Toxicol*. 49: 73-96.

Seger YR, García-Cao M, Piccinin S, Cunsolo CL, Doglioni C, Blasco MA, Hannon GJ, Maestro R. 2002. Transformation of normal human cells in the absence of telomerase activation. *Cancer Cell*. 2: 401–413.

Shammas MA, Shmookler Reis RJ, Li C, Koley H, Hurley LH, Anderson KC, Munshi NC. 2004. Telomerase inhibition and cell growth arrest after telomestatin treatment in multiple myeloma. *Clin Cancer Res*. 10: 770-776.

Shamovsky I and Nudler E. 2008. New insights into the mechanism of heat shock response activation. *Cell Mol Life Sci*. 65: 855-861.

Sharp S, Boxall K, Titley J, Drysdale M, Workman P. 2003. Mechanisms of action of the novel Hsp90 inhibitor, CCT018159 in malignant melanoma cell lines. *Clin Cancer Res*. 9: 73.

Sharp S and Workman P. 2006. Inhibitors of the HSP90 molecular chaperone: current status. *Adv Cancer Research*. 95: 323-348.

Shay JW and Bacchetti S. 1997. A survey of telomerase activity in human cancer. *Eur J Cancer*. 33: 787-791.

Shay JW, Pereira-Smith OM, Wright WE. 1991. A role for both RB and p53 in the regulation of human cellular senescence. *Exp Cell Res*.196: 33-39.

Shay JW and Roninson IB. 2004. Hallmarks of senescence in carcinogenesis and cancer therapy. *Oncogene.* 23: 2919-2933.

Shay JW and Wright WE. 1996. Telomerase activity in human cancer. *Curr Opin Oncol*. 8: 66-71.

Sherr CJ. 1996. Cancer cell cycles. *Science*. 274: 1672-1677.

Shiau Ak, Barstad D, Loria PM, Cheng L, Kushner PJ, Agard DA, Greene GL. 1998. The structural basis of estrogen receptor/coactivator recognition and the antagonism of this interaction by tamoxifen. *Cell*. 95: 927-937.

Shih RS, Wong SH, Schoene NW, Lei KY. 2008. Suppression of Gadd45 alleviates the G2/M blockage and the enhanced phosphorylation of p53 and p38 in zinc supplemented normal human bronchial epithelial cells. *Exp Biol Med (Maywood)*. 233: 317-327.

Shirley SH, Rundhaug JE, Tian J, Cullinan-Ammann N, Lambertz I, Conti CJ, Fuchs-Young R. 2009. Transcriptional regulation of estrogen receptor-alpha by p53 in human breast cancer cells. *Cancer Res*. 69: 3405-3414.

Sitte N, Merker K, Grune T, von Zglinicki T. 2001. Lipfuscin accumulation in proliferating fibroblasts in vitro: an indicator of oxidative stress. *Exp Gerontol*. 36: 475-486.

Slamon DJ, Clark GM, Wong SG, Levin WJ, Ullrich A, McGuire WL. 1987. Human breast cancer: correlation of relapse and survivial with amplification of the HER2/neu oncogene. *Science*. 235: 177-182.

Slamon DJ, Godolphin W, Jones LA, Holt JA, Wong SG, Keith DE, Levin WJ, Stuart SG, Udove J, Ullrich A, Press MF. 1989. Studies of the HER-2/neu proto-oncogene in human breast and ovarian cancer. *Science*. 244: 707-712.

Slamon DJ, Leyland-Jones B, Shak S, Fuchs H, Paton V, Bajamonde A, Fleming T, Eiermann W, Wolter J, Pegram M, Baselga J, Norton L. 2001. Use of chemotherapy plus a monoclonal antibody against HER2 for metastatic breast cancer that overexpresses HER2. *N Engl J Med*. 344: 783-792.

Slijepcevic P. 2006. The role of DNA damage response proteins at telomeres-an “integrative” model. *DNA Repair*. 5: 1299-1306.

Slijepcevic P and Al-Wahiby S. 2005. Telomere biology: integrating chromosomal end protection with DNA damage response. *Chromosoma*. 114: 275-285.

Soga S, Neckers LM, Schulte TW, Shiotsu Y, Akasaka K, Narumi H, Agatsuma T, Ikuina Y, Murakata C, Tamaoki T, Akinaga S. 1999. KF25706, a novel oxime derivative of radicicol, exhibits *in vivo* antitumor activity via selective depletion of Hsp90 binding signaling molecules. *Cancer Res*. 59: 2931-2938.

Soga S, Sharma S, Shiotsu Y, Shimizu M, Tahara H, Yamaguchi K, Ikuina Y, Murakata C, Tamaoki T, Kurebayashi J, Schulte TW, Neckers LM, Skinaga S. 2001. Stereospecific antitumor activity of radicicol oxime derivatives. *Cancer Chemother Pharmacol*. 48: 435-445.

Solit DB, Zheng FF, Drobnjak M, Munster PN, Higgins B, Verbel D, Heller G, Tong W, Cordon-Cardo C, Agus DB, Scher HI, Rosen N. 2002. 17-Allylamino-17-demethoxygeldanamycin induces the degradation of androgen receptor and HER-2/neu and inhibits the growth of prostate cancer xenografts. *Clin Cancer Res*. 5: 986-993.

Son YS, Suh JM, Ahn SH, Kim JC, Yi JY, Hur KC, Hong WS, Muller MT, Chung IK. 1998. Reduced activity of topoisomerase II in an Adriamycin-resistant human stomach-adenocarcinoma cell line. *Cancer Chemother Pharmacol*. 41: 353-360.

Soti C, Racz A, Csermely P. 2002. A nucleotide-dependent molecular switch controls ATP binding at the C-terminal domain of Hsp90. *J Biol Chem*. 277: 7066-7075.

Sporn MB. 1997. The war on cancer: a review. *Ann N Y Acad Sci*. 833: 137-146.

Srinivasan D and Plattner R. 2006. Activation of Abl tyrosine kinases promotes invasion of aggressive breast cancer cells. *Cancer Res*. 66: 5648-5655.

Srinivasan D, Sims J, Plattner R. 2008. Aggressive breast cancer cells are dependent on activated Abl kinases for proliferation, anchorage-independent growth and survival. *Oncogene*. 27: 1095-1105.

Stebbins CE, Russo AA, Schneider C, Rosen N, Hartl FU, Pavletich NP. 1997. Crystal structure of an Hsp90-geldanamycin complex: targeting of a protein chaperone by an antitumor agent. *Cell*. 89: 239-250.

Strik HM, Weller M, Frank B, Hermisson M, Deininger MH, Dichgans J, Meyermann R. 2000. Heat shock protein expression in human gliomas. *Anticancer Res*. 20: 4457-44662.

Su TT. 2006. Cellular responses to DNA damage: one signal, multiple choices. *Annu Rev Genet*. 40: 187-208.

Surralles J, Hande MP, Marcos R, Lansdorp PM. 1999. Accelerated telomere shortening in the human inactive X chromosome. *Am J Hum Genet*. 65: 1617-1622.

Sullivan A, Yuille M, Repellin C, Reddy A, Reelfs O, Bell A, Dunne B, Gusterson BA, Osin P, Farrell PJ, Yulug I, Evans A, Ozcelik T, Gasco M, Crook T. 2002. Concomitant inactivation of p53 and Chk2 in breast cancer. *Oncogene*. 21: 1316-1324.

Sullivan WP, Owen BA, Toft DO. 2002. The influence of ATP and p23 on the conformation of Hsp90. *J Biol Chem*. 277: 45942-45948.

Supko JG, Hickman RL, Grever MR, Malspeis L. 1995. Preclinical pharmacologic evaluation of geldanamycin as an antitumor agent. *Cancer Chemother Pharmacol*. 36: 305-315.

Suva L. Griffin R. Makhoul I. 2009. Mechanisms of bone metastases of breast cancer. *Endocr Relat Cancer*. 14: ahead of print.

Sydor JR, Normant E, Pien CS, Porter JR, Ge J, Grenier L, Pak RH, Ali JA, Dembski MS, Hudak J, Patterson J, Penders C, Pink M, Read MA, Sang J, Woodward C, Zhang Y, Grayzel DS, Wright J, Barrett JA, Palombella VJ, Adams J, Tong JK. 2006. Development of 17-

allylamino-17-demethoxygeldanamycin hydroquinone hydrochloride (IPI-504), an anti-cancer agent directed against Hsp90. *Proc Natl Acad Sci USA*. 103: 17408-17413.

Ta HQ, Thomas KS, Schrecengost RS, Bouton AH. 2008. A novel association between $p130^{Cas}$ and resistance to the chemotherapeutic drug Adriamycin in human breast cancer cells. *Cancer Res*. 68: 8796-8804.

Taldone T, Gozman A, Maharaj R, Chiosis G. 2008. Targeting Hsp90: small-molecule inhibitors and their clinical development. *Cur Opin Pharmac*. 8: 370-374.

Tewey KM, Rowe TC, Yang L, Halligan BD, Liu LF. 1984. Adriamycin-induced DNA damage mediated by mammalian topoisomerase II. *Science*. 226: 466-468.

Tian ZQ, Liu Y, Zhang D, Wang Z, Dong SD, Carreras CW, Zhou Y, Rastelli G, Santi DV, Myles DC. 2004. Synthesis and biological activities of novel 17-aminogeldanamycin derivatives. *Bioorg Med Chem*. 12: 5317-5329.

Tong WM, Hande MP, Lansdorp PM, Wang ZQ. 2001. DNA strand break-sensing molecule poly(ADP-Ribose) polymerase cooperates with p53 in telomere function, chromosome stability, and tumor suppression. *Mol Cell Biol.* 21: 4046-4054.

Ulrich E, Boehmelt G, Bird A, Beug H. 1992. Immortalization of conditionally transformed chicken cells: Loss of normal p53 expression is an early step that is independent of cell transformation. *Genes Dev*. 6: 876-887.

Van Limbergen E and Weltens C. 2006. New trends in radiotherapy for breast cancer. *Curr Opin Oncol*. 18: 555-562.

Van Slooten HJ, van De Vijver MJ, Borresen AL, Eyfjord JE, Valgardsdottir R, Scherneck S, Nesland JM, Devilee P, Cornelisse CJ, van Dierendonck JH. 1999. Mutations in exons 5-8 of the p53 gene, independent of their type and location, are associated with increased apoptosis and mitosis in invasive breast carcinoma. *J Pathol*. 189: 504-513.

Vasquez A, Bond EE, Levine AJ, Bond GL. 2008. The genetics of the p53 pathway, apoptosis, and cancer therapy. *Nat Rev Drug Disco*. 7: 979-987.

Verdun RE and Karlseder J. 2007. Replication and protection of telomeres. *Nature*. 447: 924-931.

Vilenchik M, Solit D, Basso A, Huezo H, Lucas B, He H, Rosen N, Spampinato C, Modrich P, Chiosis G. 2004. Targeting wide-range oncogenic transformation via PU24FCl, a specific inhibitor of tumor Hsp90. *Chem Biol*. 11: 787-797.

Villeneuve DJ, Hembruff SL, Veitch Z, Cecchetto M, Dew WA, Parissenti AM. 2006. cDNA microarray analysis of isogenic paclitaxel- and doxorubicin-resistant breast tumour cell lines

reveals distinct drug-specific genetic signatures of resistance. *Breast Cancer Res Treat*. 96: 17-39.

von Zglinicki T, Saretzki G, Döcke W, Lotze C. 1995. Mild hyperoxia shortens telomeres and inhibits proliferation of fibroblasts: a model for senescence? *Exp Cell Res.* 220:186-193.

von Zglinicki T, Saretzki G, Ladhoff J, d'Adda di Fagagna F, Jackson SP. 2005. Human cell senescence as a DNA damage response. *Mechanisms of Ageing and Development*. 126: 111-117.
Wai LK. Telomeres, Telomerase, and Tumorigenesis – A review. Med Gen Med 2004;6:19.

Vousden KH and Lu X. 2002. Live or let die: the cell's response to p53. *Nat Rev Cancer*. 2: 594-604.

Wang J. 2000. Regulation of cell death by the Abl tyrosine kinase. *Oncogene*. 19: 5643-5650.

Weidner N, Folkman J, Pozza F, Bevilacqua P, Allred EN, Moore DH, Meli S, Gasparini G. 1992. Tumor angiogenesis: a new significant and independent prognostic indicator in early-stage breast carcinoma. *J Natl Cancer Inst*. 84: 1875-1887.

Weigelt B and Bissell MJ. 2008. Unraveling the microenvironmental influences on the normal mammary gland and breast cancer. *Semin Cancer Biol*. 18: 311-321.

Weinberg RA. 1995. The retinoblastoma protein and cell cycle control. *Cell*. 81: 323-330.

Wenger SL, Senft JR, Sargent LM, Bamezai R, Bairwa N, Grant SG. 2004. Comparison of established cell lines at different passages by karyotype and comparative genomic hybridization. *Biosci Rep*. 24: 631-639.

Wesche J, Małecki J, Wiedłocha A, Skjerpen CS, Claus P, Olsnes S. 2006. FGF-1 and FGF-2 require the cytosolic chaperone Hsp90 for translocation into the cytosol and the cell nucleus. *J Biol Chem*. 281: 11405-11412.

White LK, Wright WE, Shay JW. 2001. Telomerase inhibitors. *Trends Biotechnol*. 19: 114-120.
Whitesell L and Lindquist S. 2005. Hsp90 and the chaperoning of cancer. *Nature Reviews Cancer*. 5: 761-772.

Whitesell L and Lindquist S. 2005. Hsp90 and the chaperoning of cancer. *Nat Rev Cancer*. 5: 761-772.

Whitesell L, Mimnaugh EG, De Costa B, Myers CE, Neckers LM. 1994. Inhibition of heat shock protein Hsp90-pp60v-src heteroprotein complex formation by benzoquinone ansamycins: essential role for stress proteins in oncogenic transformation. *Proc Natl Acad Sci USA*. 91: 8324-8328.

Whitesell L, Shifrin SD, Schwab G, Neckers LM. 1992. Benzoquionoid ansamycins possess selective tumoricidal activity unrelated to src kinase inhibition. *Cancer Res*. 52: 1721-1728.

Wiley HS. 2003. Trafficking of the ErbB receptors and its influence on signaling. *Exp Cell Res*. 284: 78-88.

Wright WE and Shay JW. 1992. The two-stage mechanism controlling cellular senescence and immortalization. *Exp Gerontol.* 27: 383-389.

Wright WE and Shay JW. 2005. Telomere biology in aging and cancer. *J Am Geriatr Soc*. 53: S292-S294.

Wolf D, Harris N, Rotter V. 1984. Reconstitution of p53 expression in a nonproducer Ab-MuLV-transformed cell lines by transfection of a functional p53 gene. *Cell*. 38: 119-126.

Wong KB. DeDecker BS, Freund SMV, Proctor MR, Bycroft M, Fersht AR. 1999. Hot-spot mutants of p53 core domain evince characteristic local structural changes. *Proc Natl Acad Sci USA*. 96: 8438-8442.

Workman P. 2004. Altered states: selectively drugging the Hsp90 cancer chaperone. *Trends Mol Med.* 10: 47-51.

Wu X, Hawse JR, Subramaniam M, Goetz MP, Ingle JN, Spelsberg TC. 2009. The tamoxifen metabolite, endoxifen, is a potent antiestrogen that targets estrogen receptor α for degradation in breast cancer cells. *Cancer Res*. 69: 1722-1727.

Wynford-Thomas D. 1999. Cellular senescence and cancer. *J Pathol*. 187: 100-111.

Xiao K, Liu W, Qu S, Sun H, Tang J. 1996. Study of heat shock protein HSP90 alpha, HSP70, HSP27 mRNA expression in human acute leukaemia cells. *J Tongji Med Univ*. 16: 212-216.

Yamamoto K, Garbaccio RM, Stachel SJ, Solit DB, Chiosis G, Rosen N, Danishefsky SJ. 2003. Total synthesis as a resource in the discovery of potentially valuable antitumor agents: cycloproparadicicol. *Angew Chem Int Ed*. 42: 1280-1284.

Yano M, Naito Z, Tanaka S, Asano G. 1996. Expression and roles of heat shock proteins in human breast cancer. *Jpn J Cancer Res*. 87: 908-915.

Yano M, Naito Z, Yokoyama M, Shiraki Y, Ishiwata T, Inokuchi M, Asano G. 1999. Expression of hsp90 and cyclin D1 in human breast cancer. *Cancer Letters.* 137: 45-51.

Yashima K, Milchgrub S, Gollahon LS, Maitra A, Saboorian MH, Shay JW, Gazdar AF. 1998. Telomerase enzyme activity and RNA expression during the multistage pathogenesis of breast carcinoma. *Clin Cancer Res*. 4: 229-234.

Yoo DY, Park JK, Choi JY, Lee KH, Kang YK, Kim CS, Shin SW, Kim YH, Kim JS. 1998. CDK4 down-regulation induced by paclitaxel is associated with G1 arrest in gastric cancer cells. *Clin Cancer Res*. 4: 3063-3068.

Young JC, Moarefi I, Hartl FU. 2001. Hsp90: a specialized but essential protein-folding tool. *J Cell Biol*. 154: 267-273.

Young JC, Obermann WMJ, Hartl FU. 1998. Specific binding of tetratricopeptide repeat proteins to the C-terminal 12-kDa domain of Hsp90. *J Biol Chem*. 273: 18007-18010.

Young JC, Schneider C, Hartl FU. 1997. In vitro evidence that hsp90 contains two independent chaperone sites. *FEBS Lett*. 418: 139-143.

Yu CX, Amies CJ, Svatos M. 2008. Planning and delivery of intensity-modulated radiation therapy. *Med Phys*. 35: 5233-5241.

Yun BG, Huang W, Leach N, Hartson SD, Matts RL. 2004. Novobiocin induces a distinct conformation of Hsp90 and alters Hsp90-cochpaerone-client interactions. *Biochemistry*. 43: 8217-8229.

Zagouri F, Nonni A. Sergentanis TN, Papadimitriou CA, Michalapoulos NV, Lazaris AC, Patsouris E, Zografos GC. 2008. Heat shock protein 90 in lobular neoplasia of the breast. *BMC Cancer*. 8: 312-318.

Zhan Q. 2005. Gadd45a, a p53- and BRCA1-regulated stress protein, in cellular response to DNA damage. *Mutat Res*. 569: 133-143.

Zhang H and Burrows F. 2004. Targeting multiple signaling transduction pathways through inhibition of Hsp90. *J Mol Med*. 82: 488-499.

Zhang Y, Yoshida T, Zhang B. 2009. TRAIL induces endocytosis of its death receptors in MDA-MB-231 breast cancer cells. *Cancer Biol Ther*. 8:1-6.

Zhang Y and Zhang B. 2008. TRAIL resistance of breast cancer cells is associated with constitutive endocytosis of death receptors 4 and 5. *Mol Cancer Res*. 6: 1861-1871.

Zheng YL, Loffredo CA, Shields PG, Selim SM. 2009. Chromosome 9 arm-specific telomere length and breast cancer risk. *Carcinogenesis*. 30: 1380-1386.

Zou J, Guo Y, Guettouche T, Smith DF, Voellmy R. 1998. Repression of heat shock transcription factors HSF1 activation by HSP90 (HSP90 complex) that forms a stress-sensitive complex with HSF1. *Cell*. 94: 471-480.

Zuo L, Weger J, yang Q, Goldstein AM, Tucker MA, Walker GJ, Hayward N, Dracopoli NC. 1996. Germline mutations in the $p16^{INK4A}$ binding domain of CDK4 in familial melanoma. *Nat Genet*. 12: 97-99.

Zunino F, Gambetta R, Di Marco A. 1975. The inhibition *in vitro* of DNA polymerase and RNA polymerases by daunomycin and adriamycin. *Biochem Pharmacol*. 24: 309–311.

Appendix

Telomere-associated TRF2 Expression during Breast Cancer Progression

A.1 Introduction and Rationale

Telomeres are specialized structures found at the ends of linear chromosomes that contain non-coding DNA distinguished by a 5'-TTAGGG-3' sequence (Blackburn, 1991). The end replication problem produces a stretch of unreplicated DNA between the final RNA priming event and the terminus. To counteract this problem, the processive ribonucleoprotein enzyme, telomerase, extends these continuously shortened ends. An internal RNA template (in humans, hTR) recognizes the single stranded overhang produced as a result of normal replication, and a catalytic reverse transcriptase (hTERT) uses the hTR template to add on telomeric DNA (Nugent and Lundblad, 1998). Telomerase maintains telomeres in the vast majority of tumor cells thus providing for unlimited proliferative potential (Holt and Shay, 1999; Shay and Bacchetti, 1997). However, despite high levels of telomerase activity in cancer cells, telomeres are nevertheless maintained at a relatively short length. In fact, telomere length abnormalities are seen as early events in the initiation of epithelial carcinogenesis, including ductal carcinoma *in situ* (DCIS) of the breast (Meeker *et al*., 2004a; 2004b).

In light of these abnormalities, a host of telomere binding proteins are critical for assuring that telomeres do not trigger a DNA damage response, since an unfolded telomere could be sensed as a double strand DNA break (Deng and Chang, 2007). Some of the telomere binding proteins that provide this capping function include telomeric repeat binding protein factor 1 and 2 (TRF1 and 2), TIN2, POT1, RAP1, MRE11 complex, PTOP/PIP1, and tankyrase

1/2 (Shay and Bacchetti, 1997). These proteins cooperatively establish the t-loop, in which the single-stranded 3'overhang folds back onto itself and invades duplex DNA (de Lange, 2005; Kanoh and Ishikawa, 2003). The region of invasion is referred to as the D-loop (Neidle and Parkinson, 2003). Without a capping mechanism, the ends of chromosomes are eroded to such a critically short length that telomere dysfunction ensues.

Shelterin is a complex consisting of six integral telomere binding proteins, TRF1, TRF2, TIN2, Rap1, TPP1, and POT1. Unlike other telomere-associated proteins, this complex is abundant only at chromosome ends and remains associated at the telomere throughout the cell cycle (de Lange, 2005). Two of the shelterin components, TRF1 and TRF2, are necessary for the proper formation of the T/D-loop. Both proteins contain DNA-binding domains and form homodimers and higher order oligomers (de Lange, 2005). TRF2 has emerged as the major protective factor at chromosome ends, acting as a positive regulator of telomere length (Karlseder, 2003). In support of this role, overexpression of TRF2 results in increased telomere shortening, without an associated increase in replicative senescence rate (Karlseder, 2002). This finding indicates that TRF2 acts to stabilize and protect shortened telomeres and prevents the induction of senescence. Functional inactivation of TRF2 results in a loss of t-loop invasion, leading to non-homologous end joining-mediated formation of end-to-end fusions. These fusions arise from the cells' inability to distinguish natural ends and broken DNA. In addition to fusions, normal cells without a capping mechanism may also undergo recombination due to their highly repetitive sequence (Baykal *et al*., 2004). Other downstream chromosomal instabilities may occur at later rounds of cell division, including translocations, non-disjunction, and aneuploidy, which all likely contribute to tumorigenesis. Thus, maintaining telomere integrity and avoiding dysfunction are critical for genomic stability.

Previous data indicate that TRF2 may also assume additional (non-telomeric) cellular roles. For instance, TRF2 has been implicated in sensing and responding to irradiation-induced non-telomeric interstitial DNA damage (Bradshaw *et al*., 2005). Currently very little is known about the involvement of TRF2 in mammary carcinogenesis. One study has reported that TRF2 is upregulated in ductal carcinoma *in situ* (DCIS) and invasive breast cancer (Nijjar *et al*., 2005). However, this analysis only included six clinical specimens and mainly served as confirmatory data for *in vitro* cell culture findings, suggesting that TRF2 is upregulated during mammary cancer progression. The present study seeks to examine TRF2 expression in full scale microarrays of normal, DCIS, and invasive breast cancer tissue. It may be possible that breast cancer cells overexpress TRF2 to protect short telomeres, thus allowing for continued cell proliferation. TRF2 expression in normal, DCIS, and malignant breast tissues in immunohistochemically stained sections were compared in terms of reactivity, intensity, and cellular localization. Telomere length in these tissues was assessed using telomere-specific FISH analysis. Finally, we determined whether there was any correlation between TRF2 expression and progression of disease stage and between telomere length and advancement of breast cancer.

A.2 Results

A.2.1 Invasive breast carcinomas express less nuclear TRF2.

Based on the immunostaining results, cellular distribution of TRF2 was almost exclusively localized in the nucleus in normal, DCIS, and malignant cores. Cores in which no primary TRF2 antibody was applied do not show any positive staining (Figure 49A, C, E). Normal breast ductal epithelial cells exhibit moderately high levels of TRF2 staining in the nucleus (Figure 49B). Out of all the normal breast cores examined, the majority (73.35% ±

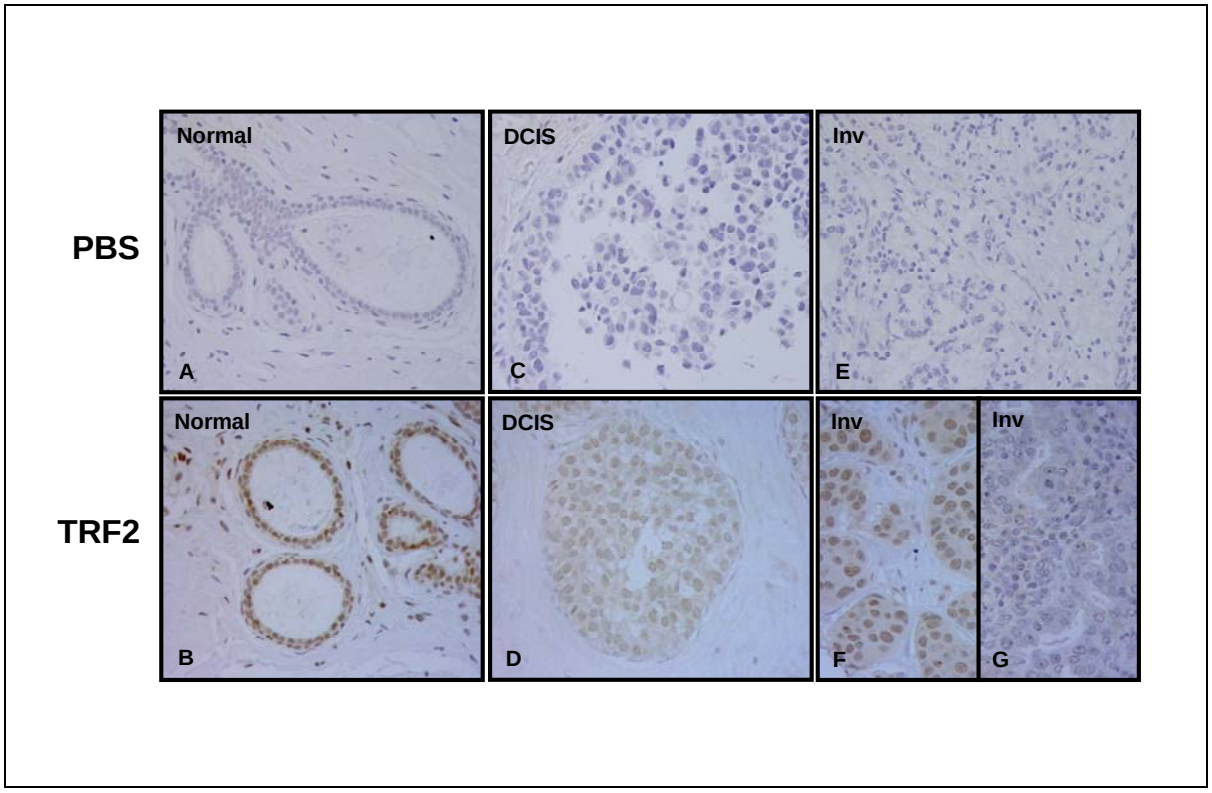

Figure 49: TRF2 expression in normal, DCIS, and invasive breast carcinomas from tissue arrays. Representative images of PBS treated sections of normal (A), DCIS (C), and invasive (E) cores. Immunostaining with an antibody against TRF2 shows that it is localized to the nucleus of normal (B), and DCIS (D) cores and shows variability in expression in invasive cores (F, G). Total numbers of cores stained was n = 113 for normal, n = 56 for DCIS, and n = 459 for invasive carcinomas. Overall weighted kappa value is 0.5495. All representative images shown are at 40x.

3.55%) were scored as 2, corresponding to moderate intensity (Table 10). Similarly, the greatest proportion of DCIS cores (66.8% ± 4.2%) was also moderately stained in intensity (Figure 49D, Table 10). The remainder of the cores for both normal and DCIS tissues could be categorized into weakly and strongly staining, but these fractions were considerably smaller and thus may represent outliers in the data.

Unlike normal and DCIS cores, invasive carcinomas show a greater variability in TRF2 staining, ranging from very low intensity or negative immunoreactivity to strongly reactive (Figure 49F, G). Again, the majority of invasive cores were given a score of 2 for moderate staining (59% ± 3.65%) (Table 10). It is interesting to note that although moderately intense TRF2 expression was seen in the largest proportion of each disease type, this proportion decreased with increasing malignancy. Specifically, a smaller fraction of invasive breast carcinomas stained moderately intense than normal breast, with DCIS scores falling in the middle. Furthermore, out of the three disease types, invasive cores had a greater proportion of very weakly expressing TRF2 cores (5.35% ± 1.35%) than both normal (3.45% ± 0.7%) and DCIS (0.95% ± 0.4%) specimens. However, invasive cores also had the largest proportion of strongly expressing TRF2 cores (12.2% ± 2.85%) relative to normal (9.25% ± 2.3%) and DCIS (5.4% ± 1.6%) tissues.

A.2.2 Consistently high levels of nuclear TRF2 in breast and non-breast cell lines.

In addition to breast tissue, immortalized and cancer cell lines were assessed for TRF2 expression. Included in duplicate in this array were the breast cancer cell lines MCF7 and T47D, the immortalized non-tumorigenic epithelial cell line MCF-10A, prostate cancer cell line PC3, and the colon adenocarcinoma HT-29 cell lines. Unlike the variability observed in

Table 10: TRF2 nuclear immunostaining

	Nuclear Score % (stdev)			
Intensity	**Normal**	**DCIS**	**Invasive**	**Cell Lines**
0	3.45 (0.70)	0.95 (0.40)	5.35 (1.35)	0
1	14.05 (2.45)	26.8 (3.0)	23.45 (3.85)	0
2	**73.35 (3.55)**	**66.8 (4.20)**	**59.0 (3.65)**	26.65 (4.45)
3	9.25 (2.30)	5.4 (1.60)	12.2 (2.85)	**73.35 (4.45)**

invasive breast carcinomas, established cell lines consistently exhibit very intense TRF2 immunostaining, that is primarily localized in the nucleus (Figure 50). Specifically, the great majority of cell lines stains strongly (73.35% ± 4.45%), while only a fraction stain moderately intense (26.65% ± 4.45%) (Table 10). Additionally, the frequency of strong TRF2 staining in established cell lines is noticeably higher than normal, DCIS, and invasive breast tissue. It is striking that none of the cell lines have weak TRF2 expression, indicating that TRF2 may be an important growth regulator in established cancer cell lines.

A.2.3 Highly variable FISH signal indicative of nonhomogeneous telomere length.

TRF2 has emerged as a major protective protein at the telomere. In pursuance of the variability in TRF2 immunostaining, we wanted to determine whether the differences in TRF2 intensity within breast carcinomas were influenced by telomere length. Fluorescence *in situ* hybridization (FISH) was performed on breast tissue arrays to assess telomere length in normal, DCIS, and invasive carcinoma cores. The pantelomeric PNA probe specific for telomeric sequences produces multiple, punctate, nuclear hybridization signals. In general, normal cores generally had brighter telomeric signal, corresponding to longer telomeres (data not shown). Representative results indicate that invasive breast carcinomas displayed a range of telomeric signal intensities, with some cores showing intense fluorescence signal and other cores showing very weak, but still readily detectable signal, corresponding to short telomeres (Figure 51). These invasive carcinomas were found to include both weak (shorter) telomeric signals as well as strong (longer) telomeric signals. Telomere length as noted in the surrounding normal architecture was generally longer, since FISH signals were consistently larger (Figure 52). DCIS cases also seemingly displayed some variability in telomeric signal, but there were fewer

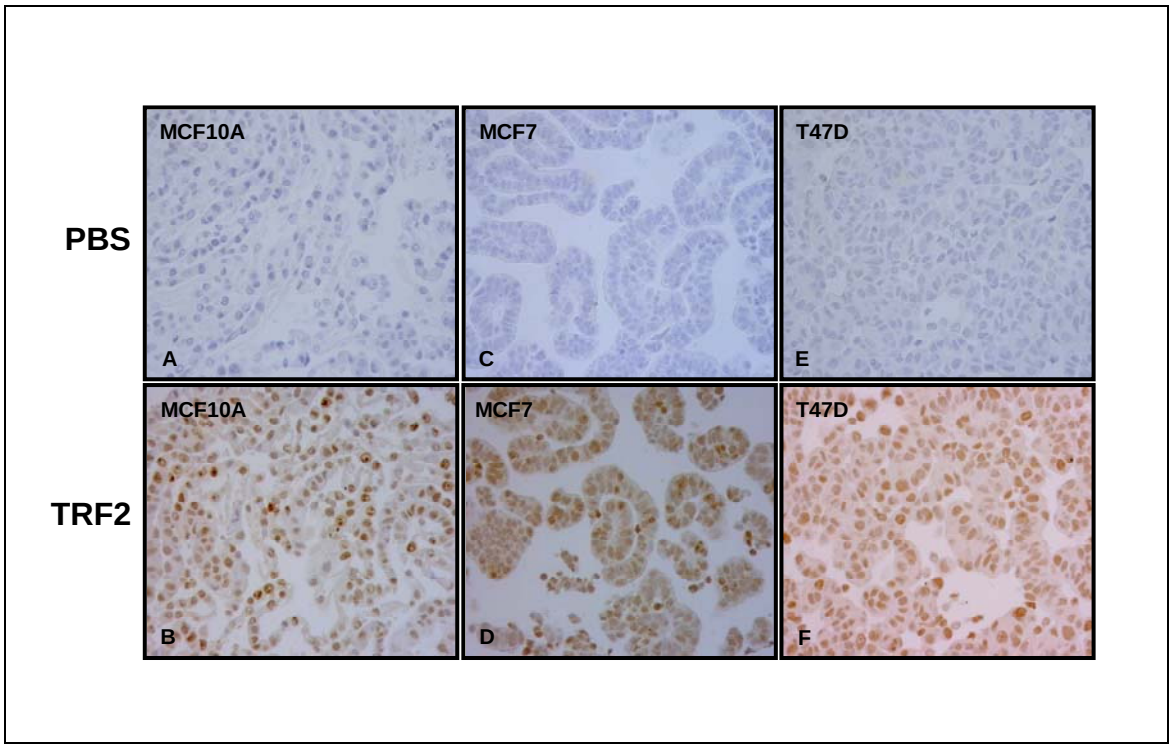

Figure 50: Established cell lines consistently express high levels of nuclear TRF2. Control cores in each array included breast cancer cell lines MCF7 and T-47D; immortalized epithelial cell line MCF-10A; prostate cancer cell line PC-3 (not shown); and colon cancer cell line HT-29 (not shown). These cores display significantly strong nuclear staining, more so than normal, DCIS, or invasive breast carcinomas. Representative images of MCF10A (B) and breast cancer cell lines MCF7 (D) and T47D (F) are shown stained with an antibody against TRF2. PBS-treated MCF10A (A), MCF7 (C), and T47D (E) served as negative controls (no primary antibody). Total numbers of cell line cores stained was n = 108. Overall weighted kappa value is 0.5495. All images shown are at 40x.

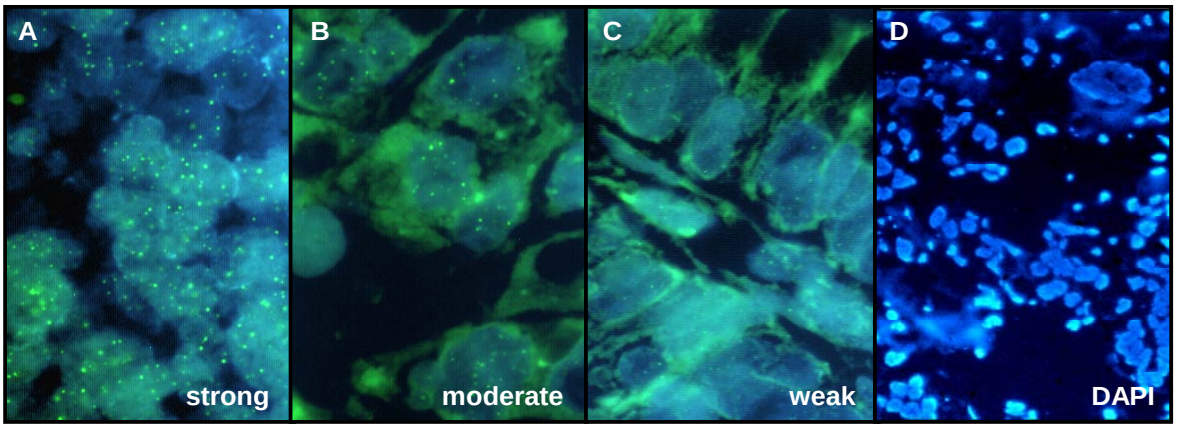

Figure 51: Variability in telomeric signal in invasive cores. Invasive breast carcinoma cores display varied telomere length, as can be seen by the diversity in intensity of the telomeric signal. Since tissues are three-dimensional, there are multiple planes of telomeric signal. (A) Representative images of tissue with telomeres longer than normal show strong telomeric signal. (B) Tissue with telomeres comparable in size to that of normal cores have moderate signal intensity. (C) Tissue with telomeres shorter than that of normal tissue, but are still detectable. (D) Low power image of core with DAPI staining.

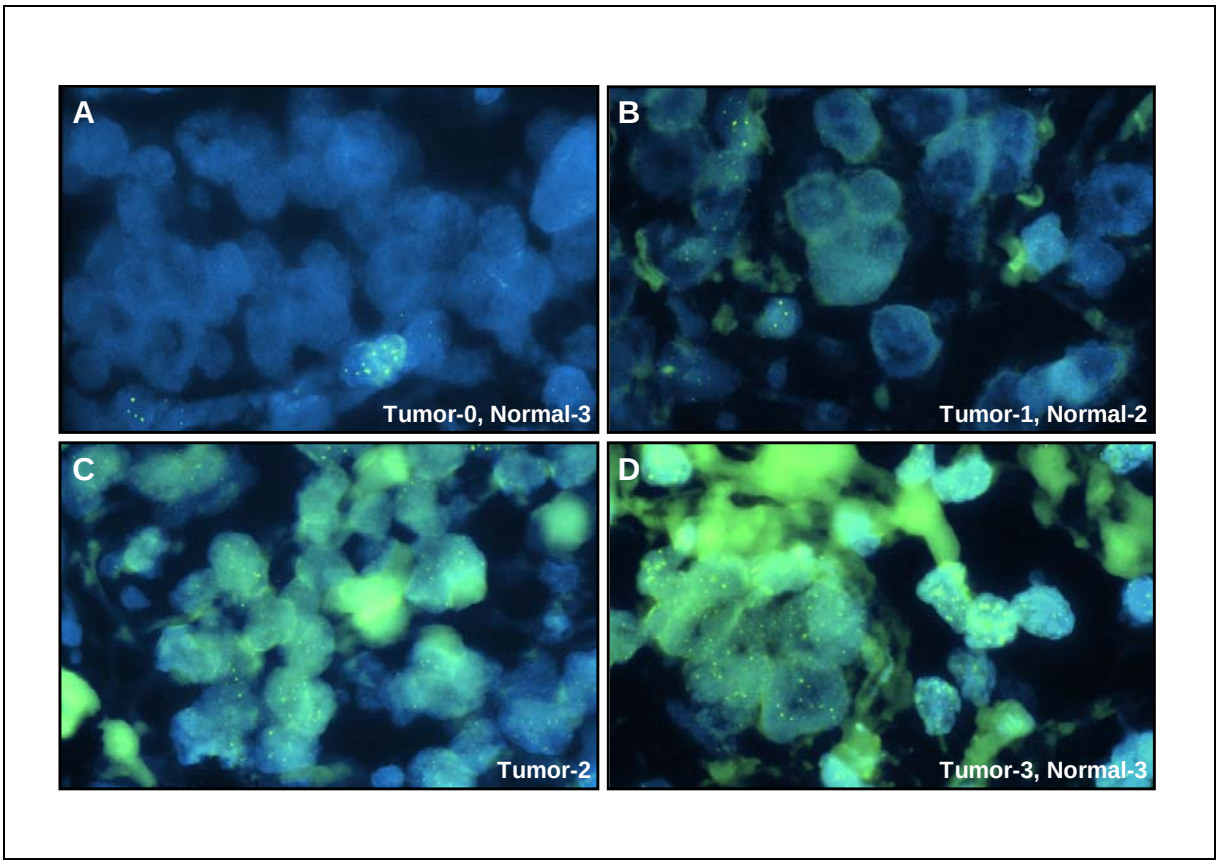

Figure 52: Tumor and surrounding normal tissue express varying telomeric intensity. Pantelomeric FISH detects varying telomeric signal between tumor cells and the surrounding normal cells within an invasive breast carcinoma core. Representative images show undetectable signal in tumor cells with strong signal in normal cells (A); weak signal in tumor cells and moderate signal in normal cells (B); moderate signal in tumor cells (C); and strong signal in both tumor and normal cells (D).

cores staining brightly (data not shown). Taken together with the TRF2 finding, the variability of FISH signals in invasive cores is in accordance with the wide distribution of TRF2 intensity that was observed with immunostaining. Thus, malignant breast cancers display variable TRF2 protein expression as well as telomere length.

A.2.4 No difference in TRF2 score, but considerable difference in FISH score.

As a group in terms of TRF2 immunostaining, normal cores on average score at 1.8967 ± 0.5897 while DCIS cores score at 1.7685 ± 0.5767 and invasive cores at 1.7806 ± 0.7235 (Table 11). Based on these observed means, there is no significant difference between the three disease types when examining TRF2 expression in the nucleus ($p = 0.0810$). This finding suggests that invasive breast carcinomas more frequently express both very low and very high TRF2 levels than normal and DCIS tissues, highlighting the inherent variability of malignant breast tissue. Although proportions of weakly, moderately, and strongly staining cores appear to appreciably differ between the disease types, there is a lack of any real difference as a disease group.

Although no significant differences emerged between the disease types in terms of TRF2 expression, telomeric signal is considerably different as assessed by FISH. Normal breast tissue generally displays moderately strong FISH signal (2.2111 ± 0.1981), corresponding to telomere lengths characteristically found in normal stroma and mammary epithelial cells (Table 11). DCIS and invasive carcinomas express relatively weaker telomeric signal, 1.1915 ± 0.47 and 1.3786 ± 0.2942, respectively, reflecting shorter telomeres. Thus, normal breast tissue contains significantly longer telomeres than pre-invasive and malignant breast specimens ($p<0.0001$).

Table 11: Average TRF2 immunostaining and FISH scores

	Observed means (s.e.)			
	Normal (n = 113)	**DCIS (n = 56)**	**Invasive (n = 459)**	**p-value***
TRF2	1.8967 (0.5897)	1.7685 (0.5737)	1.7806 (0.7235)	0.0810
FISH	2.2111 (0.1981)	1.1915 (0.4700)	1.3786 (0.2942)	**<0.0001**

*p<0.05 are significant

A.2.5 Age influences TRF2 expression.

Despite the lack of significant difference in TRF2 expression between all disease types, we nevertheless observed great variability in invasive breast carcinomas. Since TRF2 is a tight regulator of telomere maintenance, it may be possible that the TRF2 variability in malignant tissue reflects alterations in telomere length. In order to address this finding, we wanted to determine if TRF2 protein is influenced by chronologic age, which is closely associated with telomeric length. As shown in Table 12, no significant correlations emerge between chronologic age and TRF2 intensity in invasive breast carcinomas. However, TRF2 expression in both normal breast tissue ($p<0.0001$) and pre-invasive DCIS tissue ($p = 0.0017$) reveals significant positive correlations with age. Additionally, we wanted to determine if the variability in invasive cores was impacted by breast cancer stage as designated by TNM grading. We do not observe significant correlations between TNM and TRF2 score ($p = 0.7052$), suggesting that the degree of malignancy is not associated with TRF2 expression (Table 12).

A.2.6 Association of TRF2 and telomere length.

Although chronologic age at diagnosis does not appear to be a driving factor in TRF2 expression in invasive cores, physiologic age as assessed by measuring telomere length may possibly be more influential. We find that TRF2 negatively correlates with FISH intensity, indicating that greater TRF2 expression is associated with weaker FISH signals in invasive carcinomas ($p = 0.0491$, Table 13). As an extension of this finding, we determined that a greater FISH signal also significantly correlates with a lower TNM grade ($p = 0.0250$, Table 13). When examining chronologic age, no apparent correlations emerge with FISH signal.

Table 12: Correlations between chronologic age or TNM stage and average TRF2 score

	Tissue Type	Correlation	p-value*
Age	Normal	+	**<0.0001**
	DCIS	+	**0.0017**
	Invasive	None	0.8766
TNM	Invasive	None	0.7052

*p<0.05 are significant

Table 13: Correlations between TRF2 score or clinical parameters and FISH

Parameter	Tissue Type	Correlation	p-value*
TRF2	Invasive	-	**0.04913**
TNM	Invasive	-	**0.02496**
Age	Normal	None	0.6069
	DCIS	None	0.254
	Invasive	None	0.6411

*p<0.05 are significant

Thus, telomere length is mainly associated with TRF2 expression and influenced by the cancer stage in invasive carcinomas.

A.3 Discussion

Many telomere-binding proteins are required at the telomere to avoid triggering a DNA damage response, since an unfolded telomere could be interpreted as a double strand break. TRF2 is part of the shelterin complex and implicated in assisting in the formation of the protective t-loop. To study the role of TRF2 in breast cancer progression, tissue microarrays were used since they allow for the simultaneous investigation of a large number of tissue specimens on a single slide. Although normal, DCIS, and invasive subdivisions are by no means an exhaustive grouping of breast cancer types, they closely represent the natural progression of this disease.

The present study confirms that TRF2 is almost exclusively localized in the nucleus. In addition to its protective role, the nuclear localization of TRF2 suggests that it may also be involved in non-telomeric functions. Bradshaw, *et al*., 2005 have shown that TRF2 associates with irradiation-induced double strand breaks, forming transient foci in these regions. Also, Ning, *et al*, 2006 published data indicating that adriamycin or etoposide treatment had no effect on telomere length, but did upregulate TRF2 in gastric cancer cells.

Similar to the study by Nijjar, *et al*., 2005, our study also showed marked nuclear staining in normal, DCIS, and invasive breast tissue. However, contrary to their study, the results presented here show that TRF2 is not significantly upregulated in DCIS and invasive breast carcinomas compared to normal breast tissue. These differences may be due to experimental power, since only a few clinical specimens were analyzed and no statistical

analyses were included in their study. Our study examined hundreds of cores simultaneously and included internal controls within each slide.

Presently, we found that the majority of normal cores stained moderately intense for TRF2, implying that normal breast tissue is associated with more TRF2 protein bound to telomeres. The presence of this protein protects telomeres by promoting t-loop formation at chromosome ends, thereby avoiding the cellular growth arrest that accompanies a critically short telomere. So although normally dividing cells have longer telomeres, it is the telomere state that actually regulates senescence onset (Karlseder, 2003).

A comparison of normal and invasive tissues showed that there were fewer normal cores but more invasive cores that exhibited weak TRF2 expression. In other words, invasive breast tissue expressed less TRF2 levels relative to normal breast tissue. This finding may be reflective of the inherently shorter telomere length in cancer cells. The vast majority of cancer cells, including breast cancer, display elevated levels of telomerase due to reactivation of this enzyme. Due to this phenomenon, telomeres are maintained in cancer cells, although at shorter lengths than normal (Shay and Bacchetti, 1997). Applied to the data presented here, it is possible that shorter telomeres provide fewer repeat sequence (TTAGGG) sites for TRF2, and so less TRF2 can stably bind in the malignant state (Nijjar, *et al*., 2005). This working model is supported by chromatin immunoprecipitation studies performed in our lab showing less TRF2 bound at the telomere in cancer cells without exogenous telomerase expression.

Unlike clinical breast tissue, immortalized and cancer cell lines consistently displayed elevated levels of nuclear TRF2 expression. This finding was also observed previously in our lab, which showed that immortalized and breast cancer cell lines have increased TRF2 levels as analyzed by immunoblotting. The elevated TRF2 expression in this case may reflect an artifact

of cultured cell lines. These cells may need to upregulate TRF2 as a protective mechanism to ensure continued proliferation under the selective pressures of growing in culture, which breast tissue specimens do not experience.

Since TRF2 is a tight regulator of telomere maintenance, it may be possible that the TRF2 variability in malignant tissue reflects alterations in telomere length. Since aging and alterations in telomere length are closely related (Aubert and Lansdorp, 2008), we assessed the association of TRF2 with chronologic age. We found that TRF2 expression in both normal and pre-invasive breast tissue significantly correlates with age. These positive correlations indicate that greater TRF2 expression is associated with greater age at diagnosis in benign tissue or less aggressive cancers. It is possible that in normal breast cells, more TRF2 is recruited to impart telomeric protection in older individuals. In invasive carcinomas, we do not observe any significant correlation to chronologic age. However, the observed variability in TRF2 intensity in invasive cores could also be due to the heterogeneous nature of malignant breast tissue in terms of telomeric or physiologic age. FISH data indicated that normal breast tissue show longer telomeres, while invasive carcinomas have generally shorter and varied telomere length. This is in agreement with a previous study (Meeker, *et al*., 2004a) in which invasive and DCIS breast tissues displayed variable telomere length. The presence of stronger telomeric signal in normal breast tissue and weaker signal in malignant breast tissue is supported by studies reporting telomere shortening occurring as part of tumorigenic conversion (Meeker, *et al*., 2004a; 2004b). Our finding that longer telomere lengths in invasive carcinomas as assessed by FISH correlates with weaker TRF2 expression suggests that these larger lengths may require less stabilization by TRF2. Thus, the weaker TRF2 intensity in this subset of invasive tissue may reflect a less protected telomere state, allowing the cell to become more genetically

unstable. Furthermore, since TNM stage does not correlate with TRF2 expression, it is possible that TRF2 only provides a growth potential or advantage to premalignant and malignant cells without imparting any tumorigenic potential. However, we did show that a significant negative association exists between TNM stage and FISH signal, such that a greater telomeric signal is indicative of a lesser degree of malignancy.

Collectively, the results presented reflect a model in which TRF2 behaves in a differential manner depending on the presence or absence of malignancy. In normal cells or in "young" cells, telomeres are generally longer and thus require less TRF2 association for protection of the t-loop. However, in invasive carcinomas, TRF2 acts in a bimodal capacity. For those cancers that contain longer lengths, less TRF2 is localized to the telomere and may provide less protection, predisposing the cell to a malignant state. In contrast, in those cancers with shorter telomeres, we find higher TRF2 expression, suggesting that TRF2 may be heavily recruited to these sites. These short telomeres may be inducing a damage response such that TRF2 attempts to impart more protection. Indeed, telomere-binding proteins, in forming a protective cap on telomeres, aid in length regulation and stabilization of the t-loop structure (De Boeck *et al.*, 2009).

In summary, there are clear trends in the data based on degree of malignancy, which may ultimately serve as the basis for mechanistic studies of breast cancer progression and the role of telomere binding proteins in this process. The importance of telomere-binding proteins at the telomere in imparting protection and avoidance of activating a DNA damage response is clearly evident, as telomere dysfunction leads to genomic instability and/or transformation. Thus, maintenance of telomeric structure and function in part by TRF2 is critically essential in cell homeostasis and the evasion of tumorigenesis.

Vita

Malissa Chang Diehl was born in Shenyang, China on July 15, 1980 with the surname Liu. She immigrated with her family to the United States in 1986 and became a naturalized citizen. Growing up in North Wales, PA, she attended North Penn High School and graduated in 1998. Her undergraduate studies at the Pennsylvania State University, University Park Campus were completed in 2002. Following this, Malissa relocated to Richmond, Virginia to attend graduate school. Her future plans include pursuing a post-doctoral position at the University of Pennsylvania in Philadelphia, PA.